UNIVERSIDAD COMPLUTENSE DE MADRID

FACULTAD DE CIENCIAS QUÍMICAS
Departamento de Bioquímica y Biología Molecular

TESIS DOCTORAL

Molecular mechanisms of mitotic cell death

Mecanismos moleculares de la muerte celular en mitosis

MEMORIA PARA OPTAR AL GRADO DE DOCTOR

PRESENTADA POR

Elena Doménech Cruz

Director

Marcos Malumbres

Madrid, 2015

Universidad Complutense de Madrid
Facultad de Ciencias Químicas
Departamento de Bioquímica y Biología Molecular

Molecular Mechanisms of Mitotic Cell Death

Elena Doménech Cruz
Degree in Biochemistry

Thesis Director:
Dr. Marcos Malumbres

Centro Nacional de Investigaciones Oncológicas (CNIO), Madrid

Acknowledgements

Summary/Resumen

Summary

Throughout the process of neoplastic transformation cells progressively acquire functional capabilities that allow cancer cells to survive, proliferate and disseminate. These functions are acquired in different tumor types via distinct mechanisms during the course of multistep tumorigenesis. The most fundamental trait of cancer cells is their ability to sustain chronic proliferation (Malumbres and Barbacid, 2001; Hanahah and Weinberg, 2011). Selective cancer chemotherapy is based on the assumption that tumor cells proliferate rapidly and cytotoxic drugs gain specificity from their ability to preferentially kill rapidly proliferating cells (Chabner *et al*., 2006). Targeting the deregulated cell cycle of cancer cells seems to be a good therapeutic options.. The fragility of cancer cells when they undergo division serves as a critical point for intervention in chemotherapy (Chan *et al*., 2011). Mitosis is considered the most fragile period of the cell cycle, during which is highly susceptible to cell death when exposed to several insults.

The great clinical success of microtubule poisons in clinics, such as taxanes and vinka-alkaloids, and the susceptibility of cells to mitotic arrest, has encouraged the development of agents that inhibit mitotic progression. However, microtubules are also necessary for multiple cellular processes in interphase and the use of this spindle poisons is associated with side-effects such as neurotoxicity, that can lead to irreversible neuropathies. The generation of anti-tumoral therapies that target proteins with specific functions in mitosis, although promising, has not achieved the desired efficiency in patients. In general, this new generation of mitosis targeted inhibitors show less anti-tumor activity than taxol, although the problem of neurotoxicity has been solved effectively. One of the reasons of the limited effect of these drugs may be the low mitotic rate in human tumors, much lower than in preclinical models (Malumbres and Doménech, 2013). Besides, the drug development programs have traditionally focused on developing inhibitors of Plk1 and Aurora A and B as anti-tumor targets. Recently, several members of the family of kinesins are emerging as potential anti-tumor targets, however, there are a variety of kinases mitotic whose potential as a therapeutic target has not yet been explored, as is the case for: Nek, Mps1, Mast or Haspin.

The arrest imposed by anti-mitotic drugs is often transient and the cells are able to exit from mitosis (i.e. DNA decondensates and the nucleus re-assemble in the absence of chromosomal segregation) in a process known as mitotic slippage (Brito and Rieder, 2006; Topham and Taylor, 2013). Mitotic slippage is considered one of the major mechanisms of resistance against anti-mitotic drugs, leading to the appearance of aneuploid cells that may continue proliferating, an undesirable outcome.

Eukaryotic cells have evolved mechanisms of control to detect errors that may occur during cell cycle and blocking progression until it is repaired. One of these mechanisms is mediated by the APC/C (Anaphase Promoting Complex or cyclosome), a multimeric complex with E3 ubiquitin ligase activity necessary for chromosome segregation, that target for degradation several cell cycle regulators. The APC/C recognizes its substrates through two adapter proteins; Cdh1 and Cdc20, being Cdc20 responsible for the function of APC/C during the initial stages of mitosis and for triggering the transition from metaphase to anaphase. When the chromosomes are perfectly aligned at the metaphase plate attached to microtubules of the bipolar spindle, the activation of APC/C by Cdc20 results in the elimination of two critical substrates; securin (separase inhibitor) and cyclin B (Cdk1 activator), which leads to mitotic exit (Manchado *et al*. 2010). In the absence of Cdc20, cells are unable to exit mitosis and remain arrested in metaphase for 6-36 hours till they inevitably die in mitosis (Manchado *et al*. 2010). Inhibition of the APC/C has recently been proposed as a therapeutic option for preventing mitotic slippage (Malumbres and Doménech, 2013;. Huang *et al.*, 2009; Machado *et al.*, 2011;. Rieder and Medema, 2009).

How cells die in the absence of Cdc20 is an issue of great interest. The cellular alterations resulting from aberrant mitosis are collectively known as mitotic catastrophe (Vitale *et al*., 2011). Mitotic catastrophe (MC) can be defined as a type of cell death resulting from aberrant mitosis which takes place in the ongoing

mitosis or in the following interface (Galluzi *et al*, 2012;. Vitale *et al*., 2011). It is therefore different from apoptosis, necrosis or senescence and is driven by a poorly understood signaling cascade. MC can be considered a tumor-suppressor mechanism (Vitale *et al*., 2011) preventing chromosomal instability and the appearance of aneuploid cells. MC favors the disruption of tumor progression and its induction is a therapeutic endpoint. Despite the broad use of this concept, the exact molecular mechanism that determine cell death in response to these changes are still unknown. Furthermore, it is unclear whether these cell death pathways are functional during mitosis, or arise in the next cell cycle as a result of changes during mitosis. For instance, in a prolonged mitotic arrest specific caspases are activated, causing DNA damage and the induction of p53-dependent apoptosis in the following interface (Orth *et al*., 2012). Multiple evidences have established a link between the intrinsic or mitochondrial apoptotic pathway in response to mitotic aberrations (Huang *et al*, 2009;. Topham and Taylor, 2013), by contrast, the extrinsic pathway of apoptosis is not functional at this stage of the cell cycle (Matthess *et al*., 2010).

This pathway is of great interest since, can be induced by treatment with several anti-tumoral agents, such as taxol. Despite its clinical relevance, little is known about the molecular pathways that mediate death in mitosis, mainly for the lack of a homogeneous model in which this process can be induced in an efficient and controlled manner. The generation of Cdc20 conditional knockout cells opens the possibility to analyze molecular pathways of death in mitosis in a controlled genetic model (Manchado *et al*., 2010).

Material and Methods

We made use of the mouse embryonic fibroblasts Cdc20(*lox/lox*), RERT (*+,Cre*) in which the conditional deletion of Cdc20 becomes effective after 4-OHT addition (Manchado *et al*., 2010). We have developed a strategy to follow individual cells for video microscopy expressing a histone reporter, H2B-GFP, after elimination of Cdc20 or chemical inhibition of mitosis. Mitotic onset is characterized by cell rounding, DNA condensation and the formation of the metaphase plate and cell death becomes evident by the addition to the culture media of To-Pro 3, a DNA dye which diffuses into the cell after membrane permeabilization that precedes death. This system allows the interrogation of the consequences of modulating several signaling pathways using siRNA or chemical inhibitors. Transfections of siRNA or plasmids were performed either with the Amaxa or Lipofectamine 2000 system following the manufacturer's instructions. For High-throughput studies the same experimental set up was followed (staining with To-Pro 3) but Opera microscope (Perkin Elmer) was used instead. For FRET the protocol described in Tsou *et al*., 2011 was followed and the fluorescence microscope (CCD) was used. For other life-cell studies SP5 confocal microscope was used-WLL.

Metabolic studies were performed in the Seahorse analyzer for measuring oxygen consumption and use extracellular acidification (Faubert et al, 2013;.. Wu et al, 2006). The analysis of extracellular metabolites was made by nuclear magnetic resonance (NMR) following the protocol described in Bradley *et al*., 2010. Determination of ATP levels was carried out as described in Saha *et al*., 2004. For the in vivo experiments MDA-MB-231 cells were injected subcutaneously in nude mice. When tumors reached an average volumen of 150-200 mm^3 received different treatments by intraperitoneal injection. All statistical analysis were performed with Prism 5 (GraphPad).

In the search for specific mitotic killers, the massive screening was performed in the Opera microscope, whereas the single cell fate analysis was performes using Delta Vision microscope following the same protocols introduced earlier in this section.

Results

1. Mitotic cell death pathways

Using the Cdc20(*lox/lox*) RERT(*+/Cre*) or human cell lines arrested in mitosis by treatment with APC/C inhibitors, we have shown that depletion of pro-survival Bcl-2 family factors results in a dramatic reduction survival in mitosis. These results are consistent with recent data suggesting the importance of these factors in mitosis (Huang *et al*, 2009;. Inuzuka *et al*, 2011;. Topham and Taylor, 2013; Wertz *et al.,* 2011). Intrinsic mitochondrial apoptotic pathway requires mitochondrial pore formation by Bak and Bax dimerization which precedes the release of cytochrome C and other pro-apoptotic factors and eventually caspase activation. The fact that Bax/Bak deficient cells die primarily by necrosis and autophagy during prolonged mitotic arrest suggest that other forms of cell death, in addition to apoptosis, may contribute to cell death in mitosis. Morphological characteristics of necrosis during mitosis were observed, however mitotic cell death seems to be independent of RIPK1 and RIPK3 activity and therefore programmed necrosis is not involved in MCD. Surprisingly, we identified autophagy as a pathway of great importance in controlling death during mitosis. Although traditionally, it is assumed that the processes of autophagy does not occur during this phase of the cell cycle (Eskelinen *et al*., 2002; Furuya *et al*, 2012;. Tasdemir *et al*., 2008), in this work we shown that autophagy remains during mitosis. It is a dynamic and progressive macro-autophagic process, which becomes massive at later mitotic arrest (24 hours). This autophagy can be enhanced by using inhibitors of mTOR and cooperates with apoptotic cell death in mitosis.

Mitotic spindle assembly and chromosome segregation requires proper mitochondrial activity. It has recently been shown that Cdk1 is required to phosphorylate and activate various components of mitochondrial complex I, leading to an increase in mitochondrial respiration during G2/M (Wang *et al*., 2014). Therefore, inhibition of Cdk1 results in decreased mitochondrial activity (Wang *et al*., 2014) accompanied by reduced respiration and reduced ATP levels. During prolonged mitotic arrest observed a decrease in mitochondrial mass is observed, which becomes apparent after 3 hours in mitosis, initially it is due to the lack of organelles renewal during mitosis. This decrease in mitochondrial mass is further enhanced by the presence of mitophagy, an active process of autophagy which particularly target damaged mitocondria for elimination (Okamoto *et al*., 2014; Youle and Narendra, 2011). The balance between mitochondrial biogenesis and mitophagy determines the amount of healthy mitochondria present in the cell. The absence of biogenesis is probably due to the reduced transcription and translation, which perpetuates mitochondrial dysfunction, and is the cause of the decreased ATP levels during mitotic arrest. Mitochondrial integrity may therefore set the limit for cell survival for its key role in the regulation of metabolism and cell death. As a consequence of the loss of mitochondrial respiration, ATP production decreased (concomitantly increased AMP levels) leading to an energetic crisis which ultimately triggers AMPK activation, the bioenergetic sensor of the cell. In parallel to the decrease in oxidative phosphorylation, increase in glucose uptake is observed. AMPK boost glucose uptake and glycolysis through PFKFB3 activation. PFKFB3 (also known as PFK-2) is a key enzyme in the regulation of the glycolytic flux, modulating PFK-1 activity, which catalyzes a primary checkpoint in glycolysis. PFK-1 catalyzes the conversion of fructose-6-phosphate (F6P) to fructose 1,6-bisphosphate (F1, 6BP), an irreversible and limiting reaction in the pathway, frequently hyperactivated in cancer (Bando *et al*., 2010). AMPK phosphorylates and activates PFKFB3 at ser-461 resulting in an increased Vmx of the kinase activity and a decreased phosphatase activity, leading to increased production of Fru-6-P, the allosteric regulator of PFK-1, (Marsin *et al*., 2002; Novellasdemunt *et al*., 2012) and the concomitant increase in PFK-1 activity and glycolysis. PFKFB3 is often expressed in transformed cells and tumors (Almeida *et al*., 2010; Bando *et al*., 2005; Calvo *et al*., 2006; Chesney *et al*., 1999; Duran *et al*, 2008; Kesseler *et al*., 2008; Novellasdemunt *et al*., 2006; Riera *et al*., 2020; Yalcin *et al*., 2009) and it has been linked to Warburg effect (Marsin *et al*., 2002; Bando *et al*., 2005). While PFKFB3 is nuclear during interphase, AMPK is predominantly cytoplasmic (Tsou *et al*., 2011). Whereas in mitosis, upon nuclear envelope breakdown cytoplasmic compartments mix their content and this interaction is favoured. Genetic inhibition or

the use of chemical inhibitors of both PFKFB3 and AMPK results in a reduced survival in mitosis. Similarly, the addition of glucose to the culture medium delays mitotic cell death. Therefore the induction of the glycolytic pathway during mitotic arrest is a mechanism that contributes to cell survival.

2. Anti-mitotic compounds

In the second part of this doctoral thesis we have focused on the search for compounds that reduce specifically cell viability of mitotic cells, that is, compounds that induce cell death in mitosis. To do this, we made use Cdc20 conditional knockout cells and we tested a library of 300 compounds in its ability to specifically kill cells in mitosis.

This study has allowed us to identify Haspin kinase as a potential anti-mitotic target. Haspin is considered an atypical mitotic kinase responsible for phosphorylation of histone 3 in the threonine-3, which acts as an docking site for the chromosome passenger complex (CPC), consisting of survivin, Aurora B, Borealin and INCENP (Cuny *et al*., 2012). Haspin inhibition in Cdc20-null cells enhanced cell death in mitosis, while inhibition of Haspin in asynchronous cultures leads to a transient mitotic arrest often followed by cell death in mitosis, in agreement with previous data (Dai *et al*., 2005; Niedzialdhowska *et al*, 2012; Wang *et al*., 2011). Haspin inhibitors results in a longer mitotic arrest than taxol treatment and it seems to be dependent on the activity of the mitotic checkpoint (SAC) given that treatment with reversine, an inhibitor of Mps1, the kinase activity of the SAC, rescued the normal duration of mitosis. However, it has been recently published that Haspin inhibition can abrogate SAC activity (De Antoni *et al*., Wang *et al*., 2010).

Discussion

1. Mitotic cell death pathways

Here we have stablished that inhibition of survival pathways or induction of cell death pathways in mitosis enhanced cell death during mitosis before mitotic slipagge occurs. This finding may have important implications in cancer therapy avoiding the accumulation of aneuploid cells and increasing the therapeutic efficacy of anti-mitotic drugs currently used in clinics. The combination of microtubule poisons and apoptosis inducers has been extensively studied (Inuzuka *et al*, 2011; Oltersdorf *et al*., 2005; Topham and Taylor., 2013; Wertz *et al*., 2011) and are of particular interest in specific celular settings, for example in tumors overexpressing Bcl-2 (Oakes *et al*., 2011). Similarly, combinations of taxol and mTOR inhibitors or inhibitors of enzymes involved in metabolism have been extensively tested in xenograft models (Campone *et al*, 2009; Lieber *et al*., 2011; Meier *et al*., 2009). However, in this study we show for the first time the molecular basis underlying this synergistic effect. Together these data provide the molecular basis for new combination therapies directed against cell cycle and metabolism in cancer.

2. Anti-mitotic compounds

The molecular mechanism by which inhibition of Haspin results in cell death in mitosis is still unknown. As Haspin activity is responsible for the proper localization of the CPC, lack of Haspin activity could lead to misslocalization and deficient activation of Aurora B, therefore Aurora B inhibition might affect mitosis in the same way that inhibition of Haspin. However, genetic deletion of Aurora B in mouse embryonic fibroblasts, as well as the use of inhibitors of Aurora B leads to a shorter mitosis compared to control fibroblasts, as a results from premature inactivation of mitotic checkpoint point. Survivin, given its ability to prevent apoptosis by direct inhibition of caspases (Chan et al., 2012), seems to be a good candidate to explain the reduced survival after inhibition of Haspin in mitosis. Indeed, Survivin silencing shorten survival in mitosis, although this is something that needs to be further studied. Inhibition of Haspin in Survivin overexpressing tumors could be beneficial as anti-tumor therapy.

Resumen

Introducción

A lo largo del proceso de transformación neoplásica las células adquieren de manera progresiva una serie de alteraciones que les otorgan de la capacidad de sobrevivir, proliferar y diseminarse. Estas funciones son adquiridas por los distintos tipos tumorales mediante diferentes mecanismos y a varios tiempos durante el proceso secuencial de tumorigenesis. Un rasgo principal de las células tumorales es la capacidad de proliferación incontrolada (Malumbres and Barbacid, 2001; Hanahah and Weinberg, 2011). Por ello la quimioterapia actual se centra en atacar específicamente células con alta tasa proliferativa (Chabner *et al.,* 2006) y las estrategias que interfieren con el ciclo celular parecen ser una buena opción terapéutica. Entre otras estrategias, el bloqueo específico de la progresión mitótica parece un buen candidato para evitar el avance tumoral. La mitosis es la fase del ciclo celular de mayor fragilidad y de mayor sensibilidad a muerte en respuesta a daño, lo que la convierte en un punto crítico para la intervención terapéutica (Chan et al., 2011).

El gran éxito clínico alcanzado por los venenos de microtubulos, como taxanos y vinka-alkaloides, ha potenciado el desarrollo de agentes que inhiban la progresión mitótica. Sin embargo, el hecho de que el citoesqueleto de tubulina desempeñe funciones fundamentales tanto en mitosis como en interfase, ha hecho replantear si el efecto observado por estos agentes se debe exclusivamente a su acción durante mitosis. De hecho, uno de los grandes problemas del uso de estas drogas es la gran neurotoxicidad asociada, lo que conlleva frecuentemente el cese del tratamiento. Se hace necesario el desarrollo de inhibidores de reguladores de mitosis; proteínas involucradas en la formación del huso y la progresión mitótica y que carezcan de estos efectos secundarios. De hecho, inhibidores selectivos de kinesinas y kinasas mitóticas están actualmente en diferentes fases de ensayos clínicos, aunque los resultados en pacientes no han alcanzado las expectativas. En general, esta nueva generación de inhibidores dirigidos a mitosis muestran menor eficacia anti-tumoral que el taxol, aunque el problema de la neurotoxicidad haya sido resuelto. Una de las razones por las que el efecto de estas drogas puede verse limitado es por la baja tasa mitótica en tumores humanos, mucho más reducida que en modelos preclínicos (Doménech and Malumbres, 2013). Además los programas de desarrollo de drogas se han centrado tradicionalmente en el desarrollo de inhbidores de Plk1 y Aurora A y B como dianas anti-tumorales. Recientemente varios miembros de la familia de las kinesinas están emergiendo como potenciales dianas anti-tumorales, sin embargo, hay una gran variedad de kinasas mitóticas cuyo potencial como diana terapéutica aún no ha sido explorado, como es el caso de: Nek, Mps1, Mast o Haspin.

La parada en mitosis observada como consecuencia del tratamiento con drogas anti-mitóticas es frecuentemente transitoria y las células son capaces de salir de mitosis (es decir, son capaces de descondensar el ADN y ensamblar el nuevo núcleo en ausencia de segregación cromosomal), a pesar de la permanente actividad del punto de control mitótico en un proceso conocido como "escape mitótico" (Brito and Rieder, 2006; Topham and Taylor, 2013). El escape mitótico es considerado uno de los principales mecanismos de resistencia ante drogas anti-mitóticas. En estas condiciones es frecuente la aparición de células aneuploides que pueden continuar proliferando.

Las células eucariotas poseen mecanismos de control para detectar errores que puedan ocurrir durante el ciclo celular interrumpiendo la progresión y si es posible permitiendo su reparación. Uno de estos mecanismos está mediado por el APC/C (Anaphase Promoting Complex o ciclosoma), un complejo multimérico con actividad enzimática ubiquitina ligasa E3 necesario para la segregación cromosómica, que marca con ubiquitina diversos reguladores del ciclo celular para su posterior eliminación por el proteasoma. El APC/C reconoce sus sustratos gracias a dos proteínas adaptadoras; Cdh1 y Cdc20. Cdc20 es responsable de la función de APC/C durante las fases iniciales de mitosis y por desencadenar la transición

de metafase a anafase. Cuando los cromosomas están perfectamente alineados en la placa metafásica y anclados mediante los microtúbulos a ambos polos del huso, la activación de APC/C por Cdc20 resulta en la eliminación de dos sustratos críticos; securina (inhibidor de separasa) y ciclina B (activador de Cdk1), lo que conlleva salida de mitosis (Manchado et al. 2010). En ausencia de Cdc20, las células no son capaces de salir de mitosis y permanecen bloquedadas en metafase durante 6-36 horas e irremediablemente mueren (Manchado et al. 2010). La inhibición del APC/C ha sido recientemente propuesta como opción terapéutica para la prevención del escape mitótico (Doménech and Malumbres, 2013; Huang *et al*., 2009; Machado *et al*., 2011; Rieder and Medema, 2009).

Cómo mueren las células que carecen de Cdc20 es una incógnita de gran interés. Se sabe que las células no pueden permanecer bloqueadas en mitosis durante mucho tiempo, ya que se lanza una cascada de muerte conocida como muerte celular en mitosis. En general, las alteraciones consecuencia de mitosis aberrantes se conocen como catástrofe mitótica (Vitale et al., 2011). La catástrofe mitótica (CM) puede ser definida como un tipo de muerte celular resultado de una mitosis aberrante que sucede en mitosis o en la interfase siguiente (Galluzi *et al*., 2012; Vitale *et al.,* 2011). Es por tanto diferente de apoptosis, necrosis o senescencia y está conducida por una cascada de señalización apenas conocida. CM puede ser considerada un mecanismo oncosupresor (Vitale *et al*., 2011) ya que evita inestabilidad cromosómica y previene la aparición de células aneuploides. La interrupción de CM favorece la progresión tumoral y su inducción constituye un punto final terapéutico. A pesar del amplio uso que se hace de este concepto, no se conocen adecuadamente los mecanismos moleculares que determinan la muerte celular en respuesta a estas alteraciones. Además, no está claro si estas rutas de muerte celular son funcionales durante mitosis, o si por el contrario surgen como una consecuencia de alteraciones durante mitosis que se efectúan en el ciclo celular siguiente. Por ejemplo, un arresto mitótico prolongado activa parcialmente caspasas específicas, causando daño al ADN y la inducción de apoptosis dependiente de p53 en la interfase siguiente (Orth *et al.,* 2012). Entre las rutas de muerte celular múltiples pruebas han establecido una conexión entre la vía intrínseca o mitocondrial de apoptosis en respuesta a aberraciones mitóticas (Huang *et al*., 2009; Topham and Taylor, 2013), por el contrario, la ruta extrínseca de apoptosis no es funcional en este estadio del ciclo celular (Matthess e*t al*., 2010).

Esta ruta es de gran importancia ya que, como se ha introducido anteriormente, se puede inducir por tratamiento con diversos compuestos químicos, como taxol, empleados en la terapia del cáncer. Pese a su gran relevancia clínica, no se conoce mucho sobre las rutas moleculares que median la muerte en mitosis, principalmente por falta de un modelo homogéneo en el que suceda este proceso de una manera eficiente y controlada. La generación de células con una deleción condicional en el gen Cdc20 inducible con 4-hidroxi-tamoxifeno, abre la posibilidad de analizar las rutas moleculares de muerte en mitosis en un modelo genético controlado (Manchado et al., 2010).

Materiales y Métodos

Hemos usado los fibroblastos embrionarios de ratón Cdc20(*lox/lox*), RERT(+,Cre) en los que la deleción condicional del alelo Cdc20 se hace efectiva tras adición de 4-hidroxitamoxifen (4-OHT) por la presencia de la versión inducible de Cre (Manchado *et al*., 2010). Hemos desarrollado una estrategia por videomicroscopía, mediante la cual es posible seguir a cada célula de manera individual tras parada mitótica por eliminación de Cdc20 o inhibición química de mitosis. El comienzo de la mitosis se caracteriza por que la célula comienza a redondearse y el ADN a condensarse, hasta que se hace evidente la formación de una placa metafásica, para ello usamos células que expresen histona H2B-GFP, mientras que la muerte celular se hace evidente por la adición al medio de To-Pro3, un colorante de ADN que difunde al interior de la célula tras permeabilización de la membrana plasmática que antecede a la muerte. Este sistema permite

caracterizar las consecuencias de la alteración de varias rutas de señalización usando ARN inteferente (ARNi) o inhibidores químicos. Las transfecciones de ARNi o plásmidos fueron realizadas con el sistema Amaxa o con Lipofectamina 2000 siguiendo las instrucciones del fabricante. Para un análisis a mayor escala de estas rutas de muerte mitótica, se empleó el mismo desarrollo experimental (tinción con To-Pro 3), pero se utilizó un microscopio de análisis masivo: Opera (Perkin Elmer). Para los estudios de FRET se siguió el protocolo descrito en Tsou *et al.,* 2011 un microscopio de fluorescencia (CCD) y para otros ensayos en células vivas se empleó el microscopio confocal SP5-WLL.

Para los estudios metabólicos se empleó el analizador Seahorse, para medidas de consumo de oxígeno y acidificación extracelular (Faubert *et al*., 2013; Wu *et al*., 2006) y para el análisis de metabolitos extracelulares se emplearon técnicas de resonancia magnética nuclear (RMN) siguiendo el protocolo descrito en Bradley *et al*., 2010. La determinación de niveles de ATP se llevó a cabo según lo descrito en Saha *et al*., 2004. Para los experimentos in vivo se utilizaron ratones "desnudos" a los que se inyectó de manera subcutánea células de la línea MDA-MB-231 y cuando los tumores alcanzaron un volumen entre 150-200 mm^3 recibieron un tratamiento intraperitoneal con diferentes drogas. Todos los análisis estadísticos fueron realizados con Prism 5 (GraphPad).

Para la búsqueda masiva de compuestos que inducen muerte mitótica y su posterior análisis más detallado se emplearon los mismos protocolos descritos al inicio de este apartado.

Resultados

1. Rutas de muerte en mitosis

Haciendo uso de estas células *Cdc20*(lox/lox) RERT(+/Cre) y al mismo tiempo en células humanas bloqueadas en mitosis por inhibición del APC/C hemos mostrado que la eliminación de factores pro-supervivencia de la familia Bcl-2 resulta en una reducción dramática de la supervivencia. Estos resultados están en concordancia con datos recientes que sugieren la relevancia de estos factores en mitosis (Huang *et al.,* 2009; Inuzuka *et al.,* 2011; Topham and Taylor, 2013; Wertz *et al.,* 2011). La vía intrínseca mitocondrial de apoptosis requiere la formación del poro mitocondrial por dimerización de Bak y Bax que precede a la liberación de citocromo c y otros factores pro-apoptóticos y a la activación de caspasas. El hecho de que las células deficientes en Bax/Bak mueran principalmente por necrosis y autofagia durante bloqueo mitótico prolongado, sugiere que otras formas de muerte celular, además de apoptosis, pueden colaborar en la muerte celular en mitosis (MCM). De hecho, observamos características morfológicas de necrosis durante mitosis, aunque este tipo de muerte parece ser independiente de RIPK1 y RIPK3 y por tanto no se trata de un proceso necrótico programado o necroptosis. Sorprendentemente, hemos identificado a la autofagia como una ruta de gran importancia en el control de muerte durante mitosis. Aunque tradicionalmente se asume que los procesos de autofagia no suceden durante esta fase del ciclo celular (Eskelinen *et al*., 2002; Furuya *et al.,* 2012; Tasdemir *et al.,* 2007; Tasdemir *et al.,* 2008), en este trabajo hemos demostrado que la autofagia permanece durante mitosis. Se trata de una macro-autofagia dinámica y progresiva, que se induce de forma masiva a tiempos tardíos (24 horas) de arresto mitótico. Esta autofagia puede ser potenciada mediante el uso de inhibidores de mTOR y coopera con la apoptosis en muerte celular en mitosis.

La formación del huso mitótico y segregación cromosómica requiere una correcta actividad mitocondrial. Se podría decir que la fosforilación oxidativa es la principal fuente de ATP en mitosis y que es esencial para la transición G2/M. De hecho, recientemente ha sido demostrado que Cdk1 es requerida para fosforilar y activar varios componentes del complejo I mitocondrial, lo que lleva a un aumento de la respiración mitocondrial durante G2/M (Wang et al., 2014). Por el contrario, la inhibición de Cdk1 da lugar a una disminución en la actividad mitocondrial (Wang et al., 2014) acompañada de caída de la respiración y reducción en los niveles de ATP disponibles. Durante un bloqueo mitótico prolongado, hemos observado una

caída en la masa mitocondrial, que se hace evidente después de varias horas de arresto en mitosis y que inicialmente se debe a la falta de renovación de orgánulos durante mitosis. Esta caída en masa mitocondrial se ve potenciada por la presencia de mitofagia, un proceso activo de autofagia especialmente dirigido a la eliminación de mitocondrias dañadas y que suponen un daño potencial para la célula (Okamoto, 2014; Youle and Narendra, 2011). El balance entre biogenesis mitocondrial y mitofagia determina la cantidad de mitocondrias sanas presentes en la célula. La reducción en biogenesis se debe probablemente a la reducida transcripción y traducción en células mitóticas que perpetua la disfunción mitocondrial y es la causa de la reducción en los niveles de ATP durante arresto mitótico. La integridad mitocondrial puede tratarse del límite en cuanto a supervivencia celular ya que juega un papel fundamental en regulación de metabolismo y muerte celular.

La pérdida de respiración mitocondrial conduce a una caída en la producción de ATP (y consecuente aumento en los niveles de AMP) lo que origina una crisis energética desencadenante de la activación de AMPK, el sensor bioenergético de la célula. Paralelamente a la reducción en fosforilación oxidativa hemos observado un aumento en el consumo de glucosa. Este aumento del consumo de glucosa y de glicólisis se debe a la regulación que ejerce AMPK sobre PFKFB3. PFKFB3 (también conocida como PFK-2) es una enzima clave en la regulación del flujo glicolítico, ya que modula la actividad PFK-1 que cataliza un punto primario de control de glicólisis. PFK-1 cataliza la conversión de fructosa-6-fosfato (F6P) a fructosa 1,6-bifosfato (F1, 6BP), una reacción limitante e irreversible en la ruta que establece la velocidad del flujo glicolítico y aparece frecuente hiperactivada en cáncer (Bando *et al*., 2010). AMPK fosforila y activa PFKFB3 en el residuo ser-461 que experimenta un incremento en la velocidad máxima de la reacción kinasa y disminución de la actividad fosfatasa, lo que da lugar a un incremento en la producción de Fru-6-P (Marsin *et al*., 2002; Novellasdemunt *et al*., 2012) que en consecuencia aumenta la actividad PFK-1 y la glicólisis. PFKFB3 se expresa en células transformadas y tumores (Almeida *et a*l., 2010; Bando *et al*., 2005; Calvo *et al.,* 2006; Chesney *et al*., 1999; Duran *et al.,* 2008; Kesseler *et al.,* 2008; Novellasdemunt *et al*., 2006; Riera *et al.,* 2020; Yalcin *et a*l., 2009) y se ha relacionado a esta proteína con el efecto Warburg (Marsin *et al*., 2002; Bando H *et al*. 2005). PFKFB3 es nuclear durante interfase, mientras que la de AMPK es predominantemente citoplasmática (Tsou *et al*., 2011). En mitosis, esta interacción se ve favorecida, ya que la rotura de la envuelta nuclear resulta en la combinación de los compartimentos núcleo y citoplasma. La inhibición genética y el uso de inhibidores químicos de ambos AMPK y PFKFB3 da lugar a una reducción de la supervivencia en mitosis. Similarmente, la adición de glucosa al medio de cultivo de células mitóticas retrasa su muerte. Por tanto la inducción de la ruta glicolítica durante el bloqueo mitótico se trata de un mecanismo que contribuye a la supervivencia celular.

2. Compuestos anti-mitóticos

En la segunda parte de esta tesis doctoral nos hemos centrado en la búsqueda de compuestos que reduzcan, específicamente, la viabilidad en células mitóticas; es decir, compuestos que induzcan muerte celular en mitosis. Para ello, hemos usado de nuevo como modelo de estudio los fibroblastos embrionarios de ratón del modelo de eliminación condicional para Cdc20 y hemos testado una librería de 300 compuestos, en su habilidad para matar específicamente células en mitosis.

Este estudio nos ha permitido identificar la kinasa Haspin como una potencial diana anti-mitótica. Haspin se considera una kinasa atípica encargada de la fosforilación mitótica de la histona 3 en la treonina-3, que actúa como un sitio de anclaje para complejo pasajero cromosómico (formado por survivina, Aurora B, borealina e INCENP) (Cuny *et al*., 2012). En células deficientes en Cdc20, la inhibición de Haspin potencia la muerte celular, mientras que la inhibición de Haspin en cultivos asíncronos conduce a una parada mitótica transitoria y muerte en mitosis, de acuerdo con datos previos (Dai J *et al*., 2005; Niedzialdhowska *et al*., 2012; Wang et al., 2011). Los inhibidores de Haspin son capaces de producir una parada mitótica más prolongada que el taxol y al mismo tiempo son más. Esta parada en mitosis parece ser dependiente de la

actividad del punto de control mitótico, ya que tratamiento con reversina, un inhibidor de Mps1, la actividad kinasa del punto de control, es capaz de rescatar la duración normal de mitosis. Sin embargo, recienetemente ha sido publicado que, la inhibición de Haspin puede inhibir la actividad del punto de control mitótico (De Antoni et al., Wang et al., 2010).

Discusión

1. Rutas de muerte celular en mitosis

Estos datos son de gran relevancia en la terapia anti-tumoral ya que establecen que la inhibición de las rutas que mantienen supervivencia en mitosis o la inducción de rutas de muerte favorecen la muerte celular en mitosis antes de que tenga lugar el escape mitótico. Este hallazgo puede ayudar a prevenir la acumulación de células aneuploides y aumentar la eficacia terapéutica de estas drogas. La combinación entre venenos de microtúbulos e inductores de apoptosis ha sido extensamente estudiada (Inuzuka *et al*., 2011; Oltersdorf *et al*., 2005; Topham and Taylor, 2013; Wertz *et al*., 2011) y son de particular interés en escenarios concretos, por ejemplo en tumores que sobreexpresan Bcl-2 (Oakes *et al.,* 2011). Del mismo modo, las combinaciones de taxol e inhibidores de mTOR o inhibibores de enzimas involucradas en el metabolismo han sido ampliamente probados en modelos murinos de xenotransplantes (Campone *et al*., 2009; Lieber *et al.,* 2011; Meier *et al*., 2009). Sin embargo, en este estudio mostramos por primera vez las bases moleculares de este efecto sinergístico. En conjunto estos datos proporcionan las bases moleculares para nuevas terapias combinadas dirigidas contra el ciclo celular, rutas de muerte celular y metabolismo en cáncer.

2. Compuestos anti-mitóticos

Parece lógico pensar que la inhibición de Haspin produzca el mismo resultado que la inhibición de Aurora B, ya que puede resultar en deslocalización del complejo pasajero cromosómico, y en consecuencia la deficiente activación de Aurora B. Sin embargo, la eliminación genética de Aurora B en fibroblastos embrionarios de ratón, así como el uso de inhibidores de Aurora B, resulta en una mitosis más corta que en fibroblastos control que es consecuencia de la inactivación prematura del punto de control mitótico, es decir, el resultado opuesto. Survivin, por su habilidad de prevenir apoptosis por inhibición directa de caspasas (Chan et al., 2012), parece ser un buen candidato para explicar la reducida supervivencia en mitosis tras inhibición de Haspin. De hecho, el silenciamiento de Survivin reduce la supervivencia en mitosis. Aunque es algo que necesita ser estudiado en profundidad, la inhibición de Haspin en tumores que sobreexpresan Survivin podría ser beneficioso como terapia anti-tumoral.

Contents

Abbreviations

4-OHT	4-hydroxy-tamoxifen
Ab	Antibody
AMP	Adenosine monophosphate
APC/C	Anaphase Promoting Complex/Cyclosome
ATP	Adenosine triphosphate
C3A	Active caspase 3
Cdk	Cyclin-dependent kinase
cKO	conditional Knock out
Cre	Cre-recombinase
CsA	Cyclosporyn A
Ctrl	Control
DAPI	4´, 6-diamidino-2-phenylindole
DMEM	Dubelcco´s Modified Eagle´s Medium
DMSO	Dimetil sulfoxide
DOM	Duration of mitosis
DTT	Ditriotreitol
EDTA	Ethylenediaminetetraacetic acid
EGTA	Ethyleneglycoltetraacetic acid
FBS	Fetal Bovine Serum
FRET	Fluorescence resonante energy transfer
GFP	Green fluorescence protein
H2B	Histone 2B
HTM	High-throughput miccrscopy
I	Interphase
IF	Inmunofluorescence
IHC	Inmunohistochemistry
KD	Knock down
KO	Knock out
LDH	Lactate dehydrogenase
MCC	MItotic Checkpoint Complex
MEFs	Mouse Embryonic Fibroblast
M	Mitosis
NE	Nuclear envelope
NEBD	Nuclear Envelope Break-down
NMR	Nuclear Magnetic Resonance
OA	Okadaic acid
OXPHOS	Oxidative Phosphorylation
PCR	polymerase chain reaction
pH3	phosphorylated Histone 3
Plk1	Polo-like-kinase 1
PP1	Protein Phosphatase 1
PP2A	Protein Phosphatase 2A
pRb	Retoniblastoma protein
RT	Room Temperature
SAC	Spindle Assembly Checkpoint
SCF	Skp1/Cullin /F-box protein complex
Scr	Scramble
SD	Standart Deviation
SDS-PAGE	sodium dodecyl sulfate polyacrylamide gel electrophoresis
SEM	Standart Error of the Mean

siRNA	small-interference RNA
TBS	Tris Buffer Saline
TCA	Tricarboxylyc Cicle Acid
TMSP	Sodium 3-Trimethylsilylpropionate
WT	Wild Type

Introduction

1. The mammalian cell cycle

Cell division requires two major sequential steps: duplication of the genome, achieved during S-phase (or DNA synthesis phase), and chromosome segregation of newly replicated genomes into two daughter cells a process known as mitosis (M-phase; Figure 1). Two gap phases alternate: G2 in between S and the M-phase and G1 in between M and the S-phase of the subsequent cell cycle. Upon unfavorable conditions, cells enter a resting state known as G_0 or quiescence, a stage in which the majority of the cells in adult tissues are when they reach maturity. The three previous steps to M-phase are grouped and termed as interphase.

Cell-cycle progression is based on highly ordered events forming a dependent sequence. If an early event is blocked, then usually none of the following events takes place, and a complex system of control at different levels allows the activation of each process at the right time in an ordered and irreversible way. Molecular basis of this mechanism of control relies in the activity of a family of cyclin-dependent protein kinases (Cdks) (Hartwell and Weinnert, 1989; Hunt, 1989; Hunt, 2001; Nurse, 1990; Nurse, 1994) that activates or inactivates target proteins to coordinate entry into the next phase of the cell cycle. Cdks are inactive in the absence of a partner cyclin, which form the regulatory subunits, and Cdks the catalytic subunits of an activated heterodimer. Different cyclin-Cdk combinations determine the downstream proteins targeted. Whereas Cdks levels remain constant throughout the cell cycle cyclins are synthesized and degraded at specific stages of the cell cycle. Proper progression through the cell cycle also depends on the timely phosphorylation-dephosphorylation, which may influence positively or negatively Cdks activity. Cdk2 phosphorylation at Thr-160 activates, whereas Cdk1 phosphorylation at Thr-14 and Tyr-15 inhibits Cdk1 activity (Gu *et al*., 1992; Lindqvist *et al.,* 2009). The rise and fall of Cdks activity is also regulated by binding of Cdks inhibitor proteins, named CKI. CKI are grouped in two molecular families: INK4 whose four members ($p16^{INK4a}$, $p15^{INK4b}$, $p18^{INK4c}$, $p19^{INK4d}$) exclusively bind to and inhibit the D-type cyclin-dependent kinases (Cdk4 and Cdk6), and the CIP/KIP family, whose three members ($p21^{CIP1/WAF1}$, $p27^{KIP1}$, $p57^{KIP2}$) are able to inhibit the activity of all Cdks (Sherr and Roberts, 1999). Expression of any of the CKIs results in growth arrest in the G1 phase and prevents entry into the DNA synthetic phase (Sherr and Roberts, 1999). The expression of cell cycle regulators is also controlled at the transcriptional level during early phases. Growth arrest is accomplished by repression of the E2F transcription factors by pRb binding, which are required for the transcriptional activation of genes necessary for DNA synthesis (Dyson, 1998). Mitogenic signals induce cyclins D expression that binds and activate Cdk4 and Cdk6 (Malumbres and Pellicer, 1998), which in turn phosphorylates pRb promoting its dissociation from E2F that is now able to induce the expression of essential proteins for cell cycle regulation.

In addition, Cdks activity is regulated by proteolysis: ubiquitin ligases recognize cyclins at specific points of the cell cycle and target them for proteasome degradation. The major proteolytic activities are the SCF (Skp1/Cullin/F-box), which controls G1/S through G2/M transitions and the Anaphase-promoting complex (APC/C) (Acquaviva and Pines, 2006; Cardozo and Pagano, 2004; Harper *et al*., 2002; King *et al.,* 1996; Peters, 2006) that is responsible for targeting critical regulators for degradation during mitosis and G1 until its activity is inhibited at the G1/S transition. The SCF complex participates in the ubiquitylation of cyclins D, E, A, and some Cdks inhibitors (CKIs) during G1 and S-phases, whereas the APC/C ubiquitylates cyclins A and B during mitosis.

In summary, progression through the cell cycle is subject to several mechanisms of control at different levels in order to ensure a unidirectional sequence of events that follows each other. This complex system of control has the ability to delay progression into the subsequent phase when a defect has been detected providing of extra time for error correction and avoidance of damage accumulation. Hartwell and Weinert introduced this concept as 'checkpoints' in 1989. Checkpoint pathways are the mechanism by which an uncompleted cell cycle event sends an inhibitory signal to later events stopping progression. The eukaryotic cell cycle is guarded by at least by three checkpoints: at the G1/S boundary (G1 checkpoint), the G2/M boundary (G2 or DNA damage checkpoint), and the metaphase/anaphase boundary (mitotic or spindle assembly checkpoint; SAC).

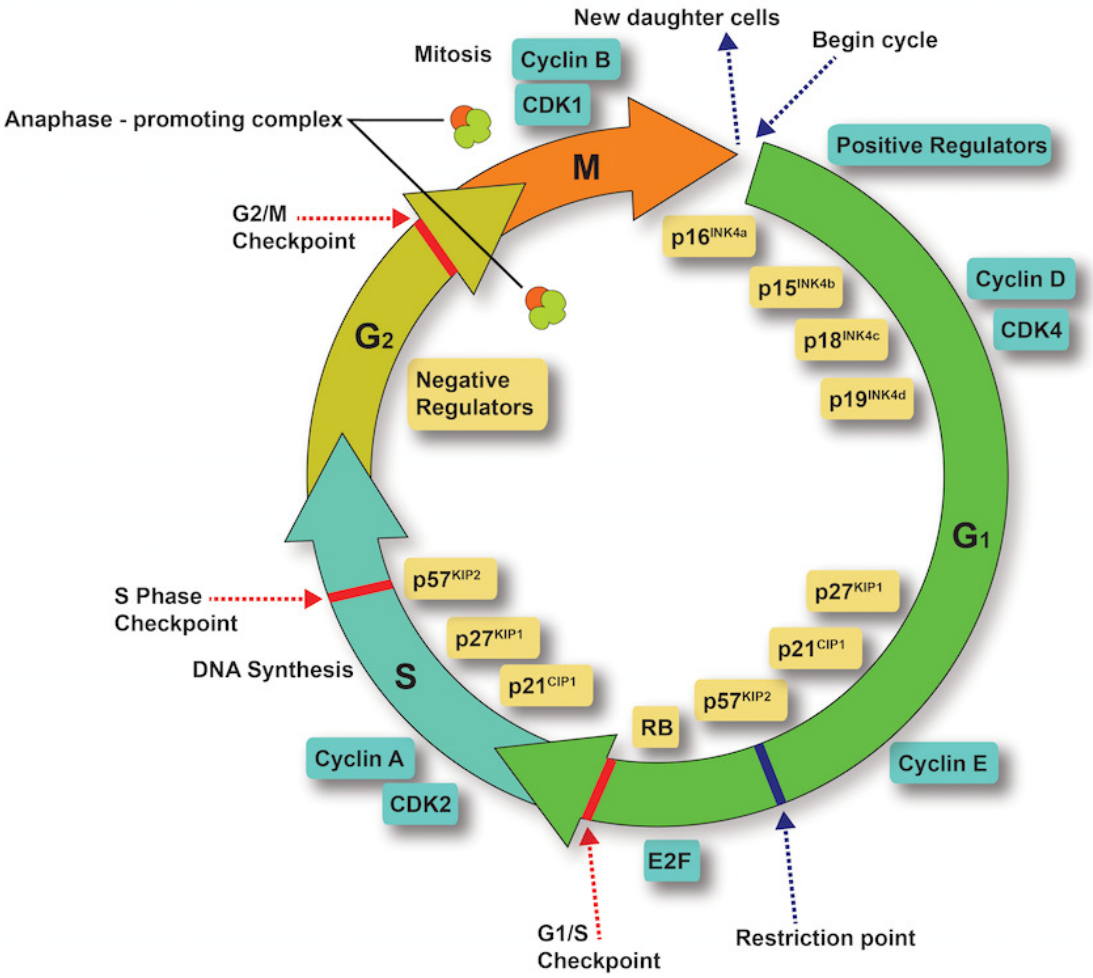

Figure 1. The cell division cycle. Interphase consists on three phases: G1, S and G2 phases. During S-phase cell duplicate their genome that will be distributed giving rise to two complete daughter cells. G1 and G2 are the interval in between M-S and M-S respectively. These two gap phases are of relevant importance because provide time for growing and the accumulation of cellular components and organelles that afterward will distribute between the two daughter cells. When extracellular conditions are unfavorable cells can enter a resting state named G0. Most cells in adults are in a quiescent state that resembles G0 that in some cases can be bypassed upon mitogenic signals. Cell cycle progression is regulated by several checkpoints pointed out by arrows; G1 checkpoint, G2 checkpoint or DNA damage checkpoint and the mitotic checkpoint or SAC. (Adapted from Kong et al., 2010). Cdks are inactive in the absence of a partner cyclin and different cyclin-Cdk combinations determine the downstream proteins targeted. Whereas Cdks levels remain constant throughout the cell cycle cyclins are synthesized and degraded at specific stages of the cell cycle. The rise and fall of Cdks activity is also regulated by binding of Cdks inhibitor proteins: INK4 whose four members ($p16^{INK4a}$, $p15^{INK4b}$, $p18^{INK4c}$, $p19^{INK4d}$) exclusively bind to and inhibit the D-type cyclin-dependent kinases (Cdk4 and Cdk6), and the CIP/KIP family, whose three members ($p21^{CIP1/WAF1}$, $p27^{KIP1}$, $p57^{KIP2}$) are able to inhibit the activity of all Cdks. The expression of cell cycle regulators is also controlled at the transcriptional level during early phases: repression of the E2F transcription factors by pRb binding, which are required for the transcriptional activation of genes necessary for DNA synthesis. In addition, Cdks activity is regulated by proteolysis: ubiquitin ligases recognize cyclins at specific points of the cell cycle and target them for proteasome degradation. APC/C ubiquitylates cyclins A and B during mitosis.

2. Mitosis

Mitosis is the last step of the mammalian cell cycle, by which the genetic material is equally distributed into two daughter cells. Cells undergo dramatic changes in structure at the transition from interphase to mitosis; despite being the shortest phase of the cell cycle it orchestrates major changes in multiple cellular components. This extraordinary conversion is required to successfully divide the entire cellular content to generate two viable daughter cells, each one containing an identical copy of the entire genome. The overall

changes need to be carefully controlled because a failure in cell division can lead to unequal segregation of chromosomes and genetic imbalance. Multiple kinases contribute to the transition into mitosis by phosphorylation of a large number of substrates (Dephoure *et al*., 2008) (Figure 1). The activity of these kinases induce cell rounding, chromosome condensation, nuclear envelope breakdown, organelle fragmentation, and spindle assembly, that is, turn the cell into a mitotic state consisting on 5 sequential phases: prophase, prometaphase, metaphase, anaphase and telophase (Figure 2). During prophase chromosomes start to condense, which is usually accompanied by the formation of microtubule asters around centrosomes and centromere separation. Microtubule dynamics results in the formation of the mitotic spindle, nuclear pores start to disassembly, followed by nuclear lamina depolimeryzation. NEBD (nuclear envelope breakdown) indicates the advent of prometaphase (Álvarez-Fernández and Malumbres, 2014; Guttinger *et al*., 2009). In this phase microtubules bind to kinetochores and metaphase is marked by the attachment and alignment of the chromosomes at the metaphase plate. Upon anaphase onset, sister chromatids separate towards the spindle poles, and during telophase chromosomes decondense giving rise to two identical daughter nuclei, in parallel cytokinesis begins, resulting in separation of cytoplasm and cell division.

Nuclear and cytoplasmic compartments, which were separated during interphase, upon mitotic onset mix their content resulting in a dilution of nuclear and cytoplasmic activities, changes in stoichiometry of different enzymatic complexes or dissipation of the molecular gradients from nuclei to cytoplasm, which might affect the molecular environment of the cell, specifically its phosphorylation status that condition some enzymatic activities (Álvarez-Fernández and Malumbres, 2014). The Cdk1-cyclin B1 complex, through its cytoplasmic, nuclear and centrosomal localization, synchronize multiple of these different events during mitotic entry (Hunt 1989 and Nurse, 1990; Takizawa and Morgan, 2000). The microtubule spindle binds to condensed chromosomes, Golgi membranes clusters are divided into individual stacks (Lowe *et al*., 2000), nuclear envelope membranes are retracted into the ER (endoplasmic reticulum) and mitochondria are fragmented through the Cdk1-dependent phosphorylation of Drp1, the dynein responsible for mitochondrial fission (Taguchi *et al.,* 2007). All these processes take place in an average time of an hour, in physiological conditions, and in the almost complete absence of protein synthesis. At this stage transcription is strongly suppressed and mitotic entry, as well as G_0, results in a global down regulation by as much as 60 to 80% of cap-dependent mRNA translation (Stumpf *et al*., 20013). However, allowed by mTORC1 activity, some levels of mRNA translation of protein needed for maintain the mitotic state, such as cyclin B, are sustained during mitosis (Quin, *et al*., 2004; Siva, *et al*., 2008).

The activation of the mitotic kinases is closely orchestrated through feedback and feed-forward loops in the mitotic entry network (Lindqvist *et al*., 2009). Cdk1-cyclin B1 complex is considered as the central component of the mitotic entry network that phosphorylates hundreds of proteins. Cdk1-dependent phosphorylation is an important determinant of the mitotic state, given that a large fraction of the mitotic phosphorylation occurs on Cdk1 consensus motifs and inhibition of Cdk1 activity forces cells to exit mitosis. In addition to Cdk1 activation, other kinases play an important role either in mitotic entry, progression through this phase or participating in additional levels of regulation of Cdk1 activity. Among this mitotic kinases are the Polo and Aurora family of kinases (Figure 1). Polo kinase family consists of five members being Plk1 (Polo-like-kinase-1) the more extensively characterized. In the G2/M transition Plk1 promotes centrosome maturation (Lane and Nigg, 1996) and activates the transcription factor FoxM1, which enhances the transcription of some genes necessary for mitotic entry such as cyclin B, Plk1 and the phosphatase Cdc25 (Fu *et al*., 2008). Plk1 also participates in the activation of Cdk1 through inhibition of Wee1 and Myt1, negative regulators of Cdk1 (Nakajima *et al.,* 2003; Watanabe *et al*., 2004). It also phosphorylates the regulatory subunit of Cdk1-cyclin B complex (Toyoshima-Morimoto *et al*., 2001). And moreover is involved in cytokinesis (Lens *et al*., 2010). Among the Aurora family of kinases, Aurora A is also involved in centrosome maturation, mitotic spindle formation and Cdk1 activation through phosphorylation and Cdc25b activation (Barr and Gerley 2007; Dutertre *et al*., 2004; Lens *et al*., 2010; Malumbres, 2011). In late G2 Aurora B phosphorylates histone H3 at Ser-10, which is involved in chromosome condensation and is a hallmark of mitosis. Aurora B, in association with inner centromere protein (INCENP), Borealin and Survivin forms the

chromosomal passenger complex (CPC), which regulates proper kinetochore-microtubule attachment and cytokinesis (Carmena *et al.,* 2012). Haspin phosphorylation of histone H3 at threonine 3 (H3T3ph) during mitosis promotes CPC components localization on mitotic chromatin, particularly at the centromere, which positions and activates Aurora B, leading to the downstream phosphorylation of a variety of substrates (De Antoni *et al.,* 2012; Kelly *et al*., 2010; Wang *et al*., 2011) to ensure chromatin cohesion, metaphase alignment and normal progression through the cell cycle. Dephosphorylation of H3T3ph at the exit from M phase is required for proper chromosome decondensation and nuclear envelope formation (Kelly *et al.,* 2010). Another family of kinases essential for mitosis is Nek kinases (NIMA-related kinases), which consist on 11 proteins, being Nek2 the most extensively characterized. Nek2 is involved in modulation and maintenance of centrosome. Some studies suggest that Nek2 activity regulates duplicated centrosomes separation upon mitotic onset by phosphorylation of centriolar proteins (Fry *et al*., 1998). The activity of all these mitotic kinases contributes to the phosphorylation of a wide spectrum of proteins involved in the necessary rearrangement that accompany mitosis

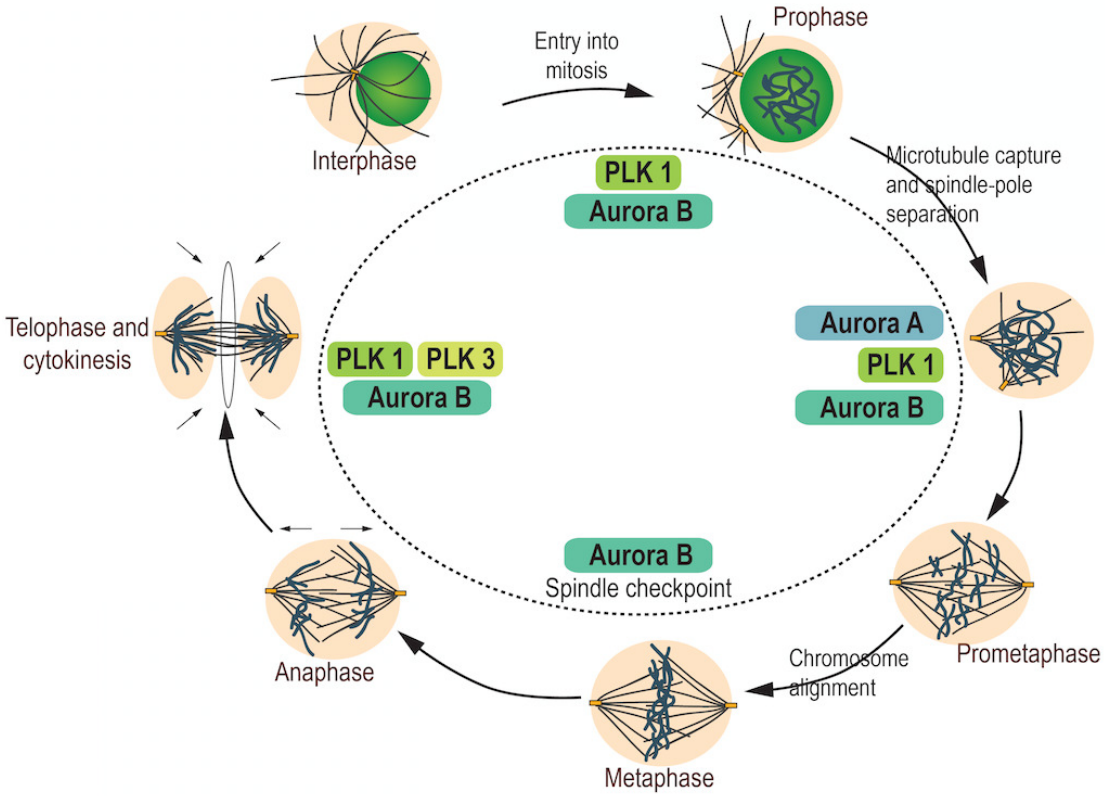

Figure 2. Phases of mitosis. Mitosis consits on 5 sequential phases: prophase, prometaphase, metaphase, anaphase and telophase. Chromosomes condensation and microtubule aster formation starts in prophase. Bipolar microtubule spindle is formed in prometaphase but is in metaphase when microtubules are perfectly attached to chromosome kinetochores at the metaphase plate. Upon anaphase onset sister chromatids separate followed by chromosome decondensation during telophase, giving rise to two genetically identical daughter cells. In addition to Cdk1, Polo and Aurora kinases family are also involved in mitotic entry and progression or participating in additional levels of regulation of Cdk1 activity. In the G2/M transition Plk1 promotes centrosome maturation and is involved in cytokinesis. Aurora B in association with INCENP, Borealin and Survivin forms the CPC which regulates proper kinetochore-microtubule attachment and cytokinesis. And Aurora A is involved in mitotic spindle formation during prometaphase.

3. The Anaphase-promoting complex/Cyclosome (APC/C)

The APC/C was discovered by Avram Heshko and Marc Kirschner and is composed of roughly a dozen subunits, measures a massive 1.5 MDa being the most complex ubiquitin ligase discovered so far. It

was first characterized as the machinery needed for cyclins degradation upon exit from mitosis and the factor responsible for their cyclic expression pattern (Glotzer *et al*., 1991; Sudakin *et al*., 1995). This discovery was based on biochemical purification by the Hershko group who called it cyclosome, as well as identification by the Kirschner group of vertebrate homologues of yeast cell cycle mutants genes, previously isolated by Lee Hartwell and colleagues in the early 1970s, who termed it APC (anaphase-promoting complex). The term APC has been taken already for other proteins in the cell, so the current terminology is APC/C to properly acknowledge these early discoveries (Peters, 2006). The APC/C is an unusual complex multi-subunit E3 ubiquitin ligase, that mediates the ubiquitylation of a broad array of mitotic regulatory proteins for its later degradation by the 26S proteasome (Peters, 2006; Thornton and Toczyski, 2006). The APC/C controls the cell cycle processes responsible for chromatid segregation at the metaphase to anaphase transition, the completion of mitosis, and the establishment and maintenance of G1. APC/C activity depends on the interaction with specific proteins known as co-activators. The best studied are the mitotic Cdc20/Fizzy and Cdh1/Hct1/Fizzy-related cofactors, which confer specificity for the substrate (Peters, 2006; Sullivan and Morgan, 2007).

Throughout S- and G2-phases the APC/C remains inactive by binding of Emi1, which is degraded upon mitotic entry by another ubiquitin ligase: the SCF (Skp1/cullin/F-box)–β –TrCP (β -transducin repeat-containing protein. Phosphorylation of many of the APC/C subunits upon mitotic onset by by Cdk-cyclin B and Plk1 (Golan *et al*., 2002) is a prerequisite for the binding of the substrate-specific cofactor Cdc20. On the contrary, the interaction APC/C-Cdh1 does not depends on the phosphorylation of APC/C subunits. Cdh1 activates the APC/C at the final phases of mitosis and G1 (Peters, 2006), while earlier in mitosis Cdh1 is phosphorylated and inhibited. Cdk2 (cyclin-dependent kinase 2) and Cdk1 are the kinases responsible for Cdh1 phosphorylation during G2, S-phase and mitotic entry, impeding its interaction with APC/C until late stages of mitosis. When cyclin B is degraded and Cdk1 activity levels fall (Blanco *et al*., 2000; Zachariae *et al*., 1998) this phosphorylation is reversed by Cdc14 phosphatase (Wurzenberger and Gerlich, 2011). Dephosphorylated Cdh1 is now ready to replace Cdc20 as co-factor of APC/C, one of the first actions of the newly formed APC/C-Cdh1 is to degrade its predecessor Cdc20. Both co-factors participates in the recognition of those substrates that are going to be ubiquitylated by the APC/C through the WD40 domain at the C-terminal, which allows specific interactions with D-box, A-box or O-box domains (Araki *et al*., 2005; Fang *et al*, 1998; Littlepage *et al*., 2002; Pfleger and Kirschner, 2000).

3.1 Relevance of APC/C-Cdc20 in mitotic exit

Cdc20 was identified for the first time in 1973 by Lee Hartwell as a mutant strain of *Saccharomyces cerevisae*, which results in a permanent mitotic arrest (Hartwell *et al*., 1973). Cdc20 is expressed during S-phase, G2 and mitosis. However it can only bind to the APC/C when various subunits of this complex have been phosphorylated by mitotic kinases (Kramer *et al*., 2000). APC/C-Cdc20 activity is regulated by several mechanisms, being the most important the spindle assembly checkpoint (SAC; Figure 3).

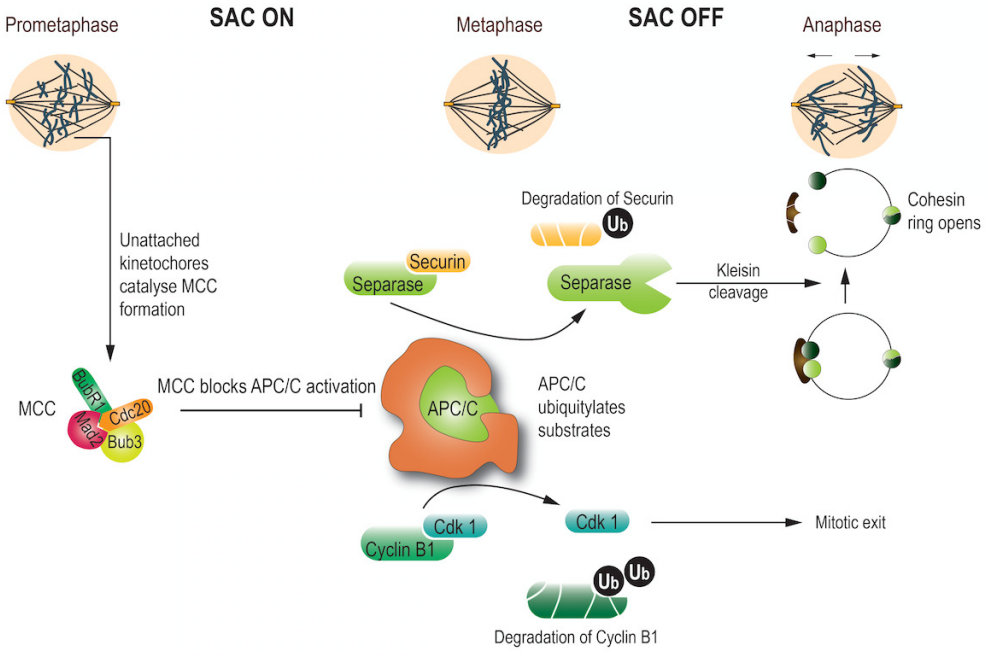

Figure 3. The role of the APC/C during mitosis. Once kinetochores are attached to microtubule spindle, the SAC is satisfied and the releasing from its inhibition the APC/C-Cdc20 complex. APC/C-Cdc20 targets cyclin B and securin for degradation by ubiquitylation. Securin degradation leads to the activation of separase and the subsequent separation of the sister chromatids.

For cells to segregate their genome, each chromosome must be attached in a bioriented manner to the mitotic spindle. The SAC monitors this attachment and in this way contributes to the fidelity of chromosome segregation and ensures that daughter cells inherit a complete copy of the genome, avoiding the generation of aneuploidy cells. The SAC negatively regulates the ability of Cdc20 to activate the APC/C, delaying anaphase onset until every chromosome is perfectly attached to microtubule spindle (Mussachio and Salmon, 2007). Unattached kinetochores in prometaphase activate the SAC by triggering a biochemical cascade that inhibits the APC/C, how exactly this signaling is performed is still controversial. The mitotic checkpoint complex (MCC) has emerged as the possible SAC effector (Varetti and Musscahio, 2008). The MCC contains three SAC proteins: Mad2, BubR1/Mad3 and Bub3, as well as Cdc20 (Musacchio and Salmon, 2007). This multiprotein complex binds the APC/C as a pseudosubstrate inhibitor (Burton and Solomon, 2007) impeding its catalytic activity and delaying the onset of the anaphase.

Several independent studies converge in proposing a model in which MCC complex formation is triggered by specific interactions between Mad1 and Mad2 at the level of the kinetochores that are not bound to the spindle. When bound to Mad1, Mad2 suffers a conformational change, adopting a conformation known as close-Mad2 (C-Mad2) (De Antoni *et al.,* 2005; Kulukian *et al*., 2009; Simonetta *et al*., 2009). This conformational change of Mad2 is needed to promote the formation of a complex with Cdc20 and BubR1 (Mussachio and Salmon, 2007). According to this model, the APC/C is kept inactive because Cdc20 has been hijacked by the MCC and also because the MCC binds APC/C through Cdc20. However the majority of the cellular Cdc20 pool is not forming a complex with Mad2 and it has been also shown that Cdc20 undergoes continuous ubiquitin-dependent degradation, and it is continuously resynthesized during mitotic arrest, in a manner that involves polyubiquitylation by the APC/C (Ge *et al*., 2009; Nilsson *et al*., 2008). In this model Mad2 catalyzes the interaction between Cdc20 and BubR1, which presents Cdc20 to the APC/C. It is believed that this SAC-mediated degradation of Cdc20 keeps Cdc20 levels bellow a threshold, which would suppress its function as an APC/C co-activator.

When all kinetochores become attached to spindle microtubules and under tension, the SAC activity is rapidly switched off, MCC dissociates from the APC/C, Cdc20 is relieved from SAC proteins and serves as an

APC/C coactivator promoting mitotic exit (Howell *et al*., 2000; Rieder *et al*., 1995). As well as with the effector mechanism of the SAC, little is known about how SAC is satisfied and how its inhibitory signal is extinguished. Several studies suggest that, polyubiquitylation of Cdc20 by APC/C is the major mechanism for SAC inactivation. Mutliubiquitylation of Cdc20 allows its rapid dissociation from the complex Mad2-BubR1-Bub3 and binding to the APC/C. Whereas de-ubiquitytilating enzymes acts on Cdc20, while the SAC is still active, stabilizing the complex Cdc20-Mad2-BubR1-Bub3 (Reddy *et al.,* 2007; Stegmeier *et al*., 2007). Moreover, checkpoint antagonists, such as p31comet, are involved in SAC silencing. This mechanism is based on $p31^{comet}$ competition for binding to C-Mad2, the Mad2 conformation that binds to Cdc20. Kinetochores negatively regulate the ability of $p31^{comet}$ to bind to C-Mad2, but reactivation of $p31^{comet}$ at metaphase, when kinetochores are bound to microtubule spindle, would trigger SAC inactivation (Vink *et al.,* 2006; Xia *et al*., 2004). However there are no obvious orthologues for $p31^{comet}$ in lower eukaryotes.

APC/C-Cdc20 mediates the anaphase onset leading to mitotic exit by polyubiquitylating two key substrates, securin and cyclin B (Lim *et al.,* 1998; Shirayama *et al.,* 1999), thereby promoting its destruction by the 26S proteasome (Basserman *et al*., 2013; Peters, 2006; Skaar and Pagano, 2009;). Securin is a stoichiometric inhibitor of the protease separase/Esp1 whereas Cdk1-cyclin B directly binds and inhibits securin (Stemmann *et al*., 2011). Upon securin and cyclin B degradation, separase can cleave centromeric cohesins that keeps sister chromatids together. Concomitantly, proteolysis of cyclin B inactivates Cdk1. It was indeed demonstrated in budding yeast that Cdc20 is not essential in cells that lack both securin and Clb2, emphasizing the importance of degradation of these two substrates for metaphase and mitotic exit (Shrirayama et al 1999, Thornton and Toczyski 2003).

Cdk1 activity is the driving force for mitotic progression; its inactivation is therefore the major molecular event that triggers mitotic exit favoring the reversion of all the changes imposed by the entry into mitosis (Sigrist *et al*., 1995). Many of the mitotic phosphorylations need to be removed and phosphatases now play its role. In budding yeast, Cdc14 phosphatase promotes mitotic exit by dephosphorylating Cdk1 targets (Queralt and Uhlmann, 2008), in contrast mammalian homologs (Cdc14a, b and c) do not seem to be required for mitotic exit (Mocciaro and Shiebel, 2010). However PP1 and PP2A-B55δ, which are inactive during mitosis, are reported to be important for mitotic exit (Mochida and Hunt, 2007; Mochida et al., 2009; Wu *et al*., 2009) in *Xenopus* egg extracts. Cdk1 inhibition leads to PP1 activation by auto-dephosphorylation and inactivation of its inhibitor I1 (Wu *et al*., 2009). In addition, a recent screen has identified PP2A-B55α as a regulator of mitotic exit in human cells, involved in DNA decondensation, reorganization of the nuclear envelope among other events (Schmitz *et al*., 2010). In an independent study premature exit of mitosis has been reported as a consequence of PP2A activation induced by Mastl knockdown in human cells (Burguess *et al*., 2010). Multiple phosphatases seem to regulate mitotic exit in mammals, but how phosphatases become actives is not well known. A feasible mechanism is that phosphatases undergo auto-dephosphorylation upon Cdk1 inactivation (Wu *et al*., 2009) and other possibility to regain activity might be that different phosphatases regulate selected steps of pospho-epitopes, generating a multilevel regulation, in a dephosphorylation cascade (Medema and Linqvist, 2011). Once the Cdk1 activity ceased and phosphatases become active, the removal of the Cdh1 phosphorylated residues, results in the formation of a new APC/C-Cdh1 complex. This complex catalyzes the degradation of Aurora A and Plk1 kinases which favors mitotic exit and G1 progression.

In addition, APC/C-Cdc20 complex promotes the degradation of additional substrates such as cyclin A, Nek2A and p21 Cip1 at the mitotic onset, independently of the SAC activity (Amador et al 2001; Di Fiore and Pines; Geley et al 2001; Wolthuis et al 2008). Cdh1 is not able to compensate for the lack of Cdc20, this is not due to differences in substrate specificity because Cdh1 is also able to target securin and cyclin B for degradation, rather, this reflects the fact that Cdc20 absence arrests cells with high Cdk1 activity, and this activity is known to inhibit Cdh1 function, because it cannot be de-phosphorylated and therefore binds APC/C.

Small residual amounts of Cdc20 are sufficient to exit mitosis (Baumgarten *et al.,* 2009; Wolthuis *et al.,* 2008). Mitotic exit is likely to be efficient with as little as 5% of cellular Cdc20 (Wolthuis *et al*., 2008), giving an explanation for previous reports indicating that Cdc20 knockdown by RNAi does not result in cyclin B stabilization or mitotic arrest (Clarke *et al*., 2009). A Cdc20 conditional knockout (KO) mouse model was generated recently in our lab (Manchado *et al.,* 2010). Genetic ablation of Cdc20 results in metaphase arrest *in vivo*. Since Cdc20 is essential for anaphase onset, conditional genetic elimination of Cdc20 results in complete metaphase arrest in embryonic or somatic cells *in vivo*. In the absence of Cdc20 cells are not able to progress to anaphase and remain arrested in mitosis in the presence of condensed DNA. In this Cdc20 KO cells are arrested in mitosis with high Cdk1 activity, in the absence of cyclin A and B degradation. These cells can only be forced to exit mitosis if Mastl is depleted and Cdks activity is suppressed simultaneously by the addition of roscovitine (a Cdks inhibitor). Inhibition of PP2A or combined knockdown of B55α and B55δ in these cells, delays Cdks-substrates dephosphorylation indicating that act cooperatively to revert mitotic phosphorylations (Manchado *et al*., 2010).

4. Metabolism and the cell cycle

The regulation of metabolism and growth must be tightly coupled in order to guarantee the efficient use of energy and anabolic substrates throughout the cell cycle. The notion that the cell cycle is fundamentally linked to something, whose intracellular abundant or activity oscillates in temporal coordination with cell-cycle progression, come from the 50´s. Early evidences shows that a preparation phase, that requires efficient respiration and carbohydrate utilization in aerobic conditions, is needed prior mitosis (Swann, 1957), however, once mitosis is initiated it could proceed in the absence of new ATP production and anaphase and cytokinesis could be completed in the presence of any energy production inhibitors. In the same way, Bullough postulated, in the “energy reservoir hypothesis”, that an active production of energy is vital only during the period that immediately precedes the prophase termed as “antephase” (Bullough, 1952), however, by the time mitosis becomes recognizable, it is highly independent of external conditions. Thus, it seems that the critical importance of the active production of energy in the antephase may be related either to a demand for energy at this time, or to the necessity for energy storage in the maintenance of the cell during division (Bullough, 1952). In line with these observations, Gelfant in 1969 observed that glycolytic waves precede mitosis and claimed that the inhibition of the energy pathways during mitosis does not affect the undergoing mitosis but prevents the following mitotic entry. In agreement with this need of glucose accumulation it has been recently reported that glycogen is required for microtubule assembly in meiotic extract (Aaron *et al*., 2013). Mitosis is a phase in which several high-energy consuming processes are active, such as chromosome condensation, microtubule network organization, mitotic spindle formation (Álvarez-Fernández and Malumbres 2014; Janssen and Medema 2011; Medema and Lindqvist 2011) and a prolonged mitosis could therefore result in energy deprivation. Specific depletion of ATP pools with DNP, azide or AMP-PNO, results in a rapid prolonged mitotic arrest in mammalians cells (Burgess *et al*., 2014; Lee *et al*., 1989; Spurck *et al.,* 1987). ATP is needed for microtubule disassembly and therefore depletion of ATP stabilizes microtubules. Moreover, the depletion of ATP also depletes Mad2 and BubR1 from kinetochores, with both proteins accumulating at spindle poles, however this does not appear to affect their ability to bind Cdc20 and inhibits the APC/C (Howell *et al.,* 2000; Hoffman *et al.,* 2000; Howell *et al.,* 2001). G1/S and G2/M checkpoints are also energy-sensitive and require pronounced bioenergy supply for de novo synthesis of biomasses needed for cell-cycle phase transitions (Sweet and Singh, 1995; Sweet and Singh, 1999).

Accumulating molecular evidences suggest that mitochondrial respiration is linked with cell-cycle regulation: cyclinD1 coordinates mitochondrial biogenesis in G1 progression (Sakamaki *et al.,* 2006), cyclin E controls the formation of high energy-charged mitochondria in the G1/S transition (Mitra *et al*., 2009) and Cdk1-cyclin B1 is involved in the integration of mitochondrial fission with the onset of G2/M transition (Taguchi *et al.,* 2007). Moreover, mitochondrial metabolism cooperates with the process of cell division, a functionally efficient mitochondrial complex I in OXPHOS is required not only for overall mitochondrial respiration

(Roessler *et al*., 2010), but also for successful cell-cycle progression (Osusu-Ansah *et al*., 2008). Cdk1-cyclin B1 regulates mitochondria metabolism to coordinate G2/M progression: a fraction of Cdk1-cyclin B1, located in the matrix of mitochondria, is responsible for the phosphorylation of some components of mitochondrial complex I. This phosphorylation is responsible for the upregulation of its enzymatic activity and boost ATP generation (Wang *et al*., 2014a).

4.1 APC/C-Cdh1 and metabolism

APC/C-Cdh1 regulates the glycolysis-promoting enzyme PFKFB3 (6-phosphofructo-2-kinase/fructose-2, 6-biphosphatase isoform 3) and GLS1 (glutaminase 1), a critical enzyme in glutaminolysis. Decreased activity of APC/C-Cdh1 in mid-to-late G1 releases both proteins for being ubiquitylated and targeted for degradation, which explains the simultaneous increase in the utilization of glucose and glutamine for cell proliferation. This occurs at a time consisting with the nutrient-sensitive G1 restriction point, described as the stage in G1 beyond which cells no longer require the presence of mitogenic signals for progression along the cell cycle. PFKFB3 is also a substrate for the ubiquitin ligase SCF at the onset of S-phase. For these reasons, the activity of PFKFB3 is short lasting, coinciding with a peak in glycolysis in mid-to-late G1, whereas the activity of GLS1 remains high throughout S-phase. Both glucose and glutamine are required for progression through the restriction point, whereas only glutamine is necessary for progression through S-phase into cell division (Colombo *et al*., 2010), suggesting that glycolysis and glutaminolysis plays different roles at different stages of the cell cycle.

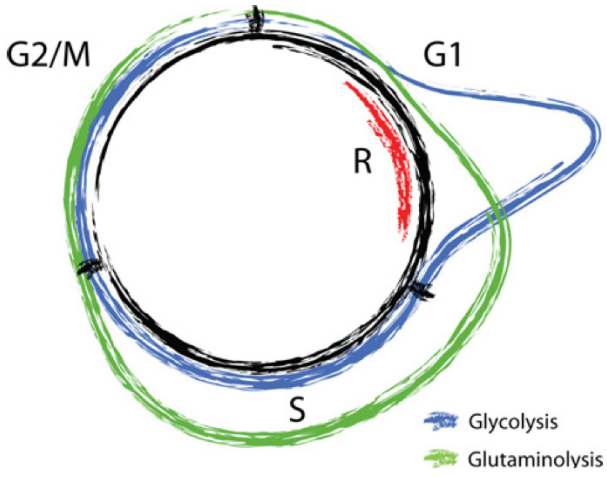

Figure 4. Levels of PFKFB3 are controlled by APC/C-Cdh1 and SCF-b-TrCP. Glycolysis peaks in late G2 due to the non-degradation of PFKFB3 by this two complexes, whereas glutaminolysis takes place late G2 till G27M transition coincident with the inactivation of APC/C-Cdh1. The R represents the restriction point beyond what a cell has committed to cycle. (Adapted from Moncada et al., 2012).

PFKFB3 (also known as PFK-2) is a key regulator of glycolytic flux by modulating PFK-1 activity, which catalyzes a primary control point of glycolysis: the conversion of fructose-6-phosphate (F6P) to fructose 1,6-biphosphate (F1, 6BP), a rate-limiting and irreversible early reaction in the pathway constituting the pacemaker of glycolysis. PFK-1 is an allosteric enzyme subjected to extensive regulation by various metabolites in the glucose metabolism pathway. Cells can increase or decrease the rate of glycolysis by controlling PFK-1 through allosteric activation or inhibition. A total of six ligand binding sites are found in PFK-1: the substrate-binding sites for ATP and F6P, activator-binding sites: for AMP and fructose-2, 6-biphosphate (F2, 6BP), and inhibitors binding sites for ATP and citrate. Binding of citrate enhances the inhibitory effect of ATP, which is inhibitor and substrate. When the tricarboxylic acid cycle (TCA cycle) is highly active, ATP and citrate accumulate, indicating an adequate supply of energy, which in turn inhibits glycolysis. However increasing evidences suggest that cancer cells may have acquired ability to evade this feedback regulation (Mor, *et al*., 2011). F2, 6BP is generated from F6P through phosphorylation by phosphofructokinase-2 (PFK-2). Increased glucose uptake and hexokinase activity (first enzyme of glycolysis) leads to elevated levels of

F6P, yielding more F2, 6BP, which represents an allosteric feedforward mechanism that enhances glycolysis when glucose is abundant. The steady-state concentration of F2,6BP depends on the enzymatic activity of PFK-2, which is a bifunctional enzyme that catalyzes either the phosphorylation of F6P to F2, 6BP (kinase activity) or the dephosphorylation of F2,6BP to F6P (phosphatase activity). The enzyme exists in multiple isoforms, sharing 85% of sequence homology, encoded by four genes termed from PFKFB1 to PFKFB4. Among them PFKFB1, PFKFB2 and PFKFB4 localize to the cytoplasm, where glycolysis takes place, whereas PFKFB3 localizes in the nuclei. Nuclear PFKFB3 did not stimulate the glycolytic flux, but its cytoplasmic mutant was able to enhance glycolytic rate (Yalcin *et al.,* 2009) suggesting the possibility for cellular compartmentalization of F2, 6BP. Depending on the stimuli there may exist a concentration gradient between nucleus and cytoplasm, so that a relative increase of F2, 6BP in the cytoplasm might activate glycolysis, whereas in the nucleus might signal cells to a more efficient use of glucose to proliferate (Yalcin *et al*., 2009). The relative functions of PFKFB3 and PFKFB4 are of particular interest because they are activated in human cancers and increased by mitogens and low oxygen.

5. Cell cycle, metabolism and cancer

5.1 Altered cell cycle and metabolism, two hallmarks of cancer

Cell cycle deregulation is a common feature of human cancers (Malumbres and Barbacid, 2001). Tumor cells accumulate mutations that results in unscheduled proliferation, genomic instability and chromosomal instability. Normal cells evolve progressively to a neoplastic state, by successive acquisition of several capabilities. Hanahan and Weinberg gather the different alterations that accompany cell transformation and define six hallmarks of cancer as acquired functional capabilities that allow cancer cells to survive, proliferate and disseminate. These functions are acquired in different tumor types via distinct mechanisms and at various times during the course of multistep tumorigenesis. The most fundamental trait of cancer cells is their ability to sustain chronic proliferation. Normal tissues carefully control the production and release of growth-promoting signals in order to ensure a homeostasis of cell number and maintenance of tissue architecture, whereas cancer cells can acquire the capability to sustain proliferative signaling and evading the anti-proliferative signals in many ways (Witsch *et al.,* 2010). Growth factor independence may also derive from the constitutive activation of components of signaling pathways operating downstream of the receptors bypassing the need to stimulate these pathways by its ligand. Somatic mutations may activate these downstream pathways resulting in constitutive signaling. Activating K-RAS mutations are frequently found in human cancers, they are common in: pancreatic cancer, colorectal cancer, lung adenocarcinoma, gall bladder cancer, bile duct cancer, and thyroid cancer. Similarly, mutations in the catalytic subunit of phosphoinositide 3-kinase (PI3K) which hyperactivate the signalling cascade including its key Akt/PKB signal transducer, are being detected in an array of tumour types (Yuang and Cantley, 2008). Acquisition of the multiple hallmarks depends in a large part on a succession of alterations in the genomes of neoplastic cells. The development of genomic instability in cancer cells enables tumorigenesis, by generating random mutations, including chromosomal rearrangements that further contribute to tumor development.

Cancer is a disease arising from genetic and epigenetic alterations in oncogenes and tumor suppressors genes, many of which are also able to reprogram metabolism. Thus, the metabolic changes occurring in cancer might be considered a secondary effect to the transformation process, however, as altered metabolism is a universal property of cancer cells, Hanahan and Weinberg have recently included the capability to reprogram cellular metabolism as a hallmark of cancer (Hanahan and Weinber, 2011). Compared to normal cells, cancer cells strongly upregulate glucose uptake and glycolysis to give rise to increased yield of intermediate glycolytic metabolites and the end product pyruvate in order to fulfill the requirements for neoplasic proliferation. Moreover, glycolysis is uncoupled from the mitochondrial tricarboxylic acid cycle (TCA) and oxidative phosphorylation (OXPHOS) in cancer cells. Consequently, the majority of glycolysis-derived pyruvate is diverted to lactate fermentation, converted to lactate in the cytoplasm by lactate

dehydrogenase (LDH) and secreted, rather from being oxidized through mitochondrial metabolism. This metabolic phenotype is known as the Warburg effect and occurs even in the presence of sufficient oxygen to support mitochondrial respiration. This metabolic phenomenon was first described by Otto Warburg in 1956 and is also referred as to aerobic glycolysis. Although human cancers display a diverse range of metabolic profiles, the Warburg metabolic phenotype is a widespread cancer-associated trait. Indeed, enhanced glucose uptake by cancer cells has become the basis for positron emission tomography (PET) with 18-fluorodeoxyglucose (FDG), which preferentially accumulates in tumor cells as a result of their rapid uptake of glucose. Several oncogenes and associated proteins such as HIF-1, RAS, C-MYC, Oct, SRC and p53 can influence energy substrate utilization by affecting cellular targets, leading to metabolic changes that favor cancer cell survival independently of the control of cell proliferation. These oncogenes stimulate the enhancement of aerobic glycolysis and at least some of them can directly target the OXPHOS machinery, i.e. RAS E1A affects early steps of tumorigenesis, increase in oxygen consumption and superoxide production, (Jose *et al.,* 2011). To which extent normal and neoplastic cells share metabolic pathways remains unknown and is of particular interest since the existence of relevant differences in the metabolic pathways of cancer and normal cells would suggest the possibility of developing therapeutic approaches that selectively interfere with cancer metabolism without side-effects related to the mechanism of action.

5.2 Mitotic targeted therapies:

Deregulated cell cycle is a common feature of cancer cells and multiple strategies have been proposed in the last few years to impair tumor cell proliferation, current efforts can be broadly divided into three different groups. Initial strategies were designed to inhibit the machinery that drives the entry into the cell cycle imposed by oncogenic signals (G1 phase) and DNA synthesis (S phase) (Malumbres, 2001). Mechanistically, inhibition of cell cycle entry (i.e., by inhibiting interphase Cdks) is likely to induce cell cycle arrest or quiescence but not apoptosis, generating viable quiescent cells. The use of small-molecule inhibitors for interphase Cdks may result in certain levels of apoptosis, although the lack of specificity of these compounds prevents any detailed molecular conclusion. Interfering with the G1/S machinery or abrogation of the DNA damage checkpoint generally prevents DNA replication (Bucher *et al*., 2008; Toledo *et al*., 2011), thus rendering diploid interphase cells that cannot proliferate but are viable. For instance, inhibition of Cdk4 prevents the development of lung tumors induced by K-Ras oncogene by triggering senescence, a permanent arrest in G_0/G1. The two first approaches are clearly based on the specific signals originated from the oncogenic stress in tumour cells. This has been far more difficult to achieve in targeted therapies directed against mitosis given the conservation in the essential mechanism that regulates chromosome segregation in normal or tumour cells.

The fragility of cancer cells when they undergo division serves as a critical point for intervention in chemotherapy (Chan *et al*., 2011). Mitosis is considered the most fragile period of the cell cycle, during which is highly susceptible to cell death when exposed to various insults. The chromosomes are in highly condensed state and not protected by the nuclear envelope, in fact it has been shown that mitotic cells have enhanced sensitivity for example to radiation treatment (Stobbe *et al*., 2002). The great success of spindle poisons in clinics and the susceptibility of cells to mitotic arrest have led in the last years to a search for improved therapeutic strategies based on specific mitotic targets (Figure 4). The discovery of centrosome and mitotic regulators that function during S phase, or M phase provided further additional targets, such as mitotic kinases or the mitotic spindle machinery, required for chromosome segregation. Thus, targeting mitosis offers several possibilities to kill cancer cells that we will discuss right after.

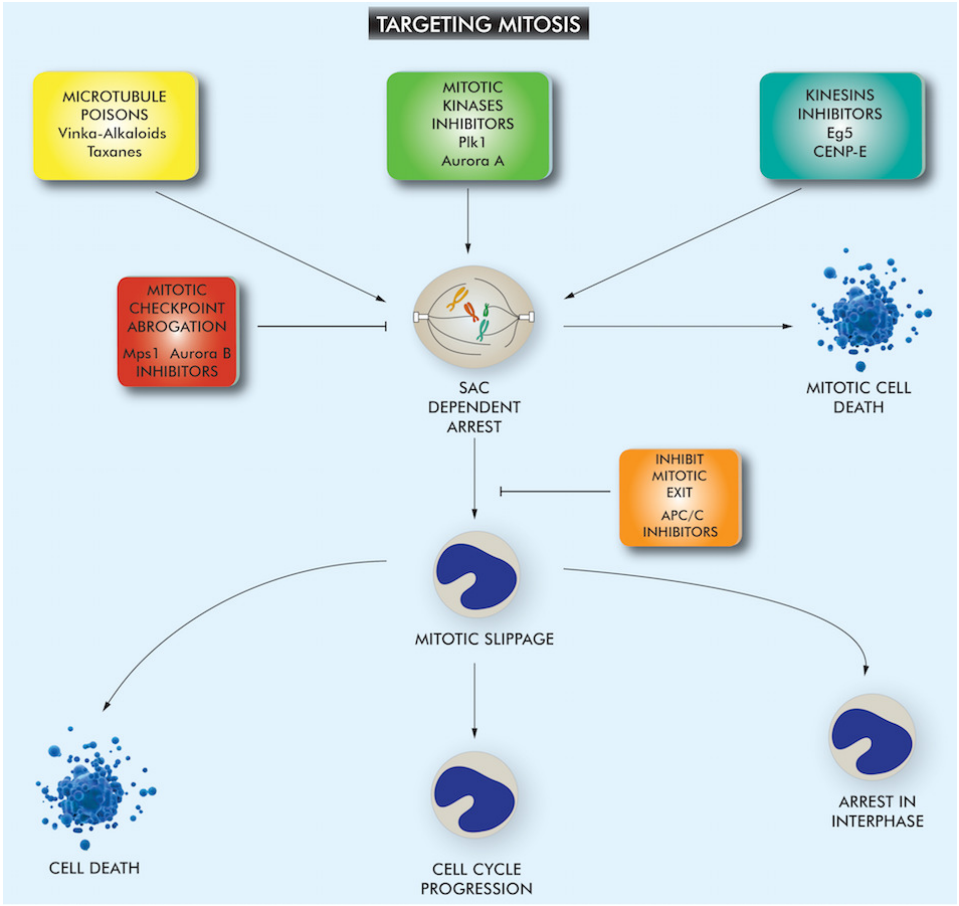

Figure 5. Strategies for targeting mitosis in cancer therapy. Inducing an aberrant mitosis by targeting microtubules, inhibition of mitotic kinases or kinesins induces a SAC dependent mitotic arrest that eventually leads to cell death in mitosis, if not cell will slip out mitosis without segregating their genome, therefore giving rise to viable aneuploid cells that may die in the subsequent interphase or remain viable. Other possible approach is the abrogation of the SAC activity, leading to a similar outcome. However the more efficient therapeutic approach, it has been recently proposed is the inhibition of mitotic exit forcing cell to die in mitosis (Domenéch & Malumbres, 2013).

a) Targeting mitotic entry: Cdk1 is the major kinase activity that drives entry into mitosis. Inhibition of Cdk1 prevents mitotic entry leading to G2 arrest. Strong inhibition of Cdk1 is likely to be toxic for normal cells limiting its therapeutic use, however it can be useful in specific cellular settings and synthetic lethal interactions exist with GSK3B (Mayes *et al.,* 2011), in Myc-overexpressing tumors (Goga *et al*., 2007) and partial inhibition of Cdk1 sensitize BRCA-proficient cancer cells to inhibit PARP (Johnson *et al*., 2011).

b) Targeting spindle dynamics: classical antimitotic therapies have made use of the spindle poisons that bind tubulin subunits and either stabilize, for example taxanes (paclitaxel, Nab-paclitaxel and docetaxel) now widely used to treat breast and ovarian tumors, non-small-cell lung cancer and Kaposi's sarcoma, or de-stabilizing, for example; vinka-alkaloids (vinorelbine, vinblastine, vincristine) used in a broad range of hematological malignancies. All this compounds prevents microtubule dynamics, a process required for the generation of a functional bipolar spindle and for chromosome segregation during mitosis. This situation is monitored by the SAC which delays mitosis until errors in microtubule–kinetochore attachment are resolved (Musacchio *et al*., 2007; Kops *et al*., 2005) by inhibiting APC/C-Cdc20, thus inhibiting mitotic exit (see above section 2.1). The SAC-dependent delay in mitosis increases the susceptibility of cells to undergo cell death. Alternatively, cells can escape from the mitotic arrest by slowly degrading cyclin B, a process known as mitotic slippage even in the presence of an active SAC. Mitotic slippage is thought to be one of the major mechanisms of resistance against antimitotic drugs. Microtubules are also necessary for multiple cellular

processes in interphase and the use of this spindle poison is associated with side-effects such as neurotoxicity, that can lead to irreversible neuropathies due to the effect of this drugs in microtubules, the basic components of neurons. Patients treated with these drugs develop severe myelosuppression derived from proliferation impairment of cycling bone marrow cells. Besides the fact that mitosis is not a key target of microtubule agents in patient tumors (Komlodi and Pasztor, 2011) it is expected that dividing cells are more vulnerable to these microtubule-disturbing agents due to the increased rate or microtubule turnover during mitosis. In addition, patients treated with microtubule poisons often acquire resistance to these drugs. Thus, although inhibiting microtubule function has demonstrated a significant antitumor activity, the side effects of these drugs limit their use and have prompted to identify alternative antimitotic drugs.

c) Mitotic targets: Most current efforts have mostly focused on the inhibition of Plk1 and Aurora (A and B) kinases. These proteins are overexpressed in multiple tumors and are essential components of cell division since their inactivation results in lack of chromosome segregation, polyploidy and, eventually, cell death. Multiple small-molecule inhibitors have been developed in the last years and some of them have been tested in clinical trials. Mitotic targets also include kinesins, a class of motor proteins with ATPase activity that move along microtubule filaments and are required for proper microtubule function. Several members of the kinesin superfamily, such as Eg5 and CENP-E are now emerging as putative anticancer targets. The main side effect observed was reversible hematological toxicity and some limited, but encouraging antitumor activity was observed promoting Phase II studies in monotherapy (Table 1) and combination (Table 8) in solid and hematopoietic tumors. However, the evidence for clinical efficacy was reduced with very limited objective responses and these compounds were mostly ineffective in patients.

Target	Inhibitor	Tumour types	Description
Plk1	BI2536	Phase I/II in solid tumours and relapsed hematopoietic malignancies	Partial antitumor activity. Reversible neutropenia.
	BI6727	Phase I advanced solid tumours	Some partial responses and stable disease. Most trial ongoing
	GSK461364	Phase I in advanced solid tumors and Non-Hodgkin's lymphoma	Prolonged stable disease in 15% of the patients.
	ON 01910. Na	Phase I/II Hematopoietic and advanced solid cancer	Propose AKT2 phosphorylation and cyclin D1 expression as biomarkers. Mostly ongoing / no results published
Aurora		Solid tumour cell lines	Growth inhibition and apoptosis in vivo and in vitro.
	AZD1152 (AurkB-specific)	Phase I/II study AML and Phase I trials patients with advanced solid malignancies.	Overall hematologic response rate 27%. One out of the four entered complete remission for AML. But No objective tumour responses observed, but stable disease in 23% of the patients.
	MLN8237 (AurkA-specific)	Phase I Advanced solid tumours and phase I/ II AML. Phase I refractory ovarian, fallopian tube or primary peritoneal carcinoma	Good tolerability and favourable pharmacokinetics, produces neutropenia and stomatitis. Modest response as a single agent, durable disease.
	MLN8054 (AurkA-specific)	Phase I advanced solid tumor	Dose-escalating study. Recommended dose for phase II clinical trials was not established
	VX-680 (MK-0457, pan Aurk inhibitor)	Phase I/II Advanced hematopoietic and solid tumors	Ongoing / no results published
	AMG 900 (pan-Aurora inhibitor)	Phase I acute leukaemia and solid tumor	Ongoing / no results published
Mps1	NMS-P715	Cultured cells	Aneuploidy and cell death in a variety of tumour cell lines. Inhibits tumour growth.

Target	Inhibitor	Tumour types	Description
	MPI-0479605	Colon carcinoma cell lines	Aberrant mitosis and growth arrest. Cells undergo mitotic catastrophe and/or apoptosis
	Reversine	Colon carcinoma cell lines	Low doses selectively kill p53-null cells
Cenp-E	GSK923295	Phase I in refractory cancer	Limited side effects. One patient with a durable partial response.
Eg5	AZD4877	Phase I solid tumor, phase II advanced bladder cancer	Acceptable safety profile. But little evidence of clinical efficacy
	SB-715992	Phase I metastatic cancer and tumors resistant to taxanes and/or platinum	The most common toxicities were nausea, diarrhea, fatigue and neutropenia. Some partial responses. Mostly ongoing / unpublished data
	SB-743921	Phase I lymphoma, solid tumors	Partial responses.
	ARRY-520	Phase I solid advanced cancer, advanced myeloid leukaemia	Relative lack of clinical activity in solid tumours
	ARQ621	Phase I metastatic solid, hematologic	Ongoing / no results published
	LY2523355	Phase I Solid and hematopoietic tumors	Ongoing / no results published
	MK0731	Phase I Solid tumours	Lengthening of stable disease in patients with taxane resistant tumors

Table 1. Mitotic drugs: recent preclinical and clinical Studies as monotherapy.
Abbreviations: AML, acute myeloid leukemia; CLL, chronic lymphocytic leukemia; pH3, phospho-histone H3.

d) Targeting the mitotic checkpoint: SAC abrogation results in defective or abnormal chromosome segregation, generating polyploid or aneuploid cells that may lead to chromosomal instability (CIN), therefore promoting tumorigenesis. Abrogation of the mitotic checkpoint specifically generates lethal aberrations in chromosomal unstable tumour cells. As most tumors are aneuploid or display certain levels of CIN, SAC abrogation may induce further levels of instability and may be therefore used as a therapeutic strategy as it is shown by genetic elimination of Mad2 or BubR1 results in chromosome missegregation that triggers cell death (Baker *et al*., 2004; Dai *et al.,* 2004a; Dobles *et al.,* 2000; Michel *et al*., 2001). One of the SAC druggable components is the kinase Mps1 which is required for SAC activity and its inhibition results in defective chromosome segregation, mitotic catastrophe and frequent cell death in a variety of tumor cell lines, with certain preference for p53 mutant cells (Castedo *et al*., 2004). Mps1 inhibitors have been only evaluated in preclinical assays (Table 1). In a general overview, the first generation of clinical trials for mitotic targeted therapies has not reached the expectations raised from preclinical models, at least for solid tumors and a crucial question that emerge from these studies is to what extent targeting the cell cycle merely results in proliferative arrest or induces tumor cell death, and which are the major resistance mechanisms. In addition, the potential as cancer targets of many other kinases such as the Nek family, Mps1, Mastl or haspin remains to be explored.

e) Targeting mitotic exit. Cells that escape from mitotic cell death and undergo mitotic slippage, can either die at the following cell cycle, arrest in a tetraploid state or undergo several rounds of division, depending on the status of genes such as p53 (Lanni *et al*., 1998; Rieder *et al*., 2009). Remarkably, several independent studies have observed no correlation between cell death and mitotic duration, suggesting that cell fate after treatment with antimitotic drugs is not exclusively dictated by mitotic length, although inhibition of apoptosis increases mitotic slippage which may indicate that both processes are somehow linked. Gascoigne and Taylor proposed a model based on two competing networks, one that involves mitotic cell death pathways and other that regulates cyclin B1 degradation and therefore mitotic exit. These two networks have specific thresholds that compete during mitotic arrest. If cyclin B1 levels fall under a certain threshold

before caspase activation has reached its cell death threshold, then cells will exit from mitosis. On the other hand, if cyclin B1 levels fall slowly, then cell death threshold will be achieved first and cells will die in mitosis (Figure 6). This model, however, does not provide an answer to the question on how a delayed mitosis could result in caspase activation.

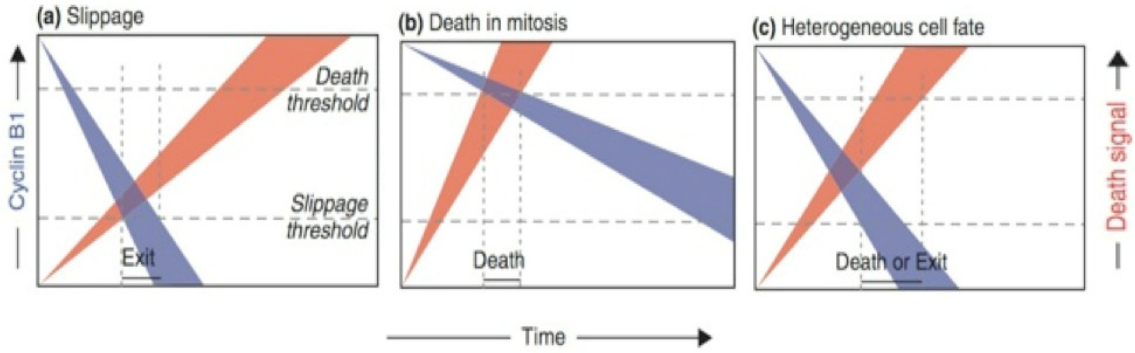

Figure 6. The model of the two competing networks. Cell fate during prolonged mitotic arrest depends on cell death pathways activation and cyclin B1 degradation with specific thresholds that compete during mitotic arrest. The network that first reaches its threshold of activation will dictate cell fate. If cyclin B1 is degraded before caspases are active cell will slip out mitosis, whereas if cyclin b levels fall slower that caspase are active, cell will die in mitosis. And cell fate does not correlate with the duration of the mitotic arrest (adapted from Gascoigne and Taylor 2009).

Multiple networks dictate cell fate during or after mitotic arrest, but preventing mitotic exit invariably results in cell death. Therefore, it is predictable that completely blocking mitotic exit might be a powerful strategy to induce mitotic cell death and may have stronger effects than targeting the spindle or mitotic entry. Preventing mitotic exit has been recently proposed as a complementary alternative since cells cannot survive for long time in mitosis and they eventually die if components of the mitotic exit pathway, such as the E3 ubiquitin ligase APC/C, are inhibited (Huang *et al*., 2009a; Zeng *et al.,* 2009). Inhibition of the APC/C, with a small-molecule inhibitor named pro-TAME, efficiently arrests tumor cells in mitosis and triggers cell death (Zeng *et al.,* 2010; Zeng and King, 2012). Our group has recently demonstrated that, impairing cyclin B1 degradation *in vivo* by genetic elimination of Cdc20 is highly efficient in killing cells in mitosis and preventing tumor growth *in vivo* (Figure 7). Moreover, preventing mitotic exit is much more efficient in killing tumor cells than targeting the spindle assembly with classical spindle poisons or new drugs inhibiting Eg5 or Plk1 (Manchado *et al*., 2010). Importantly, mitotic exit inhibition also affects pRb-null, p53-null or SAC-deficient cells suggesting widespread uses. Altogether, these results suggest that drugs that target Cdc20 or other components involved in cyclin B1 degradation, such as core components of the APC/C or the proteasome, could be quite effective in killing tumor cells. Indeed, a genome-wide RNAi screen has recently identified synthetic lethal interaction between K-RAS oncogenic signaling and the inhibition of core subunits of the APC/C, such as APC1 and APC472 (Luo *et al*., 2009). While partial inhibition of APC/C-Cdc20 may synergize with microtubule poisons, combination with Cdk1 inhibitors should be avoided. Strong inhibition of APC/C-Cdc20, however, is likely to be highly efficient in inducing apoptotic cell death and this last property should be used in therapeutic scenarios in which proliferation of normal cells is abrogated, such as after food starvation or in combination with G1-arresting agents, to selectively protect these normal cells against efficient mitotic chemotherapies. Thus, efforts to obtain fundamental insights into why some cells that arrest in mitosis die without exiting mitosis will be extremely important in enhancing our understanding sensitivity to anti-mitotic chemotherapy.

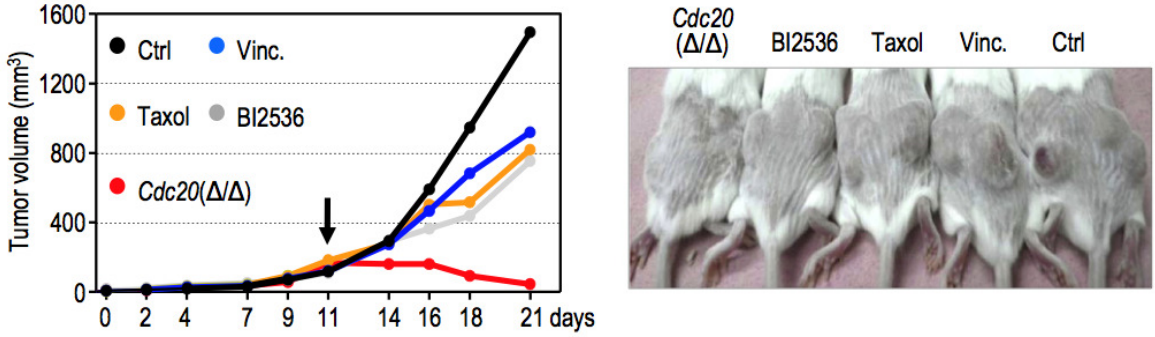

Figure 7. Cdc20 ablation is more efficient in tumor regression in vivo than current antimitotic drugs. Tumor volume diminished significantly upon in vivo ablation of Cdc20 when compared with drugs targeting mitosis (Manchado et al., 2010).

6. Mitotic catastrophe and mitotic cell death: a molecular definition

Induction of aberrant mitosis in tumor cells leads to mitotic arrest, the consequence of which can be, but not always, cell death. As a whole, the cellular alterations resulting from aberrant mitosis are known as mitotic catastrophe (Vitale *et al*., 2011). Mitotic catastrophe (MC) can be defined as a type of cell death resulting from aberrant mitosis, either in mitosis or in the subsequent interphase (Galluzi *et al*., 2012; Vitale *et al.,* 2011), that precedes and is different from apoptosis, necrosis or senescence and is driven by a poorly understood signaling cascade. MC should be considered as an oncosupressive mechanism (Vitale *et al*., 2011) avoiding chromosomal instability (CIN) by preventing aneuploidization. The disruption of MC leads to cancer progression and its induction constitutes a therapeutic endpoint. Given the lack of an accurate and consistent definition of MC, as long as cell death processes are activated within the duration of mitosis leading up to cell death thereafter, they are regarded as MCD (Figure 8). From now on, we will refer as mitotic cell death (MCD) as the special type of MC that leads to cell death during mitosis and therefore in the absence of mitotic slippage, which results the more interesting outcome from a therapeutic point of view.

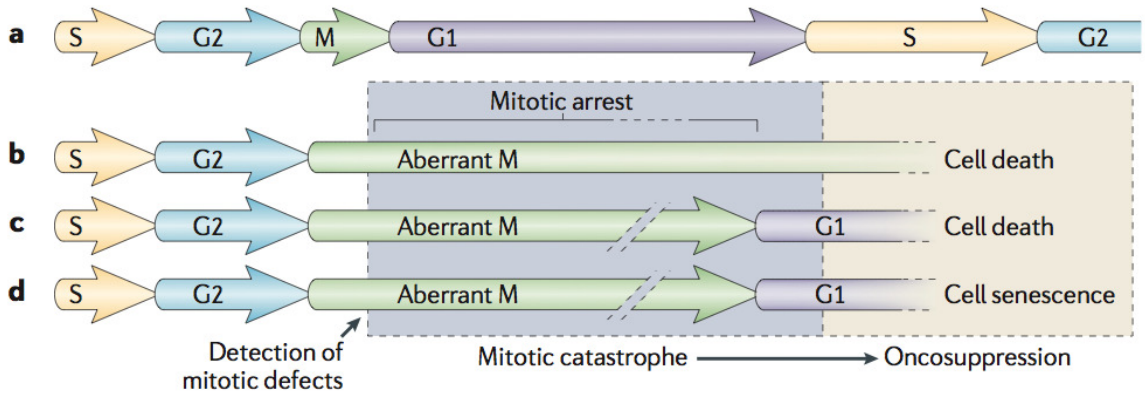

Figure 8. Definition and types of mitotic catastrophe. Normal cells progress through interphase and mitosis to complete a normal cell cycle. By contrast cells bearing mitotic perturbations that are detected during mitosis are always accompanied at some degree by mitotic arrest. Cells arrested in mitosis can have different fates: die without exit mitosis (b) mitotic cell death. (c) Undergo cell death in the subsequent cell cycle (as often occurs alter radio induced cell death). (d) Or exit mitosis and undergo senescence. (Adapted from Vitale *et al*., 2011).

MC was first described in *Schizosaccharomices pombe*, as a temperature–sensitive lethal phenotype, linked to gross abnormalities of chromosome segregation observed in some mutants strains (Ayscough *et al*., 1992; Molz *et al*., 1989). Although there is no broadly accepted definition of the term, it was first attempted to

be defined morphologically, referred to as a type of cell death resulting from abnormal mitosis which usually ends in the formation of large cells with multiple micronuclei and decondensed chromatin (Roninson *et al.,* 2001). However, reports describing mitotic catastrophe frequently show cells with some phenotypic characteristic of apoptosis, such as hypercondensed chromatin aggregates (Ianzini and Mackey, 1997; Roninson *et al*., 2001; Swanson *et al*., 1995). It has been argued that mitotic catastrophe would be fundamentally different from apoptosis because, in some scenarios, manipulations that prevent apoptosis, i.e. overexpression of Bcl-2 in etoposide-treated HeLa cells or MDR1 overexpression in irradiated tumor cells, can actually enhance the frequency of catastrophic mitosis (Lock and Stribins-kiene, 1996; Ruth and Roninson, 2000). Moreover, the fact that caspase inhibitors such as Z-VAD.fmk can fail to prevent the appearance of dying giant multinucleated cells induced, for instance by treatment with spindle poisons, has been used to conclude that mitotic catastrophe would be unrelated to apoptosis (Nabha *et al*., 2002, Niikura *et al*., 2007), assuming that apoptosis must be mediated by caspases. However, it is now well established that apoptosis may occur in a caspase-independent manner (Joza *et a*l., 2001; Susin *et a*l., 1999), meaning that failure to prevent cell death by caspase inhibitors cannot be used as an argument to define this type of cell death as non apoptotic. The co-existence of caspase-dependent and caspase-independent mechanisms in mitotic cell death can be explained by the Bcl-xL activity, which controls a switch between cell death modes during mitotic arrest. In mammary cells treated with paclitaxel or depleted in Cdc20, in the presence of Bcl-xL, die in mitosis through caspase and Bak /Bax–independent mechanisms, however, after depletion of Bcl-xL, which is required to maintain mitochondrial integrity, converts cell response to antimitotic drugs to efficient caspase and Bax-dependent apoptosis (Bah *et al*., 2014).

At least two subtypes of mitotic catastrophe can be distinguished: one that kill cells during or close to metaphase in a p53 independent manner, and a second ona that can occur after failed mitosis in a partially p53-dependent manner (Figure 9). A mitotic delay of only 2 hours can result in p53 activation and therefore, a prolonged mitosis can activate stress responses in mitotic cells (Uetake and Slunde, 2010). In fact, the loss of p53 can sensitize cells to microtubule poisons (Hawkins *et al.,* 1996). Thus cells could have evolved an intrinsic pro-apoptotic pathway responsible for clearance of cells that spend too much time in mitosis.

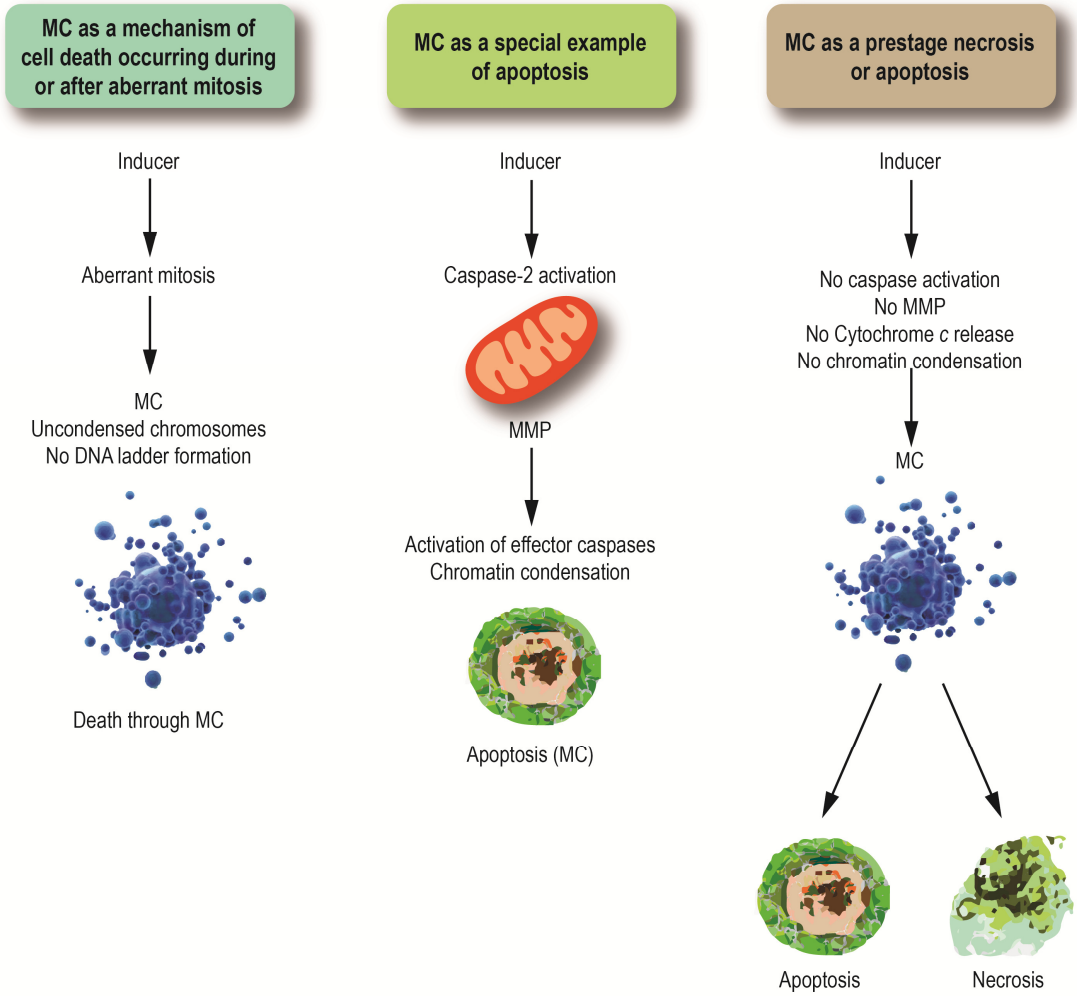

Figure 9. Mitotic cell death after mitotic catastrophe. a) Mitotic catastrophe (MC) as a death in mitosis consequence of an aberrant mitosis**. b)** It can be considered an especial form of apoptosis in which upon and stimuli, often triggered by DNA damage; caspase 2 becomes active and have a pre-mitochondrial role. c) Avoidance of mitotic catastrophe leads to aneuploid cell able to cycle**. d)** Caspase-independent cell death that shares morphological features of apoptosis and necrosis. (adapted from Vakfahmetoglu *et al.,* 2008).

From a molecular point of view, mitotic catastrophe may differ from classical apoptosis in the activation of a particular mitochondrial permeabilization pathway. During mitotic arrest caspase-2 (usually linked to DNA damage) stimulates mitochondrial membrane permeabilization facilitating the release of several caspase activators that finally lead to the caspase-3 activation, the major effector caspase (Kroemer *et al*., 2007). The BH3-only protein Bid has been proposed to be the main activity by which the caspase-2 induces mitochondrial permeability (Bonzon *et al*., 2006), its cleavage form, t-Bid (C-terminal truncated) translocate to mitochondria promoting further caspase activation (caspase-9 and the effector caspase-3, caspase-6 and caspase-7). Moreover, as cells enter mitosis, Bid is phosphorylated on ser-66 and this phosphorylated form of Bid primes cells to undergo mitochondrial apoptosis if mitotic exit is delayed (Wang *et al.,* 2014).

Cdk1-cyclinB1 has a central role in controlling both mitotic duration and the apoptotic machinery. On one hand Cdk1 activity protects mitotic cells against apoptosis by phosphorylation of caspase-9 (Allan *et al*., 2007; Castedo *et al*., 2002) and controls Fas-mediated apoptosis by regulating caspase-8 activity (Matthess *et al*., 2010), hampering their ability to trigger the intrinsic or extrinsic apoptotic pathway respectively (Figure 10 upper pannel). Cdk1-cyclin B also suppresses apoptosis upstream of mitochondrial cytochrome c release by phosphorylating caspase-2 and preventing caspase activation (Andersen *et al.,* 2009).

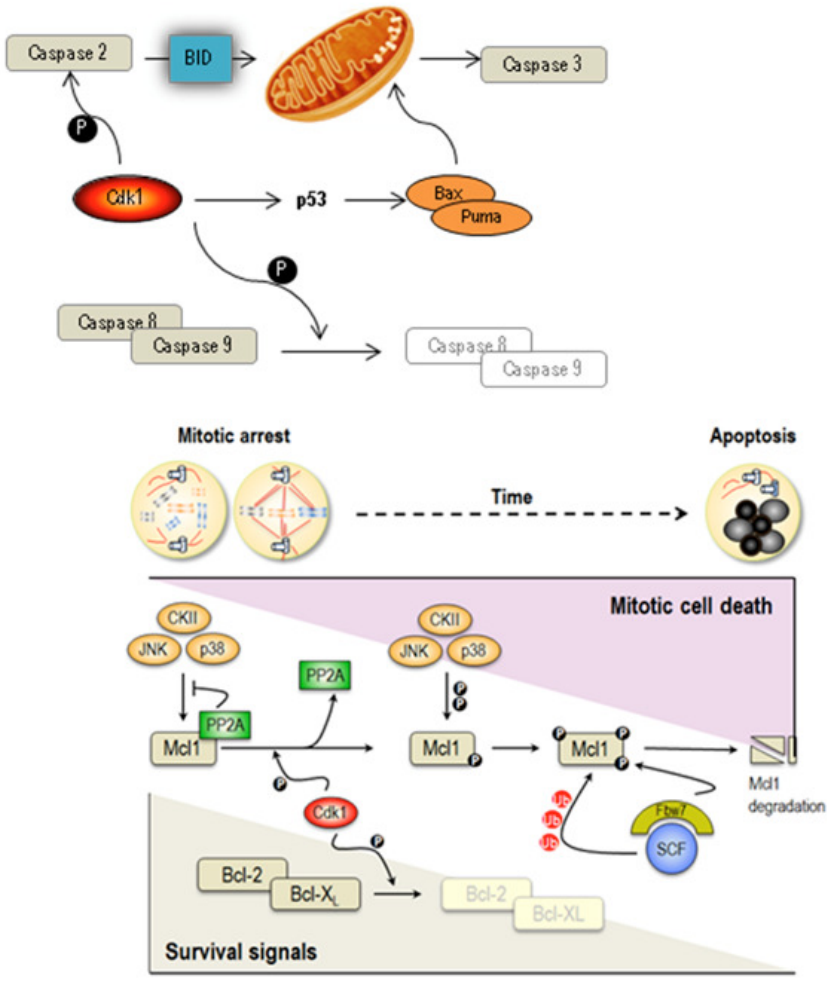

Figure 10. The dual role of Cdk1 in MCD On one hand Cdk1 sustained activation during prolonged mitotic arrest leads to phosphorylation of caspases 2, 8 and 9 protecting from caspase-dependent cell death, while on the other hand phosphorylates the pro-survival factors Bcl-1, Bcl-Xl and Mcl-1 and it also affects the turnover of Mcl-1. Hyperphosphorylation of Mcl-1 makes it more prone to phosphorylation by other kinases such as CKII, JNK and p38 and impedes dephosphorylation catalyzed by PP2A. This hyperphosphorylation makes it more susceptible to be ubiquitylated by the SCF complex and degraded by the proteasome (adapted from Manchado et al 2011).

Sensitivity to anti-tubulin chemotherapeutics is regulated by Mcl-1 and FBW7 (Wertz *et al*., 2011). Phosphorylation of Mcl-1 by Cdk1-cyclin B1 initiates its Cdc20-dependent destruction during mitotic arrest (Harley *et al.,* 2010). During a normal mitosis, transient activation of Cdk1 fails to reach the phosphorylation threshold that override the antiapoptotic activity of Mcl-1, Bcl-2 and Bcl-xL. If Cdk1 is active for too long the threshold is reached causing inactivation of the antiapoptotic function and eventually apoptosis. Recently has been shown that Cdk1 affects the turnover of Mcl-1 (Figure 10 bottom pannel). Phosphorylation of Mcl-1 makes it sensitive to the polyubuquitylation by the SCF complex. Once Mcl-1 is phosphorylated additionally by JNK, p38 and CKII kinases, it is recruited to the SCF by the tumor suppressor Fbw7 and degraded by the proteasome. During a normal mitosis phosphorylation is counteracted by PP2A and other phosphatases (Wertz *et al.,* 2011). APC-Cdc20 is also involved in the degradation of Mcl-1 when is phosphorylates by Cdk1 in cells arrested in mitosis (Harley *et al*., 2010). But Cdk1 also controls the activity of other pro-survival factor such as Bim (Fhearraigh *et al.,* 2011) which hyperphosphorylation during prolonged mitotic arrest is an important cell death signal. Cdk1-cyclin B1 phosphorylation acts as a functional link coupling mitotic arrest and apoptosis, however how Cdk1 sets the balance between cell death and survival it is not known yet. In addition to Cdk1 other mitotic regulators, such as Polo-like kinases, may also participate in balancing the activity of the pro-survival factors in mitotic arrest. Contrarily to Cdk1, Plk-1 seems to have a pro-death role by phosphorylating and weakening Bcl-xl pro-survival activity (Tamura *et al*., 2009). Moreover, sequential phosphorylation of caspase-8 by Cdk1 and Plk1 triggers apoptotic cell death during mitosis (Matthess *et al*., 2013).

While Cdk1 is clearly involved in modulating survival in mitosis, the role of the mitotic checkpoint in survival in response to mitotic inhibitors is controversial. Sustained activation of the SAC, for instance by overexpression of the Mad checkpoint proteins, leads to mitotic arrest frequently followed by apoptosis and caspases has been shown to cleave some SAC components, a phenomenon that may be linked to mitotic slippage (Castedo *et al*., 2004). However, studies in which the SAC is satisfied, in Cdc20 null cells, suggest that the SAC *per se* do not have a pro-apoptotic role (Castedo *et al*., 2004). Recent studies demonstrate that even in the absence of checkpoint activation, mitotic arrest induced by Cdc20 Knockdown (KD) or overexpression of the non-degradable form of cyclin B, leads to FLIP down regulation and sensitivity of tumor cell lines to TRAIL (Sánchez-Perez *et al.,* 2014). Consequently a pro-apoptotic signal independent of the SAC might be accumulated to trigger cell death during mitotic arrest (Jackson *et al.,* 2007). Survivin is the only functional link between mitotic machinery and apoptosis, and it has been shown to inhibit activation of caspases (Dohi *et al*., 2004; Li *et al.,* 1998; Shin *et al.,* 2001; Tamm *et al*., 1998). At the beginning of mitosis, survivin associates with mitotic spindle microtubules forming a complex with INCENP, borealin and Aurora B (O´connor *et al*., 2002; Wall *et* al., 2003) forming the chromosome passenger complex CPC. Either knockdown of survivin or INCENP has a similar phenotype, disrupted microtubule formation, polyploidy and massive apoptosis (Cutts *et al*., 1999; Uren *et al*., 2000). Recent studies provide evidence that survivin is required for a sustained mitotic arrest in response to the lack of tension at the kinetochore (Carvalho *et al* 2003; Lens *et al* 2003). Indeed, survivin depletion by siRNA leads to a prometaphase delay without effect on chromosome alignment. The APC/C complex itself may have a role in the modulation of cell death, since APC/C-Cdh1 indirectly inhibits apoptosis by degradation of MOAP-1, a Bax activator (Huang *et al*., 2012). And more importantly APC/C-Cdc20 has been implicated in inhibition of apoptosis by targeting the pro-apoptotic factor Bim for degradation (Wan *et al*., 2014).

Together this findings shown that a prolonged mitosis can result in both inhibition of the anti-apoptotic machinery and activation of a pro-apoptotic pathway, which provides a plausible mechanism to explain cells sensitivity to a delayed mitosis. Therefore preventing mitotic slippage or modulating the cell death pathways that trigger cell death in mitosis should enhance the efficacy of antimitotic drugs. This molecular pathway may have relevant implications for designing future therapeutic strategies aimed at inhibiting APC/C and for preventing adaptation to the apoptotic cell death imposed by defective mitotic exit. As previously suggested, APC/C–Cdc20 inhibitors could be useful in combination with other mitotic poisons by slowing cyclin B1 degradation and thus providing enough time to reach the apoptotic threshold of tumor cells.

Aim of the work

Blocking mitotic progression has been proposed as an attractive therapeutic strategy to impair proliferation of tumor cells. Mitotic arrest induced by anti-mitotic drugs such as taxanes and vinka-alkaloids s may lead to cell death; however, how cells survive during prolonged mitotic arrest and which are the pathways that determine survival in these conditions is not well understood. The molecular links between mitosis and apoptosis have been extensively studied, however there are also multiple evidences that death in mitosis might be apoptosis-independent. By using a genetic model of defective mitotic exit in mammalian cells, Cdc20 knockout mouse model, we aim to accomplish the following objectives

1. Understand the molecular mechanisms that govern cell survival in mitosis.

2. Evaluate the therapeutic benefit of interfering with the pathways responsible for survival during prolonged mitotic arrest.

3. Identify compounds that specifically induce cell death in mitosis.

Material and Methods

1. Cell culture and synchronization

1.1 Cell culture and synchronization

The Cdc20 conditional allele and its deletion by 4-OHT-inducible forms of Cre (RERT) were reported previously (Manchado et al., 2010). Atg5 and Bax/Bak mutant MEFs were described previously (Buytaert et al., 2006; Salazar et al., 2009; Tsukamoto et al., 2008). MEFs and human cell lines were growth in Dulbecco's modified Eagle's medium (DMEM) (Sigma) complemented with10% fetal bovine serum (FBS) and gentamycin at 37ºC and 5% CO2. For synchronization in G2, *Cdc20*(lox/lox); RERT (+/Cre) MEFs and MDA-MB-231 cells were treated with RO-3306 (Calbiochem; 5µM) for 18 hours and released in DMEM with or without 4-OHT (Sigma; 1µM), or DMEM with or without Taxol (Sigma; 700 nM) and proTAME (Boston Biochem., Inc.; 10µM). For mitotic synchronization of Cdc20-proficient mouse or human cultures, cells were treated for 12 hours with 200 nM nocodazole (Sigma) and released in fresh media containing 10 µM MG132. For synchronization in S-phase, HeLa cells were treated with thymidine (Sigma; 604 µg/mL) for 24h and released in fresh DMEM. Cells were treated with small molecule inhibitors as indicated in Table 2. One µM TO-PRO®-3 Iodide (642/661; Invitrogen T3605) was added to cultures to monitor cell death.

This is shown in Figure 11, when asynchronic cell cultures were synchronized in G2 by the addition of RO-3306, a Cdk1 inhibitor either in the presence or the absence of 4-OHT. After RO-3306 wash out cells are able to enter mitosis, but whereas in *Cdc20*(Δ/Δ) mitotic exit is completely prevented due to the lack of APC/C-Cdc20-dependent cyclin B1 degradation, Cdc20(lox/lox) cells are able to exit mitosis and progress normally through the cell-cycle. *Cdc20*(Δ/Δ) are not able to resolve anaphase and remain stuck in metaphase until cell death. Mitotic figures accumulate over time, about 40% of cells are in mitosis 0.5 h after the G2 release, reaching 80% at 8 hours after RO-3306 wash-out (Figure 11c). As previously reported (Manchado et al., 2010), no *Cdc20*(Δ/Δ) cell was able to exit from the mitotic arrest suggesting that this APC/C cofactor is essential for mitotic slippage.

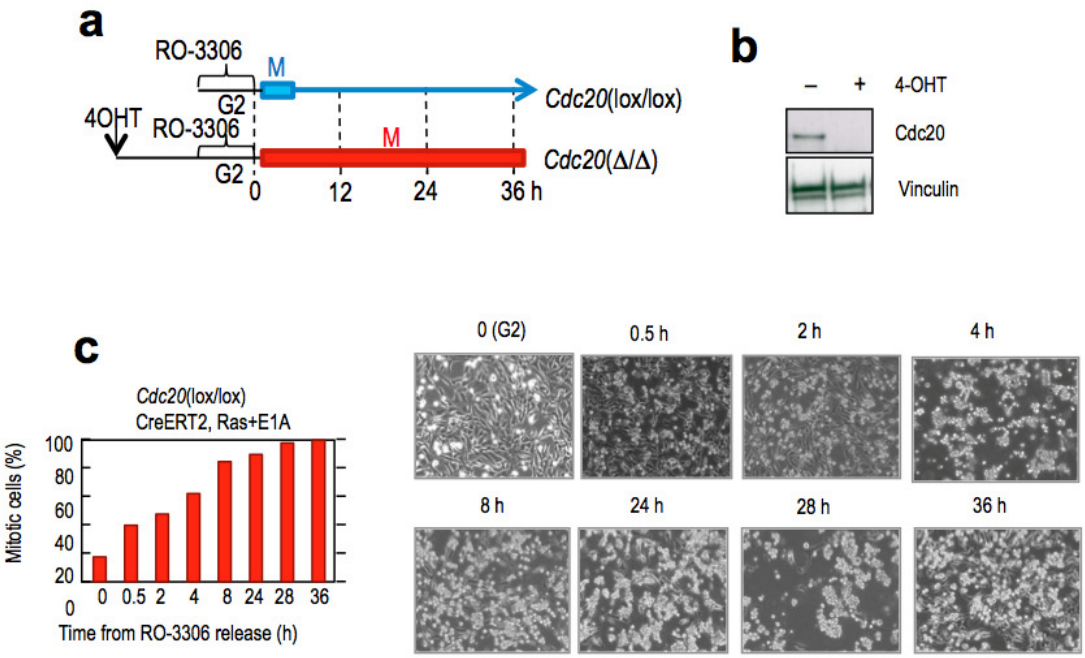

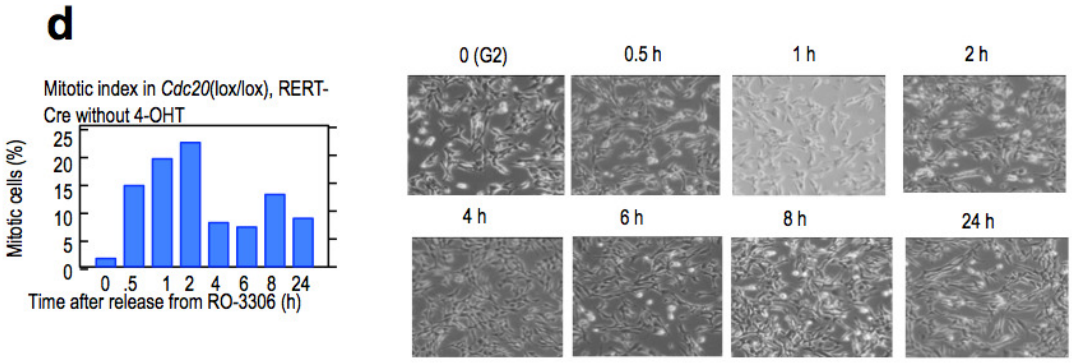

Figure 11. Synchronization of cells in mitosis. a) Schematic representation of the protocol followed for synchronization in *Cdc20*(Δ/Δ) and *Cdc20*(lox/lox). Asynchronous cells were synchronized in G2 by the addition of the Cdk1 inhibitor RO-3306, in the absence of 4-OHT (blue) presence of 4-OHT (red), added 12 hours prior RO-3306- RO-3306 is washed-out after 18 hours of treatment. **b)** Excision of Cdc20 upon 4-OHT treatment. **c)** Synchronized mitotic entry in Cdc20-null cells after release from RO-3306. *Cdc20(lox/lox)* cells were treated with 4-OHT to eliminate Cdc20 12 hours prior the addition of RO-3306, a Cdk1 inhibitor, to arrest cells in G2. This compound was washed-out 18 hours after allowing mitotic entry; in the absence of Cdc20 cells remain arrested in mitosis. Mitotic figures accumulate over time reaching 80% of mitotic figures 8 hours after RO-3306 release. **d)** Synchronized mitotic entry in *Cdc20*(lox/lox) cells after release from RO-3306. *Cdc20*(lox/lox) cells were treated with RO-3306, in the absence of 4-OHT, to arrest cells in G2. This compound was washed-out 18 hours after allowing mitotic entry in the presence of Cdc20 cells are able to exit mitosis and progress normally throughout the cell cycle.

1.2 Transfection/Nucleofection

Human cells lines and MEFs were transfected in subconfluency with Lipofectamine 2000 (Invitrogen) for plasmids transfection (LC3-GFP) and Amaxa system for siRNA against specific transcripts (Dharmacon smart pool), respectively, in accordance with the macturer´s recommendations. For Haspin knock down the following siRNA were used.

hHaspin	GGCAUCUGAUGCUGAAAAG
mHaspin	GGUCAUCUCUCUUUAGCCU

1.3 Treatments

The following drugs were used in cultured cells at the indicated concentrations:

Inhibitor	Target	Concentration	Source
2-DG	Hexokinase	5-20mM	Sigma
3MA	Vps34 (PI3KCIII)	5mM	Sigma
3PO	PFKFB3	1-100μM	Millipore
ABT-264	Bcl-2 family + Mcl-1	100nM	ActiveBiochem
ABT-737	Bcl-2 family	100nM	Selleckbio
AICAR	AMPK activator	1mM	Sigma
AKTIV	Akt	2μM	Calbiochem
Antimycin A	mitochondrial electron transport	1μM	Sigma
BEZ235	mTORC1 and PI3K	20nM	SelleckBio
C75	Fatty acid synthase	10μgr/mL	Sigma
Cyclosporin A	Cyclophilin	5μM	Sigma
Compound C	AMPK	10μM	Calbiochem

Inhibitor	Target	Concentration	Source
E64d	Cathepsin and capain	1µgr/mL	Sigma
FCCP	H+ ionophore	1µM	Sigma
LY294002	PI3K	20µM	Calbiochem
Metformin	AMPK activator	1mM	Sigma
MG132	Proteasome inhibitor	10µM	Sigma
Monastrol	Eg5	100µM	Sigma
Necrostatine-1	RIPK1	20µM	Enzo
Nocodazol	Microtubules	200nM	Sigma
Okadaic Acid	PP1/PP2A	1µM	Sigma
Oligomycin A	F0 part of the H+-ATP-synthase	2-10µM	Sigma
Oxamate	LDHA	1mM	Sigma
PD98059	MEK1 and MEK2	20µM	Calbiochem
Pepstatin A	Cathepsin and calpain	5µgr/mL	Sigma
proTAME	APC/cyclosome	10µM	Boston Biochem
PP242	mTORC1	10nM	Sigma
Rapamycin	mTORC1	500nM	Sigma
RO-3306	Cdk1	1-10µM	Sigma
Roscovitine	Cdk1	100µM	Sigma
Rotenone	mitochondrial electron transport	1µM	Sigma
SB-203580	p38MAPK	20µM	Enzo
Taxol	Microtubules	20-700nM	Sigma
Temsirolimus	mTORC1	100nM	Sigma
Z-VAD-fmk	Pan caspase inhibitor	20µM	Calbiochem

Table 2. Inhibitors used in this work.

1.4 Viral infections

Human cell lines at 60-70% confluency were infected with lentiviruses containing H2B-GFP. For IF Cdc20 (lox/lox), RERT (+, KI) MEFs at 60-70% confluency were infected either with retroviruses containing Lamina-CFP or lentiviruses containing Cherry-LC3GFP. For increasing the infection efficiency, two consecutive rounds of infection were performed. In order to generate stable cell lines cells were sorted in Influx sorted or FACs Aria.

1.5 Flow cytometry

Asynchronous cells were trypsinized for 5 min at 37ºC and resuspended in complete medium. In order to recover mitotic cells, mitotic shake-off was performed. Cell cycle profile assay were performed by adding 0.2µg/ml DAPI (Sigma) to the samples prior to run them on the LSR Fortessa (BD, San Jose). 10,000 single events were acquired. All data were analyzed using FlowJo v9.6.4 (Treestar, Oregon). For cell viability assays 1 µM TO-PRO®-3 Iodide (642⁄661; Invitrogen T3605) was added. To quantify mitochondrial mass, cells were resuspended in complete medium with 10 nM Mitotracker Deep Red FM (MTDR, M22426, Invitrogen) and 1 ⁄mL propidium iodide (P4864, Sigma) and then incubated for 15 min at 37ºC. Using an FC500 flow cytometer (Beckman Coulter), 10,000 cells were acquired in the FL3 and FL4 channels. Mean

fluorescence in the FL4 channel in the viable cell (PI-negative) population was plotted and normalized against that of untreated cells.

1.6 ROS measure

To monitor ROS, cells were grown on μCLEAR bottom 96-well plates (Greiner Bio-One), treated with specific drugs and incubated for 30 min at 37ºC as indicated in OxiSelect TM Intracellular ROS assay kit, Cell Biolabs and 5 μg/ml Hoechst 33342 (Invitrogen H3570). Images were automatically acquired from each well by an Opera High-Content Screening System (Perkin Elmer) as indicated above.

2. Immunofluorescence and biochemical analysis

2.1 Western blotting

Asynchronous cells were trypsinized for 5 min at 37ºC and resuspended in complete medium. In order to recover mitotic cells, mitotic shake-off was performed. Harvested cells were lysed in RIPA or a buffer containing 50 mM Tris HCl, pH 7.5, 1 mM phenylmethylsulfonyl fluoride, 50 mM NaF, 5 mM sodium pyrophosphate, 1 mM sodium orthovanadate, 0.1% Triton X-100, 1 μg/ml leupeptin, 1mM EDTA, 1 mM EGTA and 10 mM sodium-glicerophosphate. (Salazar *et al.,* 2009) and 30 μg of total protein was separated by SDS-PAGE in Criterion Bis-Tris geles (BioRad), transferred to nitrocellulose membranes (BioRad) by wet transference. Membranes were blocked with 5% milk in 0,005% TBS-Tween 20 and probed with antibodies against as indicated in Table 3. The secondary antibodies were HPR-conjugated (DAKO) and western blot (WB) was developed using the ECL system (PerkinElmer). Analysis of WB levels were performed in Image J.

Antigen	Source Ig	Source	Use
α-tubulin	Mouse	Sigma	WB
ACC	Rabbit	Cell Signalling	WB
AMPK	Rabbit	Cell Signalling	WB
Akt	Rabbit	Cell Signalling	WB
Bcl-2	Rabbit	Cell Signalling	WB
Bcl-X	Mouse	BD Pharmigen	WB
Bim	Rabbit	Abcam	WB
Caspase 2	Rabbit	Abcam	WB
Caspase 3	Rabbit	Cell Signalling	WB
Cdc20	Rabbit	Santa Cruz	WB
Cdc27	Mouse	Abcam	WB
ERK	Rabbit	Cell Signalling	WB
LC3b	Rabbit	Sigma	WB
Mcl-1	Rabbit	Rockland	WB
p62	Mouse	Sigma	WB
PARP	Rabbit	Cell Signalling	WB
PFKFB3	Rabbit	Cell Signalling	WB
Phospho-ACC	Rabbit	Cell Signalling	WB
Phospho-AMPK(Thr172)	Rabbit	Cell Signalling	WB
Phospho Akt (ser473)	Rabbit	Cell Signalling	WB
Phospho-Erk (Thr202/Tyr204)	Rabbit	Cell Signalling	WB
Phospho-(Ser) CDK substrates	Rabbit	Cell Signalling	WB
Phospho-Histone 3 (ser10)	Rabbit	Millipore	WB
Phospho-S6-ribosomal protein (ser235/236)	Rabbit	Cell Signalling	WB

Antigen	Source Ig	Source	Use
Survivin	Rabbit	Novus Biological	WB
Vinculin	Mouse	Sigma	WB

Table 3. WB; western blot

2.2 Inmunofluorescence

For immunofluorescence, cells were fixed in 4% buffered paraformaldehyde for 10 min at RT, permeabilized in 0.15% Triton-X 100 for 5-10 min at RT and stained with 4,6 diaminophenylindole (DAPI; Prolong Gold antifade, Invitrogen) to visualize nuclei. Images were captured using a laser scanning confocal microscope TCS-SP5 (AOBS) Leica or a Leica DMI 6000B microscope. For Lamina-CFP, a Cdc20 (lox/lox), RERT (+, KI) stable cell lines were generated. For mitophagy quantification, before fixation cells were incubated with Mitotracker Deep Red FM (MTDR, M22426, Invitrogen) for 30 min at 37 ºC.

2.3 Immunohistochemistry

For immunohistochemistry dissected tumors were fixed in 10%-buffered formalin (Sigma) and embedded in paraffin wax. Sections of 3-5 μm thickness were stained with active caspase 3 (C3A) antibody and analyzed. Table 3 the slides were digitalized by MIRAX digital slide scanner (Zeiss).

2.4 Real-time reverse-transcription PCR (qRT-PCR)

For quantitative RT-PCR studies total RNA was isolated by using the Qiagen RNeasy kit according to the manufacturer's instructions. cDNA was synthesized with a Superscript III reverse transcriptase (Invitrogen) and PCR amplification was performed using SYBR Green PCR Master mix (Applied Biosystems) with specific primers (Table 4). mRNA levels were normalized to β-actin mRNA levels in murine cells and to GAPDH for human cell lines.

Gene		Sequence
AMPKα1	Forward	AGTCAAAGCCGACCCAATGA
	Reverse	GGATTCTTCCTTCGTACACGC
AMPKα2	Forward	ATGGCTGAAGTGTACCGAGC
	Reverse	AGCTCCGACTGTCTACCAGG
Bak	Forward	CATCTTGGGTCAGGTGGGTC
	Reverse	TGGAACTCTGTGTCGTAGCG
Bax	Forward	TCTCCGGCGAATTGGAGATG
	Reverse	CGTGTCCACGTCAGCAATCA
Beclin1(BECN1)	Forward	TTGAAACTCGCCAGGATGGT
	Reverse	ATCAGATGCCTCCCCGATCA
Drp1	Forward	TCAGAAATGCTACTGGCCCC
	Reverse	TCACGGGCAACCTTTTACGA
hHaspin	Forward	TGAAACGAGAGCCATGACCG
	Reverse	CCATATGTGCGGAAAAGCCG
mHaspin	Forward	ACACGCAGGCTCTTGACTC
	Reverse	GTACGTTCGAAAGAGCCGGG
Raptor	Forward	CTGCTCGTGGCAAGTTTGTT

Gene		Sequence
	Reverse	CTGCTTACTGGGGTGCAGTT
RIPK1	Forward	ACATCAATGCAAAGCCCACG
	Reverse	TGCAGATCACGAACTGCTCA
RIPK3	Forward	GTACGTTCGAAAGAGCCGGG
	Reverse	ATCTTGTCACCAGAGCCTGC
Survivin	Forward	ATCTGGCAGCTGTACCTCAAG
	Reverse	TTCTATGCTCCTCTTCGCTCT
ULK1	Forward	CCTGACTTCCTACAGCGGAG
	Reverse	CTAGCCAACAGGGTCAGCAA
Vps34 (PI3KCIII)	Forward	AGACTTCAGGCCTTGCTTGG
	Reverse	CTTGACGCAAGTCGTCTCCA

Table 4. qRT-PCR primers used in this work.

3. Microscopy

3.1 Videomicroscopy

For videomicroscopy human and murine cell lines expressing stable H2B-GFP were plated on eight-well glass-bottom dishes (Ibidi) and imaged with a DeltaVision RT imaging system (Applied Precision, LLC; IX70/71; Olympus) equipped with a PI APO 20X/ 1.42 NA objective lens, maintained at 37 °C in a humidified CO_2 chamber. 1 μM TO-PRO®-3 Iodide (642⁄661; Invitrogen T3605) was added before start recording. Images were acquired every 10 or 15 min, and processed and analyzed using ImageJ software.

3.2 High-throughput microscopy (HTM)

For HTM cells were grown on μCLEAR bottom 96-well plates (Greiner Bio-One). After specific treatments, 1 μM TO-PRO®-3 Iodide (642⁄661; Invitrogen T3605) and 5 μg/ml Hoechst 33342 (Invitrogen H3570) were added. After 30 min of incubation at 37ºC, images were automatically acquired from each well by an Opera High-Content Screening System (Perkin Elmer). A 20x magnification lens was used and pictures were taken at non-saturating conditions. Images were segmented using the Hoechst 33342 staining to generate masks matching cell nuclei from which the mean TO-PRO®-3 signal were calculated. For the screening of 200 compounds *Cdc20*(lox/lox) MEFs expressing H2B-GFP cells were grown on μCLEAR bottom 96-well plates (Greiner Bio-One). After specific treatments at the indicated times and 1 μM TO-PRO®-3 Iodide (642⁄661; Invitrogen T3605) addition, images were automatically acquired from each well by an Opera High-Content Screening System (Perkin Elmer). A 10x magnification lens was used and pictures were taken at non-saturating conditions. Images were segmented using the GFP staining to generate masks matching cell nuclei from which the mean TO-PRO®-3 signal were calculated. Based on the distribution of TO-PRO3 intensity in untreated cells, a threshold for cell viability was established. Data were filtrated using SPSS.

3.3 FRET

For FRET analysis (Tsou *et al*., 2011), cells were plated on eight-well flow chambers (Ibidi) and Imaged with a Leica AF6000W equipped with a fast external filter wheels, Hamamatsu CCD Camera, HCX PL APO 40X/ oil 1.25 NA objective lens and AFC hardware autofocus system, maintained at 37 °C in a

humidified CO2 chamber. Images were acquired every 1 or 10 min. Images were processed and analyzed using ImageJ software.

3.4 Life-cell confocal microscopy

Images were captured using a laser scanning confocal microscope TCS-SP5 (AOBS) Leica or a Leica DMI 6000B microscope, HCX PL APO 63X/oil 1.25x objective lens, maintained at 37 °C in a humidified CO_2 chamber.

3.5 Transmission electron microscopy (TEM)

Cells were fixed for 4 hours at 4°C in 4% paraformaldehyde (w/v) and 2.5% glutaraldehyde (v/v) in 0.4 M HEPES buffer pH 7.4, washed and fixed again in aqueous 1% (w/v) osmium tetroxide, and embedded in Epon. Electron microscopy was performed with a JEOL 1230 transmission electron microscope, at 80 kV, on ultra-thin sections of 60 nm.

4. Metabolic assays

4.1 Seahorse metabolic profiling

Oxigen consumption rate (OCR) and the extracellular acidification rate (ECAR) of cells were measured with an XF96 Extracellular Flux Analyzer (Seahorse Bioscience). In brief, cells were plated at 1.5-2 $\times 10^4$ cells/well in buffered DMEM containing 25 mM glucose and 2 mM glutamine. Cells were incubated in a CO2-free incubator at 37°C for 1 h to allow for temperature and pH equilibration prior to loading into the XF96 apparatus. Assays consisted of sequential mix (2 min), pause (2 min), mix (0.33 min) and measurement (4 min) cycles, allowing for determination of OCR/ECAR every 8.33 min. Mitotic cells were obtained after shake off and plated in BD Cell-TaK coated plates (Faubert et al., 2013; Wu et *al*., 2006).

4.2 Nuclear magnetic resonance (NMR)

For NMR analysis of cell media metabolites **(**Bradley *et al*, 2010), 0.5 x10^6 MEFs were plated (in triplicate) in DMEM containing 5 mM U^{13}C-labeled glucose and 10% dialyzed FBS and were synchronized as described above. 500 μL of cell media supernatant were sampled for every time point (at 0 h, when cells are washed and fresh ^{13}C-label medium is added, and 4, 8, and 24 h, or 3, 6, 18 and 36 h afterwards), and centrifuged at 10,000 xg for 10 min using 10Kd Spin Columns (BioVision) to eliminate high molecular mass components (mainly albumin from serum). NMR samples were prepared mixing 400 uL of medium filtrate with 200 uL of NMR buffer (PBS 3X in 70% deuterated water, 0.3 mM TMSP, and 0,09% sodium azide) and transferred to 5 mm NMR tubes for measurement. High-resolution NMR spectra were registered on a Bruker Avance spectrometer operating at 16.4 T (proton Larmor frecuency of 700 MHz) at 293 K using a room temperature TXI probe with pulsed field gradient capabilities, and equipped with a BACS120 sample changer. 1D proton NMR spectra (1dH) of cell growth media were recorded using a NOESY pulse sequence (noesygppr1d in Bruker nomenclature) employing pulse field gradients during the mixing time of 10 ms and low power (50 db) presaturation of the residual water signal during the 2 s recovery delay between consecutive scans. 256 scans were accumulated using a spectral width of 20 ppm and acquisition time of 1.6 s, resulting in typical acquisitions times of 17 min per sample. Analogous parameters were used to record ^{13}C-filtered 1D proton NMR spectra (1dHC), which allows selective observation of ^{13}C-bound protons (from ^{13}C-glucose and metabolic transformation products thereof). 1dHC spectra were recorded using the first increment of a 2D sensitivity-enhanced ^{1}H-^{13}C heteronuclear single quantum coherence experiment (2dHC, hsqcetgpsisp2 in Bruker nomenclature) (Schleucher *et al*., 1994; Willker *et al*., 1993) without ^{13}C decoupling during the 1.6 s acquisition time. All 1dH and 1dHC free induction decays (FIDs) were processed with

exponential multiplication (0.5 Hz line-broadening) before Fourier transformation and baseline corrected afterwards using Topspin2.1 (Bruker). ^{1}H chemical shifts were referenced to internal TMSP (0.00 ppm). Concentrations of metabolites in 1dH spectra were obtained by comparing metabolite signal integrals to that of the added standard (TMSP), considering the number of equivalent protons in each chemical group of each metabolite. Integration regions of variable size were manually defined using the AMIX3.8 software (Bruker) in order to cover all detected signals (but water) and adjusted (to accommodate small variations in signal positions presumably due to differences of pH and ionic strength between samples) for each set of spectra. In 1dH experiments signal-specific correction factors were applied for incomplete recovery of magnetization during the incomplete relaxation delay, and the number of equivalent protons in each resonance (as well as the 9 protons in TMSP) was taken into account to calculate absolute metabolite concentrations from the corresponding signal/s, which resulted in a 5-fold saving in NMR acquisition time over the alternative method which requires recording fully relaxed spectra. These correction factors were determined from the ratio of each signal integrals in two spectra acquired on a representative sample: that in a regular 1dH experiment recorded with 2 s recovery delay, and the corresponding one in the fully relaxed spectrum, recorded with 10 s recovery delay. The total integral of the different well-resolved signals of glucose (the only ^{13}C-labeled nutrient) and that of the methyl signal of lactate in 1dHC spectra was used to quantify the relative decrease of U-$^{13}C_6$-glucose and the relative increase of $^{13}C_3$-lactate in the media. These were converted into approximate molar concentrations using the known initial concentration of $^{13}C_6$-glucose in the medium and the maximum final lactate, as measured from the two ^{13}C-satellites of the methyl resonance of lactate in 1dH spectra. Unlabeled glucose uptake and lactate production was also measured using the central (non-satellite) signals of the H4 protons of (unlabeled) glucose at 3.41 ppm (that overlap for α and β glucose) and the doublet of the lactate methyl signal at 1.33. In order to normalize for the (possibly) variable amount of cells in each plate the total metabolite signal of each 1dH NMR spectrum (calculated as the sum of all integration regions, excluding the TMSP and contaminants signals) of each polar extract sample was taken into account, and 1dH-derived integrals and 2dHC-derived intensities of samples with a reduced amount of metabolite signal were divided by the corresponding reduction factor to match the most concentrated sample in each set.

4.3 HPLC ATP

Concentration of ATP was determined spectrophotometrically as described previously (Saha *et al*., 2004).

5. In vivo studies

Mice were injected subcutaneously in the right and the left flank with 3 x10^6 MDA-MB-231 cells in 0.1 ml of PBS + 0.5% BSA. 20 days after cell injection, tumors had grown to an average volume of 150-200 mm^3. Mice were then divided into different experimental groups of 5 animals each, which received the following treatments as intraperitoneal injections: saline (control); 5 mg/kg Taxol; 5 mg/kg 3PO; 25 mg/kg 3PO; 50 mg/kg 3PO; 5 mg/kg Taxol + 5 mg/kg 3PO; 5 mg/kg Taxol + 25 mg/kg 3PO; 5 mg/kg Taxol + 50 mg/kg 3PO. The injection was repeated every two days and treatment was continued for 12 days. Tumor volumes were monitored using calliper measurements and were calculated by the formula: (4p/3) * (w/2)2 * (l/2).

6. Statistics

Statistical analysis was carried out using Prism 5 (GraphPad). All statistical tests were performed using two-sided, unpaired Student's t tests, or the Fisher's exact test. Data with $p<0.05$ were considered statistically significant (*, $p<0.05$; **, $p<0.01$; ***, $p<0.001$).

Results

1. Molecular pathways that modulate cell viability in mitosis

Inhibition of mitotic progression leads to prolonged mitotic arrest which may results in cell death in mitosis, or more frequently, mitotic exit in the absence of proper chromosome segregation and an active SAC (mitotic slippage). While many of the aneuploid cells may die because of massive chromosome imbalance, survivors may continue proliferating, which is clearly an undesirable outcome. Thus, efforts to obtain fundamental insights into the regulation of mitotic cell death will be extremely important in enhancing our understanding of drug sensitivity in cancer cells. MCD can be exploited as a strategy to increase the efficacy of chemotherapeutic agents such as microtubule poisons. Cdc20-null cells are the ideal scenario to characterize the molecular requirements for cell death in mitosis.

2.1 Mitotic cell death is modulated by the intrinsic apoptotic pathway

As previously introduced, we have developed a new strategy to follow individual cell fate by videomicroscopy after mitotic arrest caused by genetic depletion of Cdc20 or chemical inhibition of mitosis in human cells. We use H-Ras-transformed Cdc20-conditional knockout cells expressing a histone H2B-GFP reporter as well as an inducible form of the Cre recombinase. Addition of tamoxifen results in the activation of Cre, the excision of Cdc20 exons and metaphase arrest. We also use some human cell lines expressing the histone H2B-GFP reporter in which we mimic the metaphase arrest exerted by Cdc20 ablation by using proteasome inhibitor or an APC/C inhibitor. Cell death becomes evident in these cells by the use of a soluble dye, To-Pro3, which diffuses into the cells after the permeabilization of the membranes that accompanies cell death. Mitotic onset is characterized by cell rounding accompanied by DNA condensation. This system allows the interrogation of the consequences of modulating several signalling pathways by using RNA interference or specific chemical inhibitors. By measuring survival in mitosis (SiM), which is the time from mitotic entry till cell death in mitosis (To-pro3 staining).

Cdc20(Δ/Δ) cells display a variable SiM of 20 ± 14 h until they finally died in mitosis (Figure 12b,c) in the complete absence of mitotic exit, previously reported (Manchado *et al.,* 2010). Initially we evaluated the relevance of the apoptotic pathway in mitotic cell death. The two pathways of apoptotic cell death converge in the activation of caspases, but can be distinguished by the requirement of Bcl-2 family proteins and by which caspases are crucial for their execution. The intrinsic or mitochondrial pathway, regulated by Bcl-2 family proteins, generally leads to the activation of caspase-9, whereas the extrinsic or death-receptor pathway is triggered by ligation of the death receptor which can recruit and activate caspase-8, an event that leads to the subsequent activation of downstream effectors caspases-3, 6 or 7 (Youle *et al.,* 2008). Bcl-2 family proteins play pivotal roles in controlling programmed cell death and have been classically grouped into three classes: the pro-survival members; Bcl-2, Bcl-xL, Bfl-1/A1, Bcl-w, Mcl-1, Boo, NR-13, BHRF1, LMW5-HL, ORF16, KS-Bcl-2, E1B-19K, and Ced-9, and the pro-apoptotic members which includes: Bax, Bak, and Bok (Adams and Cory, 1998). A third divergent class is the BH3-only proteins (Bad, Bid, Bik, Bim, BMF, Noxa and Puma), which selectively interact with anti-apoptotic Bcl-2 family members (Huang and Strasser, 2000). The pro-apoptotic family members Bak and Bax are crucial for permeabilization of the outer mitochondrial membrane by oligomerization and formation of a pore and the subsequent release of apoptogenic molecules such as cytochrome c and DIABLO, which ultimately leads to caspase activation (Youle *et al*., 2008). The anti-apoptotic members Bcl-2 and Bcl-xL bind and prevent Bak and Bax homo or heterodimerization (Willis *et al*., 2007a-b) repressing Bak and Bax proteins. It is still controversial how BH3-only proteins can activate Bak and Bax proteins, one model states that it occurs through direct binding and inhibition of Bcl- 2 family members, but an opposing model argue that Bid, Bim and Puma directly activates Bak and Bax (Youle *et al.,* 2008, Zong *et al*., 2008).

To test the relevance of apoptosis in MCD, we transfected these cells with small interfering siRNAs (Figure 12d,e) against several apoptotic regulators following the protocol depicted in Figure 12a. Knockdow of

Mcl-1, a pro-survival regulator of the Bcl2 family involved in the response to taxol (Inuzuka *et al*., 2011; Wertz *et al*., 2011) resulted in early MCD (SiM 9.5 ± 6.5 h). Similar studies suggested the involvement of Bcl-x in preventing MCD in fibroblasts whereas the differences induced by knockdown of Bcl-2 did not reach statistical significance despite an efficient downregulation of protein levels (Figure 12c,e). Contrarily, knockdown of both caspase-2 and caspase-3 significantly delayed MCD (SiM 25.5 ± 17.2 h; Figure 12b,c). The involvement of the apoptotic machinery was also validated using the pan-caspase inhibitor ZVAD or two different inhibitors of the Bcl-2 family (Figure 12d). SiM was improved with ZVAD treated cells and significantly decreased after application of Bcl-2 family inhibitors (Figure 20d) being more dramatic in the case of ABT-263, perhaps as a consequence of the more potent effect of this compound against Mcl-1 (Rooswinkel *et al*., 2012; Tse *et al.,* 2008). Downregulation or inactivation of caspases or Bax /Bak, proteins delayed but did not prevent MCD, resulting in SiM 34 ± 28 h, as all cells died in these assays in the absence of Cdc20 (Figure 20c,d). Similar data were obtained when human cancer cells (HeLa or MDA-MB-231) were subjected to a similar protocol for synchronization (Figure 21c) and treated with either caspase or Bcl-2 family inhibitors, suggesting that apoptosis is involved but not essential for MCD.

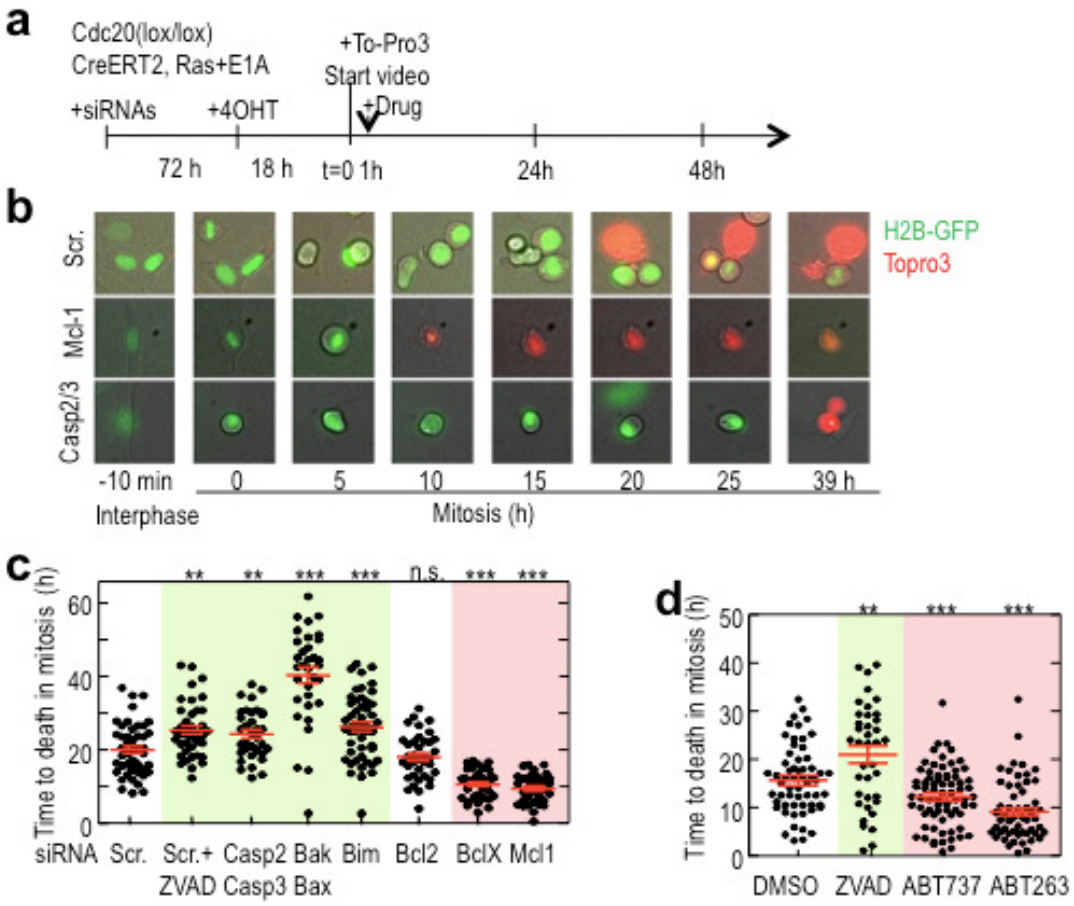

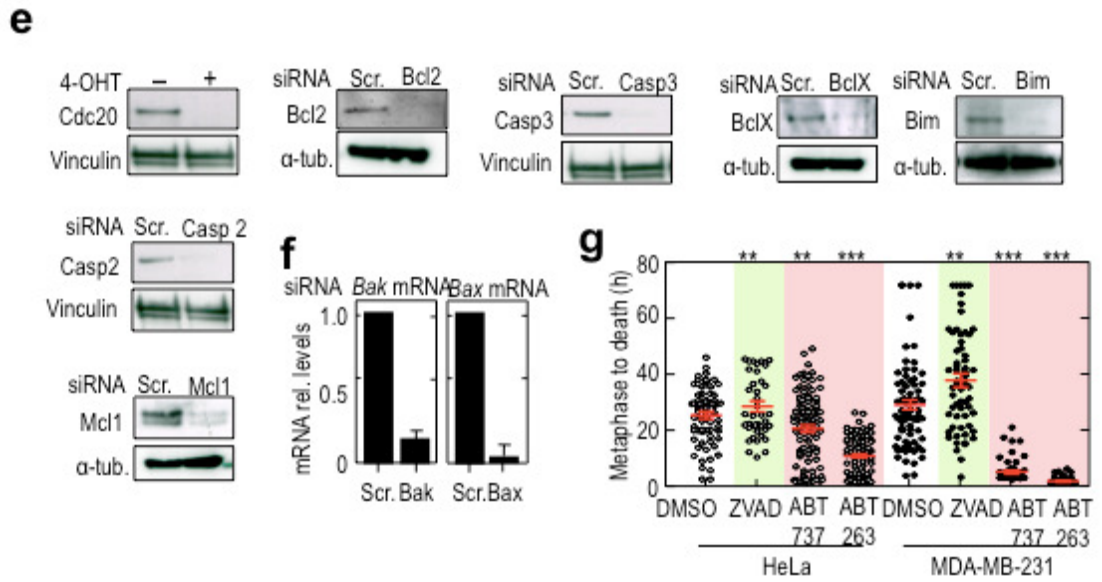

Figure 12. MCD is modulated by the intrinsic apoptotic pathway. a) Schematic representation of the protocol for time-lapse microscopy in Cdc20-deficient cells. Cells are subjected to two consecutive rounds of transfection, at 72 and 24 hours before start recording, respectively. 4-OHT was added 18 hours before the video. In contrast, for chemical inhibition, inhibitors were injected after the beginning of the video to cells that has been treated with 4-OHT for 24 hour. Only mitotic cells were considered for the analysis in order to avoid a possible detrimental effect of the indicated treatments on mitotic entry. **b)** Representative micrographs of Cdc20-deficient cells after the indicated periods of arrest in mitosis in the presence of siRNAs against Mcl-1 or caspase-2 and 3. **c)** Plots representing the duration of mitosis (from mitotic entry till cell death in mitosis) in Cdc20-null cells treated with the indicated interfering RNAs or in the presence of the caspase inhibitor ZVAD. **d)** Plots representing the duration of mitosis (from metaphase till cell death in mitosis) in Cdc20-null cells treated with the indicated Bcl-2 family inhibitors. **e)** Inmunodetection of the indicated proteins after treatment with the indicated siRNAs. **f)** Efficiency of siRNA Knockdown by qPCR analysis of mRNA levels (48 h after siRNA nucleofection). Data were normalized by β-actin mRNA levels. **g)** Plots representing the duration of mitosis (from metaphase in the presence of MG132 to cell death) in either in HeLa or MDA-MB-231 cell lines after addition of the indicated drugs. In c and g dots represent individual cells and a red line indicates the mean. n.s., not significant. **, p<0.01; ***, p<0.001 (Student's t-test).

To further understand whether this was a consequence of partial inactivation of apoptosis, we made use of Bax /Bak double knockout MEFs in which the intrinsic apoptotic pathway is completely inhibited (Lindsten *et al.*, 2000; Wei *et al.*, 2001). To mimic the metaphase arrest caused by Cdc20 ablation, cells were released from a nodazole-induced prometaphase arrest in the presence of the proteasome inhibitor MG132, thus preventing cyclin B degradation and mitotic exit (Figure 13a). This protocol resulted in a SiM of 13.0 ± 9.5 h in wild-type cells, which was significantly expanded to 39.0 ± 28.9 h in average in the absence of Bak and Bax (Figure 13b). Yet, all cells died in mitosis in these conditions.

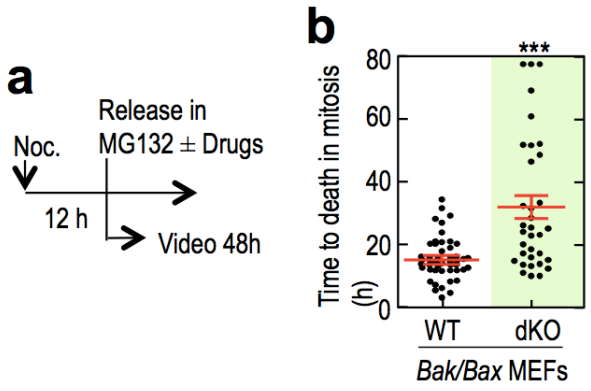

Figure 13. Apoptosis participates in MCD but is not essential. a) Schematic representation of the protocol for time-lapse microscopy in Cdc20-deficient cells. Human and murine cell lines were synchronized in prometaphase with nocodazol, after 12 hours of treatment cells are released in MG132, avoiding cyclin B proteasomal degradation. **b)** Plots representing the duration of mitosis (from metaphase in the presence of MG132 to cell death) either in Bak /Bax wild type or double-knock out cells. In b dots represent individual cells and a red line indicates the mean. n.s., not significant. **, p<0.01; ***, p<0.001 (Student's t-test).

2.2 Sustained activation of Cdk1 has a pro-death role in MCD

Cdk1 sustained activation during prolonged mitotic arrest, is known to balance pro-apoptotic and pro-survival signals. We next tested in Cdc20-null MEFs the role of Cdk1 activity. Upon Cdks inhibition, by the addition of roscovitine, in *Cdc20*(Δ/Δ) SiM was extended 5 hours in average (Figure14), whereas inhibition of PP1 and PP2A, the phosphatases that counteracts Cdk1 activity, by the addition of 1μM okadaic acid (OA), does not affects SiM. This result suggested that Cdk1 activity contributes to survival in mitosis in Cdc20-null cells.

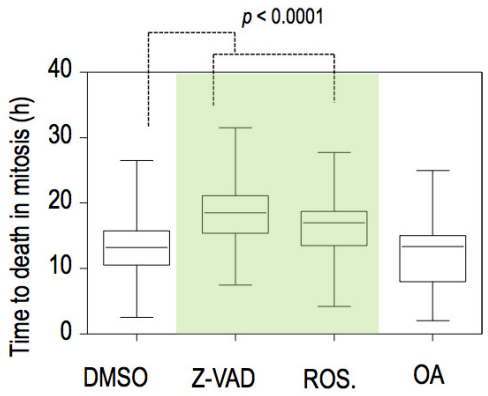

Figure 14. Cdk1 sustained activity in prolonged mitotic arrest contributes to cell death. Plots representing the duration of mitosis (from metaphase to cell death) in Cdc20-null cells after roscovitine, okadaic acid or ZVAD addition. Roscovitine addition significantly delays SiM, but caspases inhibition is more efficient in extending SiM. Boxes represent individual cells and a black line indicates the mean. n.s., not significant. **, p<0.01; ***, p<0.001 (Student's t-test). There were only considered for this assay those cells that were already in mitosis before the additon of the compounds, avoiding interferences in mitotic entry.

2.3 Necroptosis is not a major pathway for cell death in mitosis

We next investigated other pathways known to regulate cell death. Necrosis, often viewed as an accidental and unregulated cellular event, can also be executed in a regulated manner known as necroptosis (Hitomi *et al.,* 2008). The term necroptosis is used to designate one particular type of programmed necrosis that depends on the serine/threonine kinase activity of RIPK1 (receptor-interacting protein kinases) and RIPK3, which can be viewed as a form of cell death with a necrotic appearance. TNF or TRAIL triggered the formation of a RIPK1/RIPK3 complex, the initial step of the ripoptosome formation, which eventually leads to the downstream activation of caspase-8 (Golstein and Kroemer, 2007). As displayed in Figure 15, down-regulation of both RIPK1 and RIPK3 by using siRNAs, or inhibition of RIPK1 with necrostatin-1, did not alter SiM in Cdc20-null cells (Figure 15). This result suggests that necroptosis or programmed necrosis is not a major pathway for death in mitosis.

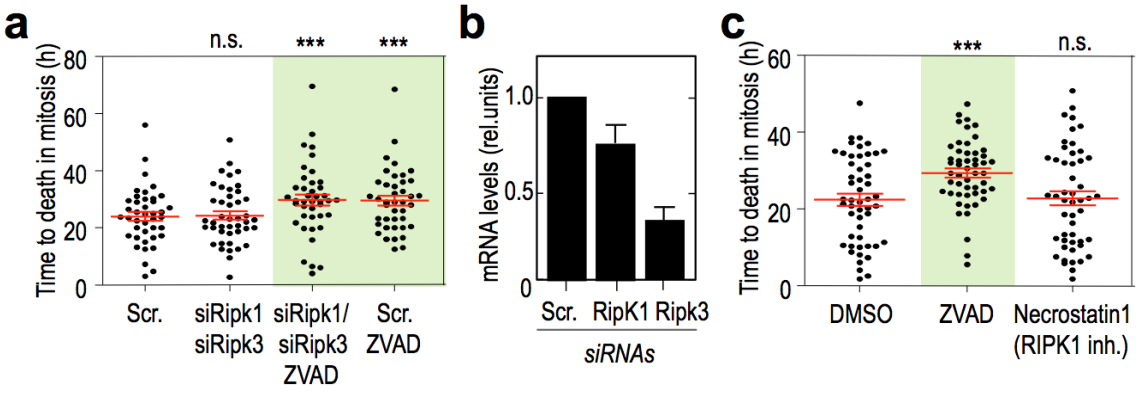

Figure 15. Necroptosis is not involved in mitotic cell death a) Plots representing the duration of mitosis (from mitotic entry till cell death) in Cdc20-null cells treated with the indicated interfering RNAs or in the presence of the caspase inhibitor ZVAD. **b)** Efficiency of siRNA Knockdown by qPCR analysis of mRNA levels (48 h after siRNA nucleofection). Data were normalized by β-actin mRNA levels. **c)** Plots representing the effect of necrostatin in duration of mitosis (from metaphase till cell death) in Cdc20-null cells. In a and c dots represent individual cells and a red line indicates the mean. n.s., not significant. **, p<0.01; ***, p<0.001 (Student's t-test).

2.4 A role for autophagy during mitotic arrest

Autophagy is a highly conserved process in which cytoplasmic content and organelles are surrounded by double-membrane vesicles called autophagosomes (De Duve *et al.,* 1963), which are delivered to lysosomes, for digestion, forming autophasolysosome (Rubinsztein *et al*., 2007). Autophagy can be both, a selective process or a non-selective pathway for degradation of bulk cytoplasmic content (Fimia *et al*., 2013). It is a cellular response to a variety of internal and external stress stimuli like nutrient deficiency, hypoxia, ER stress, oxidative stress and activated oncogenes. It is critical during starvation in order to provide essential nutrients during stress and also serves as a quality control to remove damaged and dysfunctional organelles, misfolded proteins, etc. Typically is a protective pro-survival response, however, if hyperactivated, it will ultimately kill the cell (Rosenfeldt and Ryan, 2011) considered an independent form of programmed cell death, called type II cell death (Galluzi *et al.,* 2012). Three types of autophagy are defined, depending on the route of delivery to the lysosome: microautophagy, charepone-mediated autophagy and macroautophagy. In this work we will focus on macroautophagy, hereafter simply termed autophagy.

Autophagy has been proposed to be inhibited in mitosis (Eskelinen *et al.*, 2002, Furuya T *et al.*, 2010; Gwinn *et al*., 2010; Ramírez-Valle *et al*., 2010), however, it has also been shown that autophagy can persist during mitosis (Liu *et al.,* 2009), so we tested the changes in this process during entry into mitosis and prolonged mitotic arrest. One of the hallmarks of autophagy is the conversion of the soluble form of the microtubule-associated protein 1 light-chain 3 (LC3b-I), to the lipidated and membrane-associated form (LC3b-II), which acquires a cytoplasmic dotted pattern. To gain insight into the possible role of autophagy in MCD, the autophagic flux was scored using a fluorescent-tagged LC3 sensor in which the pH sensitivity differences exhibited by GFP (green fluorescent protein) and RFP (red fluorescent protein) can monitor progression from the autophagosome to autophagolysosome (Kimura *et al.,* 2007, Mizushima *et al.,* 2010). Whereas autophagosomes emit both mRFP/GFP signals, autolysosomes emit only an acid-stable mRFP signal because the pH-sensitive GFP signal is quenched in acidic lysosomes. Cdc20-null cells were first synchronized in G2 using the Cdk1 inhibitor RO-3306 and mitotic entry and progression were monitored after release from this compound (Figure 16a and Figure 16a,b). The levels of puncta LC3 signals were modest during normal mitosis in asynchronous cultures in the absence of 4-OHT or in the initial arrest in Cdc20-null cells (Figure 16b). However, both the green and red signals accumulated with time upon prolonged mitotic arrest, indicating that autophagy is a dynamic process and that autophagic flux is not impaired in mitosis. Accumulation of puncta LC3b-II was significantly prevented in the presence of the Class III PI3K inhibitor 3-methyladenine (3MA), and increased upon treatment with the mTOR inhibitor PP242. Together this data indicates the presence of a dynamic authophagy flux in mitotic cells.

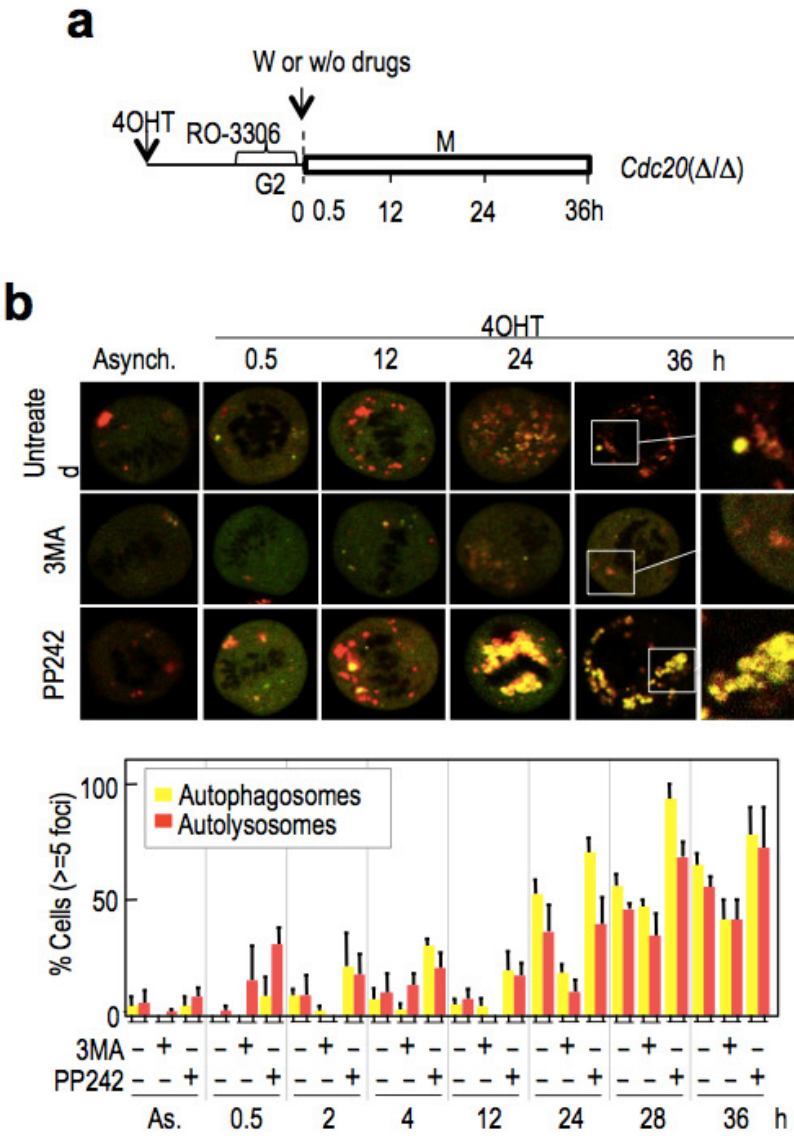

Figure 16. Dynamic autophagy in prolonged mitosis. **a)** Protocol for Cdc20-null cells synchronization, 4-OHT is added to an asynchronic culture 12 hours before the RO-3306 addition. Treatment with this Cdk1 inhibitor for 18 hours will synchronize cell at the edge of G2-M phase. RO-3306 wash out allows cell to progress to mitosis in the absence of Cdc20. **b)** Life confocal microscopy pictures of Cdc20-null cells transiently expressing the CherryLC3GFP system in the presence of an mTOR inhibitor and a 3MA. Colocalization of Cherry and GFP is present in autophagosomes, whereas in a more advanced stage of autophagy GFP is loss after acidification by the fusion of autophagosomes with lysosomes. Quantification of the autophagic flux, the criteria for considering a cell positive for autophagy is the presence of at least 5 puncta. Data are represented as the mean ± SEM (n=30 cells per condition).

The presence of double-membrane vesicles with the morphological features of autophagosomes was also verified by electron microscopy in *Cdc20*(Δ/Δ) (Figure 17). Following the same protocol for synchronization, pictures were taken after 6, 24 and 36 hours of mitotic arrest, and in asynchronous cultures. In addition, co-incubation during mitotic arrest with the lysosomal protease inhibitors E64D (a calpain and cathepsin B inhibitor) and pepstatin A (PA, an inhibitor of aspartic proteases), which blocks the last step of autophagic degradation, enhanced the accumulation of autophagic vesicles present per cell.

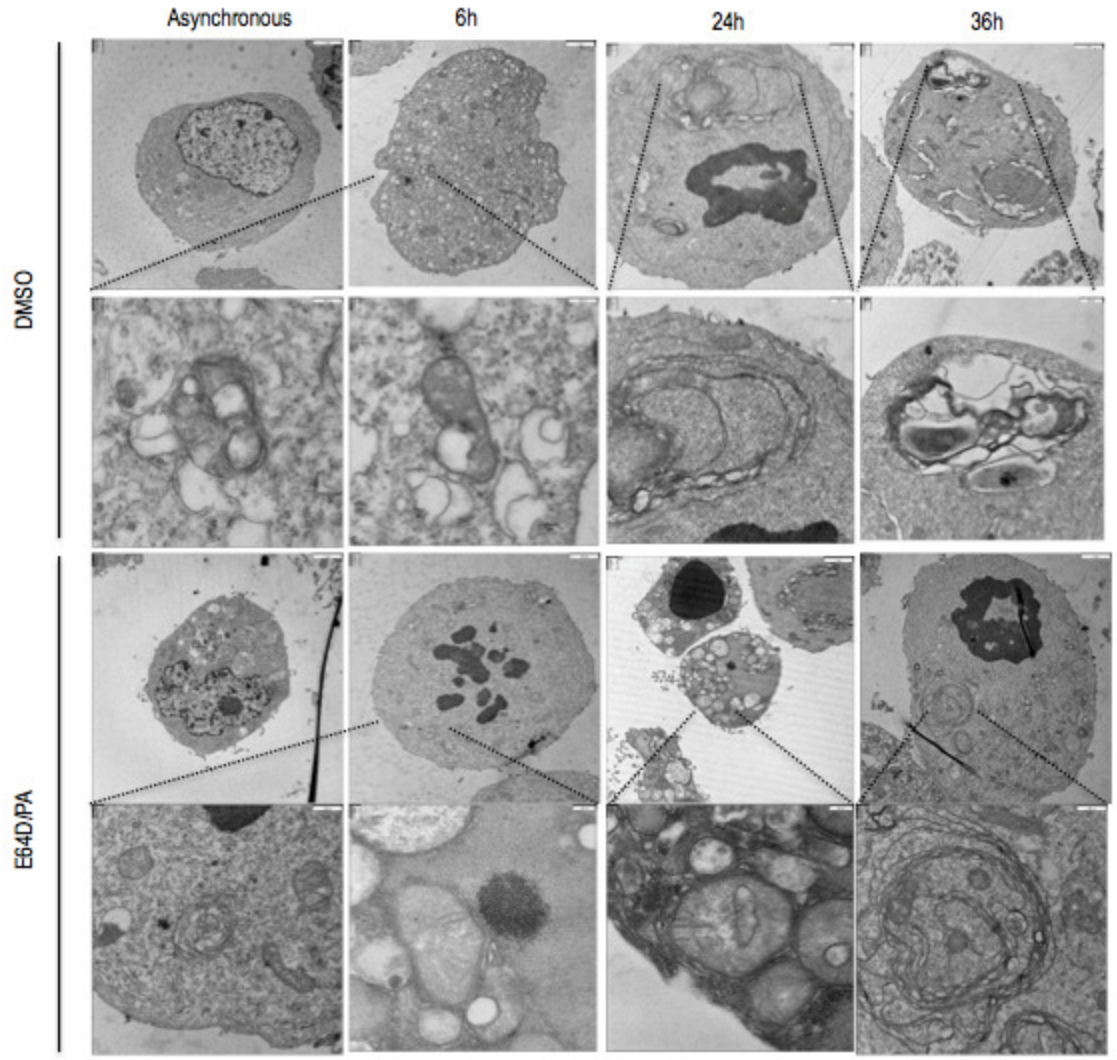

Figure 17. Presence of autophagosomes in cells arrested in mitotic. Electron microscopy pictures from Cdc20-null after 6, 24 and 36 hours of mitotic arrest and asynchronous cultures, in the presence and absence of E64D/PA. Shows an accumulation of autophagosomes in time, which is potentiated by the addition of E64D/PA. Scale bars 2µM.

The presence of LC3bII is markedly increased after 24 or 36 h of mitotic arrest in parallel to the cleavage of caspase-3, both in mouse and human cells indicating the concomitant presence of autophagy and apoptosis in these cultures (Figure 18a-b).

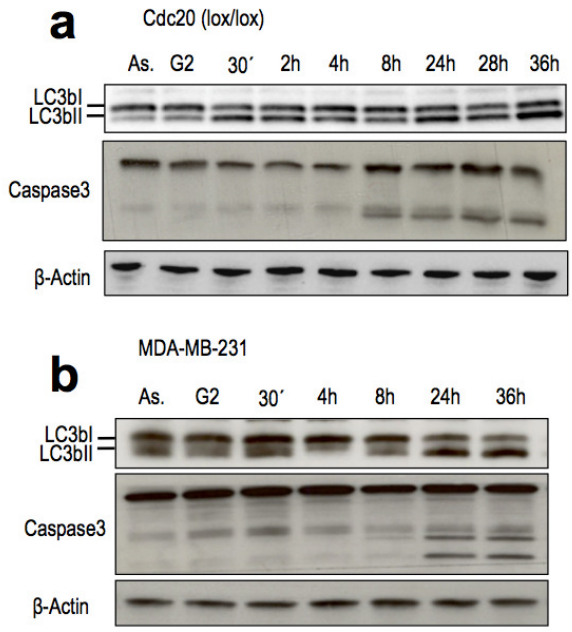

Figure 18. LC3bII increases throughout the time of mitotic arrest concomitantly to caspase-3 activation. a) Inmunodetection of the indicated proteins in Cdc20-null cells. The phosphorylated form of Akt at Ser473 rapidly decreases upon mitotic onset whereas ERK phosphorylation (Thr-202/Tyr204) fluctuates during mitotic arrest. LC3bII accumulates in time concomitantly with caspase 3 activation in Cdc20-null MEFs. **b)** Inmunodetection of the indicated proteins in MDA-MB-231 breast cancer cell line. Cdc20-null cells and human cell lines were synchronized at the G2/M boundary by inhibition of Cdk1, upon RO-3306 addition, 18 hours after cells were released from RO-3306. For human cells the release from Cdk1 inhibition is performed in the presence of taxol and proTAME (an APC/C inhibitor), mimicking the arrest imposed by Cdc20 ablation.

For a deeper characterization of autophagic flux in mitosis, we performed a LC3 turnover assay in Cdc20 null and MDA-MB-231 cells. The increased LC3bII levels after blockage of the last step of autophagic degradation by E64D/PA treatment confirms the presence of a dynamic autophagy flux during mitosis. The ratio (LC3bII vehicle/LC3bII in the presence of E64D/PA) represents the amount of LC3b that it is being loaded onto the autophagosomes at any given time (Klionsky *et al.,* 2012). This ratio was normalized to one hour after release from G2, which is the average duration of a physiological mitosis, and represented in Figure 19. There is a tendency to LC3bII accumulation over time of mitotic arrest in both murine and human cells, however, levels of LC3bII are slightly lower at 1 hour of arrest compared to the levels of asynchronous cultures, this suggest the presence of basal autophagy in interphase which is reduced upon mitotic entry, but potentiated in a prolonged mitotic arrest (Figure 19).

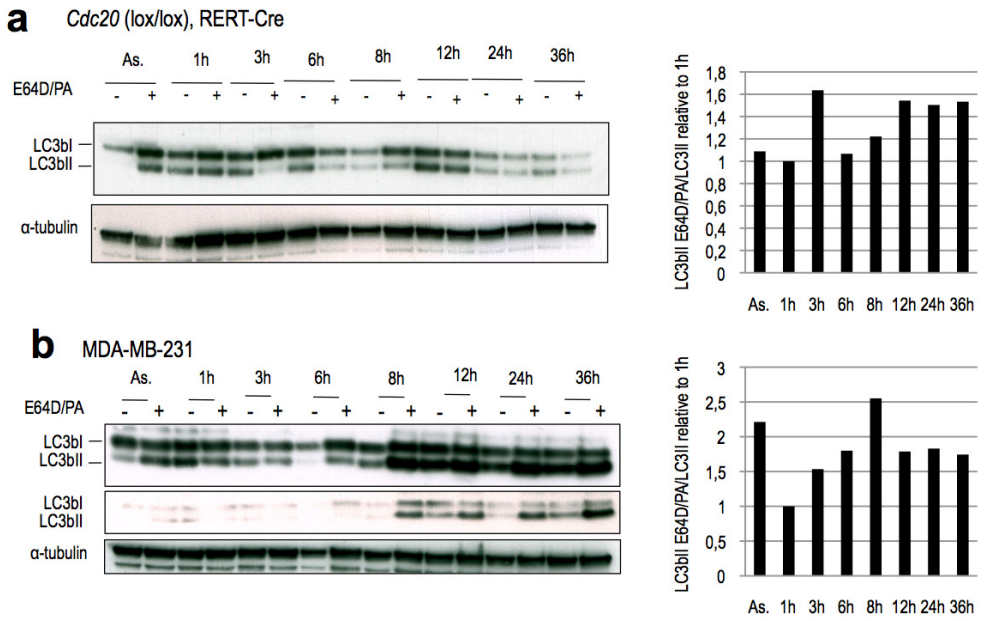

Figure 19. LC3 turnover assays show active autophagic flux in MEFs and human cell lines. **a)** Inmunodetection of the indicated proteins in Cdc20-null cells and quantification of LC3b levels in the presence and absence of E64D/PA double treatment, in asynchronic culture and Cdc20-null cells over time relative to one hour after RO-3306 release. **b)** Inmunodetection of the indicated proteins in MDA-MB-231 cells arrested in mitosis after RO-3306 release in the presence of

taxol and pro-TAME. Quantification of LC3b levels in the presence and absence of cathepsin and calpains inhibitors in asynchronic culture MDA-MB-231 cells arrested in mitosis relative to one hour after RO-3306 release. LC3bI and II levels are shown in high (upper panel) and low exposure (bottom LC3 panel).

To discard the possibility of a cell-cycle dependent regulation of autophagy HeLa cells were synchronized in S-phase by incubation with thymidine for 24 hours and protein levels of some regulators of autophagy were monitored throughout the cell cycle. Cell cycle phases were identified by flow cytometry profiles of DNA content (Figure 20). The peak of mitosis is reached at 8-10h after S-phase release, corresponding to the higher levels of Cdks substrates phosphorylation. Atg5, Atg7 and LC3b protein levels remain constant throughout the cell cycle, suggesting that autophagy is induced upon prolonged mitotic arrest, but not in a normal mitosis. In addition, LC3bII is more abundant in *Cdc20(Δ/Δ)* (cells arrested in mitosis) than in *Cdc20(lox/lox)* MEFs after RO-3306 release (Figure 20c).

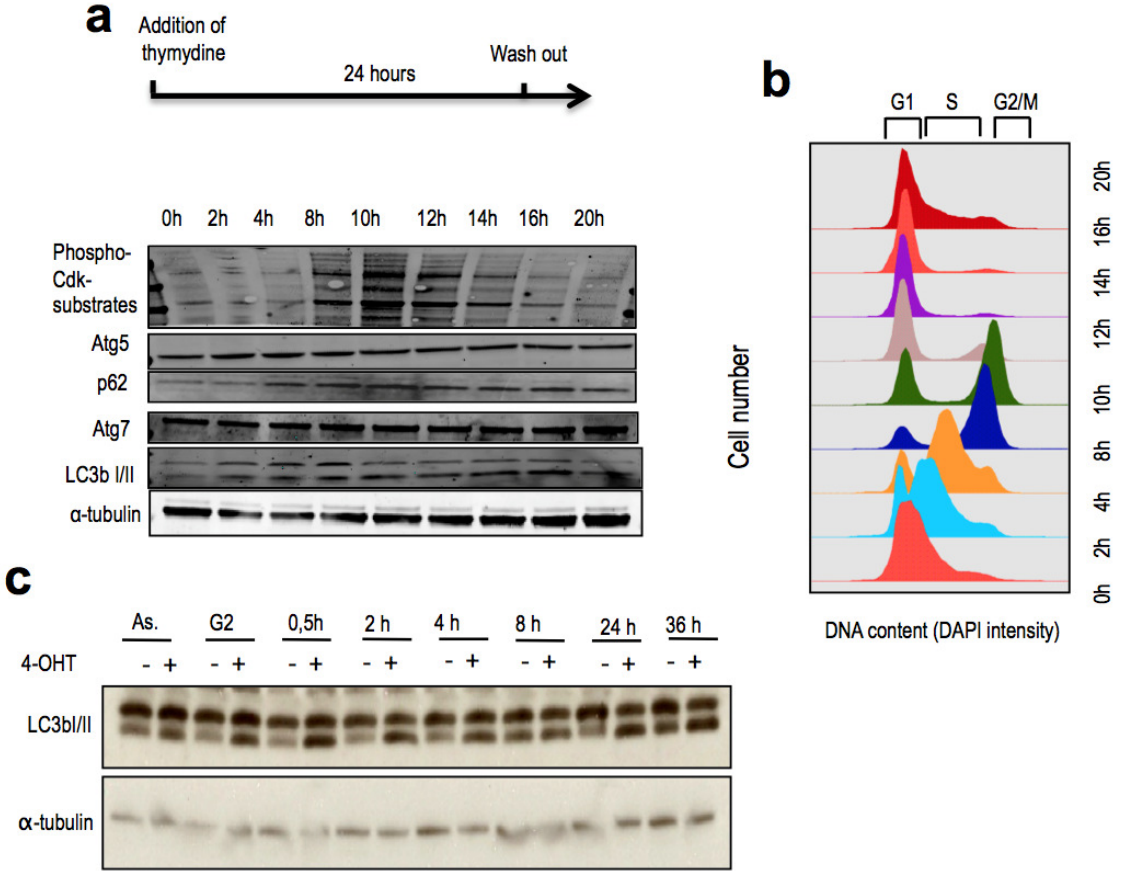

Figure 20. Autophagy is not induced in a normal-lasting mitosis. a) Schematic representation of the protocol for HeLa cells synchronization in S-phase. HeLa cells were treated with thymidine for 24 hours and released into fresh medium, protein levels were inmunodetected. **b)** DNA content y DAPI staining analyzed by flow cytometry. Initially the population is arrests before duplicate DNA content and after wash out of thymidine cell progress through the cell cycle reaching the peak of mitosis between 8-10h, exit mitosis and re-enter a new cell cycle**. c)** Inmunodetection of LC3 protein levels at different time points after release from RO-3306 in the presence (mitotic population) or absence of 4-OHT (cells that underwent normal cell cycle).

The majority of pro-autophagic events converge on the serine/threonine protein kinase mTOR (mammalian target of rapamycin). Another nutrient-sensitive signaling pathway is the class III phosphatidylinositol 3-kinase (PI3KC3 also named Vps34). While mTORC1 is usually repressing the autophagic machinery, Vps34 promotes the activation of autophagy proteins (Atgs) involved in the initial phase of the autophagosome formation. In several scenarios, triggering autophagy relies on the inhibition of mTORC1, an event that promotes the activation of downstream autophagy proteins such as Ulk1 or Vps34 in

complex with Beclin-1 (Rosenfeldt and Ryan, 2011). We next tested whether the presence of autophagy was able to modulate MCD by scoring the SiM upon downregulation of several autophagy regulators (Figure 21). Raptor, the catalytic subunit of mTORC1, is of special relevance during mitosis given that Cdk1 hyperphosphorylation of raptor during this period allows the maintenance of mTORC1 activity during mitosis (Gwinn *et al*., 2010; Ramírez-Valle *et al*., 2010). Knockdown of raptor resulted in earlier death in mitosis whereas downregulation of several proteins involved in the induction of autophagy, such as Ulk, Vps34 or Beclin1, prevented MCD to a similar extent to the apoptosis inhibitor ZVAD (Figure 21a). The requirements for autophagy in MCD were also validated during the MG132-induced mitotic arrest after nocodazole synchronization in prometaphase (protocol in Figure 13a) in Atg5 wild type and null cells (Figure 21c). While in Atg5 wild-type MEFs SiM is 27±25, in Atg5 KO MEFs the duration of mitosis before cell death is extended in 10 hours in average (SiM 30±28).

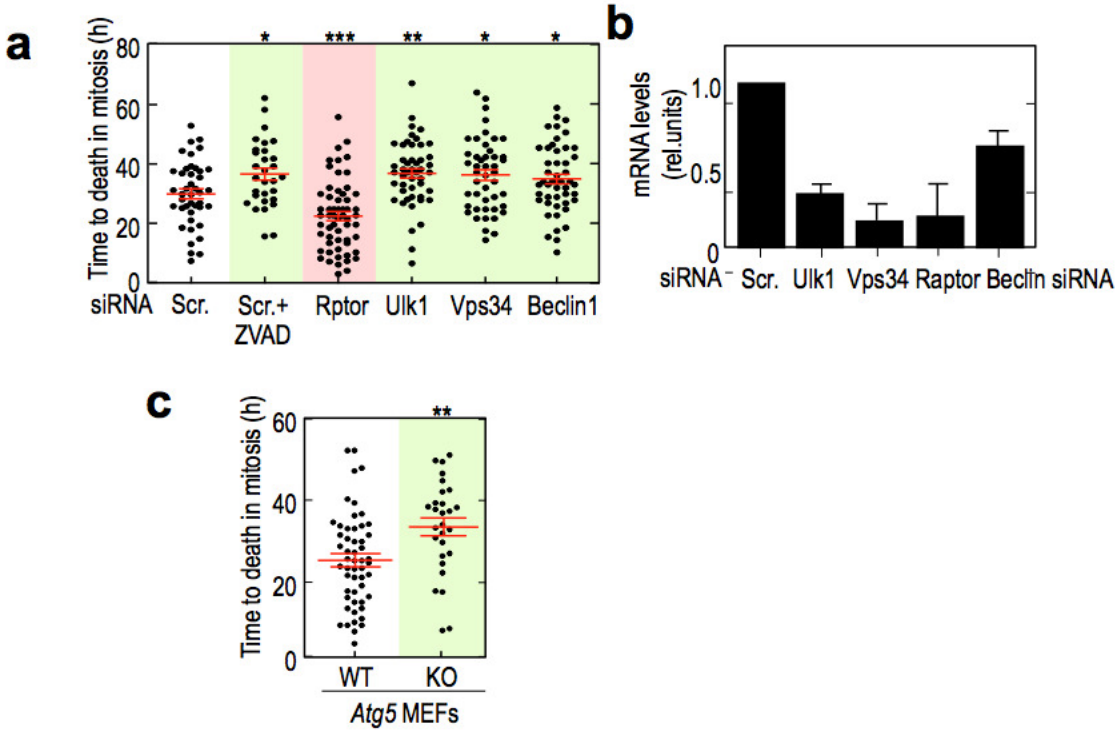

Figure 21. Autophagy modulates mitotic cell death. a) Plots representing the duration of mitosis (from mitotic entry till cell death) in Cdc20-null cells treated with the indicated interfering RNAs or in the presence of the caspase inhibitor ZVAD. **b)** Efficiency of siRNA Knockdown by qPCR analysis of mRNA levels (48 h after siRNA nucleofection). Data were normalized by β-actin mRNA levels **c)** Plots representing the duration of mitosis (from metaphase till cell death) in Atg5 Wt and Atg5 KO MEFs after synchronization in prometaphase with nocodazole treatment and released in MG132**.** In a and c dots represent individual cells and a red line indicates the mean. n.s., not significant. **, p<0.01; ***, p<0.001 (Student's t-test).

Induction of autophagy upon inhibition of mTORC1, by using a variety of mTOR inhibitors, results in premature MCD in Cdc20-null cells (Figure 22a) or mitotic human cells (Figure 22b) and increased LC3bII levels (Figure 22 c-d) in both cell types. ATP-competitors (PP242 and BEZ235) seem to be more efficient in shortening SiM, compared with rapamycin and the rapalog temsirolimus.

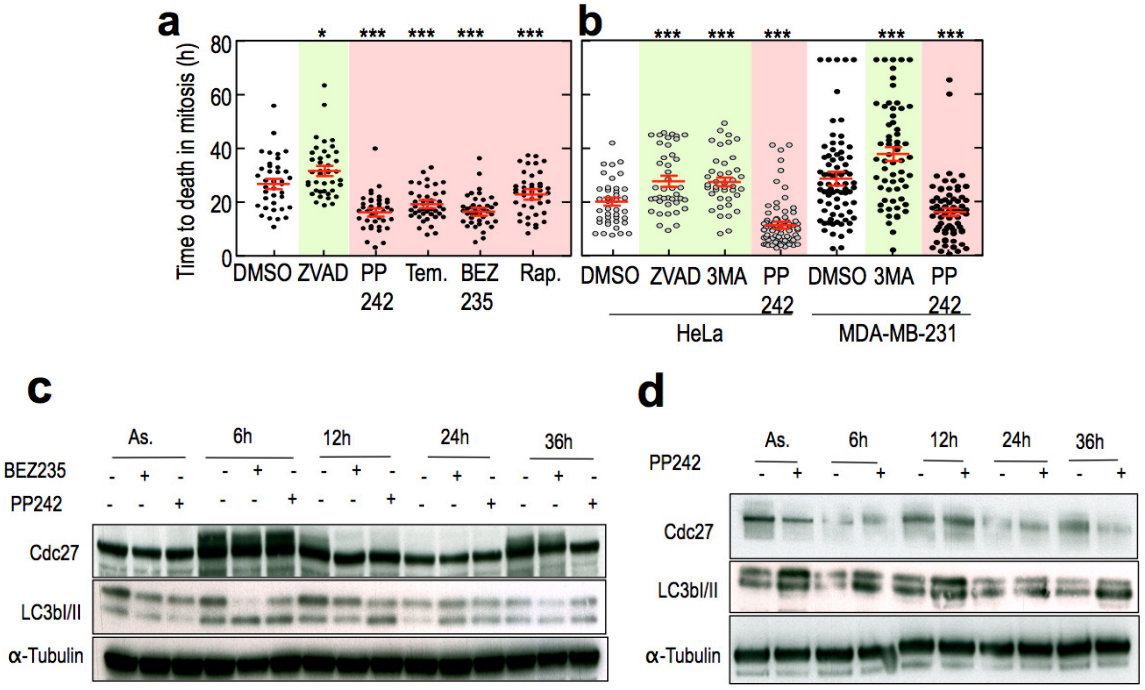

Figure 22. Inhibition of mTOR decreases the time of survival in mitosis by induction of autophagy. a) Plots comparing the duration of mitosis (from metaphase till cell death) in Cdc20-null cells treated with in the presence of the indicated drugs. **b)** Plots comparing the duration of mitosis (from metaphase till cell death) in human cell lines arrested in mitosis treated with in the indicated inhibitors. **c)** LC3bII levels in Cdc20-null cells upon mTORC1 and mTORC2 inhibition in mitosis and interphase. **d)** Inmunodetection of LC3bII levels in human cells upon mTORC1 and mTORC2 inhibition in mitosis and interphase. In a and b dots represent individual cells and a red line indicates the mean. n.s., not significant. **, p<0.01; ***, p<0.001 (Student's t-test).

Inhibition of PI3K class III kinase (Vps34) with 3MA delayed death in mitosis (Figure 23a), yet concomitant inhibition of apoptosis and autophagy by the combination of ZVAD and 3MA did not further enhance SiM and all Cdc20-null cells eventually died in the presence of these two inhibitors (Figure 23a). Moreover, E64D/PA treatment inhibits poly(ADP-ribose) polymerase (PARP-1) cleavage, suggesting that autophagy and apoptosis are tightly coupled processes (Figure 23b) and may act in parallel in driving cell death in mitosis.

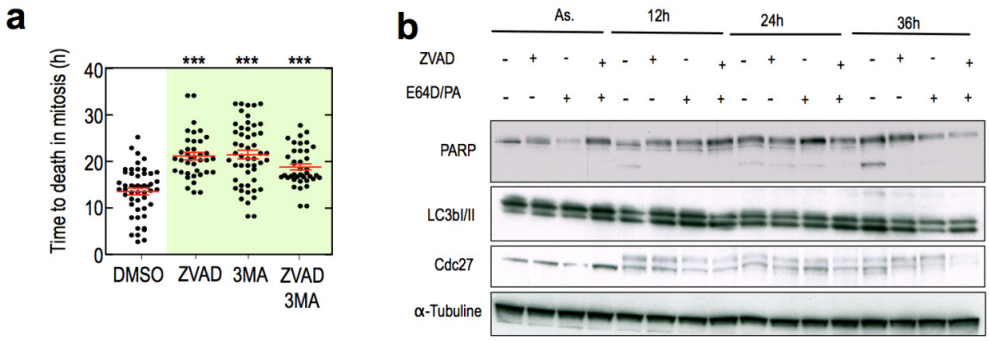

Figure 23. Inhibition of autophagy protects from cell death in mitosis and prevents PARP cleavage. a) Plots comparing the duration of mitosis (from metaphase till cell death) in Cdc20-null cells treated with in the presence of the pan-caspase inhibitor ZVAD and the Vps34 inhibitor 3MA. **b)** Western blot for total protein levels in mitotic arrested Cdc20-null cells and asynchronous cultures. In a dots represent individual cells and a red line indicates the mean. n.s., not significant. **, p<0.01; ***, p<0.001 (Student's t-test).

Due to the lack of molecular markers for necrosis, we attempt to classify MCD morphologically. Electron micrografies (Figure 24) shown in wild-type MEFs the three types of cell death routines, while in

Bak/Bax double knockout MEFs, apoptosis is completely prevented and replaced by autophagy and necrosis, as previously described (Shimizu *et al*., 2004),

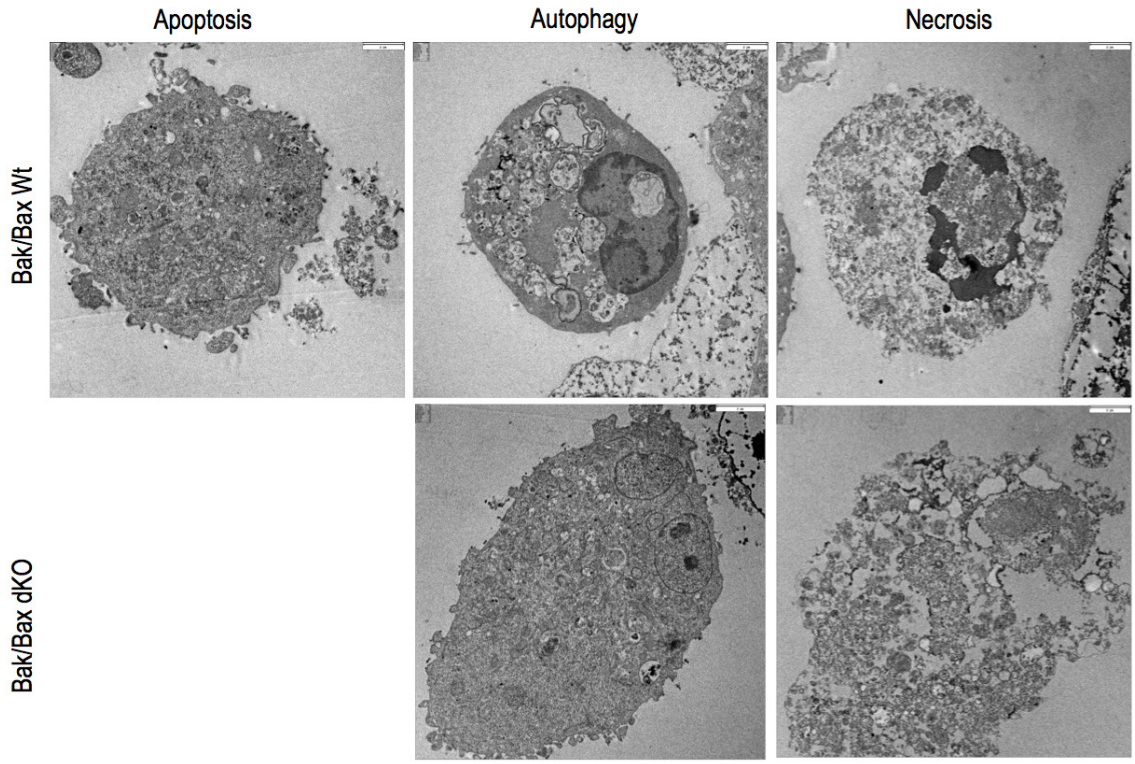

Figure 24. In the absence of apoptotic machinery MCD occurs via autophagy and necrosis. Representative EM micrographies of Cdc20-null MEFs and Bak /Bax double knockout (dKO) MEFs arrested in mitosis shows the different types of cell death. In Bak /Bax WT three types of cell death with different morphological features; apoptosis, autophagy and necrosis can occur, whereas Bak /Bax dKO undergo autophagy, which become evident by the accumulation of double-membrane vesicles and necrotic cell death characterized by pronounced dilation of organelles and empty spaces are formed. For Bak/Bax dKO, apoptotic cells were not found. Scale bars 2μM.

2.5 Mitochondrial mass decreases during prolonged mitotic arrest

Mitochondria are highly dynamic organelles that respond to cellular stress through changes in overall mass, interconnection and subcellular localization. Changes in the overall mitochondrial mass reflect an altered balance between biogenesis and clearance of damaged mitochondria. Dysfunctional mitochondria are a potential source of reactive oxygen species (ROS) and therefore need to be removed in order to prevent cellular damage. Mitophagy is the autophagic process that specifically targets malfunctioning mitochondria for degradation and consequently could be considered as a quality control that increases cellular fitness in healthy conditions (Ashrafi and Schwarz, 2013). Since biosynthesis of new organelles is limited during mitosis due to the lack of proper transcription and translation, we next tested whether mitotic arrest was accompanied by mitochondrial loss.

Mitochondrial mass started to decrease at early time of mitotic arrest (3 hours) and this reduction is potentiated further in time (from 18 h on) as detected by analysis of the intensity of a vital mitochondrial dye, by time-lapse microscopy (Figure 25a) and flow cytometry (Figure 25b). Exposure of mitotic cells to cyanide m-chlorophenyl hydrazine (CCCP, a mitochondrial respiratory chain uncoupler), resulted in decreased mitochondrial mass within the first few hours of arrest in mitosis, whereas little effect is observed during late mitotic arrest when the mitochondrial mass has considerably decreased. This may suggest that the loss of mitochondrial mass is initially due to the lack of mitochondrial biosynthesis, whereas in a more extended mitotic arrest an active process of elimination of dysfunctional mitochondria is taking place. Remarkably,

(Figure 25c) the reduction observed in mitochondrial mass after 3 hours of CCCP exposure it is equivalent to 24 hours of mitotic arrest. Inmunodetection of the mitochondrial proteins Tom20, Tim23 and Tom 40, components of the mitochondrial translocases complex, corroborated the loss of mitochondrial mass and this effect is prevented upon blockage of the last step of autophagy by E64D/PA addition, suggesting a link between the reduction in mitochondrial mass and the observed induction of autophagy.

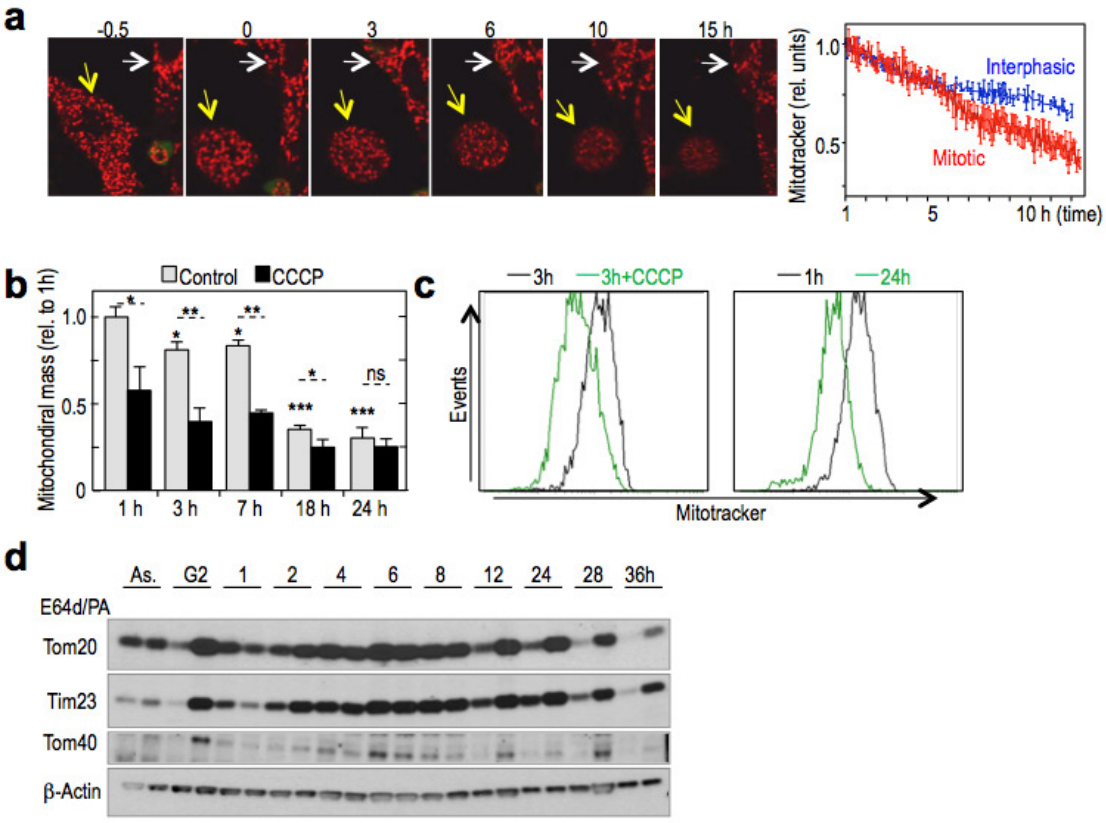

Figure 25. Mitochondrial mass significantly decreases in a prolonged mitotic arrest. a) Mitochondrial signal was followed by time-lapse microscopy at the indicated time points after release of Cdc20-null cells from G2 arrest. White and yellow arrows indicate interphasic or mitotic cells respectively. Mitotracker intensity decreases rapidly in cells arrested in mitosis (red) compared with interphasic cells (blue). Data are represented as mean ± SD (n=18 mitotic and 12 interphasic cells). **b)** Quantification of mitotracker intensity as measured by flow cytometry at the indicated time-points after release from G2 arrest (mean ± SEM). As a positive control,CCCP results in a reduction of the mitochondrial mass at early but not late time points during mitotic arrest in comparison with one hour treated cells (n=7 independent assays).**c)** Inmunodetection of the mitochondrial proteins Tom20, Tim23 and Tom40 in Cdc20-null cells at the indicated times after release from G2. As., asynchronous cultures. β-actin was used as a loading marker.

We next evaluated whether the decrease in mitochondrial mass is due to an active process of mitochondrial degeneration and further elimination through mitophagy. This decrease in mitochondrial mass was accompanied by a gradual increase in colocalization of LC3-GFP foci with mitochondria as is displayed in (Figure 26a) in life cell microscopy assays. The concurrence of LC3-GFP vesicles and mitochondria was evident from 6 hours of mitotic arrest, but this event increases in frequency at later stages of mitotic arrest. Moreover electron microscopy images shows of mitochondrial internalized into double membrane vesicles; autophagosomes (Figure 26b). The loss of mitochondrial mass is efficiently rescued by the addition of the inhibitor of autophagy 3MA and as a consequence of Cyclosporine A exposure (CsA) after 24 hours of mitotic arrest. Mitochondrial membrane permeabilization is one of the triggering events for mitophagy and cyclosporin affects mitochondria by preventing the mitochondrial permeability transition pore from opening and inhibiting cytochrome c release, a potent apoptotic stimulation factor. Thus, inhibition of autophagy (by 3MA) and inhibition of the triggering event for mitophagy (by CsA) results in a significant increase in

mitocondrial mass compared to basal conditions at 24 hours of arrest in mitosis. Together this result suggest the clearance of the mitochondrial pool by mitophagy as a major cellular process leading to the loss of mitochondrial mass during prolonged mitotic arrest, whereas in an early mitotic arrest, this might be due to the lack of mitochondrial biogenesis.

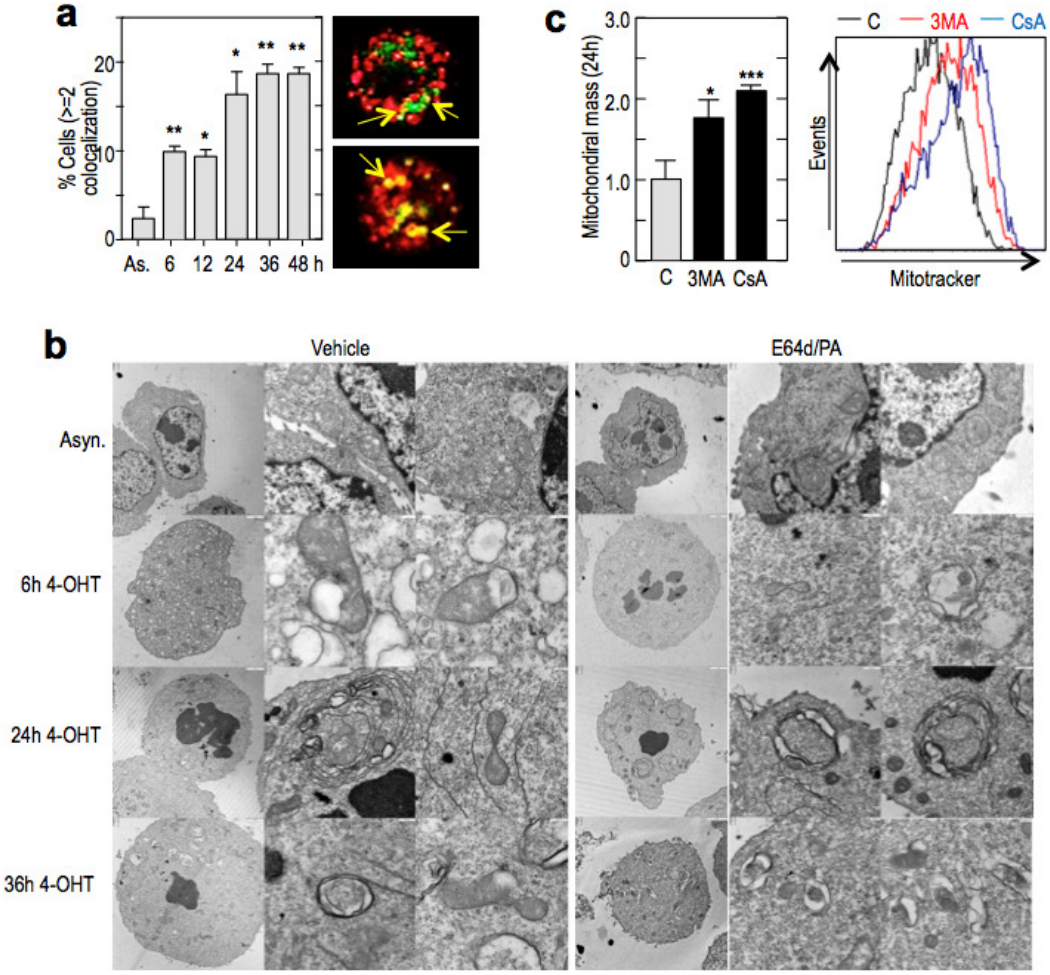

Figure 26. Mitophagy contributes to the decrease in mitochondrial mass during prolonged mitosis. a) Percentage of cells showing co-localization of LC3-GFP and Mitotracker (>2 foci per cell, see yellow arrows in the representative images) at the indicated time points after mitotic arrest. Data represent mean ± SEM; n=30 cells per condition. **b)** Representative electron microscopy micrographs showing the accumulation of autophagosomes and autophagolysosomes in Cdc20-null cells at the indicated time points of mitotic arrest, either in the presence or absence of cathepsin and calpain inhibitors (E64d/PA). Note the inclusion of mitochondria in double-membrane structures with autophagosomal features. Scale bars, 2 μM for low magnificated images and 500 nm for high magnification. **c)** Mitochondrial content as measured by flow cytometry in the presence of Mitotracker in Cdc20-null cells after 24 hours in mitosis in the presence of vehicle (C), 3MA or CsA (related to vehicle treated cells). The plots in the right represent the profile of *Cdc20*(Δ/Δ) after 24 hours in mitosis in the absence or present of 3MA (red) or CsA (blue).

Mitochondrial morphology changes can shift between small fragmented units and larger networks of elongated mitochondria. Remodeling of the mitochondrial network is regulated and takes place in response to many stimuli such as hypoxia, cell cycle regulation and also by changing energy demands and other cellular stress. Upon mitotic onset, mitochondria are fragmented to facilitate the segregation to daughter cells (Álvarez-Fernández and Malumbres, 2014). Cdk1 mediates mitochondrial fission in mitosis by phosphorylation and activation of the dynamin-related protein 1 (Drp1) at Ser-616. Many studies indicate that mitochondrial fragmentation and mitochondrial membrane depolarization precedes mitophagy and that mitochondrial fission is the major source of depolarized mitochondria (Chen *et al*., 2009). Since fragmented mitochondria are known to be more sensitive to mitophagy (Rambold *et al.,* 2011), we next tested whether

Drp1 inactivation confers some protection to mitotic mitochondria. As depicted in Figure 27a, knockdown of Drp1 prevents mitochondrial fragmentation, showing tubular organelles in interphase as well as in mitotic Cdc20-null cells. Knockdown of Drp1 also resulted in reduced co-localization of LC3-GFP foci and mitochondria (Figure 27b). This data correlates with a prevented loss of mitochondrial mass and led to increased SiM in Cdc20-deficient cells (Figure 27c).

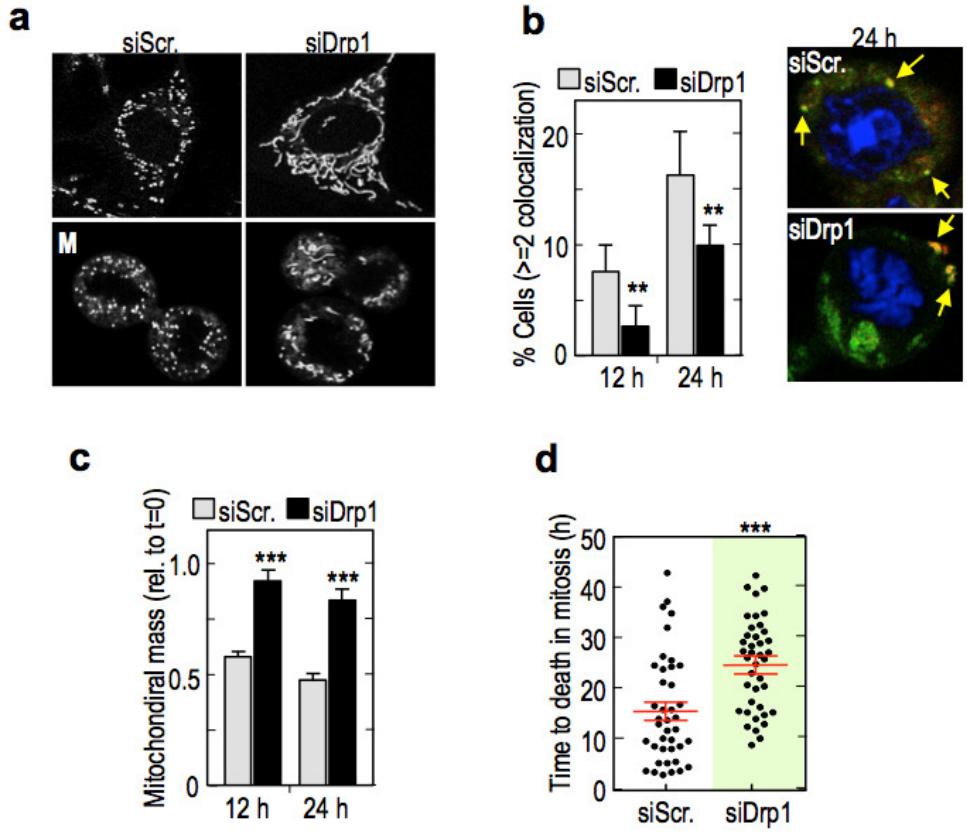

Figure 27. Fragmented mitochondria are more prone to be removed by autophagy. a) Representative confocal microscopy live images showing the mitochondrial network (Mitotracker) of mitotic (Cdc20-null) and interphasic cells in the presence (Scr.) or absence of Drp1 (siDro1) after nucleofection with siRNA against this molecule. I: Interphase and M: Mitosis. **b)** Co-localization of LC3-GFP and Mitotracker at the indicated time points after mitotic arrest in Drp1 Knock-down (siDrp1) cells. Representative confocal microscopy live images show the co-localization of LC3-GFP and Mitotracker after 24 hours of mitotic arrest in siScr. and siDrp1 treated cells. Data represent mean ± SEM (n=30 cells per condition). **c)** Quantification of Mitotracker intensity by cytometry after 12 and 24 hours of mitotic arrest relative to 1 hours of mitotic arrest in the presence (siScr.) or absence (siDrp1) of Drp1. **d)** Plots representing the duration of mitosis (from mitotic entry till cell death) in Cdc20-null in the presence or absence of Drp1In d dots represent individual cells and a red line indicates the mean. n.s., not significant. **, p<0.01; ***, p<0.001 (Student's t-test).

2.6 Mitochondrial respiration extenuates during prolonged mitotic arrest

To further investigate the functional relevance of mitochondrial loss during mitosis, we next compared the rates of mitochondrial respiration (oxygen consumption, OCR) and glycolysis (extracellular acidification rate; ECAR) from mitotic and control cells by using an Extracellular Flux Analyzer (Seahorse Bioscience). *Cdc20*(Δ/Δ) cells were arrested in G2 using RO-3306 for 16 h and released to arrest in mitosis (red) in a synchronized manner. G2-synchronized of asynchronous *Cdc20*(lox/lox) cells were used as controls (Figure 28a). Our results indicated that spare respiratory capacity quickly increased upon mitotic entry in agreement with recent data indicating the activation of the oxidative respiration during the G2/M transition in a Cdk1-dependent manner (Wang *et al*., 2014b). However, the respiratory capacity started to became extenuated

after ~12 h in mitosis (Figure 28b), coincident with mitochondrial mass depletion shown previously in Figure 33 and with cell death (Figure 28b). In parallel to decreased oxidative respiration, glycolytic capacity gradually increased during early mitotic arrest but is further boosted during late mitotic arrest in mouse (Figure 28a) as well as in human (Figure 36b) cells. This metabolic profile indicates that a progressive switch from oxidative phosphorylation to glycolysis is taking place in prolonged mitotic arrest. While cell viability in proliferating cells (blue) remains constant, cells that underwent mitotic arrest (red) show decreased cell viability with time (Figure 28b, d), therefore OCR and ECAR rates are probably being underestimated in cells arrested in mitosis.

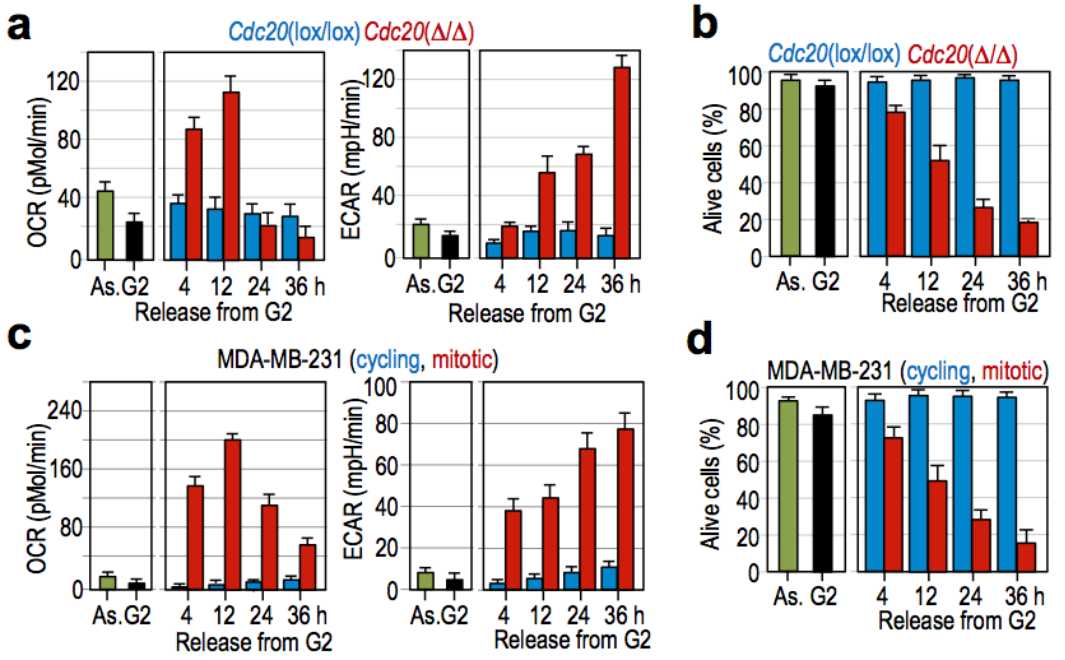

Figure 28. Mitochondrial respiration extenuates in parallel to increased glycolysis upon prolonged mitotic arrest. a) Spare respiratory capacity considered as the difference between maximal uncontrolled oxygen consumption rate (OCR), after FCCP addition, and basal OCR levels, as a measure of cells to respond to stress under conditions of increased energy demands, which is influenced by the capacity of the mitochondria. And maximum glycolytic capacity which is the difference between the maximum extracellular acidification rate **(**ECAR), after inhibition of ATP synthase by oligomycin, and the initial ECAR levels and measures in Cdc20-null (red) and *Cdc20(lox/lox)* MEFs (blue), at different time points after RO-3306 release. It is also included as G2 *Cdc20(lox/lox)* cells in the presence of RO-3306 (black) and asynchronous MEFs (green). **b)** Cell viability measured by flow cytometry in Cdc20-null (red bars) and *Cdc20(lox/lox)* after RO-3306 wash out at different time points, in the presence of RO-3306 as a G2 condition (black) and in asynchronic sells (green). Cell viability is represented as the percentage of alive cells, which are cells that do no retain To-Pro3. **c)** Spare respiratory capacity and glycolytic in MDA-MB-231 (red bars) and mitotic MDA-MB-231, which is in the presence of taxol and pro-TAME, after RO-3306 wash out at different time points, in the presence of RO-3306 as a G2 condition (black) and in asynchronic sells (green). **d)** Cell viability measured by flow cytometry in MDA-MB-231 (red bars) and mitotic MDA-MB-231, which is in the presence of taxol and pro-TAME, after RO-3306 wash out at different time points, in the presence of RO-3306 as a G2 condition (black) and in asynchronic sells (green). Cell viability is represented as the percentage of alive cells, which are cells that do no retain To-Pro3.

In line with these observations, mitochondrial dysfunction was accompanied by increase in intracellular reactive oxygen species (ROS; Figure 29a) which is attenuated by the addition of the cell antioxidant N-acetyl-L-cysteine (NAC). Prevention of ROS by NAC administration resulted in prolonged survival during mitotic arrest both in mouse and human cells (Figure 29b). It has been recently described that taxol leads to ROS accumulation (Alexandre *et al*., 2007), whether this is a consequence of the mitotic state is not known. The p38MAPK pathway is strongly activated in response to several cellular stress, among them is activated in response to ROS (Cuadrado and Nebreda, 2010; Sato *et al*., 2014). Inhibition of p38MAPK activity leads to an increase in SiM, however in combination with caspase and autophagy inhibitors did not lengthen the SiM, suggesting that are independent pathways.

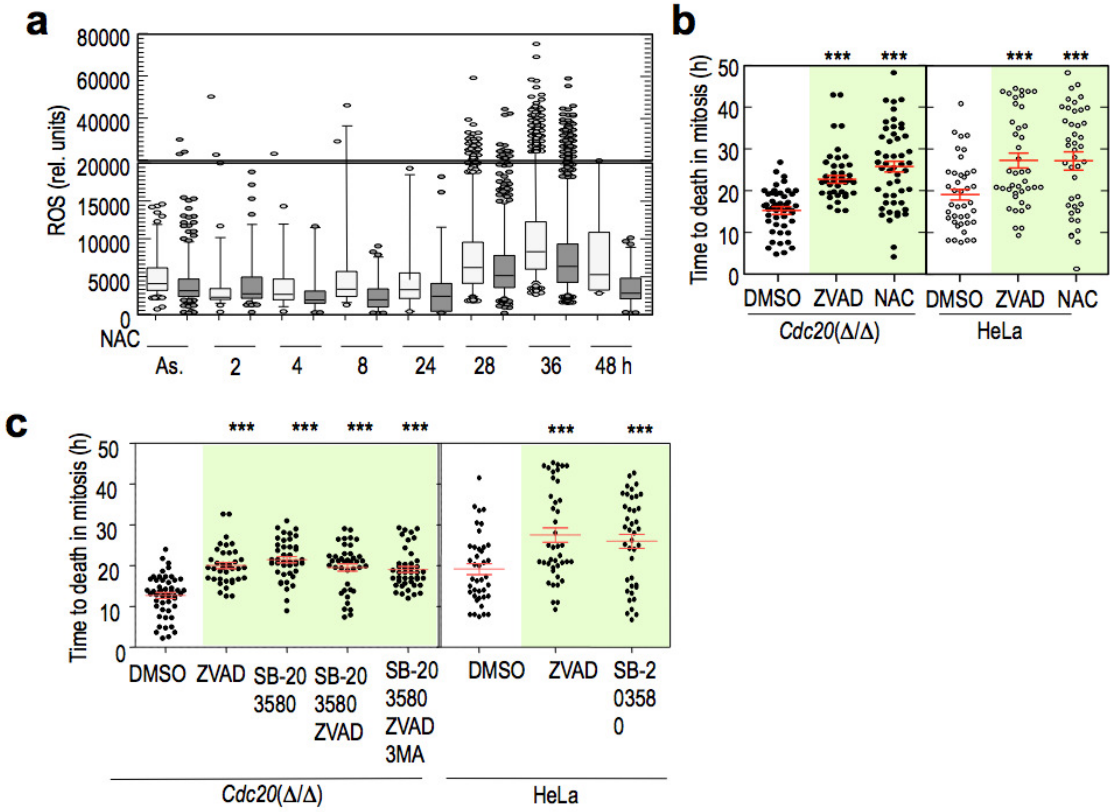

Figure 29. ROS are accumulated over time in prolonged mitotic arrest. a) ROS measure in Cdc20-null cells as determined by the Oxiselect TM intracellular ROS assay kit. Effect of NAC treatment in the accumulation of ROS at the times indicated**. b)** Plots representing the duration of mitosis (from metaphase till cell death) in Cdc20-null MEFs and human cell lines arrested in mitosis treated with a ROS scavenger. **c)** Plots representing the duration of mitosis (from metaphase till cell death) in Cdc20-null MEFs and human cell lines arrested in mitosis treated with p38MAPK inhibitor in combination with caspase and autophagy inhibitors. The differences between treatments were not statistically significant. In b and c dots represent individual cells and a red line indicates the mean. n.s., not significant. **, p<0.01; ***, p<0.001 (Student's t-test).

ROS are constantly generated as byproducts of normal mitochondrial active metabolism under physiological conditions. Mitochondrial respiration is indeed the major source of intracellular ROS, approximately 1-5% of the total oxygen consumed during normal respiration is converted to superoxide radicals. Low levels of ROS can activate various signaling pathways to stimulate cell proliferation and survival, whereas excess of ROS irreversible damage cellular macromolecular components (protein, lipids, nucleic acids) and cause cell death, including apoptosis (Cairns *et al.,* 2011). Besides, membrane depolarization and excessive ROS production are triggering events for mitophagy (Bolland *et al*., 2013).

2.7 AMPK-dependent induction of glycolysis during mitotic arrest

We next investigated the molecular changes that accompany prolonged mitotic arrest by analyzing the phosphorylation of several regulators of key pathways upon a synchronized release from G2 arrest in the absence of Cdc20. Mitotic arrest was accompanied by the accumulation of phospho-histone H3 and the reduced mobility of Cdc27 as a consequence of its mitotic phosphorylation (Figure 30b). In addition, Mcl-1 proteins decreased likely as a consequence of its ubiquitin-dependent degradation mediated by the SCF complex (Inuzuka *et al.,* 2011; Wertz et al., 2011). In contrast, the level of expression of survivin did not change. Interestingly, mitotic arrest was accompanied by a progressive activation of AMPK as detected by increased AMPK phosphorylation of a threonine (Thr-172) within the activation loop of the kinase domain both in Cdc20-null and mitotic human cells (Figure 30b,d). Phosphorylation of AMPK is followed by the inhibitory

phosphorylation of ACC (Acetyl-CoA-carboxilase) at Ser-39 (Figure 30d) inhibiting carboxylation of acetyl-CoA to produce malonyl-CoA, the initial step for synthesis of fatty acid. AMP-activated protein kinase (AMPK) plays a major role in regulating cellular energy balance by sensing and responding to increases in AMP/ADP concentration relative to ATP. Binding of AMP causes allosteric activation of the enzyme and binding of either AMP or ADP promotes and maintains the phosphorylation of Thr-172 within the activation loop of the kinase.

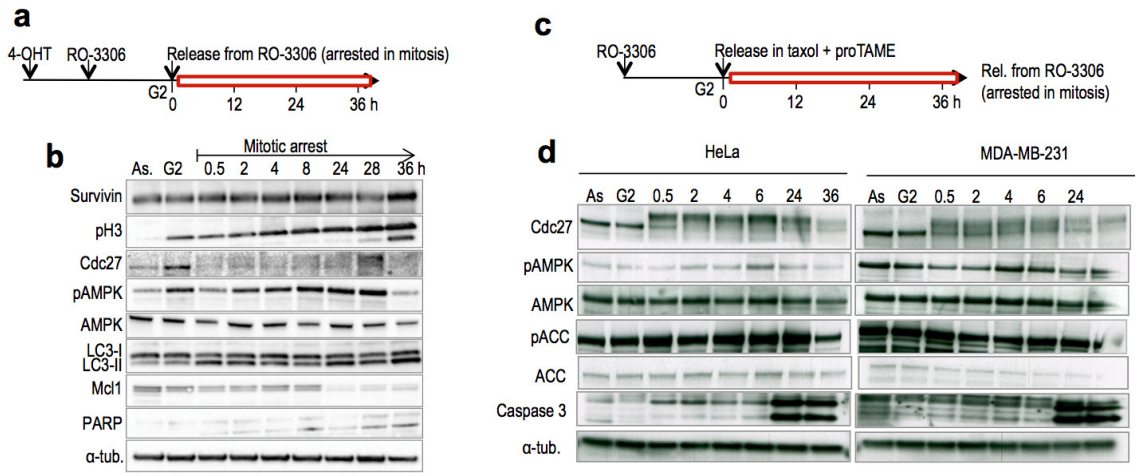

Figure 30. AMPK is reactivated in a prolonged mitotic arrest. a) Protocol performed for achieve the synchronization in Cdc20 MEFs. 4-OHT was added 12 hours before RO-3306 administration. After 18 hours of treatment, RO-3306 removal allows cell to enter mitosis. **b)** Inmunodetection of the indicated proteins in Cdc20-null cells and asynchronous cell (As) are included. **c)** Protocol performed for achieve the synchronization in human cell lines. Cells were synchronized in G2 upon RO-3306 addition. After 18 hours, cells were released from Cdk1 inhibitor in taxol and proTAME, an APC/C inhibitor used at a concentration that inhibits APC/C-Cdc20. **d)** Inmunodetection of the indicated proteins in HeLa and MDA-MB-231 cell lines arrested in mitosis and asynchronous cells (As).

Changes in AMPK activity in response to metabolic stress were also monitored at the single cell level using a FRET biosensor (Tsou *et al.*, 2011). Time-lapse microscopy assays showed that AMPK is gradually activated after ~8 h in mitotic arrest in *Cdc20*(Δ/Δ) (Figure 31a) reaching a 2-fold increase in the biosensor signal after 8 hours of mitotic arrest, in agreement with the biochemical data presented earlier. Whereas no major changes were found during a normal mitosis/G1 transition in control *Cdc20(lox/lox)* cell (Figure 31b). As a control, AMPK activity was monitored in *Cdc20*(lox/lox) MEFs in the presence of 20mM of 2-DG. Addition of 2-DG leads to an increased in the biosensor of about 2-fold, similar to 8 hours of mitotic arrest (Figure 31c). Since AMPK is activated in the presence of reduced ATP and increased AMP, we next quantify the ratio between these two nucleotides at different moments of mitotic arrest. Cells arrested in G2 displayed increased phosphorylation of AMPK (Figure 31d) in agreement with increased AMP/ATP levels (black in Figure 38d), suggesting defective ATP production in the presence of the Cdk1 inhibitor RO-3306, this defect is likely a consequence of Cdk1 inactivation by RO-3306 given the crucial role of Cdk1 in activating mitochondrial function during G2/M transition (Wang et al, 2014). The AMP/ATP ratio was normalized after release from this compound in control *Cdc20*(lox/lox) cells (blue) that underwent a normal transition through the different phases of the cell cycle. In *Cdc20*(Δ/Δ) cells, the AMP/ATP ratio displayed a gradual increase ~8 h after mitotic arrest (red in Figure 32d) in agreement with the timing of AMPK activation (Figure 31a and 31b).

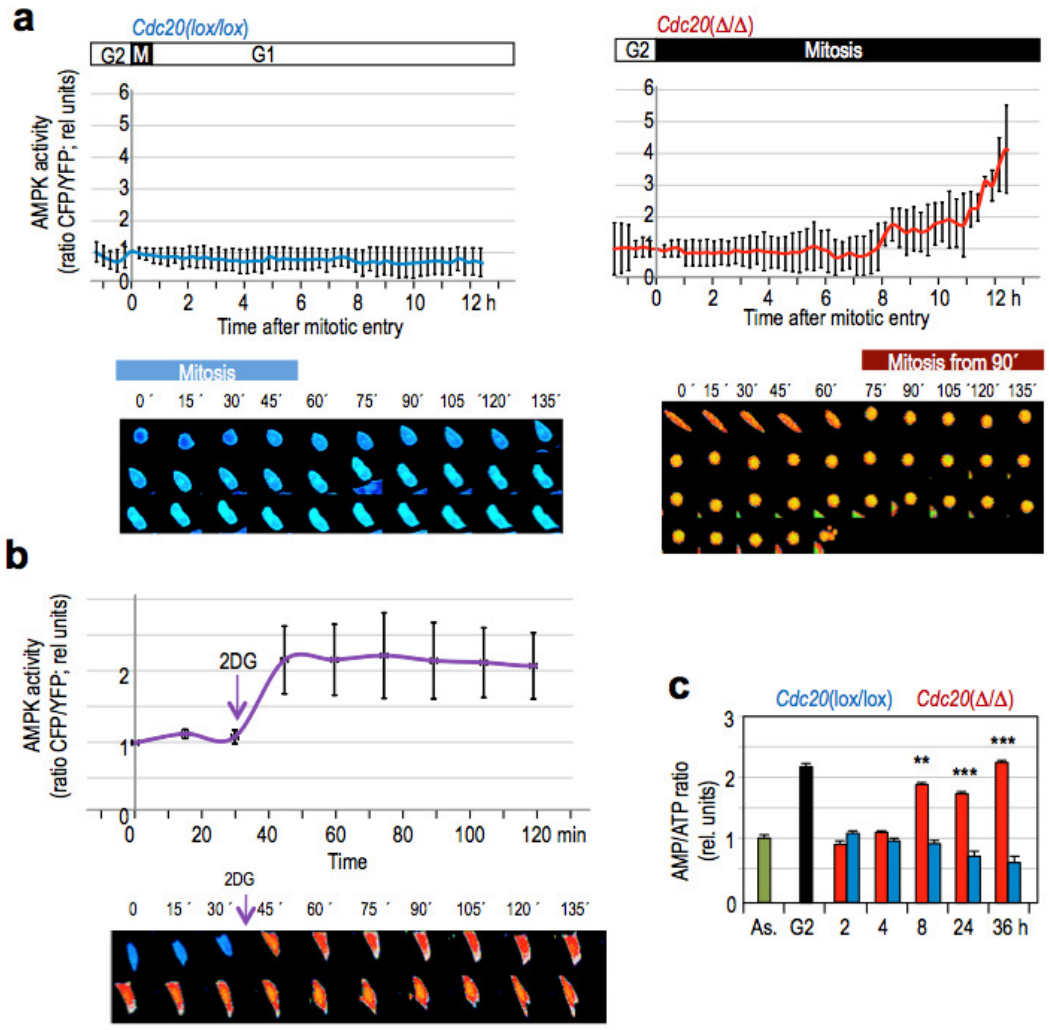

Figure 31. AMPK is reactivated in prolonged mitotic arrest a) Changes in AMPK activity were monitored using a FRET biosensor in *Cdc20*(Δ/Δ) (red) and *Cdc20*(lox/lox) (blue) Time 0 indicated mitotic entry and the length of the black bar represents the duration of mitosis. AMPK is activated giving an increase of about 2-fold in the biosensor signal at 8 hours after and reaches 4-fold at 12 hours after mitotic entry in *Cdc20*(Δ/Δ), whereas no major changes in AMPK activity are observed in *Cdc20*(lox/lox) cells. Data are represented as mean ± SD (n= 12 cells). *Cdc20*(lox/lox), after mitotic exit AMPK levels remain constant. Representative micrographies shows the level of activity of AMPK FRET biosensor indicated by the color scale, where yellow represents the, higher activity of AMPK, increased FRET, followed by red and blue, which represent the lowest activity. Pictures were taken every 15 minutes. **b)** AMPK activity FRET biosensor in *Cdc20*(lox/lox) after addition of 2-DG, AMPK is activated leading to an increase of about 2-fold in the biosensor signal, indicated in red in the images after 2-DG addition. **c)** AMP: ATP ratio measured by HPLC in Cdc20-null (red) and *Cdc20(lox/lox)* (blue) MEFs after release from RO-3306. There are also included measures from asynchronous cultures (green) and as a G2 stage, nucleotides levels were measured in the presence of RO-3306.

It has been recently reported that the inhibitory phosphorylation of ACC decreases prior to cytokinesis initiation increasing fatty acid synthesis upon division, in addition, inhibition of fatty acid synthase (FAS) arrests cells at G2/M despite the presence of abundant fatty acid in the media (Scaglia *et al*, 2014). However, in Cdc20-null cells inhibition of FAS upon C75 treatment shows no effect in cell viability in mitosis (Figure 32).

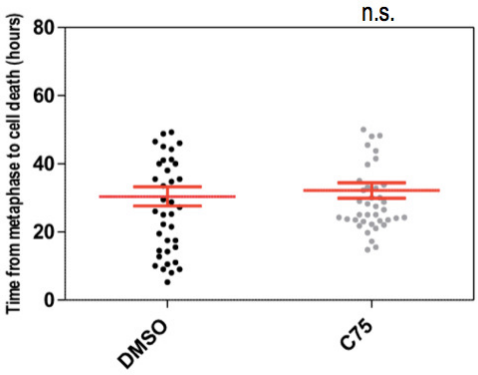

Figure 32. FAS inhibition does no affect cell viability in prolonged mitotic arrest. Plots representing the duration of mitosis (from metaphase till cell death) in Cdc20-null MEFs. Treatment with C75 did not affect cell viability in mitosis. Dots represent individual cells and a red line indicates the mean. n.s., not significant. (Student's t-test).

To further understand these metabolic changes, murine and human cells were growth in the presence of ^{13}C-labeled- glucose and the abundance of different metabolites were analyzed (Figure 33 and 34) after synchronization (Figure 33a). This analysis indicated that mitotic arrest resulted in a significantly higher consumption of glucose and a proportional generation of ^{13}C-lactate, originated from glucose breakdown, in Cdc20-null cells (Figure 33c, red) as compared to G2-released *Cdc20(lox/lox),* non-arrested cells (blue) or asynchronous cultures (green). Mitotic arrest in Cdc20-null cells was also accompanied by a significant consumption of multiple amino acids and pyruvate, whereas Ala, Glu and Gly, along several ketonic bodies, were released to the extracellular medium (Figure 33d). Synthesis of ketonic bodies can occur in response to unavailability or low glucose levels after exhaustion of cellular carbohydrate stores as a consequence of fatty acid break down. As it was previously discussed for the respirometry assays, viability in Cdc20-null cells decreases in a 50% upon 12 hours of arrest in mitosis, and therefore metabolites concentration of Cdc20-null cells were underestimated.

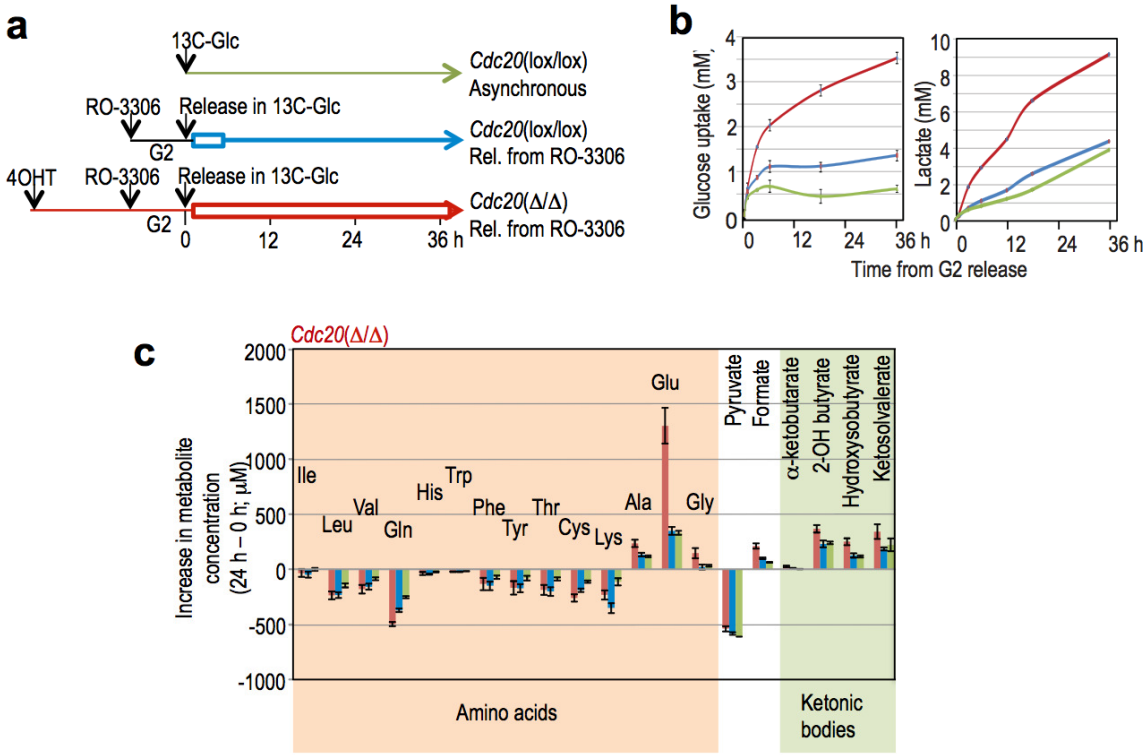

Figure 33. Metabolic profile of Cdc20 null cells. a) Schematic representation of the protocol followed for synchronized mitotic entry in *Cdc20*(lox/lox) cells (without 4-OHT) or Cdc20-null, treated with 4-OHT, to eliminate Cdc20 expression, 12 hours prior the addition of the Cdk1 inhibitor RO-3306 to trigger G2 arrest. This compound was washed-out 18 hours later, allowing cells to

progress through the cell cycle *Cdc20*(lox/lox) (blue), or arrest in mitosis (red). Green line represents asynchronous cultures. This color code is maintained throughout the manuscript to clarify the identification of the three ways of synchronization. **b)** Concentration of extracellular glucose-^{13}C and lactate-^{13}C present in the supernatant of cells in culture, which represents the glucose uptake and the concomitant production of lactate of cultured cells, monitored by NMR. Asynchronous in green, normally released from G2 (blue) or mitotic arrested (red) MEFs**. d)** Differential extracellular concentration of the indicated metabolites 24 hours after RO-3306 release compared to time zero (fresh media) as monitored by NMR. 35 metabolites were analyzed and only those exhibiting significant differences are represented (20 out of 31). No differences were found in carnosine, adenine, glyoxylate, glycerol, cholesterol, EtOH, niacinamide, acetate, inositol, asparagine and aspartic acid.

This increase in glucose uptake and generation of lactate was also observed in human cells subjected to a mitotic arrest triggered by microtubule poisons in the presence of APC/C inhibitors (proTAME) to prevent mitotic exit (Figure 41).

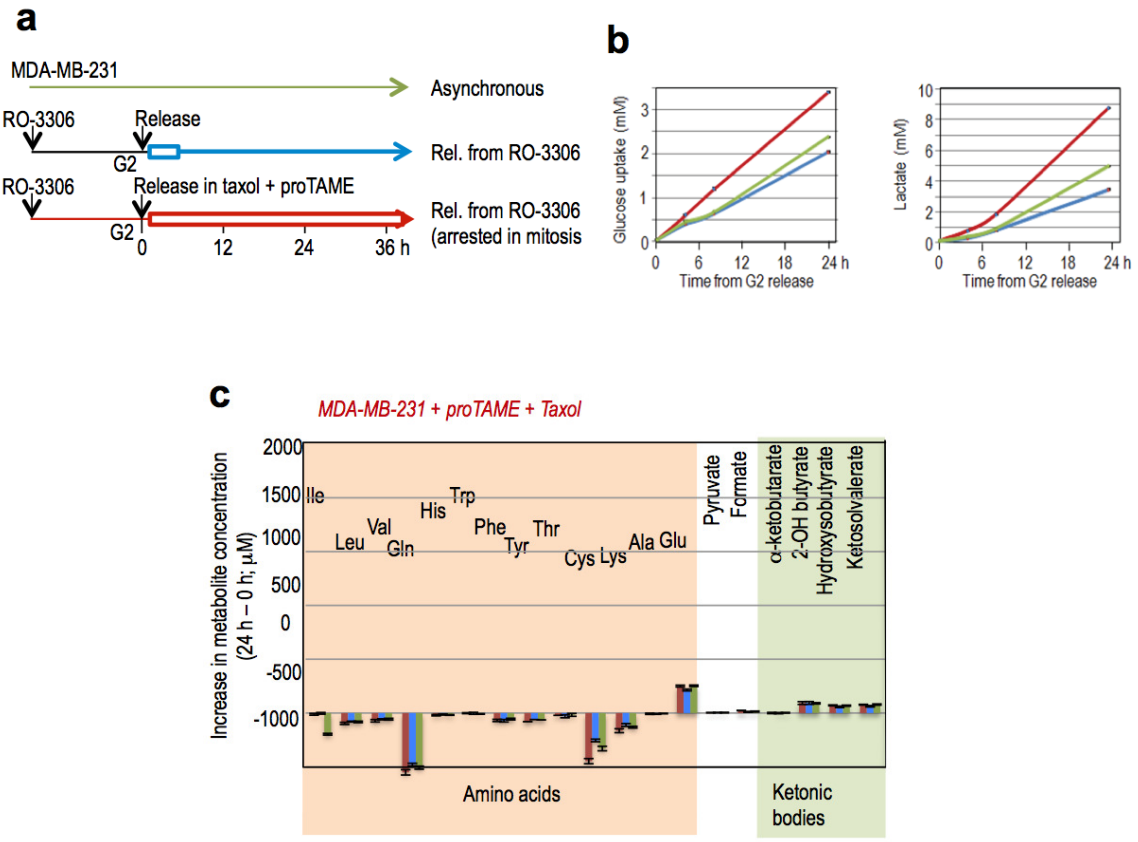

Figure 34. Metabolic profile in MDA-MD-231 cells arrested in mitosis. a) Schematic representation of the protocol followed for synchronization MDA-MB-231, cells were treated with RO-3306 to trigger G2 arrest. This compound was washed-out 18 hours later, in the presence of taxol and pro-TAME (red) in order to induce a metaphase arrest mimicking the arrest imposed in the absence of Cdc20. When cells are release from G2 arrest in the absence of mitotic inhibitors, this allows cells to progress through the cell cycle (blue). Green line represents asynchronous cultures. This color code is maintained throughout the thesis to clarify the identification of the three ways of synchronization. **b)** Concentration of extracellular glucose-^{13}C and lactate-^{13}C present in the supernatant of cells in culture, which represents the glucose uptake and the concomitant production of lactate of cultured cells, monitored by NMR. Asynchronous in green, normally released from G2 (blue) or mitotic arrested (red) MDA-MB-231 cells**. c)** Differential extracellular concentration of the indicated metabolites 24 hours after RO-3306 release compared to time zero (fresh media) as monitored by NMR. 35 metabolites were analyzed and only those exhibiting significant differences are represented (20 out of 31). No differences were found in carnosine, adenine, glyoxylate, glycerol, cholesterol, EtOH, niacinamide, acetate, inositol, asparagine and aspartic acid.

These changes in extracellular glucose and lactate were reduced after knock down of AMPKα1 and AMPKα2 in mitotically arrested Cdc20-null cells (Figure 35), suggesting the involvement of AMPK in the glycolytic induction observed in mitotic cells.

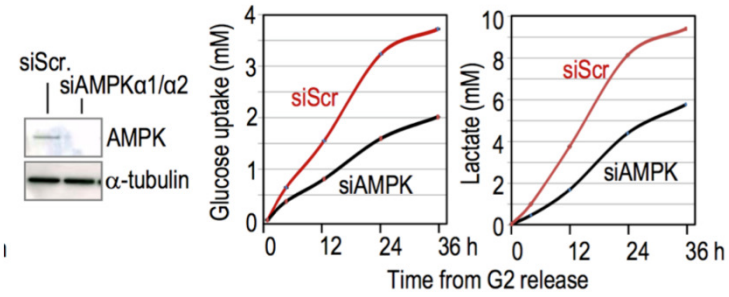

Figure 35. AMPK is involved in the glycolytic induction observed in mitosis. a) Concentration of extracellular glucose and lactate present in the supernatant of cells in culture, which represents the glucose uptake and the concomitant production of lactate of cultured cells, monitored by NMR. Extracellular levels of glucose and lactate in Cdc20-null cells after knockdown of AMPKα1/α2 using specific siRNAs. Efficiency of the indicated siRNA by inmunoblotting.

2.8 Glycolysis is a major determinant of survival in mitosis

The activation of AMPK and the subsequent glycolytic switch observed in mitotic cells raised the possibility of a dependence on energy pathways to survive in mitosis. In fact, treatment of mitotic cells with the AMPK inhibitor Compound C or with the AMPK activators AICAR (an analog of adenosine) and metformin (a compound that inhibits mitochondrial function leading to ATP depletion) resulted in reduced SiM in mitotic Cdc20-null cells (Figure 43a) or human cell lines (Figure 36b). Similar results were obtained after specific knockdown of AMPKα1 and AMPKα2 (Figure 36c). SiM after metformin treatment was rescued by the additive addition of ZVAD and 3MA, this raises the possibility that in a prolonged mitotic arrest AMPK triggers cell death by induction of both apoptosis and autophagy. Besides, Cdc20 null cells in the absence of AMPKα1/α2 shows reduced levels of LC3bII (Figure 36d).

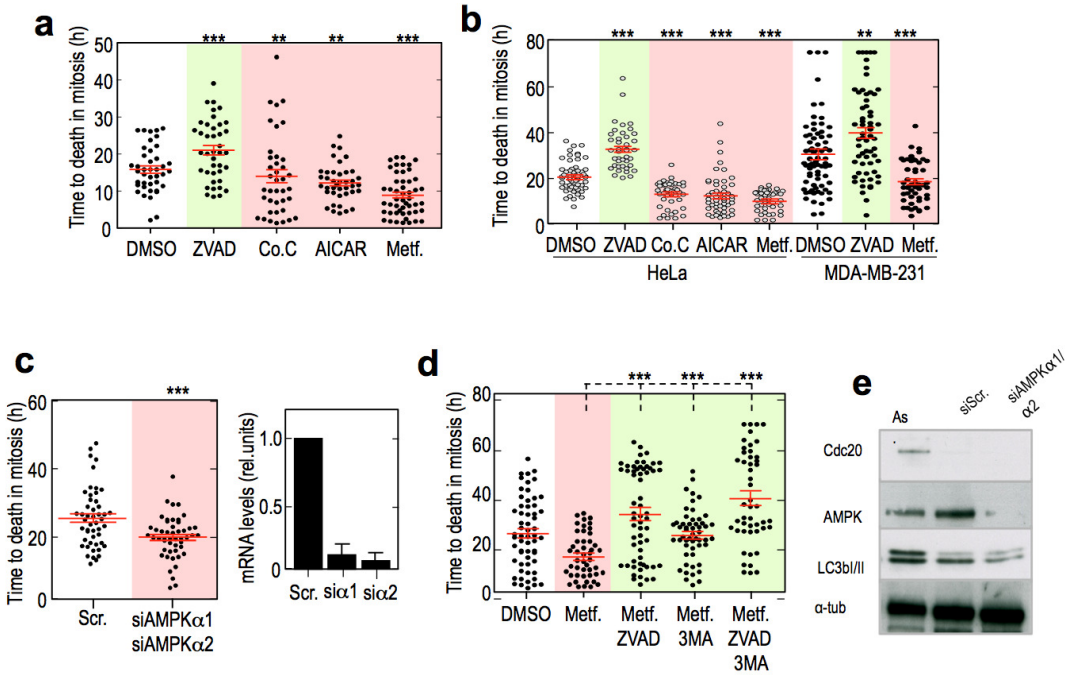

Figure 36. Either activation or inhibition of AMPK affects survival in mitosis. a) Plots representing the duration of mitosis (from metaphase till cell death) in Cdc20-null MEFs treated with AMPK activators and inhibitor. **b)** Plots representing the duration of mitosis (from metaphase till cell death) in human cell lines arrested in mitosis treated with the indicated drugs **c)** Plots representing the duration of mitosis (from mitotic onset till cell death) in Cdc20-null MEFs treated with AMPK siRNAs. Efficiency of the indicated siRNAs by qPCR analysis of mRNA levels (48 hours after siRNA nucleofection). Data were normalized with β-actin mRNA levels. **d)** Plots representing the duration of mitosis (from metaphase till cell death) Cdc20-null cells treated with the AMPK activator metformin alone or in combination with inhibitors of programmed cell death. **e)** Levels of the indicated proteins detected by inmunoblotting in MEFs. In b and c dots represent individual cells and a red line indicates the mean. n.s., not significant. **, p<0.01; ***, p<0.001 (Student's t-test).

Moreover, addition of 2-desoxi-D-glucose (2-DG; a glucose analog that cannot be metabolized inhibitor of hexokinase, the enzyme that catalyzes the first step of glycolysis) or oxamate (an isosteric and isoelectronic inhibitory analogue of pyruvate, which in turns inhibits the lactate dehydrogenase) also resulted in premature MCD, whereas supplementation of media with glucose led to a significant extension in SiM proportional to the amount of glucose added (Figure 37). When 20mM of glucose is added sequentially, SiM is expanded but only until 24h of mitotic arrest, after that survival in mitosis cannot be increased.

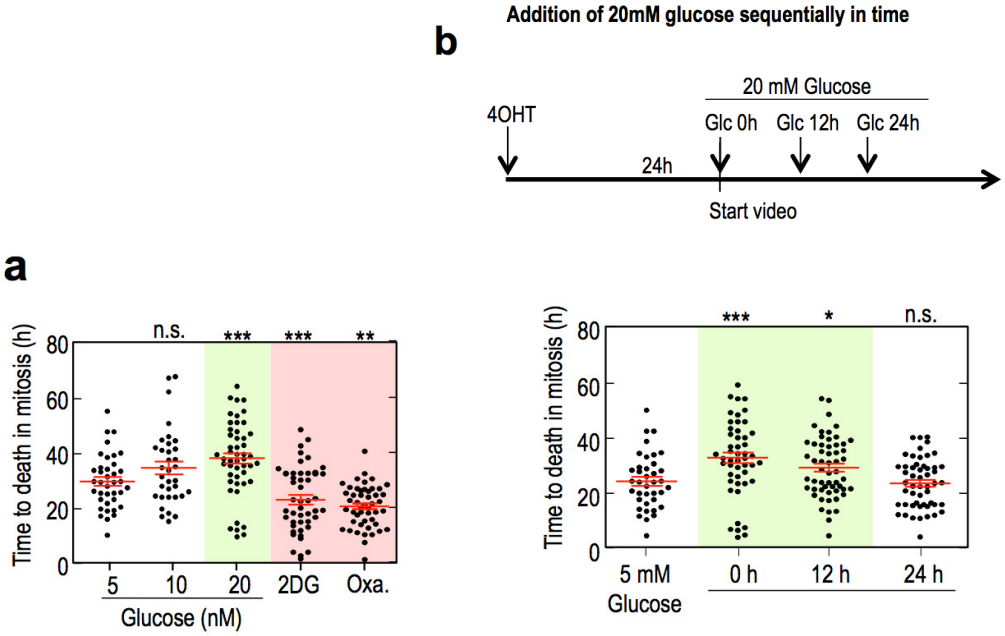

Figure 37. Glucose addition fuels cell survival in mitosis. a) Plots representing the duration of mitosis (from metaphase till cell death) Cdc20-null cells treated with the indicated glycolytic and OXPHOS inhibitors. **b)** Schematic representation of the protocol followed, video recording was initiated 24 hours of 4-OHT addition and 20mM was supplemented to the media at the indicated times after the video started. Plots representing the duration of mitosis (from mitotic entry till cell death) Cdc20-null cells in which 20mM of glucose was added sequentially in time. Dots represent individual cells and a red line indicates the mean. n.s., not significant. **, p<0.01; ***, p<0.001 (Student's t-test).

The relevance of the glycolytic pathway was directly addressed by testing the importance of 6-phosphofructo-2-kinase/fructose-2, 6-bisphosphatase 3 (PFKFB3), a key regulator of the glycolytic enzyme phosphofructokinase-1 (PFK-1), directly linked to Warburg effect (Almeida *et al*., 2010; Brooke *et al*., 2014; Cordero-Espinoza *et al*., 2013; Seo *et al*., 2011) a common feature of cancer cells. AMPK directly phosphorylates and activates PFKPB3 at residue Ser-461 (Bando *et al*., 2005; Marsin *et al*., 2000; Marsin *et al*., 2002) and highly phosphorylated PFKFB3 protein is often found in human tumor cells (Bando *et al*., 2005). Downregulation or inhibition of PFKFB3 using siRNAs or the competitive inhibitor 3-(3-pyridinyl)-1-(4-pyridinyl)-2-propen-1-one (3PO) resulted in a significant reduction in SiM in mouse (Figure 38c) or human (Figure 38d) cells, in agreement with reduced glucose consumption and lactate production during mitosis in the absence of this regulator (Figure 38e).

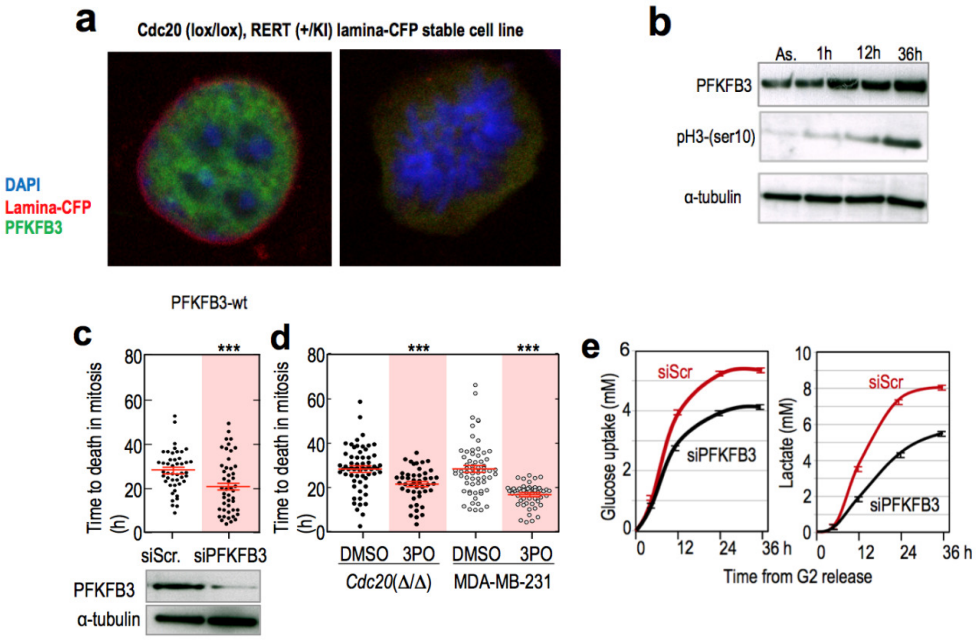

Figure 38. AMPK boost glycolysis through PFKFB3 activation. a) Confocal microscopy images of *Cdc20(ox/lox)* and *Cdc20(Δ/Δ)* transiently expressing PFKFB3-Wt in green, shows PFKFB3 localization at the nuclei in interphase and pan-cytoplasmic localization in mitosis. DNA is marker with DAPI (blue) and nuclear lamina (red), a nuclear envelope marker. **b)** Imunodetection of the indicated proteins, PFKFB3 levels are constant in prolonged mitotic arrest and interphase and phospho-Histone (Ser10) mark for mitosis**. c)** Plots representing the duration of mitosis (from mitotic entry till cell death) and a red line indicated the mean in Cdc20-null cells treated with the PFKFB3 siRNA and the efficiency of the silencing in protein levels. Efficiency of the siRNA for PFKFB3 knockdown by inmunoblotting at 48 hours post-transfection. **d)** Plots representing the duration of mitosis (from metaphase till cell death) Cdc20-null cells treated with the 3PO and the red line represented the mean. **f)** Extracellular levels of glucose and lactate in Cdc20-null cells in the presence or the absence of PFKFB3 are represented were measured by NMR. In c and d, n.s., not significant. **, p<0.01; ***, p<0.001 (Student's t-test).

Glycolytic flux was next evaluated by using a cytoplasmic FRET biosensor of glucose which activity is proportional to the concentration of intracellular glucose (Takanaga *et al*., 2007). Cells arrested in mitosis shown a more rapid fall in FRET signal compared to interphase cells in the presence of glucose-supplemented media. This decrease in FRET signal is further enhanced upon removal of glucose from the culture media, reaching its zero 10 minutes after completely removal of glucose in mitotic cells. The absence of PFKFB3 attenuates the slope in the FRET signal, which supports the role of PFKFB3 in boosting glycolytic flux in mitosis (Figure 39).

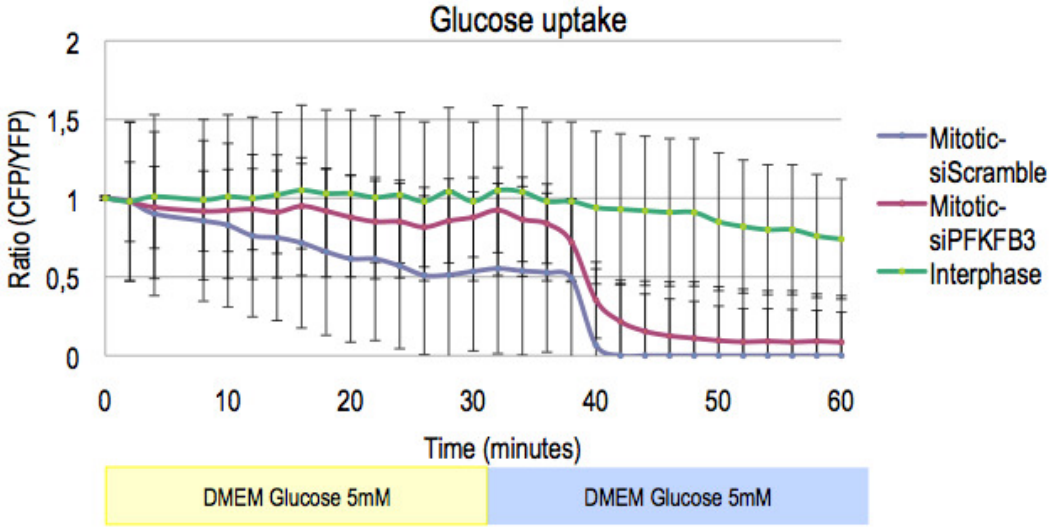

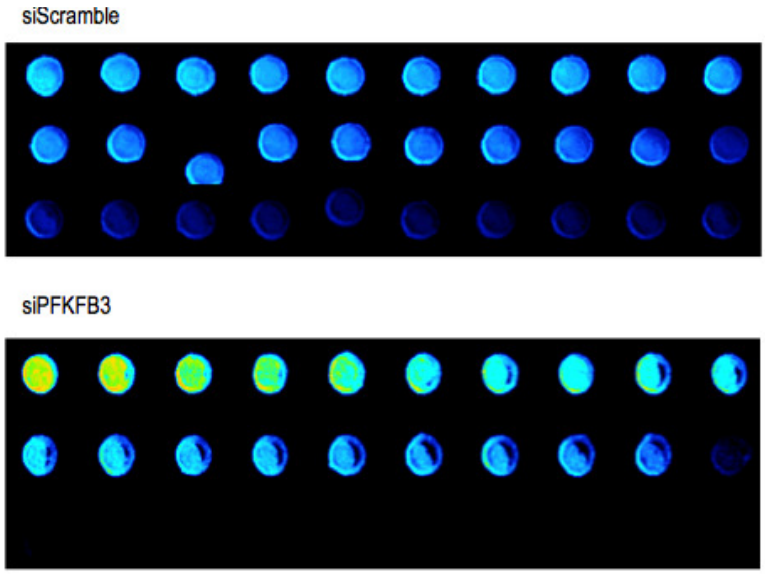

Figure 39. PFKFB3 boost glycolytic flux. a) Changes in intracellular glucose concentration were monitored using a FRET biosensor for glucose in *Cdc20*(Δ/Δ) and *Ccd20*(lox/lox). Upon removal glucose-containing media and addition of glucose-free media, FRET signal, and therefore intracellular glucose concentration, drops. Whereas in interphasic cells (green) upon glucose removal, the biosensor signal does not significantly change, in Cdc20-null cells rapidly decreases. When compared mitotic cells (cdc20-null) in the presence (siScramble) or the absence (siPFKFB3) of PFBFB3Intracellular glucose levels decreases more rapidly in Cdc20-null cells treated with PFKFB3 siRNA than scramble treated Cdc20-null or interphasic cells. This suggests that PFKFB3 is boost glycolysis in mitosis. **b)** Representative micrografies showing the activity of the FRET biosensor for glucose in color scale, yellow higher activity than blue. Data represents mean ± SD (n=12 cells).

2.9 Inhibition of glycolysis cooperates with microtubule poisons in mitotic cell death

Our results indicate that multiple pathways including apoptosis, autophagy and energy production mediate survival in mitosis. We therefore tested whether interference with these pathways could cooperate with the effect of microtubule poisons in MCD. As a first *in vitro* approach MBA-MD-231 were treated with multiple agents against the referred pathways either in the presence or absence of taxol. As indicated in Figure 40, several combinations were more efficient than the single agents in killing these breast cancer cells.

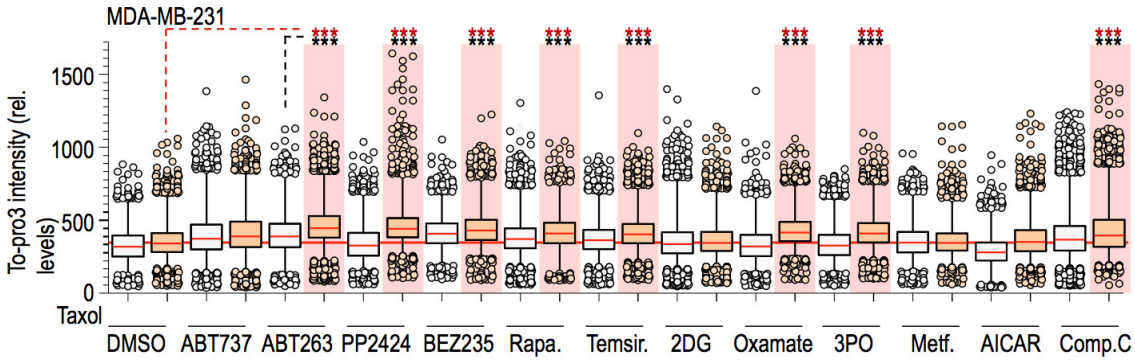

Figure 40. Taxol cooperates with different inhibitors of survival pathways to promote mitotic cell death. a) Cell death in MDA-MB-231 as determined byTo-Pro3 levels, measured using high-throughput microscopy, after the indicated treatments in the presence or absence of taxol, the intensity of the staining perfectly correlates with cell death. Pink columns indicate significative synergistic combinations when compared to single inhibitors (black dotted comparisons) or taxol (red dotted comparisons). ***, p<0.001; Student´s t-test.

The effect of ABT263, PP242, 2DG and 3PO was additionally tested in three breast cancer cell lines such as MDA-MD-468, EVSA-T or MCF7 (Figure 41).

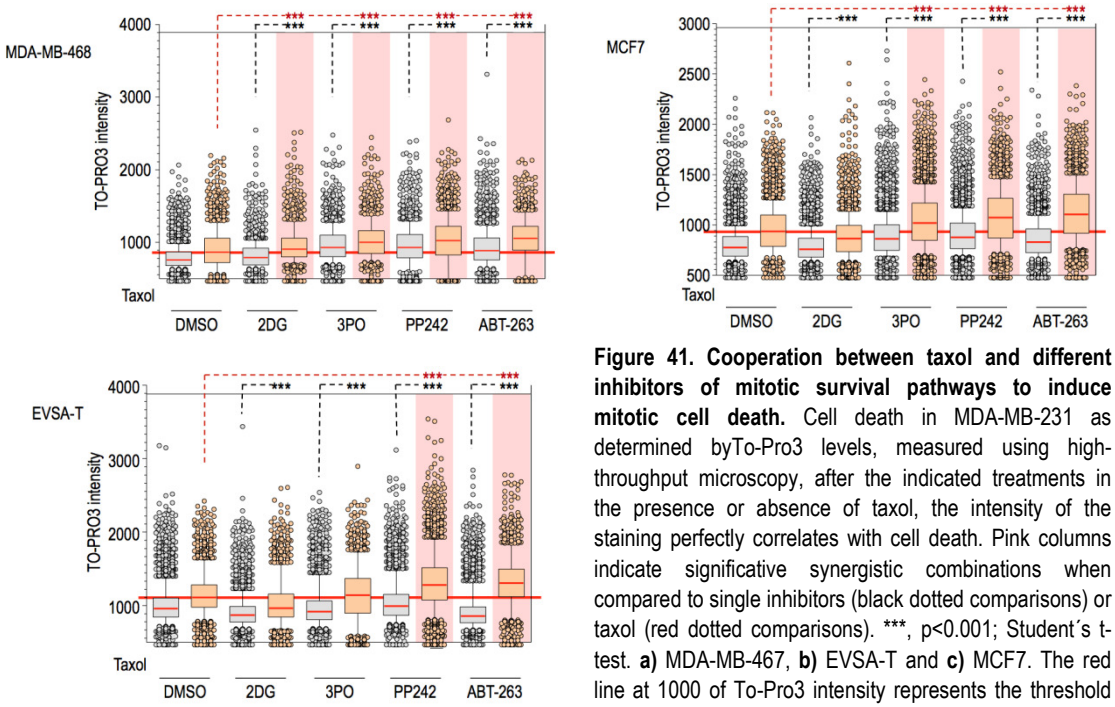

Figure 41. Cooperation between taxol and different inhibitors of mitotic survival pathways to induce mitotic cell death. Cell death in MDA-MB-231 as determined byTo-Pro3 levels, measured using high-throughput microscopy, after the indicated treatments in the presence or absence of taxol, the intensity of the staining perfectly correlates with cell death. Pink columns indicate significative synergistic combinations when compared to single inhibitors (black dotted comparisons) or taxol (red dotted comparisons). ***, p<0.001; Student´s t-test. **a)** MDA-MB-467, **b)** EVSA-T and **c)** MCF7. The red line at 1000 of To-Pro3 intensity represents the threshold considered for cell viability.

To further understand whether these combinations were effective in mitosis, we monitored cell fate of MBA-MD-231 cells treated with ABT-263, PP242, 2DG, 3PO or metformin in the absence or presence of taxol. As shown in Figure 42a, treatment of breast cancer cells with these individual drugs results in a variable efficiency in cell death ranging from 10% to 40% without affecting mitotic cells (Figure 42b,d). Single treatment with taxol also resulted in a significant percentage of death cells (21%) from which only 12% of cells died in mitosis, in agreement with previous data in transformed fibroblasts (Manchado *et al.*, 2010). Interestingly, combination of taxol with ABT-263, PP242, 3PO and metformin resulted in efficient MCD (Figure 42c,d) more than a 30% of the cells die in mitosis. We did not observe any cooperation between taxol and 2DG, probably as a consequence of reduced entry into mitosis in cells treated with 2DG (Figure 42a-d), suggesting the need of energy availability for the entry into M-phase. The combination of taxol and ABT-263 was extremely efficient and all cells died during the observation period (60 h; Figure 42c,d). About 65% of these deaths occurred in mitosis (Figure 42d) and the SiM was of 5.6 ± 4.7 h compared to 29.8 ± 18.0 in the presence of taxol alone (Figure 42e).

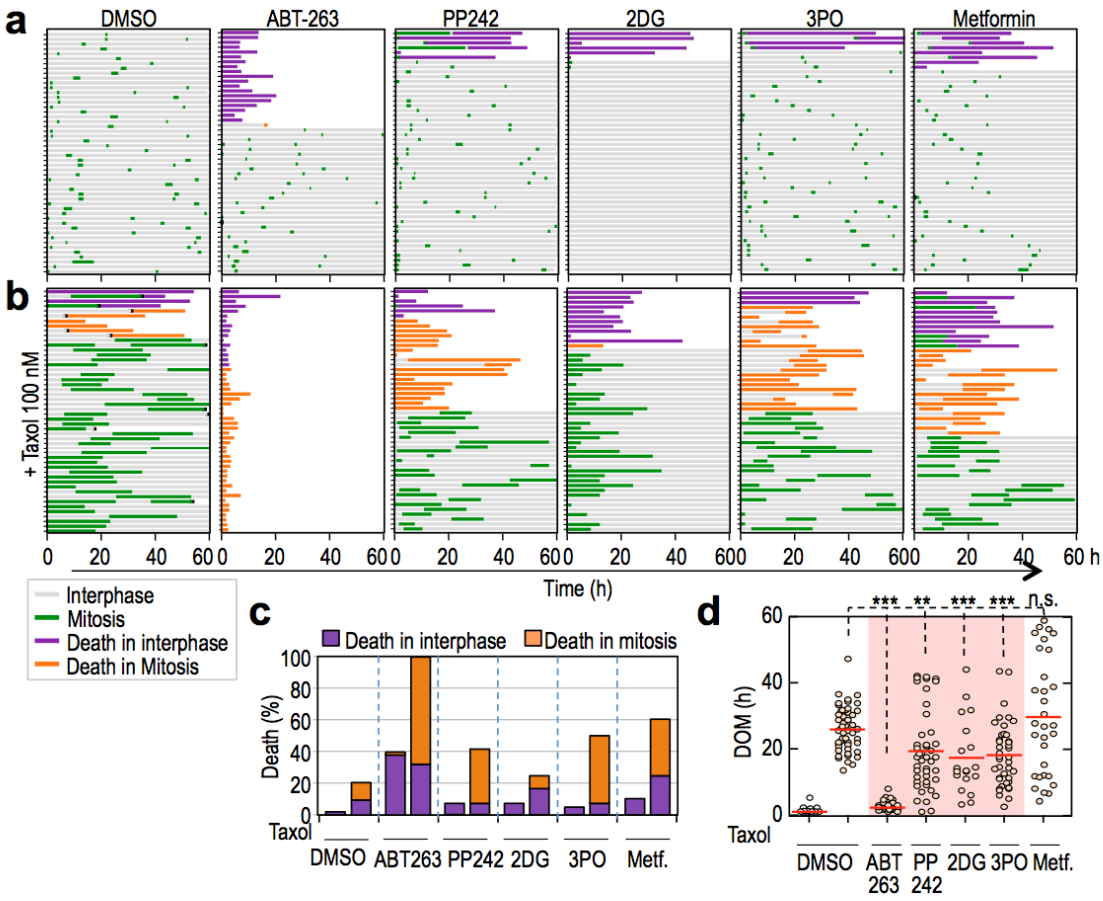

Figure 42. 3PO shows synergistic effect in vitro in MDA-MB-231 cells. a) Cell fate diagrams in which are represented the duration of interphase, represented in gray, and mitosis, green, in the presence of the indicated treatments. Each line represents an individual cell fate. Cell death in interphase is represented in violet, while cell death in mitosis is represented in orange. **b)** Cell fate diagrams in which are represented the duration of interphase, represented in gray, and mitosis, green, in the presence of the indicated treatments in combination with taxol. Each line represents an individual cell fate. Cell death in interphase is represented in violet, while cell death in mitosis is represented in orange **c)** Quantification of the percentage of cells that die in mitosis (orange) and in interphase (violet) after the indicated treatments**. d)** Duration of mitosis (DOM) from mitotic entry to cell death induced by taxol and combination treatments. n. s., not significant. **, p<0.01; ***, p<0.001 (Student´s t-test).

To investigate the cooperation between taxol and the inhibition of glycolysis in tumor development in vivo, we generated subcutaneous xenografts of MBA-MD-231 cells in nude mice. Taxol (5 mg/Kg) and 3PO (5, 25 or 50 mg/Kg) were injected i.p. when tumors reached 200 mm^3 and tumor growth was monitored during the following 12 days. Taxol was very inefficient at that doses whereas treatment with 3PO alone resulted in a significant reduction in tumor volume and weight (Figure 43a,c and d). The combination of taxol with 3PO further improved significantly the therapeutic effect when compared to single treatments (Figure 43a,c and d) and results in a significant raise in apoptotic cells in the tumors (Figure 43b). Taken together, these data suggest the potential benefit of using glycolytic inhibitors in combination with current mitotic-targeted therapies to inhibit tumor growth.

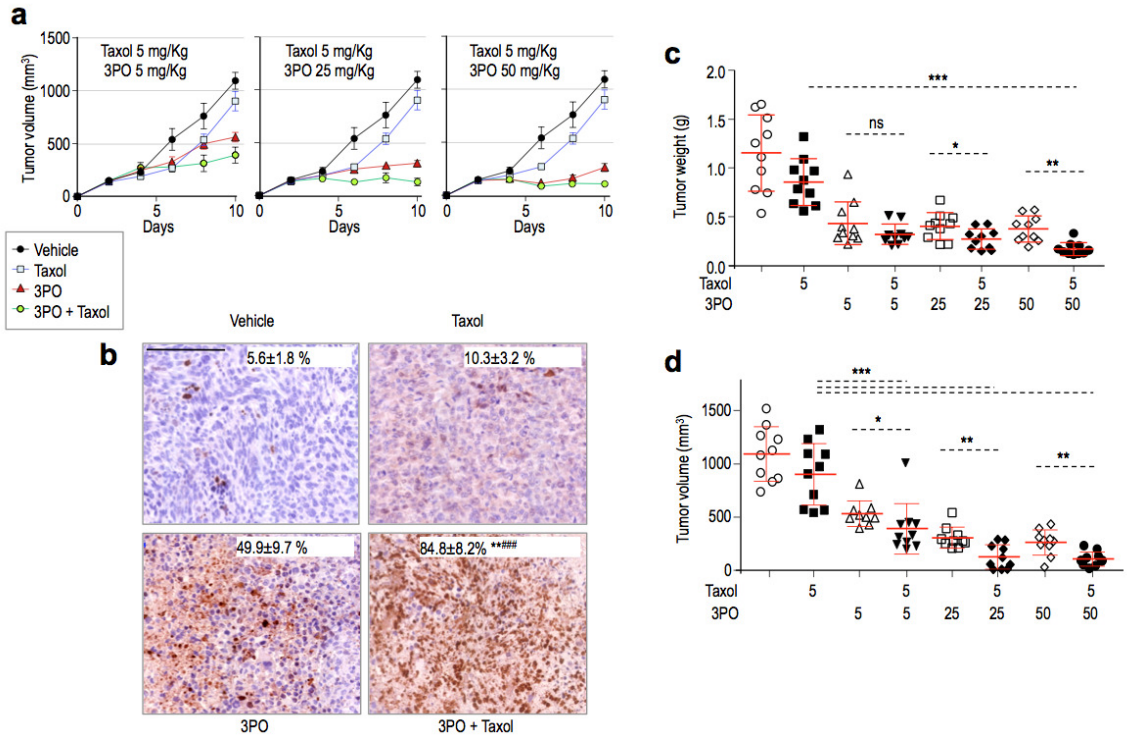

Figure 43. Anti-tumoral cooperation between microtubule poisons and PFKFB3 inhibitors *in vivo*. **a)** Effect of the combination of taxol (5mg/kg) and 3PO (5, 25 or 50 mg/kg) on the growth of tumor xenografts generated by subcutaneous injection of MDA-MB-231 cells in nude mice. **b)** Active caspase-3 inmunostainning in MDA-MB-231 derived-tumor xenografts. The numbers indicate the percentage of active caspase-3 positive cells relative to the total number of nuclei in each section ± SD. Six sections were counted for each of four dissected tumors per condition. Scale bars, 100µM. **c)** Data correspond to the weight of each of the tumors at the final time point of the experiment (n=10 tumors per condition). Red lines indicate mean ± SD. *, p<0.05; **, p<0.01; *** p<0.001 (ANOVA-test). **d)** Data correspond to the volume of each of the tumors at the final time point of the experiment. Red lines indicate mean ± SD (n=10 for each condition). *, p<0.05; **, p<0.01; *** p<0.001 (ANOVA-test).

1. A search for M-phase specific compounds

Taking advantage of Cdc20 conditional knockout mouse embryonic fibroblasts (MEFs) we tested a library of 300 compounds from a variety of molecular entities, provided by the Experimental Therapeutics Programme at CNIO, for its ability to selectively target mitotic cells. We used H-Ras transformed Cdc20 conditional knockout cells expressing an inducible form of Cre recombinase and a histone H2B-GFP reporter. Addition of tamoxifen (4-OHT) results in the inactivation of Cre, the excision of Cdc20 exons and a metaphase arrest (Manchado *et al*., 2010). Ultimately, Cdc20-null cells are not able to progress to anaphase due to the presence of active Cdk1-cyclinB1 complexes and defective activation of separase.

1.1 Screen for compounds that specifically kill cells in mitosis in Cdc20 –deficient MEFs

Mitotic entry was efficiently synchronized in *Cdc20*(Δ/Δ) cells by the addition of RO-3306, a Cdk1 inhibitor, which prevents mitotic entry arresting cells in G2 (for protocol see Material and Methods Figure 10). Upon removal of the inhibitor, Cdc20-null cells progress to mitosis and remain arrested at metaphase. One hour after G2-release, both asynchronic *Cdc20*(lox/lox) and *Cdc20*(Δ/Δ), were treated in parallel with the compounds in the presence of To-Pro3, a DNA binding dye that do not affect cell viability. To-Pro3 diffused into the cells immediately after permeabilization of the membranes that accompany cell death and was used to monitor cell viability at 6 and 24 hours after the addition of the compounds in both experimental conditions. Cell death was quantified at 6 and 24 hours after treatment, by scoring To-Pro3 levels in mitotic and interphasic cells after setting a threshold for cell viability. Cell death was normalized to To-Pro3 levels of untreated cells, and then the increment in cell death in mitosis was calculated by subtracting the percentage of dead cells in interphase from the percentage of dead cells in mitosis and was plotted in Figure 44. Scoring a positive value means that a given compound preferentially targets mitotic cells, whereas a value bellow zero corresponds to a compound which is more specific for interphasic cells. Moreover, compounds that are cytotoxic regardless of the phase of the cell cycle will score values close to zero. Finally were only considered for further analysis those compounds that show an increment in cell viability over 40 or bellow -40.

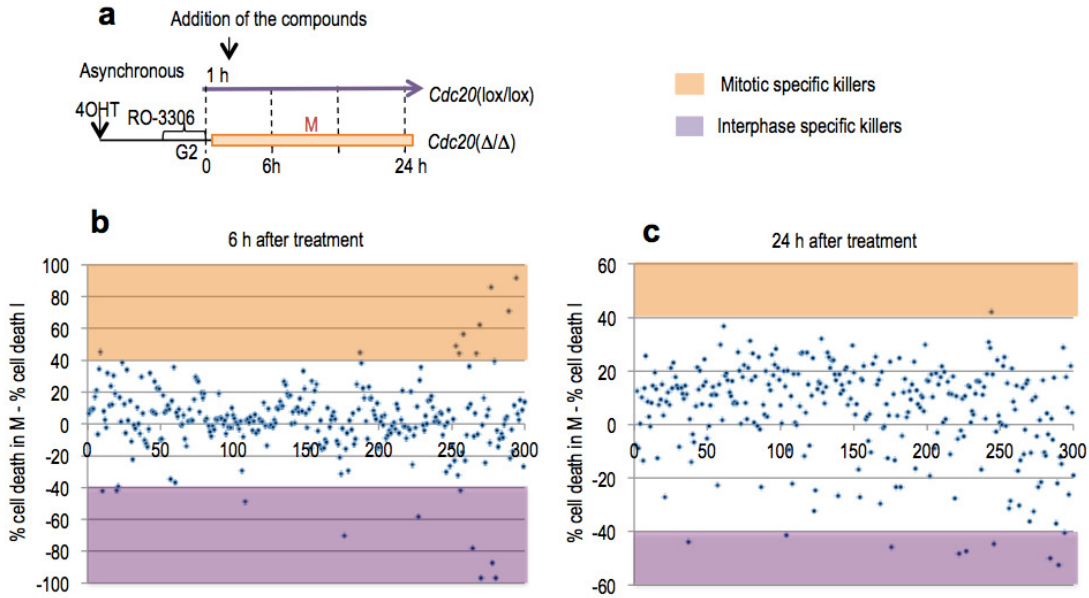

Figure 44. **Screening for selective killers in mitosis. a)** Schematic representation of the protocol followed for synchronization in *Cdc20*(Δ/Δ). *Cdc20*(lox/lox) cells were treated with 4-OHT to eliminate Cdc20 12 hours prior the addition of RO-3306, a Cdk1 inhibitor, to arrest cells in G2. This compound was washed-out 18 hours after allowing mitotic entry, but in the absence of Cdc20 cells remain arrested in mitosis. *Cdc20*(lox/lox) cells (violet) were not synchronized. 1 hour after G2 release, both interphasic

Cdc20(lox/lox) and mitotic synchronized cells, *Cdc20(Δ/Δ)* were treated with a library of 300 compounds at 10 μM in the presence of To-Pro3. **b)** Representation of the percentage of dead cells in mitosis minus percentage of dead cells in interphase scored at 6 hours after treatment. Values bellow -40 represents specific interphasic killers (in violet), whereas over 40 include compound that preferentially target mitotic cells and scoring a value in between -20 and 12 are considered non-selective killers. **c)** Representation of the percentage of dead cells in mitosis minus percentage of dead cells in interphase at 24 hours after treatment following the same criteria that at 6 hours.

A total of 15 compounds preferentially kill cells in interphase (among them 2-DG, hexokinase inhibitor which is the enzyme that catalyzes the first step of glycolysis; Table 5). Whereas 10 compounds selectively kill cells in mitosis, being 5 out of those 10, identified with an asterisk, inhibitors of the mitotic kinase haspin.

MITOSIS SPECIFIC		INTERPHASE SPECIFIC	
6 h	24 h	6 h	24 h
5-IU*	5-IU	AA1	ETP-323
ETP-460		AA2	ETP-567
ETP-084*		ETP-729	ETP-832
ETP-081*		ETP-832	ETP-823
ETP-263*		ETP-477	ETP-437
PP242		2-DG	ETP-477
RB5		2-DG	RB4
ETP-254		ETP-082	ABT-737
ETP-947		LY-294002	
ETP-340*			

Table 5. Hits from the screening. 10 compounds preferentially kill cells in mitosis, whereas 15 are kill more specifically interphasic cells. The asterisk identifies haspin inhibitors.

Haspin is an atypical ser/thr protein kinase, whose activity is limited to mitosis through autoinhibition by a basic segment (Funabiki *et al*., 2013; Zhou *et al*., 2013), and is in charge of the phosphorylation of Histone 3 at Thr-3 (H3T3). This phosphosite is a docking site for chromosomal passenger complex (CPC) composed by: survivin, INCENP, borealin and Aurora B; the catalytic subunit of the CPC, which coordinates mitotic processes through phosphorylation of key regulatory proteins. In an attempt of validation of those haspin inhibitors, we followed individual cell fate by videomicroscopy of Cdc20-null cells, in the presence of To-Pro3, and quantify survival in mitosis (SiM), which is the time that a cell spends in mitosis before cell death in mitosis (To-Pro3 positive staining). Haspin inhibition in mitosis (in Cdc20-null cells) by means of 5-IU, ETP-084 and ETP-081 leads to a reduced survival in mitosis compared to control cells, confirming that inhibition of haspin in mitosis results in reduced survival (Figure 45).

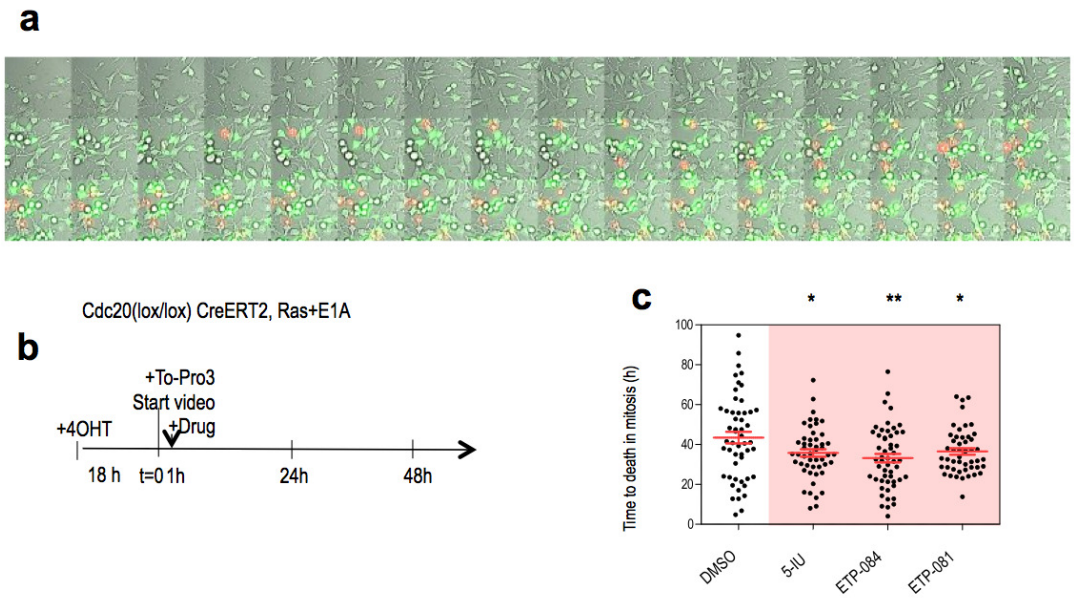

Figure 45. Validation of haspin inhibitors as mitotic cell death enhancers in Cdc20-null cells. a) Time-lapse microscopy of Cdc20-null MEFs every 15 minutes. Upon Cdc20 ablation cells will enter mitosis and remain trapped at this state for several hours, as it can be easily recognized by cell rounding and chromatin condensation, marked by Histone-2B-GFP, mitotic cells eventually die in mitosis, To-pro3 positive cells (red). **b)** Schematic representation of the protocol followed for videomicroscopy. 4-OHT was added 24 hours before the video and one hour after the beginning of the video, the indicated drugs were injected. For quantification were only taken into consideration cells that were in mitosis before the injection of the drug, in order to avoid any effect of the drug in mitotic entry. **c)** Plots representing the time of individual cells from metaphase till cell death in mitosis treated with the indicated haspin inhibitors. In c dots represent individual cells and a red line indicates the mean. n.s., not significant. **, p<0.01; ***, p<0.001 (Student's t-test).

Survivin is the only component of the CPC that shows pro-survival activity by direct binding and inhibition of caspases. The molecular mechanism still not well understood, but it seems to be linked to p53 (Chan et al., 2012). Survivin localizes to the mitotic spindle by interaction with tubulin during mitosis and may also play a contributing role in regulating mitosis. As well as haspin, depletion of survivin leads to a mitotic delay of 2-3 hours (Carvalho *et al*., 2003; Lens *et al*., 2003), however, the absence of survivin is additionally accompanied by a massive apoptosis and cells death in interphase after failing to complete cytokinesis (Cutts et al., 1999; Uren et al.,2000; Zuojun et al., 2008). As haspin activity is essential for proper localization of survivin in mitosis, we wonder whether the increased cell death observed upon haspin inhibition is an indirect consequence of survivin misslocalization and loss of functionality. For this purpose we depleted haspin and survivin protein levels by siRNA (small-interference RNA) and observed a more pronounced reduction of SiM after survivin knock-down compared to haspin siRNA and scramble (Figure 46).

.

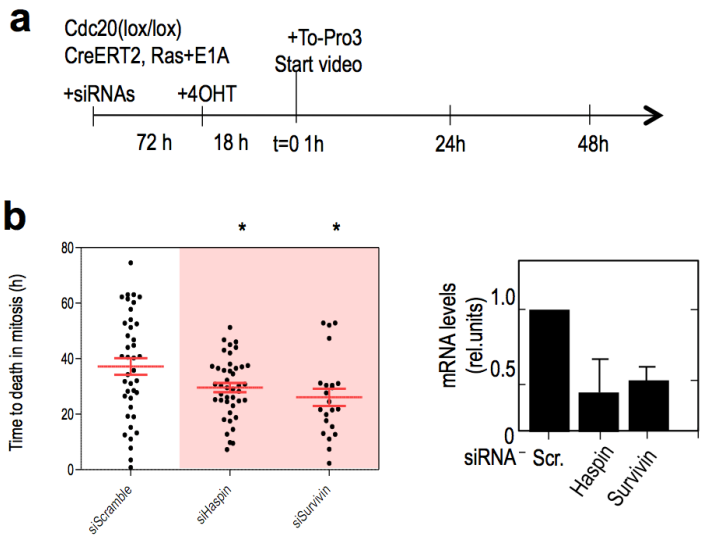

Figure 46. Haspin and survivin contribute to survival in prolonged mitotic arrest. a) Schematic representation of the protocol for time-lapse microscopy in Cdc20-deficient cells. Cells are subjected to two consecutives rounds of transfection, at 72 hours and 24 hours before start recording, respectively. 4-OHT was added 18 hours before the video. **b)** Plots representing the duration of mitosis in Cdc20-null cells treated with the indicated siRNAs. Efficiency of the indicated siRNAs by quantification of mRNA levels 48 hours after siRNA nucleofection. Data were normalized against the levels of β-actin transcripts. In b dots represent individual cells and a red line indicates the mean. n.s., not significant. **, p<0.01; ***, p<0.001 (Student's t-test).

To further characterize the effect of haspin inhibition, we monitor cell fate in asynchronic populations of *Cdc20(lox/lox)* and human HeLa cells. ETP-084 and I-iodotubercidine (5-IU) treatments results in mitotic arrest often followed by cell death in mitosis. Cells are able to successfully perform a first mitotic division in the presence of the inhibitors, however, in the subsequent mitosis cells either die in mitosis or exit mitosis in the absence of proper chromosome segregation (Figure 47a-b). Whereas ETP-00048084 treatment leads to a 50% of cell death in mitosis in HeLa cells, 5-iodotubercidine reaches only 30%. *Cdc20*(lox/lox) MEFs are more sensitive to cell death in mitosis upon haspin inhibition reaching 95% of cell death in mitosis for ETP-084 treatment and 60% in the case of 5-IU.

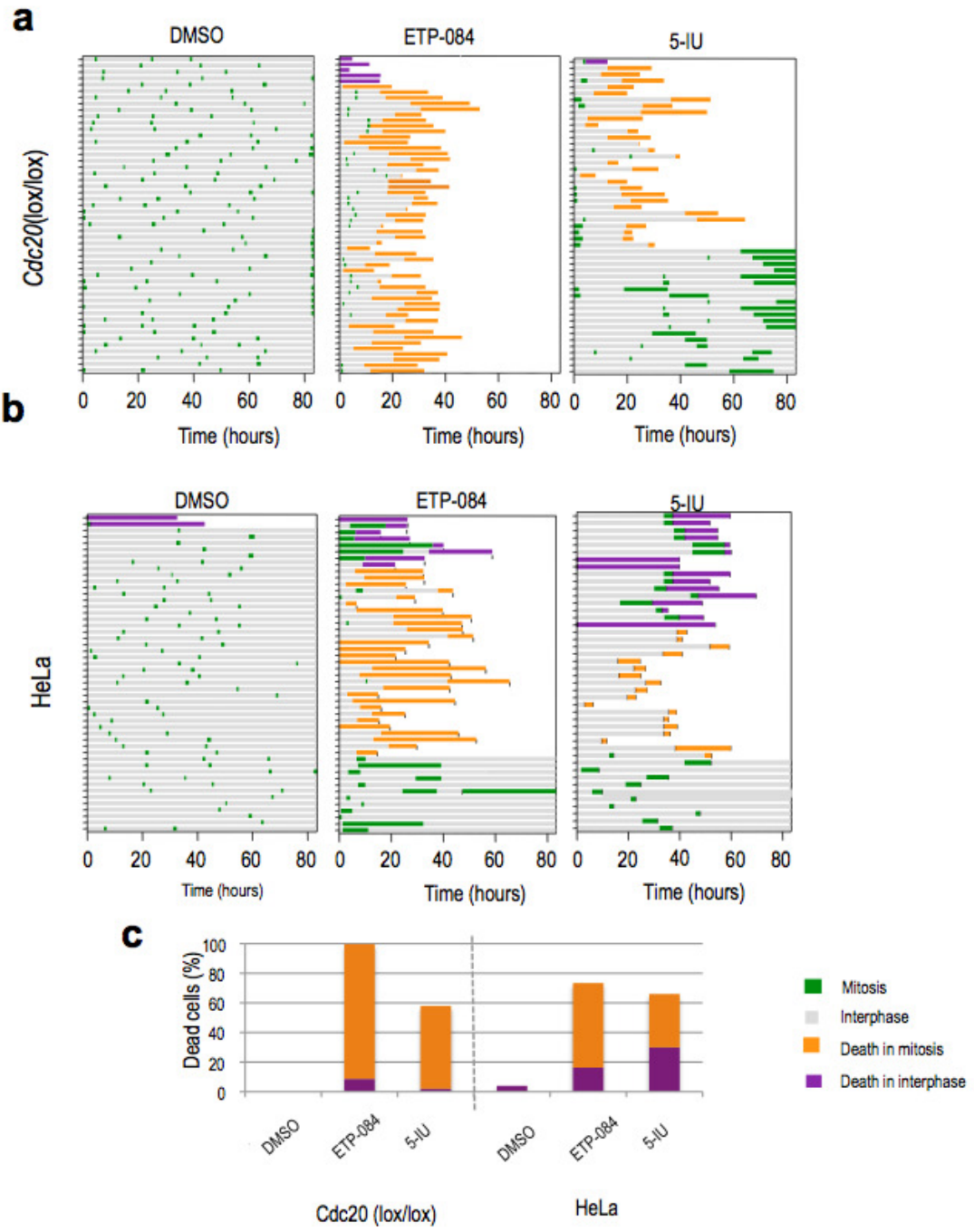

Figure 47. ETP-00048084 and 5-IU delays mitosis in MEFs and human cells. a) Cell fate diagrams of *Cdc20*(lox/lox) cells upon the indicated treatments. In gray is represented the duration of interphase and in green mitosis in the absence of segregation. Each line represents an individual cell fate in the presence of the indicated treatments. Cell death in interphase is represented in violet, while cell death in mitosis is represented in orange. **b)** Cell fate diagrams of HeLa cells. In gray is represented the duration of interphase and in green mitosis. Each line represents an individual cell fate in the presence of the indicated treatments. Cell death in interphase is represented in violet, while cell death in mitosis is represented in orange. **c)** Percentage of cell death in mitosis (orange) and interphase (violet). c) Percentage of cell death in interphase (violet) and mitosis (orange) in *Cdc20*(lox/lox) and HeLa cells upon the indicated treatments.

When haspin inhibitors were compared to current chemotherapy drugs (Figure 48), the inhibition of haspin resulted much more efficient in killing cells in mitosis. Upon taxol addition only a 30% of cell death

occurs in mitosis, whereas after ETP-340 and ETP-081 treatment more than a 60% of cells died in mitosis, suggesting that haspin inhibition is more efficient in killing cells in mitosis.

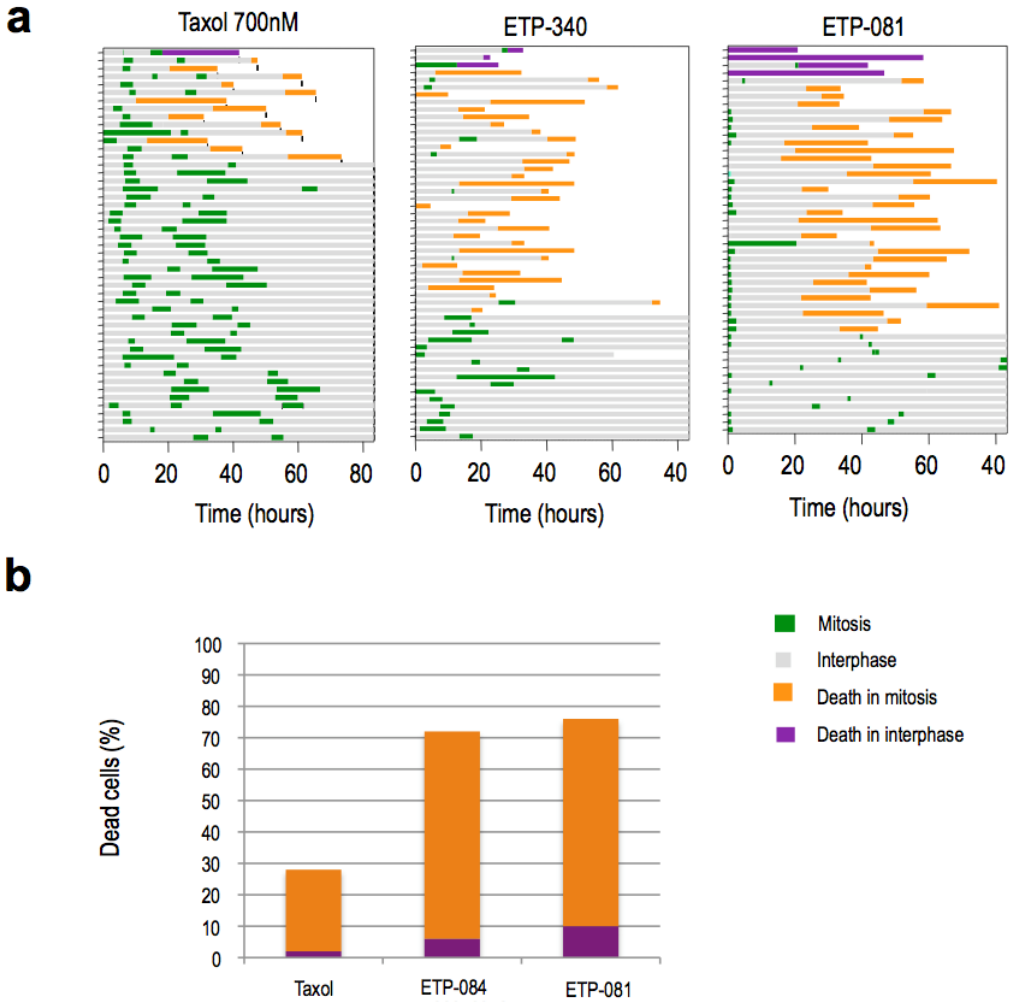

Figure 48. Inhibition of haspin is more efficient in killing cells in mitosis than current anti-mitotic drugs. **a)** Cell fate diagrams of *Cdc20*(lox/lox*)* cells upon the indicated treatments. In gray is represented the duration of interphase and in green mitosis in the absence of a proper cytokinesis. Each line represents an individual cell fate in the presence of the indicated treatments. Cell death in interphase is represented in violet, while cell death in mitosis is represented in orange in *Cdc20*(lox/lox) cells**. b)** Percentage of cell death in mitosis (orange) and interphase (violet) *Cdc20*(lox/lox) cells upon the indicated treatments.

Knock-down of haspin by siRNA means in asynchronous murine and human cells, resulted in mitotic delay followed by cell death in mitosis in more that 50% in MEFs and less than 40% in HeLa cells. Duration of mitosis in MEFs upon haspin knockdown is more prolonged than the mitotic delay induced by any of the haspin inhibitors (Figure 49). This result is not observed in HeLa cells and might be a consequence of the low efficiency achieved for haspin knockdown in those cells.

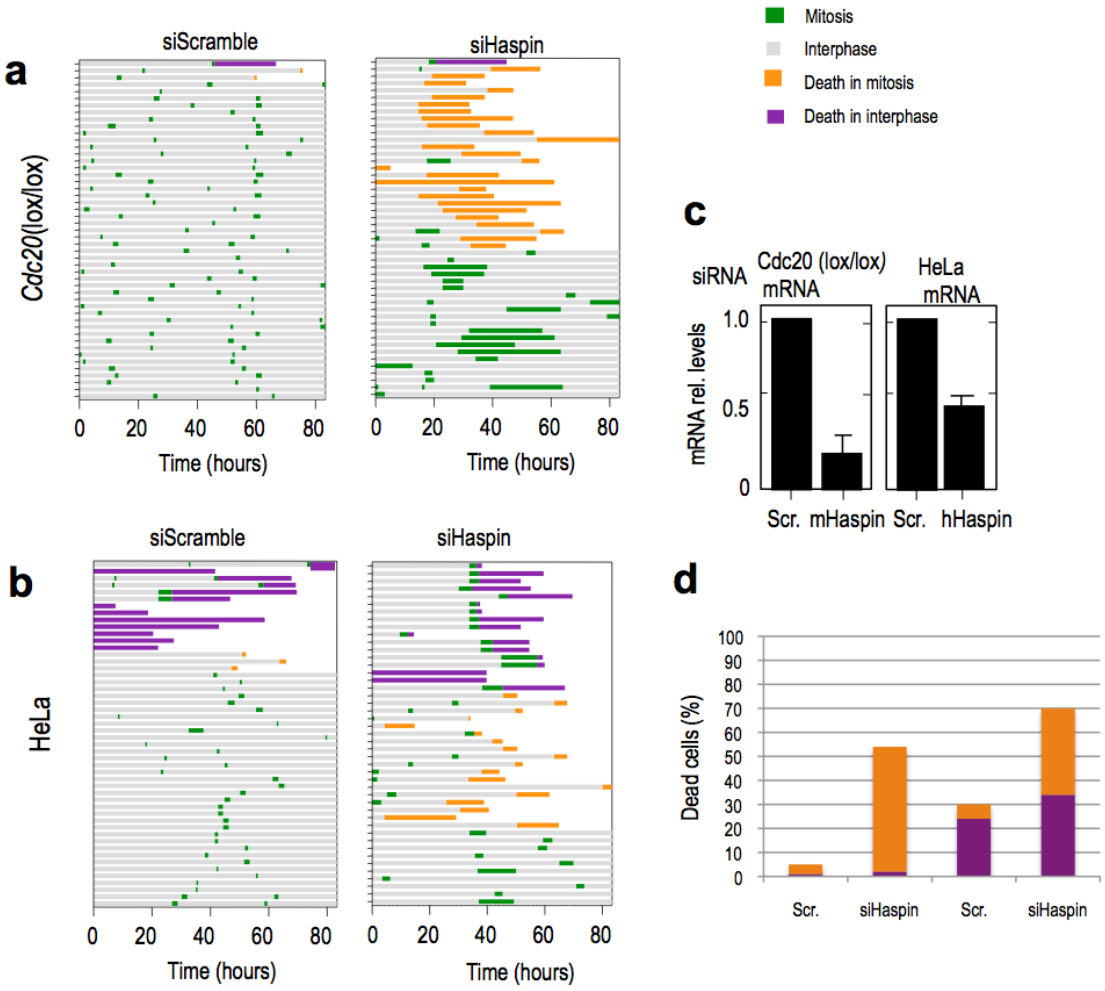

Figure 49. Inhibition of Haspin produces mitotic delay that results in either cell death in mitosis or mitotic exit in the absence of segregation. a) Cell fate diagrams of *Cdc20*(lox/lox) cells. In gray is represented the duration of interphase and in green mitosis in the absence of segregation. Each line represents an individual cell fate in the presence of the indicated treatments. Cell death in interphase is represented in violet, while cell death in mitosis is represented in orange. b) Cell fate diagrams of HeLa cells. In gray is represented the duration of interphase and in green mitosis in the absence of segregation. Each line represents an individual cell fate in the presence of the indicated treatments. Cell death in interphase is represented in violet, while cell death in mitosis is represented in orange. c) Efficiency of the indicated siRNAs by quantification of mRNA levels 48 hours after siRNA nucleofection. Data were normalized against the levels of β-actin transcripts d) Percentage of cell death in mitosis (orange) and interphase (violet).

Importantly, as is shown in Table 6, ETP-084, ETP-340 and ETP-081 are dual inhibitors for haspin and Pim, a serine/threonine kinase which expression is regulated by the JAK/STAT pathway. Pim is classified as a proto-oncogene and is directly involved in resistance to apoptosis through deactivation of Bad pro-apoptotic protein, conferring cell survival and its expression. There are three isoforms primarily expressed in B-lymphoid and myeloid cell lines, but also it solid tumors. It has been reported that Pim inhibition shows a cytostatic effect arresting cells in G1, which eventually results in cell death (Numenthaler *et al.,* 2009).

ETP compound ID	PIM1 IC_{50}	PIM2 IC_{50}	PIM3 IC_{50}	Haspin IC_{50}
ETP-340	9.27E-08	2.26E-06		1.41E-06
ETP-084	8.30E-10	1.72E-07	2.10E-08	5.34E-08

ETP-081	8.30E-09	6.51E-07	6.59E-08	6.25E-08

Table 6. Haspin inhibitors identified in the screening as M-phase selective killers. In this table are represented the IC50 for the several compound identified in the screening as haspin inhibitors. Included the IC50 against haspin and also for the dual inhibitors haspin and Pim the IC50 for the three Pim isoforms.

16 hours after ETP-084 and ETP-340 administration almost 100% of cells are in mitosis (Figure 50b) whereas the pan-Pim inhibitor ETP-00048069 does not results in accumulation of mitotic figures. This was confirmed by videomicroscopy after ETP-0048069 treatment 100% of the cells, either *Cdc20(*lox/lox) or HeLa, die in interphase before mitotic entry.

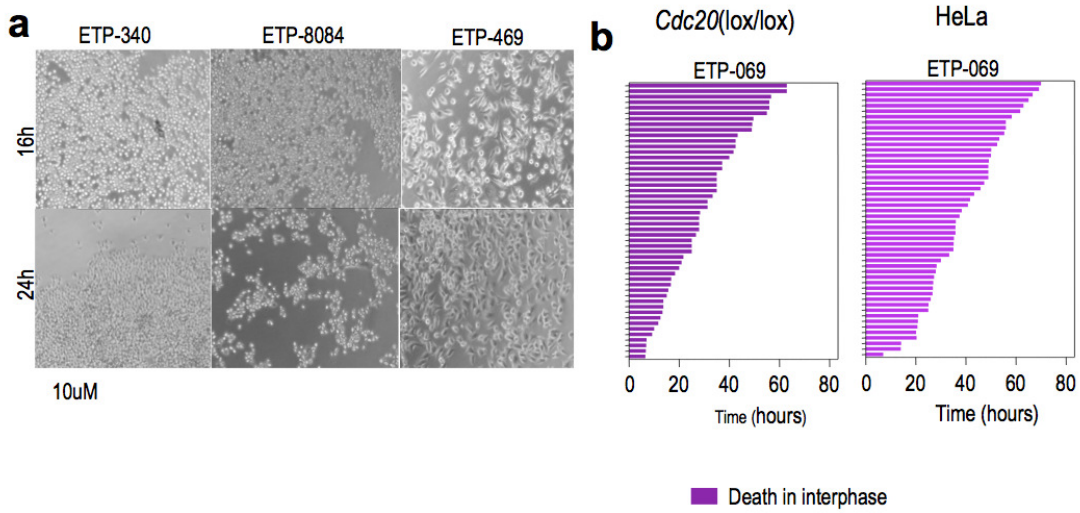

Figure 50. Inhibition of Pim leads to cell death in interphase. a) Cell fate diagrams of *Cdc20*(lox/lox) (lefts) and HeLa cells (right). In violet is represented the duration of interphase until cell death in interphase. No cell enters mitosis in the observation period. Each line represents an individual cell in the presence of the indicated treatments. **b)** Bright-field micrographies after 16 and 24 hours of the indicated treatments. Inhibition on Pim together with Haspin leads to the accumulation of cell in mitosis.

Here we have demonstrated that inhibition of haspin by 5-IU or genetic depletion by using siRNA result in mitotic arrest often followed by cell death in mitosis. A similar result is achieved upon dual inhibition of haspin and Pim by the use of: ETP-340, ETP-081 or ETP-084. Duration of mitosis (DOM) was plotted upon all these different treatments (Figure 51); green dots represent DOM of the cells that undergo mitotic slippage in the presence of the drug and in orange the DOM of cells that die in mitosis. Haspin knockdown results in a more prolonged DOM compared to chemical inhibition and is even longer than the mitotic delay imposed by taxol treatment. However, the longest DOM is achieved upon genetic ablation of Cdc20. Regarding the efficiency in the induction of cell death in mitosis, ETP-084 results more efficient than 5-IU. Taking into account that 5-IU inhibits more efficiently haspin (IC50 of 5-IU for haspin is E-09 and ETP-084 IC50 is 5E-08, see table 7 and De Antoni *et al*., 2012) this increased cell death in mitosis might be due to the concomitant Pim inhibition. These results shows that the dual inhibition of Pim and haspin enhances the efficiency of haspin inhibitors in killing cells in mitosis, suggesting that Pim activity may contribute to the pro-survival signals during mitosis.

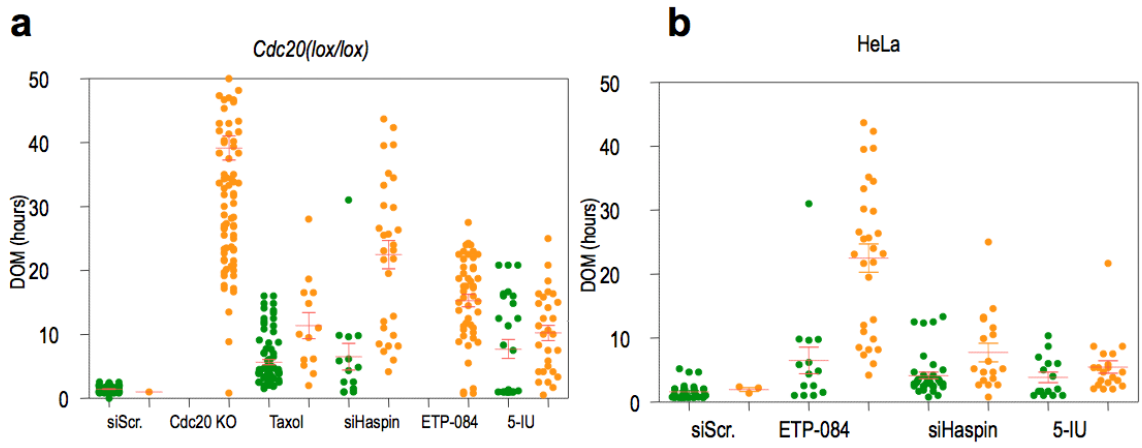

Figure 51. Pim and haspin dual inhibition results in extended DOM compared to single haspin inhibition. a) Plot representing the duration of mitosis, from mitotic entry to mitotic exit in the lack of segregation (green) and from mitotic entry till cell death in mitosis (orange) in Cdc20-null and *Cdc20*(lox/lox) MEFs. **b)** Plot representing the duration of mitosis, from mitotic entry to mitotic exit in the lack of segregation (green) and from mitotic entry till cell death in mitosis (orange) in HeLa cells.

Moreover, DOM upon haspin depletion by siRNA is in between the DOM of Cdc20-null cells, in which mitotic exit is prevented, and the DOM after treatment with taxol, which leads to mitotic delay by activation of the SAC. This prompted us to ask whether the mitotic delay observed after haspin inhibition is due to any of those two mechanisms. In order to test whether haspin inhibition is triggering SAC activity, we measure duration of mitosis upon haspin inhibition by using ETP-084 and 5-IU inhibitors in the presence of reversine, an Mps1 inhibitor, which is the kinase activity of the SAC. Reversine alone results in a reduced duration of mitosis in *Cdc20*(lox/lox) MEFs in the absence of chromosome segregation, and interestingly in combination with 5-IU or ETP-084 significantly reduces the duration of mitosis imposed by haspin inhibition (Figure 52). This result may suggest that rather than preventing mitotic exit, haspin inhibition somehow triggers the SAC.

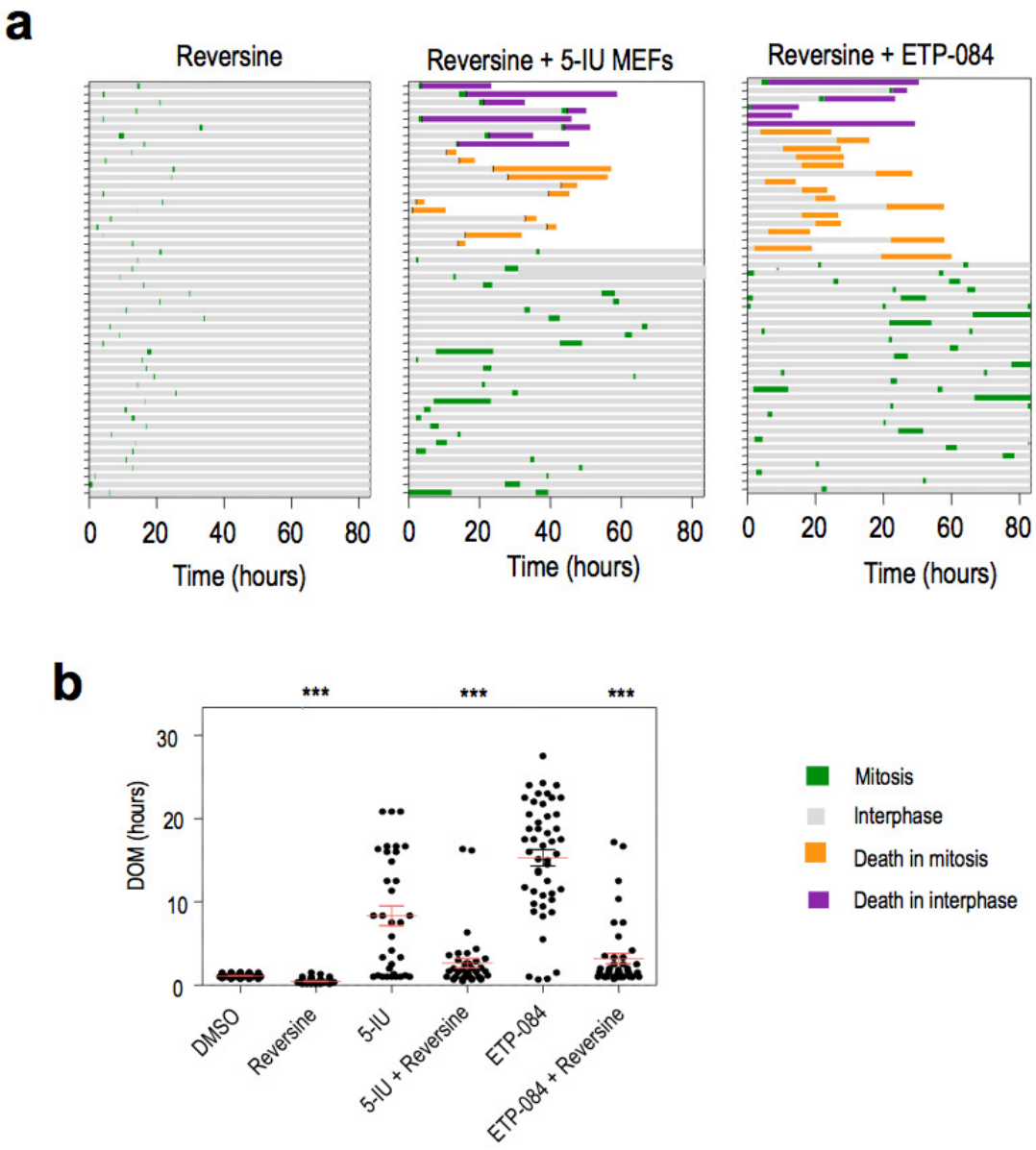

Figure 52. SAC abrogation rescues the DOM upon haspin inhibition. **a)** Duration of interphase (gray) or mitosis (green) of *Cdc20*(lox/lox) cells treated with the indicated inhibitors. Each line represents one cell. Cell death observed in interphase is represented in violet, while cell death detected during mitosis is shown in orange. Cell fate diagrams in Cdc20 wild-type MEFs upon the indicated treatments. **b)** Duration of mitosis in *Cdc20*(lox/lox) upon the indicated treatments. Reversine treatment reduces mitotic length.

All together this results suggest haspin inhibition as a potential anti-mitotic target, although its therapeutic potential for cancer therapy needs to be further analyzed in vitro as well as in vivo.

Discussion

1. Disclosing the molecular mechanism of MCD

1.1 Mitotic cell death pathways

The arrest imposed by anti-mitotic drugs is frequently transient and cells exit from mitosis (i.e. DNA decondensates and the nucleus reforms in the absence of chromosome segregation) in a process known as mitotic slippage (Brito and Rieder, 2006; Topham and Taylor, 2013). Mitotic slippage is though to be one of the major mechanisms of resistance against antimitotic drugs. Such a process does not occur in the absence of Cdc20, which instead results in a permanent mitotic arrest until cells die, providing a clean genetic model to analyze molecular pathways that determine cell fate in mitosis (Manchado *et al*., 2010). Inhibiting the APC/C has been therefore proposed as a therapeutic option to prevent mitotic slippage (Doménech and Malumbres, 2013; Huang *et al*., 2009; Machado *et al*., 2011; Rieder and Medema, 2009).

Cells are sensitive to multiple insults during mitosis and the cellular alterations resulting from aberrant mitotic progression are collectively known as mitotic catastrophe (Vitale *et al*., 2011). Despite the broad use of this concept, the molecular mechanisms that determine cell death in response to these alterations are not well understood. In addition, it is frequently unclear whether cell death pathways function in mitosis or arise as an indirect consequence of mitotic aberrations during the following cycle. For instance, prolonged mitotic arrest partially activates specific caspases, causing limited DNA damage and the induction of p53 and related apoptotic pathways in the following interphase (Orth *et al.,* 2012). Among cell death pathways, multiple evidences have established the involvement of intrinsic apoptosis in response to mitotic aberrations (Huang *et al*., 2009; Topham and Taylor, 2013), whereas the extrinsic apoptotic pathway is not functional at this stage of the cell cycle (Matthess e*t al*., 2010). Using Cdc20-null cells, as well as human cancer cells arrested in mitosis, we show here that elimination of pro-survival factors of the Bcl-2 family results in a dramatic reduction in the survival, in agreement with previous reports suggesting the relevance of this family in mitosis (Huang *et al.,* 2009; Inuzuka *et al.,* 2011; Topham and Taylor, 2013; Wertz *et al.,* 2011). It has also been recently described that Cdc20 can suppress apoptosis targeting the pro-apoptotic factor Bim (Wan *et al.,* 2014), suggesting that mitotically arrested cells in which Cdc20 is inhibited as a consequence of SAC activity are sensitive to this form of death. Despite that MCD mainly depends on Bak and Bax and caspases activation, mitotic arrested cells also die in the absence of caspase activity or in Bax /Bak double knockout cells (Figure 21) mainly by necrosis and autophagy, suggesting that other forms of cell death collaborate in MCD. The occurrence of caspase-independent cell death during mitosis has already been demonstrated (Niikura *et al*., 2007). Moreover it has been proposed that the switch between these two types of cell death is dictated by Bcl-xL. Whereas in the absence of Bcl-xL it turns to be caspase and Bak /Bax dependent (Bah *et al*., 2014), if Bcl-xL is present caspases are not needed for MCD.

In a prolonged mitotic arrest Cdk1 activity is sustained and therefore it might have a role in cell death in mitosis, whether pro-survival or pro-death not is not clear. Cdk1 controls the degradation of Bcl-2 family members and restricts the activation of caspases-2, caspase-3 and caspase-8 during mitosis through phosphorylation (Allan *et al*., 2007; Andersen *et al*., 2009; Castedo *et al.,* 2002). In addition, during mitosis Cdk1 acts as a repressor of autophagy, through phosphorylation of Vps34 (PI3K class III) at Thr-159, which impedes its interaction with Beclin1 during mitosis (Furuya *et al.,* 2010) and is also implicated in multisite phosphorylation of Raptor (Gwinn *et al*., 2010; Ramírez-Valle *et al*., 2010) allowing mTORC1 activity during mitosis.

Although we observed morphological features of necrosis in mitosis, no evidences for necroptosis were found: This can be explained by the fact that activation of RIPK1 and RIPK3 requires TNF receptor activation (Vanden Berghe *et al.,* 2014), while as previously mentioned, during mitosis the extrinsic apoptotic pathway is not functional. Strikingly, we identified autophagy as a relevant pathway for the control of cell death during mitosis. Although it was originally argued that autophagy is shut down during the later phases of the cell cycle (Eskelinen *et al*., 2002; Furuya *et al.,* 2012; Tasdemir *et al.,* 2007; Tasdemir *et al.,* 2008), here we demonstrated that autophagy could persist during mitosis, in agreement with recent studies (Liu *et*

al., 2009). In most known cases, autophagy constitutes a cytoprotective response in the attempt to cope with stress (Rosenfeldt and Ryan, 2011), however, the final outcome of autophagy depends on the cellular context and in particular the strength and the length of the stress-inducing signals, being cytoprotective in some scenarios, while considered a type II programmed cell death in some others (Levine and Kroemer, 2008; Mathew *et al.,* 2007). Here we demonstrate that inhibition of autophagy, in mitotically arrested cells, results in prolonged survival whereas induction of this process results in premature death in mitosis (Figures 29 and 30). We may hypothesize that, in an early mitotic arrest, autophagy might be initially a survival mechanism in order to fuel the highly energy consuming mitotic state, but at a late stage is massive induction contributes to cell death. Inhibition of autophagy prevents PARP cleavage, however dual inhibition of caspase and autophagy does not shows an additive effect in delaying SiM, suggesting a combined induction of autophagy and apoptosis, acting autophagy as a facilitator or cooperator of apoptosis.

1.2 Mitochondria where cell death and metabolism converge

Mitochondria may therefore set the threshold over which cell death occurs playing a central role in both energy metabolism and cell death. It has been assumed that mitochondria are particularly active during the energy intensive process driving spindle formation and chromosome segregation. In fact, recent data showed that Cdk1 activity is necessary to phosphorylate and activate several components of the mitochondrial complex I, thus enhancing mitochondrial respiration during the G2/M transition (Wang et al., 2014). Inhibition of Cdk1 results in decreased mitochondrial activity (Wang *et al.,* 2014), impaired respiratory capacity (Figure 35), and reduced ATP levels (Figure 38c). Thus, Cdk1 activity provides cells with the bioenergy required for a normal mitotic progression by enhancing mitochondrial respiration. However, upon mitotic arrest, the mitochondrial mass initially declines (after about 3 hours) presumably as a result of deficient renovation of organelles. This process occurs in the presence of mitophagy (Figure 33), a critical autophagic process responsible for the clearance of damaged mitochondria (Okamoto, 2014; Youle and Narendra, 2011) promoting further decrease in mitochondrial mass. Whereas the balance between biogenesis and mitophagy determines the maintenance of a healthy mitochondrial pool in normal cells, the reduced biogenesis resulting from impaired transcription and reduced translation in mitotic cells likely perpetuates mitochondrial dysfunction (Figure 35) and reduced ATP levels (Figure 38) during mitotic arrest. Indeed mitochondrial elongation in the absence of the dynein Drp1 (Figure 33) serves a protective function from mitophagy, in agreement with some studies that shows that in starving conditions mitochondrial elongation protects from autophagy (Rambold *et al*., 2010). Mitochondrial fusion has been linked to increased ATP production during stress and starvation (Mitra *et al*., 2012; Tondera *et al.,* 2010), therefore it is likely that elongated mitochondria in the absence of Drp1 might lead to a more efficient mitochondrial ATP production important for meeting the metabolic during mitosis.

1.3 Cell survival control by the metabolic checkpoint AMPK

The rise in the AMP/ATP ratio during mitotic arrest leads to activation of AMPK, a major homeostatic regulator of cellular ATP levels (Hardie *et al*., 2012a). AMPK stimulates catabolic pathways that generate ATP, and inhibits ATP-consuming processes such as biosynthesis and cell growth and proliferation (Hardie *et al*., 2012a). AMPK activation can acutely increase glucose uptake and glycolysis, although in the long term it promotes the more energy-efficient oxidative metabolism by upregulating mitochondrial biogenesis, however, the later process is thought to be transcription-dependent (Hardie *et al*., 2012b) and therefore inefficient in mitotic arrested cells. AMPK might be considered as a metabolic checkpoint coordinating cell growth with energy status.

Among other activities, it appears that AMPK possesses at least three different ways to release the mTORC1-mediated repression on autophagy in case of energetic stress. Activated AMPK was thought to inhibit mTORC1 activity primarily in the opposite way as growth factors stimulate it, mainly by phosphorylation and activation of the negative regulator TSC2 (Inoki *et al*., 2003). Secondly AMPK

phosphorylates Raptor generating a docking site for inhibitory 14-3-3 proteins and is required inhibition of mTORC1 and cell-cycle arrest induced by energy stress. And AMPK may also controls mTORC1 indirectly by forming stable complexes with Ulk1 and Ulk2 and directly phosphorylates Ulk1, thus triggering autophagy (Egan *et al.,* 2011; Kim *et al.*, 2011).

Additionally, it has been recently published that AMPK is active during mitosis and it is required for the completion of mitosis by phosphorylating components of the APC/C (APC1 and CDC27) and PP1 regulatory subunits (Banko et al., 2011). In these studies, it was not obvious why a kinase activated by energy stress should be required for passage through mitosis (Hardie et al., 2012b). However, it is important to note that nocodazole-arrested cells were used in these studies as a paradigm of mitotic cells (Banko et al., 2011) raising the possibility that some of these conclusions may not apply to a normal lasting (<1h in average) mitosis. In drosophila, genetic inactivation of AMPK leads to dramatic defects in cellular architecture and genomic instability. AMPK-null embryos displayed mitotic defects, including chromosome misalignment in metaphase, chromosome lagging as well as failure in cytokinesis and polyploidy (Bland et al., 2012). This phenotype is likely linked to myosin II regulatory light chain (MRLC) function (Lee et al., 2007), since it has been recently proposed that AMP-activated protein kinase (AMPK) might indirectly promote the phosphorylation of MRLC at Ser-19, by phosphorylating PPP1R12C and PAK2, to regulate the transition from metaphase to anaphase and the completion of cytokinesis. In fact Vázquez-Martín and colleagues shows that the active form of the α catalytic AMPK subunit associates dynamically with essential mitotic regulators during mitosis in human cells. Among them Plk1 conducts the AMPK-mediated activation of myosin regulatory light chain at the cytokinesis cleavage furrow independently of energy balance. The functional link between AMPK and mitosis may be more complex than initially thought, and fine-tuned biphasic activation of AMPK is required for proper cell division and faithful chromosome segregation during mitosis, whereas any alteration of AMPK expression or function (obtained by pharmacological sustained activation or AMPK depletion) alters its spatial and temporal regulation, resulting in microtubule misalignment, spindle missorientation, abnormal chromosome segregation followed by mitotic catastrophe and polyploidy (Banko et al,. 2011; Thaiparambil., et al 2012; Vázquez-Martin et al., 2009).

In addition AMPK activity is also pro-apoptotic, and necessary and sufficient for the activation of pro-apoptotic proteins such as Bim or Bmf and cell death during bioenergetics stress (Concannon *et al.*, 2010; Davila *et al*., 2012; Kilbride *et al.,* 2010). Thus, AMPK may modulate the balance between Bcl2-family pro-apoptotic and pro-apoptotic members, in favor of the later during prolonged mitotic arrest. Thus AMPK has a dual role during mitotic arrest. On one hand, it senses loss of ATP and enhances glycolysis protecting from death. On the other hand, it may enhance autophagy and apoptosis through the modulation of Ulk1/mTOR and Bim /Bmf activities, thus explaining why both the inhibition (using siRNAs or small-molecule inhibitors) and the activation of AMPK (with AICAR) results in reduced survival during mitosis (Figure 43).

1.4 AMPK drives a metabolic switch from OXPHOS to glycolysis and cell survival

The cease of respiration results in a bioenergetics crisis in which the concentration of AMP is increased, leading to AMPK phosphorylation and an increased in glucose uptake. The glycolytic activity of AMPK is mostly determined by the phosphorylation and activation of PFKFB3 which is related to Warburg effect (Marsin *et al*., 2002; Bando H *et al*. 2005). Phosphorylated PFKFB3 at ser-461 shows an increase in Vmax of the kinase activity and a decreased Km for Fru-6-P (Marsin *et al*., 2002; Novellasdemunt *et al*., 2012) leading to an increased production of F2,6BP that in turn enhances PFK-1 activity and therefore glycolysis. Interestingly PFKFB3 is expressed in transformed cells and tumors (Almeida *et a*l., 2010; Bando *et al*., 2005; Calvo *et al.,* 2006; Chesney *et al*., 1999; Duran *et al.,* 2008; Kesseler *et al.,* 2008; Novellasdemunt *et al*., 2006; Riera *et al.,* 2020; Yalcin *et a*l., 2009). And PFK-1 is often hyperactivated in cancer (Bando *et al*., 2010) (Figure 53).

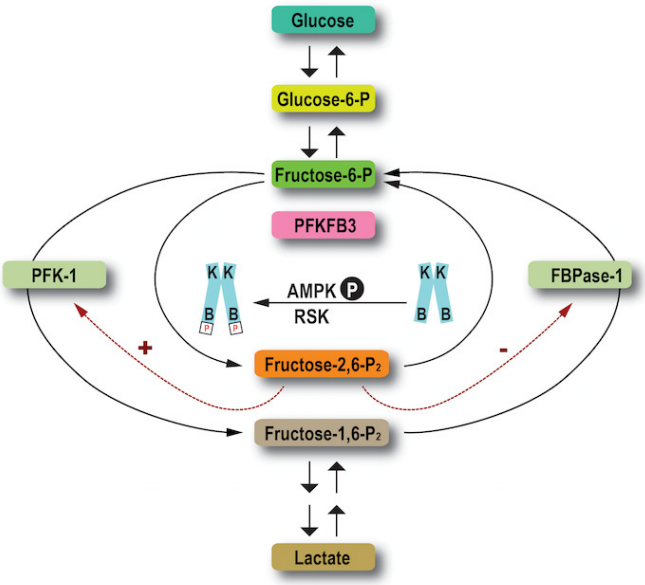

Figure 53. Mechanism of regulation of glycolysis by AMPK. The mitotic state facilitates the interaction between PFKFB3, which shows nuclear localization in interphase PFKFB3, and AMPK, mostly cytoplasmic, in absence of NE. The active form of AMPK phosphorylates PFKFB3 at serine 461, producing an increase in its kinase activity and a decreased phosphatase activity. The product of PFKFB3 kinase activity, fructose-2,6-BP, is a positive allosteric regulator of PFK-1 the first step of glycolysis, resulting in an increased glycolytic flux. In addition to AMPK, PFKFB3 is phosphorylated in the same residue by a battery of protein kinases such as: RSK, MK2, PKB/Akt and PKC.

Apart from AMPK, PFKFB3 is subject of multiregulation by several kinases. The C-terminal domain can be phosphorylated at Ser-461 by different protein kinases, such as RSK (ribosomal S6 kinase) (Novellasdemunt *et al*., 2012) and MK2 (Novellasdemunt *et al*., 2013). Is also phosphorylated at the same residue by PKA (protein kinase A), PKB/Akt (protein kinase B) (Deprez *et al*., 1007; Mouton *et al*., 2000) and PKC making it responsive to multiple external signals (Okamura and Sakakibara, 1998;). Furthermore, the PFKFB3 enzyme was found to be regulated through the PI3K (phosphoinositide 3-kinase)/Akt /mTOR pathway, turning it into a target of growth factors signaling (Duran *et al*., 2009; Garcia-Cao *et al*., 2012). PFKFB3 is also regulated in a cell cycle-dependent manner through ubiquitin-dependent targeting and degradation by APC/C-Cdh1 complexes (Herrero-Mendez *et al*., 2009). Since APC/C-Cdh1 is activated downstream of APC/C-Cdc20 after mitotic exit, the levels of PFKFB3 are high during mitosis (Fernandez-Fernandez *et al*., 2012; Moncada *et al*., 2012; Huang *et al*., 2012). PFKFB3 is mostly nuclear during interphase, whereas the activation of AMPK elicited from addition of 2-DG or AICAR has been shown to be predominantly cytoplasmic (Tsou *et al.,* 2011). During mitosis the nuclear envelope breakdown results in the combination of nuclear and cytoplasmic compartments during mitosis, likely facilitating the AMPK-mediated activation of the kinase activity. PFKFB3 in turn enhances PFK-1 activity, which results in enhanced glycolysis and increased cell survival in mitosis.

1.5 Glycolysis is a major determinant of survival in mitosis

Thus, whereas recent data suggest that Cdk1-dependent activation of mitochondrial respiration is required for the G2/M transition, our data suggest that a switch from OXPHOS to glycolysis is required during prolonged mitotic arrest modulated by AMPK and PFKFB3. This increases glycolysis can be viewed as an adaptation to loss of OXPHOS and it also may helps to evade excess ROS and alleviate oxidative stress. Warburg effect can be defined as a shift from ATP generation through oxidative phosphorylation to ATP generation through glycolysis, however this switch do not relies in an impaired mitochondrial activity; in fact the evidences of dysfunctional mitochondria in cancer are limited (Boland *et al.,* 2013). Warburg observed that the absolute rate of mitochondrial respiration in cancer cells remains comparable to that of normal cells and persist in the vast majority of tumors and remain a major source of ATP generation.

The full oxidation of one molecule of glucose produces up to 38 ATP molecules (including 2 ATP generated in glycolysis) vs only 2 ATP molecules generated in glycolysis, although is more rapid and increased glycolytic rate provide some other advantages for cell proliferation and tumor growth. Bolaños *et*

al., 2010, recently demonstrated that an enhanced glycolysis driven by PFKFB3, in astrocytes, protects from cell death by using the ATP generated in glycolysis to increase their mitochondrial membrane potential, cells become more resistant to pro-apoptotic stimuli. Moreover cancer cells boost glycolysis primarily to constantly supply of glycolytic intermediates, which as precursors can be diverted into anabolic pathways including the pentose phosphate pathways (PPP), serine and triacylglycerol synthesis pathways for *de novo* synthesis of nucleotides, aminoacids and lipids to satisfy the anabolic need of dividing cells. PPP is also a source of cellular NADPH as well as some reactions of glycolysis, and therefore boosting glycolysis replenish intracellular redox potential which can buffer increased ROS (Cairns, 2010). As it also happens in neurons, glucose metabolism may be directed to the PPP, leading to regeneration of reduced glutathione (Bolaños *et al.,* 2010). Glycolysis diminished cellular oxidative stress also by limiting the pyruvate flux into mitochondrial oxidative metabolism. In summary glycolysis confers protection to cell death by affecting metabolic pathways, but it can directly control apoptosis, as it has been recently established by Meynet *et al*., 2012, inhibition of the glycolytic metabolism of transformed cells could decrease Mcl-1 levels, but no other Bcl-2 anti-apoptotic members, through a control of its translation, and therefore inhibition of glycolysis may restore sensitivity to ABT-737- induced death.

1.6 Therapeutic implications of combination treatments

Our results indicate that multiple pathways including apoptosis, autophagy and energy production mediate survival in mitosis (Figure 54).

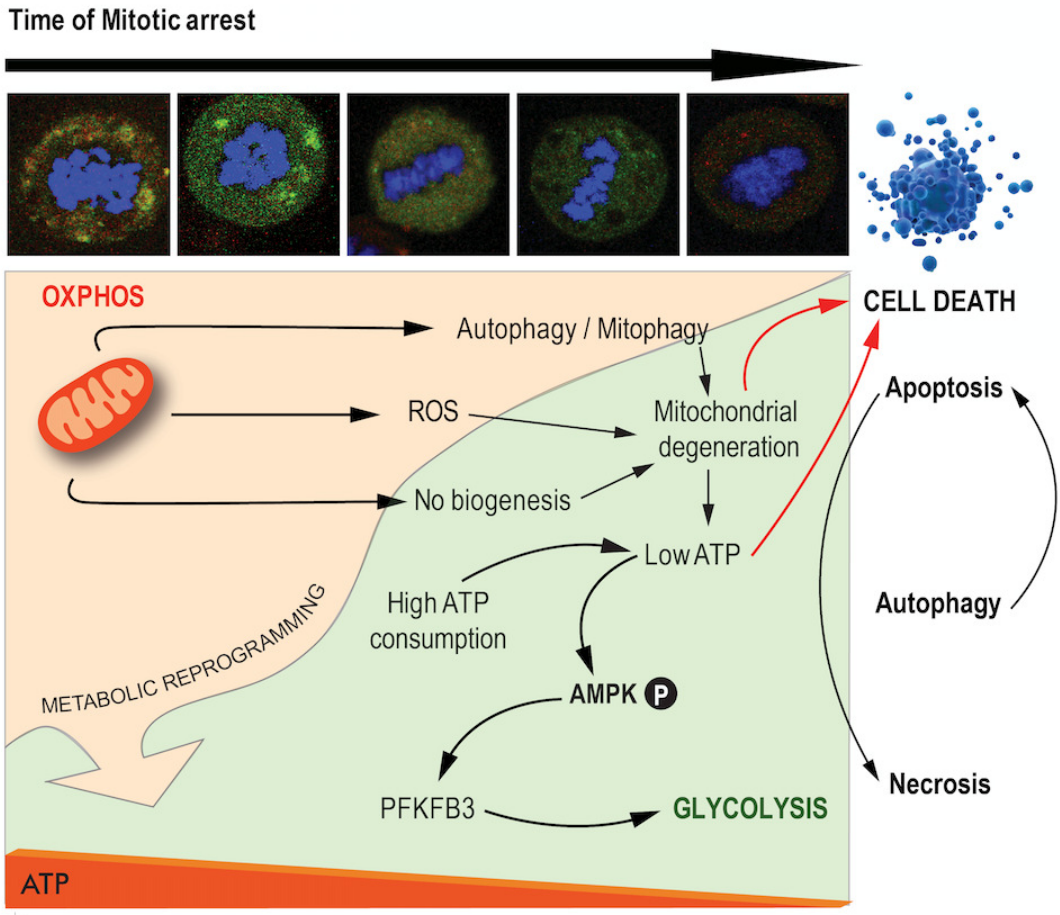

Figure 54. Mitotic cell death is dictated by cell death pathways and energy availability. Cdk1-dependent activation of OXPHOS is required for the G2/M transition, but in a prolonged mitotic arrest a metabolic switch from OXPHOS to glycolysis occurs due to, at first, of a lack o organelles biosyntesis and secondly as a consequence of an

active process of mitochondria degeneration, in part enhanced by ROS accumulation, and subsequent removal of damaged mitochondria by mitophagy. The low ATP levels, due to reduced OXPHOS and to high ATP consumption, leads to AMPK activation, which contributes to the increased glycolysis by phosphorylation and activation of PFKFB3 kinase activity. PFKFB3 in turns boost glycolysis by catalyzing the formation of the principal allosteric regulator of PFK-1, the limiting enzyme of glycolysis. Mitochondrial degeneration, low energy levels and ROS accumulation are triggers of cell death which might be further enhanced by sustained AMPK activity, which may directly modulate apoptosis and autophagy, the two major cell death pathways involved in mitotic cell death. Necrosis, apoptosis and autophagy are tightly interlinked and can be triggered and prevented among them. Whereas necrosis constituted the cell death by default that is unmasked when essential effectors of apoptosis are unmasked or in the absence of levels of ATP necessary to execute cell death programs, in prolonged mitotic arrest it seems that apoptosis and autophagy act in parallel and autophagy id pro-apoptotic.

These observations may have important implications in cancer therapy since mitotic slippage is considered as a major mechanism of resistance in mitotic-targeted therapies (Doménech and Malumbres 2013 Gascoigne and Taylor, 2008; Manchado and Malumbres, 2011) and inhibition of mitotic exit has been lately proposed as a very efficient strategy for killing tumor cells (Manchado *et al*., 2010; Huang *et al*., 2009; Luo J *et al.,* 2009; Zeng *et al*., 2009). Thus, interfering with pathways that sustain survival in mitosis or induction of cell death pathways in mitosis in combination with anti-mitotic drugs (i.e. taxol) may promote cell death before mitotic slippage and the accumulation of aneuploidy cells, ultimately improving therapeutic efficiency. Here we demonstrate that treatment with several small-molecule compounds directed against these pathways result in enhanced cell death in mitosis in cooperation with taxol and preventing cell proliferation of breast cancer cells both in vitro (Figure 49) and in vivo (Figure 50). The combination between microtubule poisons and apoptotic inducers has been extensively studied (Inuzuka *et al*., 2011; Oltersdorf *et al*., 2005; Topham and Taylor, 2013; Wertz *et al*., 2011) and are of particular interest in some particular settings, for instance in Bcl-2 expressing tumors (Oakes *et al.,* 2011). As well as combinations with mTOR and metabolic inhibitors have been thoroughly tested in xenograft mouse mode (Campone *et al*., 2009; Lieber *et al.,* 2011; Meier *et al*., 2009), however here we show for the first time the molecular basis for this synergistic effect. Single treatment with glycolytic inhibitors i.e. 3PO shows a modest effect so far, however cooperates with taxol in preventing cell proliferation of breast cancer calls both in vitro and in vivo. Collectively, these data provide the cellular basis for new combinatory therapies targeting cell cycle cell death pathways and metabolism in cancer.

2. Targeting mitosis: the need for new therapeutic options

Selective cancer chemotherapy is based on the assumption that tumor cells proliferate rapidly and cytotoxic drugs gain specificity from their ability to preferentially kill rapidly proliferating cells (Chabner *et al.,* 2006). However, proliferation rate is low in many chemosensitive human cancers, and it is not clear how a drug that only kills dividing cells could promote tumor regression. After treatment with anti-mitotic drugs only cells that enter mitosis are killed or rendered senescence (Baguley *et al.,* 1995; Blagosklonny *et al.,* 2006; Gascoigne and Taylor, 2008; Orth *et al.,* 2008; Shi *et al.,* 2008), whereas quiescent cells or cells that do not reach mitosis during the exposure time remain unaffected. According to the "fractional kill" theory, only cells that pass through the phase of the cell cycle, towards a given drug was targeted to, when drug is present above its cytotoxic threshold are killed. Therefore a cell cycle phase–specific cytotoxic drug only kills a fixed fraction of cancer cells, necessitating multiple doses to eradicate the tumor (Berenbaum, 1972). This predicts a strong correlation between proliferation rate and drug sensitivity in both cancer and normal tissues. This prediction fits well for paclitaxel in tissue culture (Baguley *et al.*, 1995), whereas data from treatment of human solid tumors are less homogeneous. A positive correlation between proliferation rate and clinical response was seen in breast cancer for mostly DNA-targeted chemotherapy (Amadori *et al.*, 1997) but not for docetaxel (Noguchi, 2006). However some studies consider mitotic index as a prognosis value. Hasebe *et al.,* in 2011 suggested that mitotic index can efficiently categorize breast carcinomas, transitional cell bladder carcinomas and ovarian carcinomas into groups of distinctly different prognoses, being the survival of patients with slowly proliferating tumors significantly better than the survival of patients with a higher mitotic frequency.

Anti-microtubule drugs such as taxanes and vinca alkaloids, has shown great clinical success encouraging the development of drugs that specifically target mitosis. Nevertheless, some of the anti-tumour effects of the tubulin drugs might be attributed to interphase interactions with the tubulin cytoskeleton. The newer targets might not afford the opportunity to alter both the mitotic spindle and the cytoskeleton, that many of these proteins appear to function solely in mitosis makes them ideal targets for the development of mitosis-specific cancer drugs. The selectivity for mitosis and the distinct ways in which these new agents interfere with mitosis provides the potential to not only overcome certain limitations of current tubulin-targeted anti-mitotic drugs, but to expand the scope of clinical efficacy that those drugs have established. Drugs that selectively inhibit mitotic kinesins involved in spindle and kinetochore functions, as well as kinases that regulate these activities, are currently in various stages of clinical trials. Although promising it have not achieved the desired efficiency in patients. Evidence for clinical efficacy was reduced with very limited objective responses and these compounds were mostly inefficient in patients. In general, the current generation of targeted mitotic inhibitors displays less anticancer activity than paclitaxel, although neurotoxicity has been abolished. It has been argued that mitotic rates in human tumors are much lower than in preclinical models and this may limit the effect of these drugs (Doménech and Malumbres, 2013). Considering these limitations it is critical to evaluate how antimitotic therapies can be improved in the clinic. One emergent strategy is the combination of antimitotic drugs with additional compounds. Examples of the combinations preclinical models and clinical trials are displayed in Table 8. Moreover drug discovery programs has mainly focused in Plk1 and Aurora A and B as cancer targets, and now several member of the kinesin superfamily are emerging as putative anticancer targets, however the are several others mitotic kinases which potential as anticancer targets remain unexplored, that is the case for Nek, Mps1, Mastl or Haspin.

Target	Combination	Model	Description
Plk1	BI2536, BI6727, ON01910 and DNA damage agents (doxorubicin, cyclophosphamide, irinotecan, etc.)	Breast cancer cell lines, Phase I/II Solid and hematopoietic tumors	Impaired tumor growth in xenografts. Combinations lead to a faster complete response and prevent relapse. Clinical trials ongoing

Target	Combination	Model	Description
	BI2536 and bortezomib (proteasome inhibitor)	Tumor cell lines	Enhanced anti-proliferative and apoptotic effects
	BI6727, BIBF1120 (VEGFR inhibitor) and BIBW2992 (EGFR inhibitor)	Phase I Advanced solid tumors	Ongoing/no results published
Aurora kinases	AZD1152, PHA-680632, MLN8237 and DNA damage agents (platinum, gemcitabine, radiation, etc.)	Solid tumor cell lines. Phase I in AML	Synergistic effects in proliferation and apoptosis. Enhance the effectiveness of the single therapy. Radisensitizer specially in p53-deficient cells
	VX-680, VE-465, AT9283, CYC3, MLN8237 and microtubule agents	Tumor cell lines. Phase I in adenocarcinoma	Synergistic or additive effect in different cell lines
	MLN8237 and bortezomid	Phase I Lymphoma and multiple myeloma	Ongoing/no results published
	MLN8237 and vorinostat (HDAC inhibitor)	Tumor celll lines. Phase I in lymphoma	Tumor growth inhibition in xenografts but additive cytotoxicity in leukemias.
	MLN8237 and rapamycin (mTOR inhibitor)	Uterine leiomyosarcoma cell lines	Synergistic antiproliferative effect (only when preadministered)
	MLN8237 and erlotinib (EGFR inhibitor)	Phase I NSCLC	Ongoing/no results published
Kinesins	SB-715992 and carboplatin or capecitabine	Phase I Solid tumors	Ongoing/no results published
	SB-715992 and docetaxel	Phase I Solid tumors	Ongoing/no results published
	ARRY-520, carfilzomib, bortezomid and dexamethalone	Phase I Relapsed or refractory multiple myeloma	Ongoing/no results published

Table 8. Therapeutic treatments using mitotic inhibitors in combination with additional compounds
Abbreviations: AML, acute mieloide leucemia; CLL, chronic lymphocytic leukemia; pH3, phospho-histine H3. Clinical trials are indicated using the ClinicalTrials.gov identifier.

By screening a library of 300 compounds for its ability to specifically kill cells in mitosis, we identified the kinase haspin as potential anti-mitotic target. Haspin inhibition in asynchronic cultures leads to mitotic delay in agreement with previous data (Dai J *et al*., 2005; Niedzialdhowska *et al*., 2012; Wang et al., 2011). This mitotic arrest is longer than the mitotic delay observed after taxol treatment and is often followed by cell death in mitosis, resulting more efficient than taxol in inducing mitotic cell death. Since reversine is able to rescue the duration of mitosis when haspin is inhibited, this may suggest that the mitotic delay observed upon haspin inhibition is dependent on SAC activation. However, recent work has suggested that chemical inhibition of haspin may impair the activation of the SAC (De Antoni et al., Wang et al., 2010), although, haspin downregulation via siRNA does not seem to produce the same SAC defect (Wang et al., 2012). Moreover, yeast cells lacking haspin paralogs, *ALK1* and *ALK2* (Panigada et al., 2013) propertly activate the SAC, and are especially sensitive to microtube deploymerizing drugs (i.e. nocodazole). Indeed, after

transient nocodazole treatment, cells lacking haspin shows a misspositioned spindle, leading to unequal segregation, but haspin does not interfere with microtubule dynamics. In summary, yeast haspin has a role in allowing cells to tolerate the mitotic delay induced by SAC activation and reestablish proper spindle positioning. Furthermore, inhibition of haspin results in some cases in problems in DNA condensation. This event might be a direct consequence of the lack of histone H3 phosphorylation at Thr-3, although the function of this modification is debated, it may facilitate chromatin condensation or the release of cohesin and ISWI chromatin-remodeling ATPases (Andrews *et al*., 2003; Pringent *et al*., 2003; Swedlow and Hirano 2003; van Hooser *et al.,* 1998). As defects in cohesion leads to SAC activation (Hoque and Ishikawa, 2002), these defects in condensation may also trigger the SAC delaying mitotic progression.

Haspin mitotic phosphorilarylation of histone 3 at threonine-3, acts as a docking site for the CPC (survivin, Aurora B, borealin and INCENP) (Cuny *et al*., 2012) and therefore haspin inhibition may lead to misslocalization of the CPC and lack of activation of Aurora B. However, the phenotype observed in Aurora B knockout MEFs and upon Aurora B chemical inhibition is the opposite: a rapid mitotic exit as a consequence of SAC abrogation, showing a shorter mitotic length compared to wild-type MEFs (Fernández-Miranda *et al*., 2010). On the other hand, as before mentioned, it has been described that survivin depletion leads to a mitotic delay of 2-3 hours and massive interphase apoptosis after failing to complete cytokinesis (Carvalho *et al*., 2003; Cutts *et al*., 1999; Lens *et al*., 2003; Uren *et al*., 2000; Zuojun *et al*., 2008). Noteworthy, survivin is the only component of the mitotic machinery that function in preventing apoptosis by directly inhibiting caspases (Chan *et al*., 2012), however the role of survivin in the CPC, wheter is mere structural or something else, is under debate. The expression of survivin reaches a maximum during G2/M and is highly expressed in many tumors being a mechanism of resistance (Rödel F *et al*., 2011). Disruption of survivin leads to increased apoptosis and decrease tumor growth, what makes survivin interesting from a therapeutic point of view. To what extent survivin is responsible for the increased cell death in mitosis observed upon haspin inhibition is not known and need to be further studied. However, if that is the case, by indirectly targeting survivin through haspin inhibition will be beneficial in survivin overexpressing tumors.

Haspin inhibitors generated by the Experimental Therapeutics Progremme at CNIO are more efficient in induction of mitotic arrest and mitotic cell death than the commercial haspin inhibitor 5-IU. The possibility that this enhanced efficacy might be due to the additional anti-Pim activity needs to be further analyzed. Interestingly, it has been reported a dynamic redistribution of Pim-1 during the cell cycle. The protein moves from the nucleus and cytoplasm in interphase to the spindle poles during mitosis (Bhatteaharya *et al*., 2002) where it interacts with NuMA, playing a role in promoting association between NuMA, HP1beta, dynein and dynactin, a complex that is necessary for mitosis. Whereas Pim-1 overexpression shows defects in the SAC, abnormal mitotic spindles, centrosome amplification, and chromosome missegregation, resulting in polyploidy and aneuploidy due to a delay in completing cytokinesis (Roh *et al.,* 2003), the absence of Pim-1 promotes apoptosis. Pim inhibitors decreased levels of the Bcl-2 family member Mcl-1, an essential pro-survival signal in mitosis, both by blocking 50-cap dependent translation and decreasing protein half life. In addition, Pim inhibition transcriptionally increased levels of the pro-apoptotic BH3 protein Noxa (Song and Kraft, 2011). In addition, inhibition of Pim kinases in prostate cancer resensitizes chemoresistant cells to taxanes (Numenthaler *et al.,* 2009). All together these evidences support the idea of a specific pro-survival role of Pim during mitosis and provides a possible molecular explanation for the fact that dual inhibition potenciates the effect of haspin inhibitors, however, this need to be further characterized.

Conclusions

Haspin inhibition leads to a SAC-dependent mitotic delay often followed by cell death in mitosis. We therefore propose that Haspin is a critical player in cell survival during prolonged mitotic arrest. In addition, chemical inhibition as well as genetic depletion of haspin is much more efficient than taxol in killing cells in mitosis. All together, these data suggest that haspin is a potential target for anti-mitotic chemotherapy whose utility in cancer therapy deserves further validation.

In conditions in which mitotic arrest is perpetuated cells eventually die. Mitotic cell death is mainly driven by the intrinsic or mitochondrial apoptotic pathway. In addition, necrosis, but not necroptosis, may also participate in mitotic cell death and it may be the major mechanism when apoptosis is inhibited.

Autophagy is induced upon prolonged mitotic arrest. In these conditions, a decrease in mitochondrial mass is observed. Since this occurs in the presence of mitophagy, and can be partially rescued by inhibiting autophagy, we conclude that autophagy also contributes to mitotic cell death, at least partially due to the destruction of mitochondria.

As an adaptation to loss of mitochondrial respiration, a glycolytic switch mediated by AMPK and PFKFB3 takes places during mitotic arrest contributing to cell survival in these conditions. Thus, mitotically arrested cells display a strong dependency on glycolysis, an observation that has important therapeutic implications. In fact, interfering with pathways that sustain survival in mitosis, such as glycolysis, promotes cell death prior to mitotic slippage. PFKFB3 inhibition cooperates in vitro and in vivo with taxol in promoting cell death and preventing tumor cell proliferation. We therefore conclude that glycolysis is a major survival mechanism in mitotically arrested cancer cells.

References

Aaron, G., Coughlin, M., Mitchison, T. M. (2013). Microtubule assembly in meiotic extract requires glycogen. Mol Biol Cell. 24 (10): 1559-1573.

Acquaviva,C. and Pines, J. (2006). The anaphase-promoting complex/cyclosome: APC/C. J Cell Sci 119: 2401-2404.

Adams J.M., Cory S. (1998) The Bcl-2 protein family: Arbiters of cell survival. Science 281:1322–1326.

Almeida, A., Bolaños, J.P., and Moncada, S. (2010). E3 ubiquitin ligase APC/C-Cdh1 accounts for the Warburg effect by linking glycolysis to cell proliferation. Pro Natl Acad Sci U S A 107: 738-741.

Álvarez, B., Martínez-A, C., Boudewjin, M. T. Burgering and Carrera A. C. (2001). Forkhead transcription factors contribute to execution of the mitotic programme in mammals. Nature Letters. 413: 744-747.

Alvarez-Fernandez, M., and Malumbres, M. (2014). Preparing a cell for nuclear envelope breakdown: Spatio-temporal control of phosphorylation during mitotic entry. Bioessays 8: 757-765.

Allan, L.A. and Clarke, P.R. (2007). Phosphorylation of caspase-p by CDK1/cyclinB1 protects mitotic cells against apoptosis. Mol Cell *26*, (2), 302-10.

Alexandre, J., Hu, Y., Lu, W., Pellicano, H., Huang, P. (2007). Novel action of paclitaxel against cancer cells: bystander effect mediated by reactive oxygen species. Cancer Res 67(8): 3512-7.

Amador, V. et al. (2007). APC/C(Cdc20) controls the ubiquitin-mediated egradation of p21 in prometaphase. Moll Cell. 27, (3): 462-73.

Amadori D, Volpi A, Maltoni R, Nanni O, Amaducci L, Amadori A, Giunchi DC, Vio A, Saragoni A, Silvestrini R. (1997) Cell proliferation as a predictor of response to chemotherapy in metastatic breast cancer: a prospective study. Breast Cancer Res Treat 43:7–14

Andersen, J. et al. (2009). Restrain of apoptosis during mitosis through interdomain phosphorylation of caspase-2. EMBO J, 28: 3216-3227.

Andrews P.D., Knatko, E., Moore, W.J., and Swedlow, J.R. 2003. Mitotic mechanics: The auroras come into view. Curr. Opin. Cell. Biol. 15: 672–683.

Araki, M., Yu, H., and Asano, M. (2005). A novel motif governs APC-dependent degradation of Drosophila ORC1 in vivo. Genes Dev, 19 (20): 2458-2465.

Ashrafi, G., and Schwarz, T. L. (2013). The pathways of mitophagy for quality control and clearance of mitochondria. Cell Death Differ 20: 31-42.

Bando, H., Atsumi, T., Nishio, T., Niwa, H., Mishima, S., Shimizu, C., Yoshioka, N., Bucala, R., and Koike, T. (2005). Phosphorylation of the 6-phosphofructo-2-kinase/fructose 2,6-bisphosphatase/PFKFB3 family of glycolytic regulators in human cancer. Clin Cancer Res 11: 5784-5792.

Ayscough, K., Hayles, J., MacNeill, S. A. and Nurse, P. (1992). Cold-sensitive mutants of p34cdc2 that suppress a mitotic catastrophe ohenotype in fission yeast.Mol Gen Genet. 232 (3): 344-50.

Axe, E. L. et al., Autophagosome formation form membrane compartments ebriched in phosphatidylinositol 3-phosphate and dynamically connected to the endoplasmic reticulum. J Cell Biol. (2010).141: 656-657.

Bah, N. et al. (2014). Bcl-xL controls a switch between cell death modes during mitotic arrest. Cell Death Dis. 5: e1291.

Bahatteaharya, N., Wang, Z., Davitt, C., McKenzie, I. F. Xing, P. X. Magnuson, N. S. (2002). Pim-1 associates with protein complexes necessary for mitosis. Chromosoma. 111 (2): 80-95.

Baguley BC, Marshall ES, Whittaker JR, Dotchin MC, Nixon J, McCrystal MR, Finlay GJ, Matthes JH, Holdaway KM, van Zijl P (1995)Resistance mechanisms determining the in vitro sensitivity to paclitaxel of tumour cells cultured from patients with ovarian cancer. Eur J Cancer 31A: 230-237.

Baker, D.J., Jeganathan, K.B., Cameron, J.D., Thompson, M., Juneja, S., Kopecka, A. et al. (2004). BubR1 insufficiency causes early onset of aging-associated phenotypes and infertility in mice. Nat Genet. 36: 744-749.

Bando, H. et al. (2005). Phosphorylation of the 6-phosphofructo-2-kinase/fructose 2,6-biphosphatase/PFKFB3 family of gycolytic regulators in human cancer. Clin Cancer Res. 11 (16): 5784-92.

Banko, M. R., Allen, J. J., Schaffer, B. E., Wilker, E. W., Tsou, P., White, J. L., Villen, J., Wang, B., Kim, S. R., Sakamoto, K.*, et al.* (2011). Chemical genetic screen for AMPKalpha2 substrates uncovers a network of proteins involved in mitosis. Mol Cell 44: 878-892.

Barr, A.R., and Gergely. (2007). Aurora-A: the maker and breaker of spindle poles. J Cell Sci 120 (Pt 179): 2987-2996.

Basserman, F., Eichner, R., and Pagani, M. (2013). The ubuquitin proteasome system-Implications for cell cycle control and the targeted treatment of cancer. Biochim Biophys Acta. 54(11): 584-93.

Baumgarten, A. J., Felthaus, J., and Wasch, R. (2009). Stronh inducible knockdown of APC/CCdc20 does not cause mitotic arrest in human somatic cells. Cell Cycle 8(4): 643-6.

Berenbaum MC(1972) In vivo determination of the fractional kill of human tumor cells by chemotherapeutic agents. Cancer Chemother Rep 56: 563–71.

Blagosklonny, M. V. and Pardee, A.B. (2001). Exploiting cancer cell cycling for selective protection of normal cells. Cancer Res 61(11): 4301-5.

Blagosklonny MV, Demidenko ZN, Giovino M, Szynal C, Donskoy E, Herrmann RA, Barry JJ, Whalen AM (2006) Cytostatic activity of paclitaxel in coronary artery smooth muscle cells is mediated through transient mitotic arrest followed by permanent post-mitotic arrest: comparison with cancer cells. Cell Cycle 5: 1574–1579.

Blanco, M.A. et al., (2000). APC(ste9/srw1) promotes degradation of mitotic cyclins in G(1) and is inhibited by cdc2 phosphorylation. EMBO J 19(15): 3945-55.

Bland, M.L., Lee, R-J., Magallanes, J.M., Foskett, J.K., Birnbaum, M.J. (2010). AMPK suuports growth in Drosophila by regulating muscle activity and nutrient uptake in gut. Dev Biol. 344(1): 293-303.

Bolaños, J. P., Almeida, A., and Moncada, S. (2010). Glycolysis: a bioenergetic or a survival pathway?. Trend Bioch Sci. 35 (3): 145-149.

Bolaños, J. P.(2013). Adapting glycolysis to cancer proliferation: the MAPK pathway focuses on PFKFB3. Biochem J. 452(3): e7-9.

Bolland, M. L., Chourasia A. H. , and Macleod K. F. (2013). Mitochondria dysfunction in cancer. Front Onc. 3: 292.

Bonzon, C., Bouchier-Hayes, L., Pagliari, L.J., Gree, D.R. Newmeyer, D.D. (2006). Caspase-2-induced apoptosis requires bid cleavage: a physiological role for bid in heat shock-induced death. Mol Biol Cell. 17 (2): 2150-7.

Bradley, S.A., Ouyang, A., Purdie, J., Smitka, T.A., Wang, T., Kaerner, A. (2010).Fermentanomics: monitoring mammalian cell cultures with NMR spectroscopy. J Am Chem Soc. 132(28): 9531-3.

Brito, D. A., and Rieder, C. L. (2006). Mitotic checkpoint slippage in humans occurs via cyclin B destruction in the presence of an active checkpoint. Curr Biol 16: 1194-1200.

Brooke, D. G. et al. (2014). Targeting the Warburg Effect in cancer; relationships for 2-arylpyridazinones as inhibitors of key glycolytic enzyme 6-phosphofructo-2-kinase/2,6-biphosphatase 3 (PFKFB3). Bio Med Chem. 22: 1029-1039.

Bucher, N., Britten, C.D.(2008). G2 checkpoint abrogation and checkpoint kinase-1 targeting in the treatmentof cancer. Br J Cancer. 12(3): 523-8.

Bullough, W. S. (1952). The energy relations of mitotic activity. Biol Rev. 27: 133-168.

Burguess, A. et al. (2010). Loss of human Greatwall results in G2 arrest and multiple mitotic defects due to deregulation of the cyclin B-Cdc2/PP2A balance. Proc Natl Acad Sci U S A, 107(28): 12564-9.

Burguess, A., Rasouli, M., and Rogers, S. (2014). Stressing mitosis to death. Front Onc. 4: 140.

Burton, J.L. and Solomon, M.J. (2007). Mad3p, a pseudosubstrate inhibitor of APCCdc2' in the spindle assembly checkpoint. Genes Dev 21: 655-667.

Buytaert, E., Callewaert, G., Vandenheede, J.R. and Agostinis, P. (2006). Deficiency in apoptotic effectors Bak and Bax reveals an autophagic cell death pathway initiated by photodamage to te endoplasmic reticulum. Autophagy 2: 238-240.

Cairns, R. A., Harris, I. S., and Mak, T. W. (2010). Regulation od cancer cell metabolism. 1:, 85-95.

Calvo, M. N. Bartrons, R., Castaño, E., Perales, J. C. Navarro-Sabaté, A., Manzano, A. (2006). PFKFB3 gene silencong decreases glycolysis, induces cell-cycle delay and inhibits anchorage-independent growth in HeLa cells. FEBBS Lett. 580 (13): 3308-14.

Campone, M. et al. (2009). Safety and pharmacokinetics of paclitaxel and the oral mTOR inhibitor everolimus in advanced solid tumours. British journal of cancer 100: 315-321.

Cardazo, T., and Pagano, M. (2004). The SCF ubiquitin ligase: insights into a molecular machine.

Carmena, M and Earnshaw, W.C. (2003). The cellular geography of aurora kinases. Nat Rev Mol Cell Biol 4: 842-854.

Carvalho, A., Carmena, M., Sambade, C., Earnshaw, W. C. and Wheatley, S. P. (2003). Survivin is required for stable checkpoint activation in taxol-treated HeLa cells. J Cell Sci. 116: 2987-2998.

Castedo, M., *et al*. (2002). Cyclin-dependent kinase-1: linking apoptosis to cell cycle and mitotic catastrophe. Cell Death Differ *9* (12): 1278-93.

Castedo, M., Perfettini, J-L., Roumier, T., Andreau, K,m Medema, R., and Kroemer, G. (2004). Cell death by mitotic catastrophe: a molecular definition. Oncogene. 23: 2825-2837.

Chabner BA, *et al*. (2006) in *Goodman and Gilman's The Pharmacological Basis for Therapeutics*, Antineoplastic agents, ed Brunton LL (McGraw-Hill, New York), 11th, pp: 1315–1403.

Chan, K-S., Koh C-G., and Li H-Y. (2012). Mitotis-targeted anti-cancer therapies: were they stand. Cell Death Dis. 3. e411.

Chaussepied, M., Ginsberg, D. (2003). Transcriptional regulation of Akt activation by E2F. Mol Cell. 16: 831-837.

Chen, H., Chan, D. C. (2009). Mitochondrial dynamics--fussion, fission, movement and mitophagy-- in neurodegenerative diseases. Hum Mol Genet. 18 (R2): R169-76.

Chesney, J. (2006). 6-phosphofructo-2-kinase/fructose-2,6-biphosphatase and tumor cell glycolysis. Curr Opin Clin Nutr Metab Care. 9(5): 535-9.

Clarke, D.J. (2009). Strong inducible kockdowm of Cdc20 does not cause mitotic arrest in human somatic cells: implications for cancer therapy?. Nat Cell Biol *5* (8): 748-53.

Cordero-Espinoza, L., and Hagen, T. (2013). Increased concentrations of Fructose 2,6-Biphosphate Contribute to the Warbur effect in Phosphatase and Tensin Homolog (PTEN)-deficient Cells. J Biol Chem. 288 (50): 36020-36028.

Colombo, S.L., Palacios-Callender, M., Frakich, N., De Leon, J., Schmitt, C.A., Boorn, L., Davis, N., and Moncada, S. (2010). Anaphase-promoting complex/cyclosome-Cdh1 coordinates glycolysis and glutaminolysis with transition to S-phase in human T lymphocytes. Proc Natl Acad Sci U S A 107: 2925-2932.

Colombo, S. L., Palacios-Callender, M., Frakich, N., Kovacs, I., Tudzarova, S., and Moncada, S.(2011). Molecular basis for the differential use of glucose and glutamine in cell proliferation as revealed by synchronized HeLa cells. Proc Natl Acad Sci.108 (52): 21069-21074.

Concannon, C. G., Tuffy, L. P., Weisova, P., Bonner, H. P., Davila, D., Bonner, C., Devocelle, M. C., Strasser, A., Ward, M. W., and Prehn, J. H. (2010). AMP kinase-mediated activation of the BH3-only protein Bim couples energy depletion to stress-induced apoptosis. J Cell Biol 189: 83-94.

Cuadrado, A., and Nebreda, A. R. (2010). Mechanism and functions of p38 MAPK signalling. Biochem J. 429 (3): 403-17.

Cuny, G.D. et al. (2012). Structure-activity relationship study of beta-carbonile derivatives as haspin kinase inhibitors. Bioorg Med Chem. 22(5): 2015-9.

Cutts, S. M. et al. (1999). Defective chromosome segregation, microtubule bundling and nuclear bridging in inner centromere protein gene (Incenp)-disrupted mice. Hum Mol Genet. 8: 1145-1155.

Dai, J. Sultan, S. Taylor, S., and Higgins, M. G. (2004). The kinase haspin is required for mitotic histone H3 Thr 3 phosphorylation and normal metaphase chromosome alignment. Gen Dev 19, 472-488.

Dai, W., Wang, Q., Liu, T., Swamy, M., Fang, Y., Xie, S et al. (2005).Slippage of mitotic arrest and enhanced tumor development in mice with BubR1 haploinsufficiency. Cancer Res. 64, 440-445.

Datta, S.R., Brunet, A., Greenberg, M.E. (1999). Cellular survival: a play in three Akts. Gen Dev 13: 2905-2927.

Davila, D., Connolly, N. M., Bonner, H., Weisova, P., Dussmann, H., Concannon, C. G., Huber, H. J., and Prehn, J. H. (2012). Two-step activation of FOXO3 by AMPK generates a coherent feed-forward loop determining excitotoxic cell fate. Cell Death Differ 19: 1677-1688.

De Antoni, A.et al. (2005). The Mad1/Mad2 complex as a template for Mad2 activation in the spindle assembly checkpoint. Curr Biol. 15 (3): 214-25.

De Antoni, A., Maffini, S., Knapp, S., Musacchio, A., Santaguida, S. (2012). A small-molecule inhibitor of Haspin alters kinetochore function of Aurora B. J Cell Biol. 199 (2): 269-84.

Deprez, J., Vertommen, D., Alessi, D.R., Hue, L., Rider, M.H. (1997). Phosphorylation and activation of heart 6-phosphofroctu-2-kinase by protein kinase B and other protein kinases of the insulin signaling cascades. J Biol Chem. 272(28):17269-75.

Dephoure, N., et al. (2008). A quantitative atlas of mitotic phosphorylation. Proc Natl Sci U S A. *105* (31): 10762-7.

Di Fiore, B. and Pines, J. How cylin A destruction scapes the spindle assembly checkpoint. J Cell Biol. *190* (4): 501-9.

Dobles, M., Liberal, V., Scott, M.L., Benezra, R., Sorger, P.K., (2000). Chromosome missegregation and apoptosis in mice lacking the mitotic checkpoint protein Mad2. Cell. 101: 635-645.

Dohi, T., Beltrami, E., Wall, N. R., Plescia, J., Altieri, D.C. (2004). Mitochondrial survivin inhibits apoptosis and promotes tumorigenesis. J Clin Invest. 114 (8): 1117-27.

Doménech, E., and Malumbres, M. (2013). Mitosis-targeting therapies: a troubleshooting guide. Curr Opin Pharmacol. 13(4): 519-28.

Driessens, G., Harsan, L., Robaye, B. Watoquier, D., Browaeys, P., Giannakopoulos, X., Velu, T and Bruyns, C. (2003). Micronuclei to detect in vivo chemotherapy damage in a p53 mutated solid tumor. Br J. Cancer. 89 (4): 727-29.

Duran, J. et al .(2009).Pfkfb3 is transcriptionally upregulated in diabetic mouse liver through proliferative signals. FEEBS J. 276(16): 4555-68.

Duran, J. et al. (2008). Overexpression of ubiquitous 6-phosphofructo-2-kinase in the liver of transgenic mice results in weight gain. Biochem Biophys Res Commun. 365(2): 291-7.

Dutrertre, S. et al., (2004). Phosphorylation of CDC25B by Aurora-A at the centrosome contributes to G2-M transition. J Cell Sci 117, (Pt117): 2523-31.

Dyson, N. (1998). The regulation of E2F by pRB-family proteins. Genes Dev. 12(15)2245-62.

Elstrom, R.L. et al. (2004). Akt stimulates aerobic glycolysis in cancer cells. Cancer Res. 64(11): 3892-9.

Egan, D. F., Shackelford, D. B., Mihaylova, M. M., Gelino, S., Kohnz, R. A., Mair, W., Vazquez, D. S., Joshi, A., Gwinn, D. M., Taylor, R.*, et al.* (2011). Phosphorylation of ULK1 (hATG1) by AMP-activated protein kinase connects energy sensing to mitophagy. Science 331: 456-461.

Eskelinen, E. L., Prescott, A. R., Cooper, J., Brachmann, S. M., Wang, L., Tang, X., Backer, J. M., and Lucocq, J. M. (2002). Inhibition of autophagy in mitotic animal cells. Traffic *3*: 878-893.

Fang, G., Hongtao, Y., Kirschner, M. W. (1998). The checkpoint protein MAD2 and the mitotic regulator CDC20 form a ternary complx with the anaphase-promoting complex to control anaphase initiation. Genes Dev. 12 (12): 1871-1883.

Faubert, B. et al. (2013). AMPK is a negative regulator of Warburg effect and supresses tumor growthin vivo. Cell Metab 17: 113-24.

Fernández-Miranda, G. et al. (2010). SUMOylation modulates the function of Aurora-B kinase. J Cell Sci. 123 (16): 2823-2833.

Fernandez-Fernandez, S., Almeida, A., Bolaños, J.P., (2012). Antioxidant and bioenergetic coupling between neurons and astrocytes. Biochem J., 443(1): 3-11.

Fhearraigh, S. M. and Mc Gee, M. M. (2011). cyclin B1 interacts with the BH3-only protein Bim and mediates its phosphorylation bt Cdk1 during mitosis. Cell Cycle. 10 (22): 3886-3896.

Fimia, G. M. et al. (2013). Ambra1 regulates autophagy and development of the nervous system. Nature. 447: 1121-1125.

Fry, A. M., Meraldi, P., and Nigg, E. A. (1998). A centrosomal function for the human Nek2 protein kinase, a member of the NIMA family of cell cycle regulators. EMBO J *17* (2): 470-81.

Fu, Z., et al. (2008). Plk1-dependent phosphorylation of FoxM1 regulate a transcriptional programme required for mitotic progression. Nat Cell Biol *10* (9): 1076-82.

Funabiki, H., and Wynne, D. J. (2013). Making an effective switch at the kinetochore phosphorylation and dephosphorylation. Chrmosoma. 122 (3): 135-158.

Furuya, T. et al. (2010). Negative regulation of Vps34 by Cdk1 mediated phosphorylation. Mol Cell. 38: 500-511.

Galluzi, L., and kroemer, G. (2008). Necroptosis: a specialized pathway of programmed necrosis. Cell. 136 (7): 1161-3.

Galluzi, L. et al. (2012). Molecular definitions of cell death subroutines: recommendations of the Nomenclature Committee on Cell Death 2012. Cell Death Differ. 19: 107-120.

Garcia-Cao, I. et al. (2012). Systemic elevation of PTEN induces a tumor-suppresive metabolic state. Cell. 149 (1): 49-62.

Gascoigne, K. E., and Taylor, S. S. (2008). Cancer cells display profound intra- and interline variation following prolonged exposure to antimitotic drugs. Cancer Cell 14: 111-122.

Ge, S., Skaar, J. R. and Pagano, M. (2009). APC/C-and Mad2-mediated degradation of Cdc20 during spindle checkpoint activation. Cell Cycle 8 (1): 167-71.

Gheniou, C., Wheelock, M.S., Funabiki, H. (2013). Autoinhibition and Polo-dependent multisite phosphorylation restrict activity of the kinase Haspin to mitosis. Mol Cell.51: 1-12.

Geley, S., et al (2001). Anaphase-promoting complex/cyclosome-dependent proteolysis of human cyclin A starts at the beginning of mitosis and is no subject to the spindle assembly checkpoint. J Cell Biol 1*53* (1): 167-71.

Gelfant, S. (1969). The energetic requiements for mitosis. Ann New York Acad Sci. 536-549.

Goga, A., Yang, D., Tward, A.D., Morgan, D.O., Bishop, J.M. (2007). Inhibition of CDK1 as a potential therapy for tumors over-expressing MYC. Nat Med. 13: 820-827.

Golan, A., Yudokovsky, Y., and Hershko, A. (2002). The cyclin-ubiquitin ligase activity of cyclosome/APC is jointly activated by protein kinases Cdk1-cyclin b and Plk1. J Biol Chem *277* (18): 15552-7.

Golstein, P., and Kroemer , G. (2007). Cell death by necrosis: towadrs a molecular definition. Trends Biochem Sci. 32 (1): 37-43.

Goltzer, M., Murray, A.W., and Kirschner, M.W. (1991). Cyclin is degraded by the ubiquitin pathway. Nature 349*:* 132-138.

Gomes, L. C., Benedetto, G. D., and Scorrano, L. (2011). During autophagy mitochondria elongate, are spared from degradation and sustain cell viability. Nat Cell Biol. 13: 589-598.

Gu, Y., Rosenblatt, J., and Morgan, D. O. (1992). Cell cycle regulation of CDK2 activity by phosphorylation of Thr160 and Tyr16. EMBO J *11* (11): 3995-4005.

Guttinger, S., Laurell, E., Kutay, U., (2009). Orchestrating nuclear envelope dissasembly and reassembly during mitosis. Nat Rev Mol Cell Biol, 10: 78-91.

Gwinn, D. M., Asara J. M., Shaw, R. J. (2010). Raptor is phosphorylated by cdc2 during mitosis. PLoS One. 5 (2): e9197.

Hanahan, D., and Weinberg, R. D. (2000). The hallmarks of cancer. Cell *100* (1): 57-70.

Hanahan, D., and Weinberg, R.D. (2011). Hallmarks of cancer: the next generation. (2001). Cell. 144(5): 646-74.

Hailey, D. W. et al. (2010). Mitochondria supply membranes for autophagosome biogenesis during starvation. Cell 141: 656-667.

Hardie, D. G., Ross, F. A., and Hawley, S. A. (2012a). AMP-activated protein kinase: a target for drugs both ancient and modern. Chem Biol 19: 1222-1236.

Hardie, D. G., Ross, F. A., and Hawley, S. A. (2012b). AMPK: a nutrient and energy sensor that maintains energy homeostasis. Nat Rev Mol Cell Biol 13: 251-262.

Harding, A., Giles, N., Burguess, A., Hancock, J-F., Gabrielli, B.G. (2003). Mechanism of mitosis-specific activation of MEK1. J Biol Chem. 278 (9): 16747-54.

Harper, J.W., Burton, J.L., and Solomon, M.J. (2002). The anaphase-promoting complex: it´s not just for mitosis anymore. Genes Dev 16: 2179-2206.

Harley, M. E., Allan, L. A., Sanderson, H. S. and Clarke, P. R. (2010). Phosphorylation of Mcl-1 y CDK1-cyclin B1 initiates its Cdc20-dependent destruction during mitotic arrest. EMBO J, 29: 2407-2420.

Hartwell, L. H., et al. (1973) Genetic control of the Cell Division Cycle in Yeast: V. Genetic analysis of Cdc Mutants. Genetics *74* (2): 267-86.

Hartwell, L. H. and Weinberg, T. A. (1989). Checkpoints: controls that ensure the order of cell cycle events. Science *246* (4930): 629-34.

Herrero-Mendez, A., Almeida, A., Fernandez, E., Maestre, C., Moncada, S., and Bolanos, J. P. (2009).The bioenergetic and antioxidant status of neurons is controlled by continuous degradation of a key glycolytic enzyme by APC/C-Cdh1. Nat Cell Biol 11: 747-752.

Hitomi, J., et al. (2008). Identification of a molecular signaling network that regulates a cellular necrotic cell death pathway. Cell. 135 (7): 1311-23.

Hoffman, D-B., Pearson, C.G., Yen, T.J., Howell, B.J. SAlmon, E.D. (2001). Microtubule-dependent changes in assembly of microtubule motor proteins and mitotic spindle checkpointproteins at Ptk1 kinetochores. Mol Biol Cell. 12(7):1995-2009.

Hoque , Md. T., Ishikawa, F. (2002). Cohesion defects lead to premature sister chromatid separation, kinetochore dysfunction, and spindle-assembly checkpoint activation. J Exp Chem. 277 (44): 42306-42314.

Howell, B.J., Hoffman, D.B., Fang, G., Murray, A.W. Salmon, E.D. (2000). Visualization of Mad2 dynamics at kinetochores, along spindle fibers, and at spindle poles in living cells. J Cell Biol. 150(6):1233-50.

Huang, D. C. and Strasser, A. (2000). BH3-Only proteins-essential initiators of apoptotic cell death. Cell. 108 (6): 449-61.

Huang, H. C., Shi, J., Orth, J. D., and Mitchison, T. J. (2009a). Evidence that mitotic exit is a better cancer therapeutic target than spindle assembly. Cancer Cell 16: 347-358.

Huang, J., Manning, B.D. (2009b). A complex interplay between Akt, TSC2, and the two mTOR complexes. Biochem Soc Trans. 37: 217-222.

Huang, N. J. Zhang, L., Tang, W., Chen, C., Yang, C. S. Kornbluth, S. (2012) The Trim39 ubiquitin ligase inhibits APC/CCdh1-mediated degradation of the Bax activator MOAP-1. J Cell Biol. 197 (3): 361-7.

Hunt, T. (1989). Embriology. Under arrest in the cell cycle. Nature 342: 483-484.

Hunt, T. (2001). Protein synthesis, proteolysis and cell cycle transitions. Les Prix Nobel;: 274-297.

Hyde, B.B., Twig, G., Shirihai, O.S. (2010). Organellar vs cellular control of mitochondrial dynamics. Semin Cell Dev Biol. 21(6): 575-81.

Ianzini, F., and Mackey, M.A. (1997). Spontaneous premature chromosome condensation and mitotic catastrophe following irradiation of HeLa S3 cells. Int J Radiat Biol. 72 (4), 409-21.

Inoki, K., Li, Y., Xu, T., Guan , K. L. (2003). TSC2 mediates cellular energy response to control cell growth and survival. Cell. 115 (5): 577-90.

Inuzuka, H., Shaik, S., Onoyama, I., Gao, D., Tseng, A., Maser, R. S., Zhai, B., Wan, L., Gutierrez, A., Lau, A. W.*, et al.* (2011). SCF(FBW7) regulates cellular apoptosis by targeting MCL1 for ubiquitylation and destruction. Nature 471: 104-109.

Jain, V. M. et al. (2013). Interconnections between apoptotic, autophagic and necrotic pathways: implications for cancer therapy development. J Cell Med. 17 (1): 12-29.

Jackson, J. R., Patrick, D. R., Dar, M. M., and Huang, P. S. (2007). Targeted anti-mitotic therapies: can we improve on tubulin agents?. Nat Rev Cancer 7: 107-117.

Janssen, A., and Medema, R. H. (2011). Mitosis as anti-cancer target. Oncogene. 30, 2799-2809.

Jhonson, N. et al (2011). Compromised CDK1 activity sensitizes BRCA-proficient cancers to PARP inhibition. Nat Med. 17: 875-882.

Jose, C., Bellance, N., and Rossignol, R. (2011). Choosing between glycolysis and oxidative phosphorylation: A tumor´s dilemma?. Bioch Bioph Acta.1807: 552-561.

Joza, N. et al. (2001). Essential role of the mitochondrial apoptosis-inducing factor in programmed cell death. Nature. 410 (6828): 549-54.

Kelly, A. F., Ghenoiu, C., Xue, J. Z., Zierhurt, C., Kimura, H., Funabiki, H. (2010). Survivin reads phosphorylated histone H3 threonice 3 to activate the mitotic kinase Aurora B. Science 330 (6001): 235-9.

Kessler, R., Bleichert, F., Warnke, J. P., Eschrich, K. (2008). 6-Phosphofructo-2-kinase/fructose-2,6-biphosphatase (PFKFB3) is up-regulated in high-grade astrocytomas. J Neurooncol. 86 (3): 257-64.

Kilbride, S. M., Farrelly, A. M., Bonner, C., Ward, M. W., Nyhan, K. C., Concannon, C. G., Wollheim, C. B., Byrne, M. M., and Prehn, J. H. (2010). AMP-activated protein kinase mediates apoptosis in response to bioenergetic stress through activation of the pro-apoptotic Bcl-2 homology domain-3-only protein BMF. J Biol Chem 285: 36199-36206.

Kim, J., Kundu, M., Viollet, B., and Guan, K. L. (2011). AMPK and mTOR regulate autophagy through direct phosphorylation of Ulk1. Nat Cell Biol 13: 132-141.

Kimura, S., Noda, T., and Yoshimori, T. (2007). Dissection of the autophagosome maturation process by a novel reporter protein, tandem fluorescent-tagged LC3. Autophagy 3: 452-460.

King, R. W., Peters, J. M., Tugendreich, S., Rolfe, M., Hieter, P., Kirschner, M. W. (1995). A 20S complex containing CDC27 and CDC16 catalyzes the mitosi-specific conjugation of ubuquitin to cyclin B. Cell. 81 (2): 279-88.

Klionsky, D. J. et al. (2008). Guidelines for the use and interpretation of assays for monitoring autophagy in higher eukaryotes. Autophagy. 4 (2): 151-75.

Komlodi-Pasztor, E., Sackett, D. L., and Fojo, A. T. (2012). Inhibitors targeting mitosis: tales of how great drugs against a promising target were brought down by a flawed rationale. Clin Cancer Res 18: 51-63.

Kops, G. J. P. L., Weaver, B. A. A., Cleveland D. W. (2005). On the road to cancer: aneuploidy and the mitotic checkpoint. Nat Rev Cancer. 5: 773-785.

Kovacis, S et al. (2003). Akt activity negatively regulates phosphorylation of AMP-activated protein kinase in heart. Met Bio. 278(41): 39422-39427.

Kramer, E.R., Scheuringer, N., Podtelejnikov, A.V., Mann, M., and Peters, J.M. (2000). Mitotic regulation of the APC activator proteins CDC20 and CDH1. Mol Biol Cell 11: 1555-1569.

Kristensen, A. R. et al. (2008). Ordered organelle degradation during starvation-induced autophagy. Mol Cell Proteomics 7: 2419-2428.

Kulukian, A., Han, J. S. Cleveland, D. W. (2009). Unattached kinetochores catalyze production of an anaphase inhibitor that requires a Mad2 template to prime Cdc20 for BubR1 binding. Dev Cell. 16 (1): 6-8.

Kutik, S., Guiard, B., Meyer, H. E. Wiedemann, N., Pfanner, N. (2007). Cooperation of translocase complex in mitochobdrial protein import. J Cell Biol. 179 (4): 585-91.

Lane, H. A. and Nigg, E.A. (1996). Antibody microinjection reveals an essential role for human polo-like kinase 1 (Plk1) in the functional maturation of mitotic centrosomes. J Cell Biol 135 (6 Pt 2*):* 1701-13.

Lanni, J.S., Jacks, T. (1998). Characterization of the p53-dependent postmitotic checkpoint following spindle disruption.Mol Cell Biol. 18: 1055-1064.

Lee, J. H., Koh, H., Kim, M., Kim, Y., Lee, S. Y., Karess, R. E., Lee, S. H., Shong, M., Kim, J. M., Kim, J., and Chung, J. (2007). Energy-dependent regulation of cell structure by AMP-activated protein kinase. Nature 447, 1017-1020.

Lens, S. M., Wolthuis, R. M., Klompmaker, R., Kauw, J. Agami, R, Brummelkamp, T., Kops, G and Medema R. H. (2003a) Survivin is required for a sustained spindle checkpoint arrest in response to lack of tension.EMBO J. 22: 2934-2947.

Lens, S.M., Voest, E.E. Medema, R.H. (2010). Shared and separate functions of polo-like kinases and aurora kinases in cancer. Nat Rev Cancer 10, 825-41.

Levine, B., and and Kroemer, G. (2008). Autophagy in the pathogenesis of disease. Cell. 132 (1): 27-42.

Li, F. et al. (1998). Control of apoptosis and mitotic spindle checkpoint by survivin. Nature. 396 (711): 580-4.

Lieber, J et al., (2011). The BH3 mimetic ABT-737 increases treatment efficiency of paclitaxel against hepatoblastoma. BMC cancer 11: 326.

Lim, H. H.Goh, P. Y., and Surana,u. (1998). Cdc20 is essential for the cyclosome-mediated proteolysis of both Pds1 and Clb2 during M-phase in budding yesat. Curr Biol. *8* (2): 231-4.

Lindsten, T. et al. (2000). The combined functions of proapoptotic Bcl-2 family members bak and bax are essential for normal development of multiple tissues. Moll Cell. 6 (6): 1389-99.

Lindqvist, A., et al. (2005). Cdc25B cooperates with Cdc25A to induce mitosis but has a unique role in activating cyclin B1-Cdk1 at the centrosome. J Cell Biol. *171* (1): 35-45.

Lindqvist, A. Rodriguez-Bravo, V., and Medema, R. H. (2009). The decision to enter mitosis feedback and redundancy in the mitotic entry network. J Cell Biol. *185* (1): 193-202.

Littlepage, L. E. et al. (2002). Identification of phosphorylated residues that affect the activity of the mitotic kinase Aurora-A. Proc Natl Acas Sci U S A. 99 (24): 15440-5.

Liu, L., Xie, R., Nguyen, S., Ye, M., and McKeehan, W. L. (2009). Robust autophagy/mitophagy persists during mitosis. Cell Cycle 8: 1616-1620.

Lock, R. B. and Stribins-kiene, L. (1996). Dual modes of death induced by etoposide in human epithelial tunor cells allow Bcl-2 to inhibits apoptosis without affecting clonogenic survival. Cancer Res. 56 (17): 40006-12.

Lowe, M., Gonatas, N. K., Warren, G. (2000). The mitotic phosphorylation cycle of the cis-Golgi matrix protein GM13o J Cell Biol. 149: 341-56.

Lu, J., Tan, M., Cai, Q. (2014). The Warburg effect in tumor progression: Mitochondrial oxidative metabolism as an anti-metastasis mechanism. Cancer Lett.

Luo, J., Solimini, N. L. and Elledge, S. J. (2009a). Principles of cancer therapy: oncogene and non-oncogene adiction. Cell. 136 (5): 827-37.

Luo, J., Emanuele, M.J., Li, D., Creighton, C.J., Schlabach, M.R., Westbroock, T.F. et al. (2009b). A genome-wide RNAi screen identifies multiple synthetic lethsl interactions with the Ras oncogene. 137, 835-848.

Malumbres, M. and Pellicer, A. (1998) RAS pathway to cell cycle control and cell transformation. Front Biosci. 3: d887-912.

Malumbres, M., and Barbacid, M. (2001). To cycle or not to cycle: a critical decision in cancer. Nat Rev Cancer 1: 222-231.

Malumbres, M. (2011). Physiological relevance of cell cycle kinases. Physiol Rev 91: 973-1007.

Manchado, E., Guillamot, M., de Carcer, G., Eguren, M., Trickey, M., Garcia-Higuera, I., Moreno, S., Yamano, H., Canamero, M., and Malumbres, M. (2010). Targeting mitotic exit leads to tumor regression in vivo: Modulation by Cdk1, Mastl, and the PP2A/B55alpha,delta phosphatase. Cancer Cell 18: 641-654.

Manchado, E., Guillamot, M., and Malumbres, M. (2012). Killing cells by targeting mitosis. Cell Death Differ 19: 369-377.

Marsin, A. S., Bertrand, L., Rider, M. H., Deprez, J., Beauloye, C., Vincent, M. F., Van den Berghe, G., Carling, D., and Hue, L. (2000). Phosphorylation and activation of heart PFK-2 by AMPK has a role in the stimulation of glycolysis during ischaemia. Curr Biol 10: 1247-1255.

Marsin, A.S., Bouzin C., Bertrand, L., Hue, L. (2002). The stimulation of glycolysis by hypoxia in activated monocytes is mediated by AMP-activated protein kinase and inducible 6-phosphofructo-2-kinase. J Biol Chem. 277 (34): 30228-83.

Matthess, Y., Raab, M., Sanhaji, M., Lavrik, I. N., and Strebhardt, K. (2010). Cdk1/cyclin B1 controls Fas-mediated apoptosis by regulating caspase-8 activity. Mol Cell Biol 30: 5726-5740.

Mayes, P.A., Dollof, N.G., Daniel, C.J., Liu, J.J, Hart, L.S. Kuribayashi, K. et al. (2011). Overcoming hypoxia-induced apoptotic resistance through combinatorial inhibition of GSK-3(beta) and CDK1. Cancer Res. 71: 5265-5275.

Medema, R. H., and Linqvist, A. (2011). Boosting and suppressing mitotic phosphorylation. Trends Bioch Sci. 36 (11): 578-584.

Meier, F. et al. (2009). Significant response after treatment woth the mTOR inhibitor sirolimus in combination with carboplatin and paclitaxel in metastatic melanoma patients. Journal of the American Academy of Dermatology 60: 863-868.

Meynet, O. et al. (2012). Glycolysis inhibition targets Mcl-1 to restore sensitivity of lymphoma cells ABT-737-induced apoptosis. Leukemia. 26 (5): 1145-7.

Michel, L.s. et al. (2001). MAD2 haploinsifficiencycauses premature anaphase and chromosome instability in mammalian cells. Nature. 409: 355-359.

Mitchison, T. J. (2012). The proliferation rate paradox in antimitotic chemotherapy. Mol Biol Cell *23*: 1-6.

Mitra, K., Wunder, C., Roysam, B., Lin, G., Lippincott-Schwartz, J. (2009). A hyperfused mitochondrial state achieved at G1-S regulates cyclin E builduo and entry into S phase. Proc Natl Acad Sci U S A. 106: 11960-11965.

Mizushima, N., and Levine, B. (2010). Autophagy in mammalian development and differentiation. Nat Cell Biol. 12 (9): 823-30.

Mocciaro, A., and Shiebel, E. (2010), Cdc14: a highly conserved family of phosphatases with non-conserved functions? J Cell Sci. 123: 2867-76.

Mochida, S. and Hunt, T. (2007). Calcineurin is required to release Xenopus egg extracts from meiotic M phase. Nature. 449 (7160): 336-40.

Mochida, S., Hunt, T. (2012). Protein phosphatases and their regulation in the control of mitosis. EMBO Rep, 13: 197-203.

Mochida, S., Ikeo, S., Gannon, J., Hunt, T. (2009). Regulated activity of PP2a2-B55 delta is crucial for controlling entry and exit from mitosis in Xenopus egg extracts. EMBO J. 28: 2777-85.

Molz, L. Booher, R., Young, P., Beach, D. (1989). cdc2 and the regulation of mitosis: six interacting mcs genes. Genetics. 122 (4): 773-82.

Mor, I., Cheung, E.C. and Vousden, K.H. (2011). Control of glycolysis through regulation of PFK1: old friends and recent additions. Cold Spring Harb Symp Quant Biol.76; 211-216.

Mouton, V., Toussaint, L., Vertommen, D., Gueuning, M. A., Maisin, L., Havaux, X., Sanchez-Canedo, C., Bertrand, L., Dequiedt, F., Hemmings, B. A. et al. (2010) Heart 6-phosphofructo-2-kinase activation by insulin requires PKB (protein kinase B), but not SGK3 (serum- and glucocorticoid-induced protein kinase 3). Biochem. J. 431: 267–275

Moncada, S., Higgs, E. A., and Colombo, S.L. (2012). Fulfilling the metabolic requirements for cell proliferation. Biochem J. 446, 1-7.

Musacchio, A., and Salmon, E. D. (2007). The spindle-assembly checkpoint in space and time. Nat Rev Mol Cell Biol 8: 379-393.

Nabha, S. et al. (2002). Combretastatin-A4 prodrug induces mitotic catastrophe in chronic lymphocytic leukemia cell line independent of caspase activation and poly(ADP-ribose) polymerase cleavage. Clin Cancer Res, 8 (8): 2735-41.

Nasmyth, K. and Haering, C. H. (2009). Cohesin: its role and mechanism. Annu Rev Genet. 43: 525-58.

Nakajima, H. et al. (2003). Identification of a consensus motif for Plk (Polo-like kinase) phosphorylation revelas Myt1 as a Plk1 substrate. J Biol Chem. 278 (28): 25277-80.

Nevins, J. R. (1998). Towards an understanding of the functional complexity of the E2F and retinoblastoma families. Cell Growth Differ. 9 (8): 585-93.

Niedzialdhowska, E., Wang, F., Porebski, P.J., Minor, W., Higgins, J.M., Stukenberg, P.T. (2012). Molecular basis for phosphospecific recognition of histone H3 tails by Survivin paralogs at inner centromeres. Mol Biol Cell. 23 (8): 1457-66.

Niikura, Y., Dixit, A., Scott, R., Perkins, G., and Kitagawa, K. (2007). BUB1 mediation of caspase-independent mitotic death determines cell fate. J Cell Biol 178: 283-296.

Nilsson, J. et al. (2008). The APC/C maintains the spindle assembly checkpoint by targeting Cdc20 for destruction. Nat Cell Bio, 10 (12): 1411-20.

Noguchi S (2006) Predictive factors for response to docetaxel in human breast cancers. Cancer Sci 97: 813–820.

Novellasdemunt, L. et al. (2012). Progestins activate 6-phosphofruto-2-kinase/fructose-2,6-biphosphatase 3 (PFKFB3) in breast cancer. Biochem J. 442: 345-356.

Novellasdemunt, L., Bultot, L., Manzano, A., Ventura, F., Rosa, J.L., Vertommen, D., Rider, M.H.,

Navarro-Sabate, À., Bartons, R. (2013). PFKFB3 activation in cancer cells by the p38/MK2 pathway in response to stress stimuli. Biochem J. 452(2): 10640-51.

Nurse, P. (1990). Universal control mechanism regulating onset of M-phase. Nature. 344: 503-508.

Numenthaler, S.M. et al., (2009). Phamacologic inhibition of Pim kinases alters prostate cancer cell growth and resensitizes chemoresistant cells to taxanes. Mol Cancer Ther 8(10): 2882-93.

Nurse, P. Ordering S phase and M phase in the cell cycle. (1994). Cell. 79: 547-550.

O´Connor, D. S., Wall, N. R., Porter, A. C., Altieri, D. C. (2002). A p34(cdc2) survival checkpoint in cancer. Cancer Cell, 2: 43-54.

Okamoto, K. (2014). Organellophagy: Eliminating cellular building blocks via selective autophagy. J Cell Biol 205: 435-445.

Okamura, N., and Sakakibara , R. (1998). A common phosphorylation site for cyclic AMP-dependent protein kinase and protein C in human placental 6-phosphofructo-2-kinase/fructose-2,6-biphosphatase. Biosci Biotechnol Biochem. 62 (19): 2039-42.

Oltersdorf, T., Elmore, S. W., Shoemaker, A. R., Armstrong, R. C., Augeri, D. J., Belli, B. A., Bruncko, M., Deckwerth, T. L., Dinges, J., Hajduk, P. J., *et al.* (2005). An inhibitor of Bcl-2 family proteins induces regression of solid tumours. Nature 435: 677-681.

Orth, J. D., Loewer, A., Lahav, G., and Mitchison, T. J. (2012). Prolonged mitotic arrest triggers partial activation of apoptosis, resulting in DNA damage and p53 induction. Mol Biol Cell 23: 567-576.

Osusu-Ansah, E., Yavari, A., Mandal, S., Banerjee, U. (2008). Distinct mitochondrial retrograde signals control the G1-S cell cycle checkpoint. Nature Genet. 40 (3): 356-61.

Pardee, A. B. (1974). A restriction point control of normal animal cell proliferation. Proc Natl Acad Sci U S A. 71 (4): 1286-90.

Peters, J. M. (2006). The anaphase promoting complex/cyclosome: a machine designed to destroy. Nat Rev Mol Cell Biol *7*, 644-656.

Prigent C. and Dimitrov, S. 2003. Phosphorylation of serine 10 in histone H3, what for? *J. Cell. Sci.* 116: 3677–3685.

Pfleger, C.M., and Kirschner, M.W. (2000). The KEN box: an APC recohnition signal distinct from the D box targeted by Cdh1. Genes Dev 14: 655-665.

Queralt, E. and and Uhlmann, F. (2008). Cdk-counteracting phosphatases unlock mitotic exit. Curr Opin Cell Biol. 20 (6): 661-8.

Quin, X., Sarnow, P. (2004). Preferential translation of the internal ribosome entry site-containing mRNAs during the mitotic cell cycle in mammalian cells. J Biol Chem. 272(14), 13721-13728.

Rabinowitz, J. D. White, E. (2010). Autophagy and metabolism. Science 330: 1344-1348.

Raffagello, L. et al. (2008). Starvation-dependent differential stress resistance protects normal but not cancer cells against high-dose chemotherapy. Proc Natl Acad Sci U S A. 105 (24): 8215-20.

Rambold, A. S., Kostelecky, B., Elia, N., and Lippincott-Schwartz, J. (2011). Tubular network formation protects mitochondria from autophagosomal degradation during nutrient starvation. Proc Natl Acad Sci U S A 108: 10190-10195.

Ramírez-Valle, F., Badura, M. L., Braunstein, S. ,Narasimhan, M., Scheneider, R.J. (2010). Mitotic raptor promotes mTORC1 activity, G(2)/M cell cycle progression, and internal ribosome entry site-mediated mRNA translation. Mol Cell Biol. 30 (13): 3151-64.

Reddy, S. K. et al. (2007). Ubiquitination by the anaphase-promoting complex drives the spindle checkpoint inactivation. Nature, 446 (7138): 921-5.

Rieder, C. L. and Maiato, H. (2004). Stuck in division or passing through: what happens when cells cannot satisfy the spindle assembly checkpoint. Dev Cell, 7(5): 637-51.

Rieder, C. L. and Medema, R. H. (2009). No way out of tumor cells. Cancer Cell 16: 274-275.

Riera, L., Obach, M., Navarro-Sabate, A., Duran, J., Perales, J. C., Vinals, F., Rosa, J. L., Ventura, F. and Bartrons, R. (2003) Regulation of ubiquitous 6-phosphofructo-2-kinase by the ubiquitin-proteasome proteolytic pathway during myogenic C2C12 cell differentiation. FEBS Lett. 550(1-3): 23-29.

Rödel, F. et al. (2011). The role of survivin for radiation omcology: moving beyond apoptosis inhibition. Curr Med Chem. 18 (2), 191-9.

Roessler, M. M. (2010 : Direct assignment of EPR spectra to structurally defined iron-sulfur clusters in complex I by double electron resonance. Proc Natl Acad Sci U S A. 107: 1930-1935.

Roh, M. et al. (2003). Overexpression of the oncogenic kinase Pim-1 leads to genomic instability. Cancer Res. 63 (23): 8079-84.

Roninson, I. B., Broude, E.V. Chang, B.D. (2001). If not apoptosis, then what? Treatment-induced senescence and mitotic catastrophe in tumor cells. Drugs Resist Updat. 4 (5): 303-13.

Rooswinkel, R. W. van de Kooj, B., Verheij, M., Borst, J. (2012). Bcl-2 is a better ABT-737 target than Bcl-xL or Bcl-w and only Noxa overcomes resistance mediated by Mcl-1, Bfl-1, or Bcl-B. Cell Death Ds. 9 (3): e366.

Rosenfeldt, M. T., and Ryan, K. (2011). The multiple roles of autophagy. Carcinogenesis, 32 (7): 955-963.

Rubinsztein, D- C., Gestwicki, J.E., Murphy, L.O, Klionsky, D.J. (2007). Potential therapeutic applications of autophagy. Nat Rev Drugs Discov. 6 (4): 304-12.

Rudner, A.D. and Murray , A. W. (2000). Phosphorylation by Cdc28 activates the Cdc20-dependent activity of the anaphase-promoting complex. J Cell Biol. 146 (7): 1377-90.

Ruth, A. C. and Roninson , I. B. (2000). Effects of the multidrug transporter P-glycoprotein on cellular responses to ionizing radiation. Cancer Res. 69 (10): 2576-8.

Saha, A-K. et al. (2004). Pioglitazone treatment activates AMP-activated protein kinase in rat liver and adipose tissue in vivo. Biochem Biophys Res Commun 314: 580-585.

Salazar, M., Carracedo, A., Salanueva, I. J., Hernandez-Tiedra, S., Lorente, M., Egia, A., Vazquez, P., Blazquez, C., Torres, S., Garcia, S*., et al.* (2009). Cannabinoid action induces autophagy-mediated cell death through stimulation of ER stress in human glioma cells. The Journal of clinical investigation 119: 1359-1372.

Sánchez-Pérez, T., Medema, R. H., López-Rivas, A. (2014). Delaying mitotic exit downregulates FLIP expression and strongly sensitizes tumor cells to TRAIL. Oncogene doi: 10.1038/onc.2013.601.

Sato, A. et al. (2014). Pivotal role for ROS activation of p38 MAPK in the control of differentiation and tumor-initiating capacity of glioma-initiating cells. Stem Cell Res. 12 (1): 119-31.

Sakamaki, T., Casimiro, M.C.., Ju, X., Quong, A.A., Katiyar, S., Liu, M., Jiao, X., Li, A., Zhang, X X., Lu, Y., et al. (2006). Cyclin D1 determines mitochondrial function in vivo. Mol Cell Biol 26: 5449-5469.

Scalaglia, N., Tyekucheva, S., Zadra, G., Photopoulos C., Loda M. (2014). De novo fatty acid synthesis at the mitotic exit is required to complete cellular division. Cell Cycle. 13 (5): 859-68.

Schleucher, J., MS, Sattler, M.S., . Schmidt, M., Schedletzky, P., S. J. Glaser, O. W. Sørensen, S.J. and Griesinger, C. (1994). A general enhancement scheme in heteronuclear multidimensional NMR employing pulsed field gradients. J Biomol NMR 4: 6.

Schmitz, M. H. et al. (2010). Live-cell imaging RNAi screen identifies PP242-B55alpha and importin-beta1 as key mitotic exit regulators in human cells. Nat Cell Biol, 12 (9), 886-93.

Seo , M., Kim, J. D., Neau, D., Sehgai, I., Lee, Y. H. (2011). Structure-based development of small molecule PFKFB3 inhibitors: a framework for potential cancer therapeutic agents targeting the Warburg effect. PLoS One. 6 (9): e24179.

Sheer, C.J., and Roberts , J.M. (1999). Cdk inhibitors: positive and negative regulators of G1-phase progression. Gen Dev. 13(12):1503-12.

Shi J, Orth JD, Mitchison T (2008) Cell type variation in responses to antimitotic drugs that target microtubules and kinesin Cancer Res 68:3269–3276.

Shimizu, S. et al.(2004). Role of Bcl-2 family proteins in a non-apoptotic programmed cell death dependent on autophagy genes. Nat Cell Biol. 6 (12): 1221-8.

Shin S, Sung BJ, Cho YS, Kim HJ, Ha NC, Hwang JI, Chung CW, Jung YK, Oh BH. (2001). An anti-apoptotic protein human survivin is a direct inhibitor of caspase-3 and -7. Biochemistry. 40 (4): 117-23.

Shirayama,M., Zachariae, W., Ciosk, R., and Nasmyth, K. (1998). The Polo-like kinase Cdc50 and the WD-repeat protein Cdc20p/fizzy are regulators and substrates of the anaphase-promoting complex in Saccharomyces cerevisae. EMBO J 17: 1336-1349.

Sigrist, S. et al. (1995). Exit from mitosis is regulates by Drosophila fizzy and the sequential destruction of cyclins A, B and B3. EMBO J, 14 (19): 4827-38.

Simonetta M, Manzoni R, Mosca R, Mapelli M, Massimiliano L, Vink M, Novak B, Musacchio A, Ciliberto A.(2009) The influence of catalysis on mad2 activation dynamics. PLoS One.7 (1): e10.

Siva, G., and Elroy-Stein, O. (2008). Regulation of mRNA trnaslation during cellular division. Cell cycle. 7(6): 741-4.

Skaar, J.R. and Pagano, M. (2009). Control of cell growth by the SCF and APC/C ubuquitin ligases. Curr Opin Cell Biol 21: 816-824.

Solaini, G., Sgarbi, G., and Baracca, A. (2011). Oxidative phosphorylation in cancer cells. Bioch Bioph Acta. 1807: 534-542.

Song, J.F. and Kraft, A.S.(2012). Pim kinase inhibitors sensitize prostate cancer cells to apoptosis triggered by Bcl-2 family inhibitor ABT-737. Cancer Research. 72 (1): 294-303.

Spankuch-Shmitt, B. et al. (2002). Downregulation of human polo-like kinase activity by antisense oligonucleotides induces growth inhibition in cancer cells.Oncogene, 21: 3162-3171.

Spurck, T-P. (1987). On the mechanism of anaphase A: evidence that ATP is needed for microtubule disassembly and not generation of polewards force. J Cell Biol. 105 (4): 1691-705.

Steigmer, F et al, (2007). Anaphase initiation is regulated by antagonistic ubiquitination and deubiquitination activities. Nature. 446 (7138): 876-81.

Stemmann, O., et al (2001). Dual inhibition of sister chromatid separation at metaphase. Cell. 107 (6): 715-26.

Stobbe, C.C., Park, S.L. Chapman, J.D. (2002). The radiation hypersensitivity of cells at mitosis. Int J Radiat Biol. 78 (12): 1149-57.

Stumpt, C.R., Moreno, M.V., Olshen, A.B., Taylor, B.S., Roggero, D. (2013). The translational landscape of the mammalian cell cycle. Mol Cell. 52 (4): 574-82.

Sudakin, V. et al. (1995). The cyclosome, a large complex containing cyclin-selective ubiquitin ligase activity, targets cyclins for destruction at the end of mitosis. Mol Biol Cell. 6 (2): 185-197.

Sullivan, M and Morgan, D. O. 2007). Finishing mitosis, one step at a time. Nat Rev Mol Biol Cell. 8 (11): 894-903.

Susin, S. A. et al. (1999). Molecular characterization of mitochondrial apoptosis-inducing factor. Nature. 397(6718)441-6.

Swann, M. M. (1957). The control of cell division: a review. I . Gneral mechanisms. Cancer Res. 17: 727-757.

Swanson, P.E., Carrol, S.B. Zhang, X.F., Mackey, M.A. (1995). Spontaneous premature chromosome condensation, micronucleus formation, and non-apoptotic cell death in heated HeLa S3 cells. Ultrastructural observations. Am L Pathol. 146 (4): 963-71.

Swedlow J.R. and Hirano, T. 2003. The making of the mitotic chromosome: Modern insights into classic: al questions. Mol. Cell 11: 557–569.

Sweet, S., and Signh, G. (1999). Changes in mitochondrial mass, membrane potential, and cellular adenosine triphosphate content during the cell cycle of human leukemic (HL-60) cells. J Cell Physiol 180: 91-96.

Taguchi, N., Ishihara, N., Jofuku, A., Oka, T., and Mihara, K. (2007). Mitotic phosphorylation of dynamin-related GTPase Drp1 participates in mitochondrial fission. J. Biol Chem 282: 11521-11529.

Takanaga, H., Chaudhuri, B., and Frommer, W. B. (2008). GLUT1 and GLUT9 as major contributors to glucose influx in HepG2 cells identified by a high sensitivity intramolecular FRET glucose sensor. Biochim Biophys Acta 1778: 1091-1099.

Takizawa, C- G. and Morgam, D.O. (2000). Control of mitosis by changes in the subcellular location of cyclin-B1-Cdk1 and Cdc25C. Curr Opin Cell Biol. 12(6): 658-65.

Tamm, I., Wang, Y., Sausville, E., Scudiero, D.A., Vigna, N., Ottersdorf, T., Reed, J.C. (1998). IAP-family protein survivin inhibits caspase activity and apoptosis induced by Fas (CD95), Bax, caspases and anticancer drugs. Cancer Res. 58(23): 5315-20.

Tamura, Y., Simizu, S., Muori, M., Takagi, S., Kawatani, Watanabe, N., Osada, H. (2009). Polo-like kinase 1 phosphorylates and regulates Bcl-x(L) during pironectin-induced apoptosis. Oncogene. 28 (1): 107-16.

Tao, R., Gomg, J., Luo, X., Zang, M., Guo, W., Wen, R., Luo, Z. (2010). AMPK exert dual regulatory effects on the PI3K pathway. J Mol Signal 5(1):1.

Tasdemir, E., Maiuri, M. C., Orhon, I., Kepp, O., Morselli, E., Criollo, A., and Kroemer, G. (2008). p53 represses autophagy in a cell cycle-dependent fashion. Cell Cycle *7*: 3006-3011.

Tasdemir, E., Maiuri, M. C., Tajeddine, N., Vitale, I., Criollo, A., Vicencio, J. M., Hickman, J. A., Geneste, O., and Kroemer, G. (2007). Cell cycle-dependent induction of autophagy, mitophagy and reticulophagy. Cell Cycle *6*: 2263-2267.

Thaiparambil, J.T., Eggers, C.M. Marcus, A.I. (2012). AMPK regulates mitotic spindle orientation through phosphorylation of myosin regukatory light chain. Mol Cell Biol. 32 (16): 3203-17.

Thornton, B.R. and Toczyski, D.P. (2003). Securin and B-cyclin/CDK are the only essential targets for the APC. Net Cell Biol. 5 (12): 1090-4.

Thornton, B.R. and Toczyski, D.P. (2006). Precise destruction: an emerging picture of the APC. Genes Dev 20: 3069-3078.

Toledo, L-I., Murga, M., Fernandez-Capetillo, O. (2011). Targeting ATR and Chk1 kinases fot cancer treatment: a new model for new (and old) drugs. Mol Oncol. 5 (4): 368-73.

Tondera, D. et al. (2012). SLP-2 is required for stress-induced mitochondrial hyperfussion. EMBO J. 28(11): 1589-600.

Tooze, S. A. (2010). The role of membrane proteins in mammalian autophagy. Semin Cell Dev Biol. 21: 677-682.

Topham, C. H., and Taylor, S. S. (2013). Mitosis and apoptosis: how is the balance set? Curr Opin Cell Biol *25*: 780-785.

Toyoshima-Morimoto, f. et al. (2001). Polo-loke kinase 1 phosphorylates cyclin B1 and targets it to the nucleus during prophase. Nature. 419 (6825): 215-20.

Tse, C., Shoemaker, A. R., Adickes, J., Anderson, M. G., Chen, J., Jin, S., Johnson, E. F., Marsh, K. C., Mitten, M. J., Nimmer, P., *et al.* (2008). ABT-263: a potent and orally bioavailable Bcl-2 family inhibitor. Cancer Res 68: 3421-3428.

Tsou, P., Zheng, B., Hsu, C. H., Sasaki, A. T., and Cantley, L. C. (2011). A fluorescent reporter of AMPK activity and cellular energy stress. Cell Metab 13: 476-486.

Tsukamoto, S et al. (2008). Autophagy is essential for preimplantation development of mouse embryos. Science 321: 117-120.

Uetake, Y., Sluder, G. (2004). Cell cycle progression after cleavage failure: mammalian somatic cells do not possess a "tetraploid checkpoint". J Cell Biol. 165, 609-615.

Uetake, Y., and Sluder, G- (2010). Prolonged prometaphase blocks daugther cell proliferation despite normal completion of mitosis. Curr Biol. 20: 1666-1671.

Uren, A. G. et al. (2000). Survivin and the inner centromere protein INCEP show similar cell-cycle localization and gene knockout phenotype.Curr Biol 10: 1319-1328.

Vanden Berghe, T. et al. (2014). Regulated necrosis: the expanding network of non-apoptotic cell death pathways. Nat Rev Mol Cell Biol. 15: 135-147.

Vander Heiden, M.G., Cantley, L.C., Thompson, C.B. (2009). Understanding the Watburg effect: the metabolic requirements of cell proliferation. Science. 324 (5930):1029-33.

Van Hooser, A., Goodrich, D.W., Allis, C.D., Brinkley, B.R., and Mancini, M.A. (1998). Histone H3 phosphorylation is required for the initiation, but not maintenance, of mammalian chromosome condensation. J Cell Sci (Pt23): 3497-3506.

Varetti , G. and Mussachio, A. (2008). The spindle assembly checkpoint. Curr Biol. 18 (14), R591-5.

Vakifahmetoglu, H., Olsson, M., and Zhivotovsky, B. (2008). Death through a tragedy: mitotic catastrophe. Cell Death Differ.15: 1153-1162.

Vázquez-Martín, A., Oliveras-Ferraros, C., Menendez, J.A. (2009). The active form of the metabolic sensor: AMP-activated protein kinase (AMPK) directly binds the mitotic apparatus and travels from centrosome to the spindle midzone during mitosis and cytokinesis. Cell Cycle 8(15): 2385-98.

Vink, M., et al. (2006). In vitro FRAP identifies the minimal requirements for Mad2 kinetochore dynamics. Curr Biol. 16(8): 755-66.

Vitale, I., Galluzzi, L., Castedo, M., and Kroemer, G. (2011). Mitotic catastrophe: a mechanism for avoiding genomic instability. Nat Rev Mol Cell Biol 12: 385-392.

Wall, N. R, O´Connor, D. S., Plecsia, J., Pommier, Y., and Altieri, D. C. (2003). Supression of survivin phosphorylation on Thr34 by flavopiridol enhances tumor cell apoptosis.Cancer Res, 63: 230-235.

Wan, L., Tan, M., Yang, J., Inuzuka, H., Dai, X., Wu, T., Liu, J., Shaik, S., Chen, G., Deng, J.*, et al.* (2014). APC(Cdc20) Suppresses Apoptosis through Targeting Bim for Ubiquitination and Destruction. Dev Cell *29*: 377-391.

Wang, F., Dai, J., Daum, J.R., Niedzialkowska, E., Banerjee, B., Stukenberg, P.T., Gorbsky, G.J., and Higgins, J.M. (2010). Histone H3 Thr-3 phosphorylation by Haspin positions Aurora B at centromeres in mitosis. Science 330, 231-235.

Wang, F. et al. (2011). A positive feedback loop involving haspin and Aurora Bpromotes CPC accumulation at centromeres in mitosis. Curr Biol. 21(12): 1061-1069.

Wang, F., Ulyanova, N.P. Daum, J.R., Patnaik, D., Kateneva, A.V., Gorbsky, G.J., and Higgins, J.M. (2012). Haspin inhibitors reveal centromeric functions of Aurora B in chromosome segregation. J. Cell Biol. 199, 251-268.

Wang, Z., Fan, M., Candas, D., Zhang, T. Q., Qin, L., Eldridge, A., Wachsmann-Hogiu, S., Ahmed, K. M., Chromy, B. A., Nantajit, D.*, et al.* (2014a). Cyclin b1/Cdk1 coordinates mitochondrial respiration for cell-cycle G2/M progression. Dev Cell *29*: 217-232.

Wang, P., Lindsay, J., Owens, T. W., Mularczyk, E. J., Warwood, S., Foster, F., Streuli, C. H., Brennan, K., and Gilmore, A. P. (2014b). Phosphorylation of the proapoptotic BH3-only protein bid primes mitochondria for apoptosis during mitotic arrest. Cell reports *7*: 661-671.

Warburg, O. (1954). On the origin of Warburg. Science 123: 309-314.

Watanabe, N. et al (2004). M-phase kinases induce phospho-dependent ubiquitination of somatic Wee1 by SCFbeta-TrCP. Proc Natl Acad Sci U S A. 101 (13): 4419-24.

Wei, M. C., Zong, W. X., Cheng, E. H., Lindsten, T., Panoutsakopoulou, V., Ross, A. J., Roth, K. A., MacGregor, G. R., Thompson, C. B., and Korsmeyer, S. J. (2001). Proapoptotic BAX and BAK: a requisite gateway to mitochondrial dysfunction and death. Science 292: 727-730.

Wertz, I. E., Kusam, S., Lam, C., Okamoto, T., Sandoval, W., Anderson, D. J., Helgason, E., Ernst, J. A., Eby, M., Liu, J.*, et al.* (2011). Sensitivity to antitubulin chemotherapeutics is regulated by MCL1 and FBW7. Nature 471: 110-114.

Willis, S. N.et al (2007a).Proapoptotic Bax is sequestered by Mcl-1 and Bcl-XL, but not Bcl-2, until displaced by BH3-only proteins. Genes Dev. 19: 1294-1305.

Willis, S.N. et al (2007b). Apoptosis initiated when BH3 ligands engage multiple Bcl-2 homologs, not Bax or Bak. Science. 315: 856-859.

Willker WL, D.; Kerssebaum, R.; Bermel, W. (1993) Gradient selection in inverse heteronuclear correlation spectroscopy. Magn Reson Chem 31: 6.

Witsch, E, Sela, M., Yarden, Y. (2010). Roles for growth factors in cancer progression. Physiology (Bethesda). 25: 85-101.

Wolthuis, R. et al. (2008). Cdc20 and CKs direct the spindle checkpoint-independent destruction of cylin A. Mol Cell. 30 (3): 290-302.

Wu M, Neilson A, Swift AL, Moran R, Tamagnine J, Parslow D, Armistead S, Lemire K, Orrell J, Teich J, Chomicz S, Ferrick DA. (2007). Multiparameter metabolic analysis reveals a close link between attenuated mitochondrial bioenergetic function and enhanced glycolysis dependency in human tumor cells. Am J Physiol Cell Physiol. 292:125-136.

Wu, J. Q. et al. (2009). PP1-mediated dephosphorylation of phosphoproteins at mitotic exit is controled by inhibitor-1 and PP1 phosphorylation. Nat Cell Biol. 11 (4): 644-51.

Wurzenberger, C., and Gerlich, D. W. (2011). Phosphatases: providing safe passage through mitotic exit. Nat Rev Mol Cell Biol 12: 469-482.

Xia, G. et al. (2004). Conformation-specific bindinf of p31comet antagonizes the function of Mad2 in the spindle checkpoint. EMBO J. 23(15): 3133-3143.

Yalcin, A. et al. (2009). Nuclear targeting of 6-phosphofructo-2-kinase (PFKFB3) increases proliferation via cyclin-dependent kinases. J Biol Chem. 284 (36): 24223-24232.

Youle, R. J., and Narendra, D. P. (2011). Mechanisms of mitophagy. Nat Rev Mol Cell Biol 12: 9-1

Youle, R. J., and Strasser, A. (2008). The Bcl-2 protein family: opposing activities that mediate cell death. Nat Rev Mol Cell Biol. 9: 47-59.

Yuang, T.L. and Cantley, L.C. (2008). PI3K pathway alterations in cancer: variations of a theme. Oncogene, 27: 5495-5510.

Zachariae, W., et al. (1998). Control of cyclin ubiquitination CDK-regulated binding of Hct1 to the anaphase of a subunit related to cullins. Science. 279(5354): 1216-9.

Zeng, X. et al., (2010). Pharmacologic inhibition of the anaphase-promoting complex induces a spindle checkpoint-dependent mitotic arrest in the absence of spindle damage. Cancer Cell. 18 (4): 382-95.

Zeng, X., and King, R. W. (2012). An APC/C inhibitors stabilizes cyclin B1 by prematurely terminating ubiquitination. Nat Chem Biol. 8(4): 383-392.

Zhou, H., Li, X-M., Meinkoth, J., Pittman, R.N. (2000). Akt regulates cell survival and apoptosis at a postmitochondrial level. J Cell Biol. 151(3) 483-494.

Zhou. L., Tian, X., Zhu, C., Wang, F. Higgins, J.M.(2013). Polo-like kinase-1 triggers histone phosphorylation by Haspin in mitosis. EMBO Rep. 15(3): 273-81.

Zong, X. et al. (2001). BH3-only proteins that bind pro-survival Bcl-2 family members fail to induce apoptosis in the absance of Bax and Bak. Genes Dev. 15 (12): 1481-1486.

Zuojun, R. et al. (2008). Deconstructing survivin: comprehensive geneticanalysis of survivin function by conditional knockout in a vertebrate cell line. J Cell Biol. 183(2): 279-296.

Annex

Elena Doménech, David Partida, Lorena Esteban, Ramón Campos-Olivas, Manuel Pérez, Diego Megias, Katherine Allen, Miguel López, Asish K. Saha, Guillermo Velasco, Eduardo Rial, Patricia Boya, María Salazar-Roa, and Marcos Malumbres. *A glycolytic switch mediated by AMPK and PFKFB3 determines survival during mitotic arrest.* Submitted

Elena Doménech Cruz and Marcos Malumbres. *Mitotic targeted therapies: a troubleshooting guide.* Current Opinion in Pharmacology (2013) 13(4):519-528.

A glycolytic switch mediated by AMPK and PFKFB3 determines survival during mitotic arrest

Elena Doménech,1 David Partida 1,Lorena Esteban-Martínez 2, Ramón Campos-Olivas 3, Manuel Pérez 4, Diego Megias 4, Katherine Allen 5, Miguel López 6, Asish K. Saha 5, Guillermo Velasco 7, Eduardo Rial 8,Patricia Boya 2, María Salazar-Roa,1,*and Marcos Malumbres1,*

1 Cell Division and Cancer Group, Spanish National Cancer Research Centre (CNIO) Madrid 28029, Spain.
2 Department of Cellular and Molecular Biology, Centro de Investigaciones Biológicas,CSIC, E-28040, Madrid, Spain.
3 Spectroscopy and Nuclear Magnetic Resonance Unit, CNIO, Madrid.
4 Confocal Microscopy Unit, CNIO, Madrid, Spain.
5 Division of Endocrinology, Diabetes & Nutrition, Boston University School of Medicine, Boston, MA 02215.
6 Department of Physiology, CIMUS, University of Santiago de Compostela-Instituto de Investigación Sanitaria, Santiago de Compostela, 15782, Spain & CIBER Fisiopatología de la Obesidad y Nutrición (CIBERobn), 15706, Spain.
7 Department of Biochemistry and Molecular Biology I, School of Biology, Complutense University, and Instituto de Investigaciones Sanitarias San Carlos (IdISSC), 28040 Madrid, Spain.
8 Department of Cellular and Molecular Medicine, Centro de Investigaciones Biológicas, CSIC, E-28040, Madrid, Spain.

ABSTRACT

Blocking mitotic progression has been proposed as an attractive therapeutic strategy to impair proliferation of tumor cells. However, how cells survive during prolonged mitotic arrest is not well understood. By using a genetic model of defective mitotic exit in mammalian cells, we show that survival during prolonged mitotic arrest is modulated by the special energetic requirements of cells during mitotic arrest. Prolonged mitotic arrest results in mitophagy-dependent loss of mitochondria, accompanied by reduced ATP levels and the activation of AMPK. As a consequence, oxidative respiration is replaced by glycolysis in a PFKFB3-dependent manner. Induction of autophagy or inhibition of AMPK or PFKFB3 results in enhanced cell death in mitosis and increases the anti-tumoral efficiency of microtubule poisons in breast cancer cells. Thus, survival of mitotic-arrested cells is limited by their metabolic requirements, a feature with critical implications in cancer therapies aimed to impair mitosis or metabolism in tumor cells.

INTRODUCTION

Progression through the cell division cycle is modulated by multiple cellular machineries that control the biochemical and structural changes required for DNA replication in S-phase and chromosome segregation during mitosis. Entry into mitosis requires a dramatic structural re-organization including centrosome duplication and generation of the microtubule spindle, disassembly of the Golgi apparatus, breakdown of the nuclear envelope and chromosome condensation. At this stage, transcription is strongly suppressed, translation is limited to a subset of mRNAs, and the absence of the nuclear envelope temporally maintains on hold multiple regulatory mechanisms based on the separation of the nuclear and cytoplasmic compartments 1.Progression through mitosis is monitored by the Spindle Assembly Checkpoint (SAC), a regulatory pathway that delays mitotic exit until all chromosomes are bipolarly attached to the spindle 2. The target of the SAC is the Anaphase-promoting complex/Cyclosome (APC/C), an E3 ubiquitin ligase that, when activated by Cdc20, targets for degradation the separase inhibitor securin, and the Cdk1 activatory subunit cyclin B. Complete bipolar attachment of chromosomes results in APC/C-Cdc20 activation, Cdk1 inhibition and activation of separase, leading to chromosome segregation and the reformation of two new nuclei 3. These nuclei and the rest of cytoplasmic structures are physically separated after cytokinesis to form two new daughter cells. Disruption of the mechanisms that regulate the proper attachment of chromosomes to the bipolar spindle results in mitotic arrest in a SAC-dependent manner. Thus, inhibition of mitotic kinases or treatment of cells with microtubule poisons that disrupt the proper dynamics of the spindle, results in mitotic arrest, a feature that may be used to prevent tumor cell proliferation 5. Yet, the success of mitotic-4 targeted therapies is limited by two major problems: a) the low mitotic index of human tumors, and b) mitotic slippage; i.e. the ability of cells to exit from mitosis in the presence of mitotic blockers 5-8. Since mitotic slippage is APC/C-Cdc20-dependent 9, targeting the mitotic exit machinery has been proposed as an efficient method to prevent resistance to antimitotic drugs 9-12. In the absence of Cdc20, cells cannot exit mitosis and irremediably die in mitosis after a prolonged arrest 9,11.Cell fate upon mitotic arrest is thought to be determined by the balance between mitotic slippage pathways and apoptotic cell death10, 13. We therefore reasoned that interfering with the pathways that determine survival in mitosis could improve the efficiency of mitotic-targeted therapies. Although death in mitosis

is thought to be at least partly mediated by apoptosis, the molecular pathways that control survival or death in mitosis are not well understood14. Here we show that death in mitosis is modulated by the energetic balance that counteracts the loss of mitochondrial mass during mitotic arrest. Using Cdc20 knockout cells or human cells treated with microtubule poisons, we describe here that the presence of autophagy during mitotic arrest is accompanied by a gradual decline in the mitochondrial mass and oxidative respiration. This results in the activation of AMPK and the induction of glycolysis in a PFKFB3-dependent manner.Inhibition of these energetic pathways in breast cancer cells prevents mitotic slippage and results in accelerated death of mitotic cells, thus potentiating the therapeutic effect of microtubule poisons currently used in the clinic.

RESULTS

Mitotic death is modulated by the intrinsic apoptotic pathway

To analyze the molecular pathways modulating cell viability in mitosis we made use of
Cdc20 conditional knockout fibroblasts in which Cdc20 is excised upon treatment with 5 4-hydroxy-tamoxifen (4OHT)9. These cells display normal mitotic entry but mitotic exit is completely prevented due to the lack of APC/C-Cdc20-dependent cyclin B1 degradation. Mitotic cell death (MCD) can be observed in these cells by time-lapse microscopy using TO-PRO3, a dye that is internalized into the cells upon the permeabilization of membranes that precedes cell death (Fig. 1a,b). Cdc20(D/D) cells display a variable survival in mitosis (SiM, time since mitotic entry till cell death) of 22 ±14 h until they finally died in mitosis (Fig. 1b,c). No Cdc20(D/D) cell was able to exit from the mitotic arrest suggesting that this APC/C cofactor is essential for mitotic slippage.To test the relevance of apoptosis in MCD, we transfected these cells with small interfering (si)RNAs (Supplementary Fig. 1) against several apoptotic regulators following the protocol depicted in Figure 1a. Knockdown of Mcl1, an anti-apoptotic regulator of the Bcl2 family involved in the response to taxol15, 16, or BclX resulted in earlier MCD whereas knockdown of both caspase 2 and caspase 3 significantly delayed MCD (Fig. 1b,c). Double knockdown of the pro-apoptotic regulators Bax and Bak also resulted in a significant increase in SiM and delay in MCD (Fig. 1c). The involvement of the apoptotic machinery was also validated using the pan-caspase inhibitor ZVAD or two different inhibitors of the Bcl2 family (Fig. 1d). SiM was improved with ZVAD and significantly decreased with the two Bcl2 family inhibitors (Fig. 1d) being more dramatic in the case of ABT-263, perhaps as a consequence of the more potent effect of this compound against Mcl1 17.Downregulation or inactivation of caspases or Bax/Bak proteins delayed but did not prevent MCD as all cells died in these assays in the absence of Cdc20 (Fig. 1c,d).
To test whether this was a consequence of partial inactivation of apoptosis, we next used Bax/Bak double knockout cells in which the intrinsic apoptotic pathway is totally 6 inhibited18. To mimic the metaphase arrest caused by Cdc20 ablation, cells were released from a nocodazole-induced prometaphase arrest in the presence of the proteasome inhibitor MG132, thus preventing cyclin B degradation and mitotic exit (Fig. 1e). This protocol resulted in a SiM value of 13.0 ± 9.5 h in wild-type cells, which was significantly expanded to 39.0 ± 28.9 h in the absence of Bak and Bax. Yet, all cells died in mitosis in these conditions in the presence of necrotic figures (SupplementaryFig. 1). Similar data were obtained in human cancer cells (HeLa or MDA-MB-231)sSubjected to the same protocol (Fig. 1f), suggesting that apoptosis is involved but not essential for MCD.

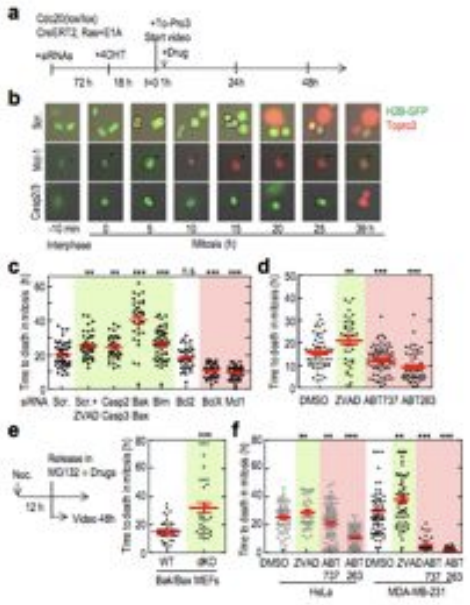

Figure 1. Mitotic cell death is modulated by the intrinsic apoptotic pathway. a)Protocol used for time-lapse microscopy in Cdc20-deficient cells. Ras/E1A-transformed Cdc20(lox/lox); CreERT2 cells were nucleofected with siRNAs, seeded at low density and treated with 4-hydroxytamoxifen (4OHT) 18h before starting the video in the presence of TO-PRO3 or other chemicals. b) Representative micrographs of Cdc20-deficient [Cdc20(D/D)] cells after the indicated periods of mitotic arrest (h after chromosome condensation and cell rounding) in the presence of siRNAs against Mcl1 or caspase 2 and 3. c) Plots representing the duration of mitosis (from mitotic entry until cell death) in Cdc20-null cells treated with the indicated siRNAs (Scr., scrambled sequences) or in the presence of the caspase inhibitor ZVAD. d) Duration of mitosis (from metaphase until cell death) in Cdc20-null cells treated with caspase or Bcl-2 family inhibitors. e) Schematic representation of the protocol followed for videomicroscopy in Bax/Bak-deficient MEFs and human cell lines cells (left panel). Cells were synchronized in prometaphase for 12 hours with nocodazole, and released in the presence of the proteasome inhibitor MG132. The duration of mitosis (from metaphase until cell death) in Bax/Bak-null and control MEFs is represented in the right panel. f) Duration of mitosis in human cell lines cells treated with caspase inhibitors or the indicated Bcl-2

family inhibitors. In (c-f) dots represent individual cells and the mean is indicated by a red line. Green or red columns indicate a significant delay or premature cell death in mitosis. n.s., not significant. **, p<0.01; ***, p<0.001 (Student's t-test).

Autophagy modulates survival during mitotic arrest

We next investigated other pathways known to regulate apoptotic-independent cell death. Downregulation of both Ripk1 and Ripk3 using siRNAs, or their inhibition using necrostatin1, did not modify MCD in Cdc20-null cells (Supplementary Fig. 1), suggesting that necroptosis or programmed necrosis is not a major pathway for death in mitosis.

Although autophagy has been previously found to be inhibited during mitosis 19, we tested the changes in this process during prolonged mitotic arrest. Cdc20-null cells were first synchronized in G2 using the Cdk1 inhibitor RO-3306 and mitotic entry and progression were monitored after release from this compound (Fig. 2a andSupplementary Fig. 2). The autophagic flux was scored using a fluorescent-tagged LC3 sensor in which the pH sensitivity differences exhibited by GFP (green fluorescent protein) and mRFP (red fluorescent protein) can monitor progression from the autophagosome to autolysosome 20. Whereas autophagosomes emit both mRFP and GFP signals (yellow in overlaid images), autolysosomes emit only an acid-stable mRFP signal because the pH-sensitive GFP signal is quenched in acidic lysosomes. Autophagy was increased after prolonged mitotic arrest in comparison with normal mitosis in asynchronous cultures in the absence of 4-OHT or with the initial arrest in Cdc20-null cells (Fig. 2b). Both the accumulation of autophagosomes and autophagolysosomeswere significantly prevented in the presence of the Class III PI3K inhibitor 3-methyladenine (3MA), and increased upon treatment with the mTOR inhibitor PP242, confirming the dynamic autophagic flux in mitotic cells. The lapidated and autophagosome membrane-associated form of LC3 (LC3-II) increased after 24 or 36 h in mitosis in parallel to the cleavage of caspase 3, both in human and mouse cells (Fig. 2d and Supplementary Fig. 2), indicating the concomitant presence of autophagy and apoptosis in these cultures. Incubation during mitotic arrest with the lysosomal protease inhibitors E64d (a calpain and cathepsin B inhibitor) and pepstatin A (PA, an inhibitor of aspartic proteases), which blocks the last steps of autophagic degradation, enhanced accumulation of LC3-II, confirming the presence of a dynamic autophagy flux during mitosis (Supplementary Fig. 2).

We then tested whether autophagy was able to modulate MCD by scoring the SiM upon downregulation of several autophagy regulators (Supplementary Fig. 2).Knockdown of Raptor, a member and positive regulator of the mTOR complex 1 that inhibits autophagy, resulted in earlier death in mitosis whereas downregulation of several proteins involved in the induction of autophagy, such as Ulk1, Vps34 or Beclin1, prevented MCD to a similar extent to the apoptosis inhibitor ZVAD (Fig. 2e). The requirements for autophagy in MCD were also validated during mitotic arrest inAtg5-null cells (Fig. 2f). Induction of autophagy by inhibitors of the PI3K-Akt-mTOR pathway resulted in premature MCD in Cdc20-null cells (Fig. 2g and SupplementaryFig. 2) or mitotic human cells (Fig. 2h), whereas 3MA delayed death in mitosis (Fig. 2h,i). Yet, concomitant inhibition of apoptosis and autophagy using a combination of ZVAD and 3MA did not further enhance SiM and all Cdc20-null cells eventually died in the presence of these two inhibitors (Fig. 2i). Finally, whereas caspase inhibition did not prevent LC3 lipidation, treatment of cells with E64d/PA inhibited poly(ADP-ribose) polymerase (PARP-1) cleavage (Supplementary Fig. 2), suggesting a pro-apoptotic activity for autophagy in mitotic arrested cells.

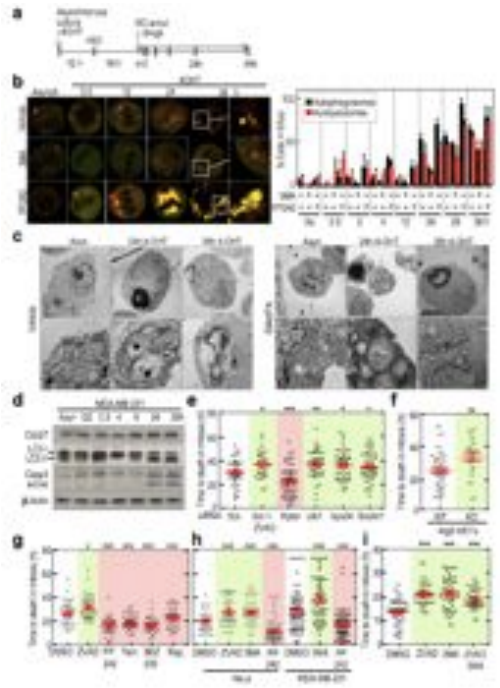

Figure 2. Autophagy modulates cell death during mitotic arrest. a) Protocol for synchronized entry into mitosis in Cdc20(D/D) cells. Cdc20(lox/lox) cells are first 25
treated with 4OHT, Cdk1 is then inhibited with RO-3306 during 18 h for G2 arrest, and cells are released to enter into mitosis in a synchronized manner (see also Supplementary Fig. 2). b) Live confocal microscopy pictures of Cdc20-null cells transiently expressing the LC3 reporter system in the presence of a mTOR inhibitor (PP242) and the autophagy inhibitor 3MA. Quantification of the autophagic flux (at least 5 puncta per cell) in asynchronous (As.) cultures or at the indicated times after release from the G2 arrest. Data are represented as mean ± SEM (n=30 cells per point).c) Electron microscopy micrographs showing the presence of autophagosomes in Cdc20-null cells after release from G2, either in the absence or presence of E64d/PA. Scale bars, 2 mm and 500 nm for low and high magnification images, respectively.

d) Immunodetection of the indicated proteins in MDA-MB-231 cells after release from the G2 arrest. b-actin is included as a loading control. e) Duration of mitosis (from mitotic entry until cell death) in Cdc20-null cells transfected with the indicated interfering RNAs or in the presence of the caspase inhibitor ZVAD. f) Duration of mitosis (from metaphase until cell death) in Atg5–null and control MEFs synchronized following the protocol depicted in Figure 1e. g) Duration of mitosis (from metaphase until cell death) in Cdc20-null cells treated with ZVAD, the indicated inducers of autophagy (mTORinhibitors PP242, temsirolimus, BEZ235), or transfected with siRNAs against Raptor (Rap.). h) Duration of mitosis (from metaphase until cell death) in human cell lines cells treated with the indicated compounds. i) Duration of mitosis in Cdc20-null cells treated with caspase and/or autophagy inhibitors. In (e-i) dots represent individual cells and the mean is indicated by a red line. Green or red columns indicate a significant delay or premature cell death in mitosis. n.s., not significant. *, p<0.05; **, p<0.01; ***, p<0.001 (Student's t-test).We then tested whether autophagy was able to modulate MCD by scoring the SiM upon downregulation of several autophagy regulators (Supplementary Fig. 2).Knockdown of Raptor, a member and positive regulator of the mTOR complex 1 that inhibits autophagy, resulted in earlier death in mitosis whereas downregulation of several proteins involved in the induction of autophagy, such as Ulk1, Vps34 or Beclin1, prevented MCD to a similar extent to the apoptosis inhibitor ZVAD (Fig. 2e). The requirements for autophagy in MCD were also validated during mitotic arrest inAtg5-null cells (Fig. 2f). Induction of autophagy by inhibitors of the PI3K-Akt-mTOR pathway resulted in premature MCD in Cdc20-null cells (Fig. 2g and Supplementary Fig. 2) or mitotic human cells (Fig. 2h), whereas 3MA delayed death in mitosis (Fig. 2h,i). Yet, concomitant inhibition of apoptosis and autophagy using a combination of ZVAD and 3MA did not further enhance SiM and all Cdc20-null cells eventually died in the presence of these two inhibitors (Fig. 2i). Finally, whereas caspase inhibition did not prevent LC3 lipidation, treatment of cells with E64d/PA inhibited poly(ADP-ribose) polymerase (PARP-1) cleavage (Supplementary Fig. 2), suggesting a pro-apoptotic activity for autophagy in mitotic arrested cells.

Mitophagy leads to loss of mitochondria during mitotic arrest

The cellular mitochondrial mass is tightly regulated by a balance between biosynthesis of new mitochondrial proteins and the removal of old mitochondria by a specific autophagy process known as mitophagy 21, 22. Since protein synthesis is limited during mitosis due to the lack of proper transcription and translation, we next tested whether mitotic arrest was accompanied by mitochondrial loss. In fact, the cellular mitochondrial content started to decrease a few hours (3-6 h) after mitotic arrest in Cdc20-null cells as detected by time-lapse microscopy (Fig. 3a) and cytometry (Fig.3b), using a mitochondrial dye resistant to loss of membrane potential. Exposure of
mitotic cells to carbonyl cyanide m-chlorophenyl hydrazine (CCCP), a classical inducer of mitophagy, resulted in decreased mitochondrial signal during the first few hours after mitotic arrest, whereas this compound had little effect during late mitotic arrest, when the mitochondrial mass was already severely reduced (Fig. 3b,c). Immunodetection of the mitochondrial proteins Tom20, Tim23 or Tom40 corroborated the loss of mitochondrial mass and this effect was prevented when the lysosomal function was inhibited with E64d/PA (Fig. 3d).9 The decrease in mitochondrial content was accompanied by a gradual colocalization of LC3 in the mitochondria suggesting the presence of mitophagy in mitotically arrested cells (Fig. 3e). In fact, the formation of autophagosomes affecting mitochondria was evident as early as 6 h after mitotic arrest and these organelles were frequently found within the autophagosomes at later stages (Fig. 3f and SupplementaryFig. 3). Prevention of mitophagy or lysosomal function with 3MA, or exposure to Cyclosporin A (CsA), a blocker of the opening of mitochondrial permeability transition pores, significantly prevented loss of mitochondrial content (Fig. 3g). In line with these observations, loss of mitochondrial function was accompanied by increased reactive oxygen species (ROS) and prevention of ROS with N-acetyl-L-cysteine (NAC) resulted in prevention of death during prolonged mitotic arrest both in mouse and human cells (Supplementary Fig. 3).

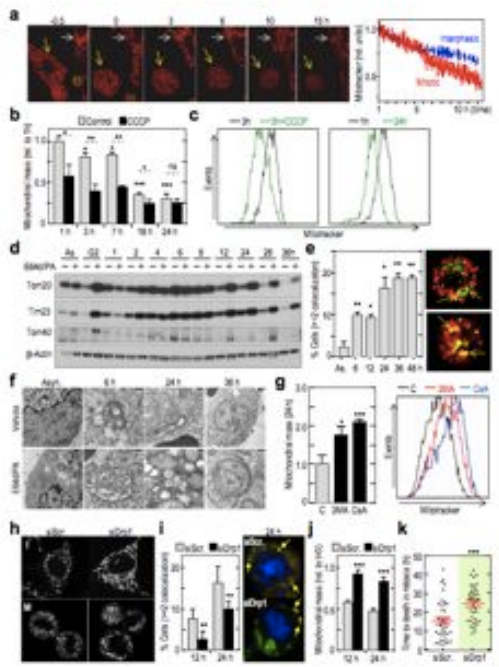

Figure 3. Reduced mitochondrial mass as a consequence of mitophagy during mitotic arrest. a) Mitotracker signal was followed by time-lapse microscopy at the indicated time points after release of Cdc20-null cells from G2 arrest. White and yellow arrows indicate interphasic or mitotic cells, respectively. Mitotracker intensity decreases rapidly in cells arrested in mitosis (red) compared with interphasic cells (blue). Data are represented as mean ± SD (n= 18 mitotic and 12 interphasic cells). b) Quantification of mitotracker intensity as measured by flow cytometry at the indicated time points after
release from G2 arrest (mean ± SEM). As a positive control, CCCP results in a reduction of the mitochondrial mass at early but not late time points during mitotic arrest in comparison with 1 h- treated cells (n=7 independent assays). c) Representative profiles of Cdc20(D/D) after 3h in mitosis in the absence or presence of CCCP (left panel), or after 1h and 24h in mitosis (right panel). d) Immunodetection of the mitochondrial proteins Tom20, Tim23 and Tom40 in Cdc20-null cells at the indicated times after release from G2. As., asynchronous cultures. b-actin was used as a loading marker. e) Percentage of cells showing co-localization of LC3-GFP and Mitotracker (>2 foci per cell; see yellow arrows in the representative images) at the indicated time

points after mitotic arrest. Data represent mean ± SEM; n=30 cells per condition. f) Representative electron microscopy images showing the inclusion of mitochondria inautophagosomes during mitotic arrest either in the absence or presence of E64d/PA.Scale bars, 200 nm in Asyn. cells and 500 nm in mitotic-arrested cells. g) Mitochondrial content as measured by flow cytometry in the presence of Mitotracker in Cdc20-null cells after 24 h in mitosis in the presence of vehicle (C), 3MA or CsA (related to vehicle-treated cells). The plots in the right represent the profile of Cdc20(D/D) after 24h in mitosis in the absence or presence of 3MA (red) or Cyclosporine A (blue). h) Representative confocal microscopy live images showing the mitochondrial network.(Mitotracker) in the presence (siScr.) or absence (siDrp1) of Drp1 after nucleofection with siRNAs against this molecule. i) Co-localization of LC3-GFP and Mitotracker (>2 foci per cell) at the indicated time points after mitotic arrest in Drp1 knock-down (siDrp1) cells. (n=30 cells per condition). Representative confocal microscopy live images show the co-localization of LC3-GFP and Mitotracker at 24 h in siScr. and siDrp1-transfected cells (right panel). j) Quantification of Mitotracker intensity by cytometry after 12 and 24 h of mitotic arrest relative to 1 hour of mitotic arrest in the presence (siScr.) or absence (siDrp1) of Drp1. k) Duration of mitosis (from mitotic entry until cell death) in Cdc20-null cells treated with specific siRNAs against Drp1 (siDrp1). n.s., not significant. *, p<0.05; **, p<0.01; ***, p<0.001, Student's t-test.

During mitosis, mitochondria are fragmented to facilitate segregation of this organelle to daughter cells 1. Mitochondrial fission is mediated by Cdk1-dependent phosphorylation and activation of the dynamin-like protein Drp1. Since fragmented mitochondria are known to be more sensitive to mitophagy23, we next tested whether inactivation of Drp1 resulted in a specific protection of mitotic mitochondria. As depicted in Figure 3h, knock-down of Drp1 by short interfering RNAs (siDrp1) in Cdc20-null cells prevented fragmentation of mitochondria and siDrp1 cells displayed longer tubular organelles during mitosis. Knock-down of Drp1 also resulted in reduced co-localization of mitophagy markers in mitochondria (Fig. 3i), prevented loss of mitochondrial mass (Fig. 3j) and led to increased SiM in Cdc20-deficient cells (Fig. 3k),in agreement with the relevance of maintaining the proper level of mitochondrial mass to prevent cell death in mitosis.

AMPK promotes glycolysis during mitotic arrest

We next investigated the functional relevance of mitochondrial loss during mitosis by comparing the rates of mitochondrial respiration (oxygen consumption, OCR) and glycolysis (extracellular acid release; ECAR) from mitotic and control cells. Cdc20(D/D) cells were arrested in G2 using RO-3306 for 18 h and released to arrest in mitosis (red) in a synchronized manner. G2-synchronized (blue) or asynchronous(green) Cdc20(lox/lox) cells were used as controls (Fig. 4a). Our results indicated that OCR quickly increased upon mitotic entry in agreement with recent data indicating the activation of the oxidative respiration during the G2/M transition in a Cdk1-dependent manner24. However, the respiratory capacity started to become extenuated after ~12 h in mitosis (Fig. 4b). ECAR levels gradually increased during mitosis but were further augmented during late mitotic arrest in parallel with the loss of oxidative respiration both in mouse (Fig. 4b) and human (Fig. 4c) cells.In agreement with increased AMP/ATP levels (black versus green in Fig. 4f). This defect is likely a consequence of Cdk1 inactivation by RO-3306 given the crucial role of Cdk1 in activating mitochondrial function during the G2/M transition24. The AMP/ATP ratio was normalized after release from this compound in control Cdc20(lox/lox) cells (blue) that underwent a normal transition through the different phases of the cell cycle. In Cdc20(D/D) cells, the AMP/ATP ratio displayed a new gradual increase ~8 h after mitotic arrest (red in Fig. 4f) in agreement with the timing of AMPK activation (Fig. 4d).

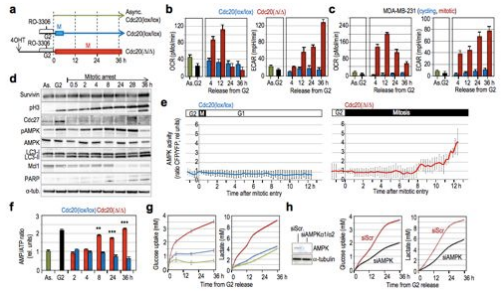

Figure 4. Metabolic switch from OXPHOS to glycolysis is mediated by AMPK. a) Protocol used to synchronize entry into mitosis. Treatment of Cdc20(lox/lox) cells with 4-OHT results in Cdc20(D/D) cells (red) which arrest in mitosis after release from the G2 arrest. Control cells include Cdc20(lox/lox) cells which do not arrest (blue) or asynchronous cultures (green). Color codes are maintained throughout the figure foreasier identification of the three cell types. b) Respirometry profile of asynchronous (As.) Cdc20(lox/lox) cells, or G2-arrested or mitotic arrested Cdc20(D/D) cells at the indicated time points after the release from G2. OCR (oxygen consumption rate) measures mitochondrial respiration, whereas ECAR (extracellular acidification rate) is a measure of glycolysis. OCR or ECAR data represent the difference between maximum (in the presence of FCCP or oligomycin, respectively) and basal values. c) Similar respirometry profile in MDA-MB-231 human breast cancer cells. b and c are representative assays from three separate experiments. d) Immunodetection of the indicated antigens in asynchronous (As.) Cdc20(lox/lox) cells, or G2-arrested or mitotic 28 arrested Cdc20(D/D) cells at the indicated time points after the release from G2. a-tubulin was used as a loading marker. e) AMPK activity is monitored by a FRET biosensor in control Cdc20(lox/lox) (blue) or Cdc20-null (red) cells upon mitotic entry at the cell single level. Time 0 indicates mitotic entry and the length of the black bar represents duration of mitosis. Data are represented as mean ± SD (n= 12 cells per genotype). f) AMP/ATP ratio measured by HPLC in control Cdc20(lox/lox) and Cdc20-null cells. **, p<0.01; ***, p<0.001, Student's t-test. g) Glucose uptake and concentration of extracellular lactate (NMR analysis) in the indicated cultures in the presence of 13C-labelled glucose. h) Similar glucose uptake and concentration of extracellular lactate in Cdc20-null cells after knock-down of AMPKa1/a2 using specific siRNAs. In g) and h) data represent mean ± SD and a spline function is used to connect the sampled points. Data in b), c) and g) are not normalized for death cells and the differences in mitotic-arrested cells are likely under-estimated.

Glycolysis is a major determinant of survival in mitosis

The activation of AMPK and the subsequent glycolytic switch observed in mitotic cells raised the possibility of a dependence on energy pathways to survive in mitosis. Treatment of mitotic cells with Compound C, a molecule known to inhibit AMPK 12 among other kinases, or with metformin, which inhibits mitochondrial function resulting in ATP depletion frequently activating AMPK, resulted in reduced SiM in mitotic Cdc20-null cells (Fig. 5a) or human cell lines (Fig. 5b). Specific knockdown of AMPKa1 and AMPKa2 transcripts also resulted in reduced viability in mitosis (Fig.5c). Furthermore, addition of two different glycolytic poisons, 2-desoxi-D-glucose (2-DG; a glucose analogue that cannot be metabolized) or oxamate (an isosteric and isoelectronic inhibitory analogue of pyruvate), also resulted in premature MCD; whereas supplementation of media with glucose led to a significant increase in SiM (Fig. 5d). The relevance of the glycolytic pathway was directly addressed by testing therelevance of 6-phosphofructo-2-kinase/fructose-2,6-bisphosphatase 3 (PFKFB3), a key regulator of the glycolytic enzyme phosphofructokinase-1 (PFK-1) that is activated by AMPK in a phosphorylation-dependent manner and frequently expressed in cancer cells 26. Downregulation or inhibition of PFKFB3 using siRNAs or the competitive inhibitor 3-(3-pyridinyl)-1-(4-pyridinyl)-2-propen-1-one (3PO) resulted in a significant reduction in SiM in mouse (Fig. 5e) or human (Fig. 5f) cells, in agreement with reduced glucose consumption and lactate production during mitosis in the absence of this
regulator (Fig. 5g).

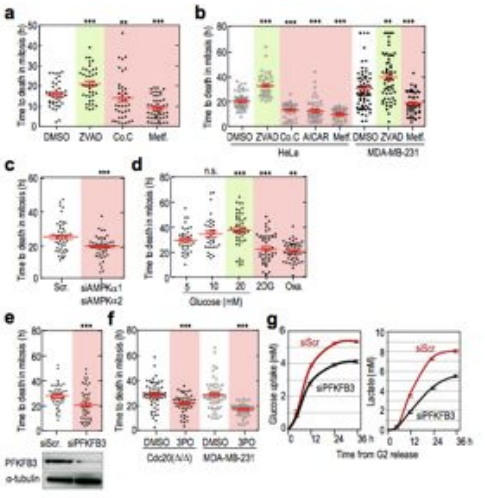

Figure 5. Glycolysis determines survival during mitotic arrest. a) Duration of mitosis (from metaphase until cell death) in Cdc20-null cells treated with the indicated AMPK modulators. b) Duration of mitosis in human cell lines treated with the indicated modulators of AMPK or the caspase inhibitor ZVAD. c) Duration of mitosis in Cdc20-null cells transfected with Scramble or AMPKa1/a2 siRNAs. d) Duration of mitosis in Cdc20-null cells treated with the indicated inhibitors of glycolysis and upon glucose addition at the indicated concentration. e) Duration of mitosis in Cdc20-null cells treated with PFKFB3 siRNAs. Bottom panel shows PFKFBP3 protein levels upon knockdown with the corresponding siRNAs. f) Duration of mitosis in Cdc20- null and in human cell lines arrested in mitosis treated with the PFKFB3 inhibitor 3PO. g) Glucose uptake (left panel) and concentration of extracellular lactate (right panel) 29measured by NMR in Cdc20-null cells transfected with Scramble or PFKFB3 siRNA.Data represent mean ± SD. In (a-f) dots represent individual cells and the mean is indicated by a red line. Green or red columns indicate a significant delay or premature cell death in mitosis. n.s., not significant. **, p<0.01; **, p<0.01; ***, p<0.001 (Student's t-test).

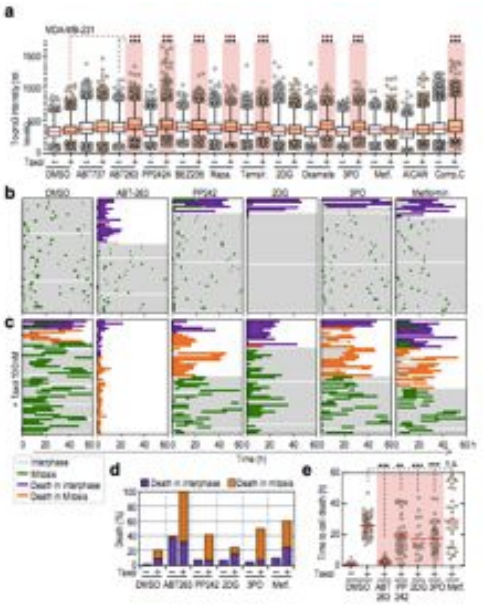

Figure 6. Taxol cooperates with different inhibitors of survival pathways to promote mitotic cell death. a) Cell death in MDA-MB-231 as determined by To-Pro3 levels, measured using high-throughput microscopy, after the addition of the indicated compounds in the presence or absence of taxol. Pink columns indicate significant synergistic combinations when compared to single inhibitors (black dotted comparisons) or taxol (red dotted comparisons). ***, p<0.001; Student's t-test. b) Duration of interphase (gray) or mitosis (green) of MDA-MB-231 cells treated with the indicated inhibitors. Each lane represents one cell. Cell death observed in interphase is represented in violet, while cell death detected during mitosis is shown in orange. c) Cell fate of single MDA-MB-231 cells treated with the indicated inhibitors in combination with Taxol. d) Quantification of the percentage of cells dying in interphase (violet) or in mitosis (orange) after the indicated treatments (n=50 cells per condition). e) Duration of mitosis (from mitotic entry until cell death) in MDA-MB-231 cells treated with the indicated drugs, alone or in combination with Taxol. n.s., not significant. **, p<0.01; ***, p<0.001 (Student's t-test).

Inhibition of glycolysis cooperates with microtubule poisons in mitotic cell death

We next tested the relevance of apoptosis, autophagy and energy production, in the therapeutic effect of microtubule poisons. MBA-MD-231 breast cancer cells were treated with multiple agents against the referred pathways either in the presence or absence of taxol. As indicated in Fig. 6a, several combinations were more efficient than the single agents in killing these breast cancer cells. The effect of ABT-263, PP242, 2DG and 3PO was also tested in additional breast cancer cell lines such as

MDA-MD-468, EVSA-T or MCF7 (Supplementary Fig. 6). To understand whether these combinations were effective in mitosis, we monitored the cell fate of MBA-MD-231 cells treated with ABT-263, PP242, 2DG, 3PO or Metformin in the absence or presence of taxol. As shown in Figure 6b-e, treatment of breast cancer cells with these individual drugs results in a variable efficiency in cell death ranging from 10% to 40% without affecting mitotic cells (Fig. 6b,d). Single treatment with taxol also resulted in a significant percentage of death cells (21%) from which only 12% of cells died in mitosis, in agreement with previous data in transformed fibroblasts 9. Notably, combination of taxol with ABT-263, PP242 and 3PO resulted in efficient MCD (Fig.6c,d) and the SiM was significantly reduced compared to the effect of taxol alone (Fig.6e).

The synergism between taxanes and Bcl2- and mTORC1-inhibitors in tumor growth has been explored in the past27-29. We therefore tested the cooperation between taxol and the inhibition of glycolysis in tumor development in vivo. Subcutaneous xenografts were generated with MBA-MD-231 cells, and taxol (5 mg/Kg) and 3PO (5, 25 or 50 mg/Kg) were injected i.p. when tumors reached 200 mm3. Taxol was very inefficient at that dose whereas treatment with 3PO alone resulted in a significant reduction in tumor volume and weight (Fig. 7a,b and Supplementary Fig. 7). The combination of taxol with 3PO further improved significantly the therapeutic effect when compared to single treatments (Supplementary Fig. 7 and Fig. 7b) and resulted in a significant raise in apoptotic cells in the tumors (Fig. 7c). Taken together, these data suggest the potential benefit of using glycolytic inhibitors in combination with current mitotic-targeted therapies to inhibit tumor growth.

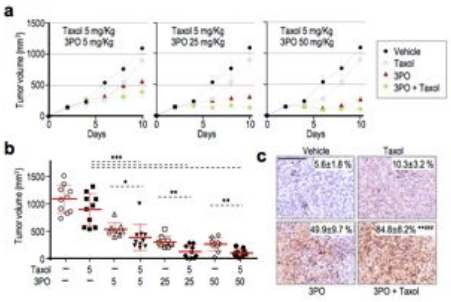

Figure 7. Anti-tumoral cooperation between microtubule poisons and PFKFB3 inhibitors in vivo. a) Effect of the combination of Taxol (5 mg/kg) and 3PO (5, 25 or 50 mg/kg) on the growth of tumor xenografts generated by subcutaneous injection of 30MDA-MB-231 cells in nude mice. b) Data correspond to the volume of each of the tumors at the final time point of the experiment (n=10 tumors per condition). Red lines indicate mean ± SD. *, p<0.05; **, p<0.01; ***, p<0.001 (ANOVA-test). c) Active caspase 3 immunostaining in MDA-MB-231-derived tumor xenografts. The numbers indicate the percentage of active caspase-3- positive cells relative to the total number of nuclei in each section ± SD. Six sections were counted for each of four dissected tumors per condition. Scale bars, 100 mm. **, p<0.01 relative to 3PO-treated tumors; ###, p<0.001 relative to taxol-treated tumors (Student's t-test).

DISCUSSION

The arrest imposed by anti-mitotic drugs is frequently transient and cells exit from mitosis in an APC/C-Cdc20-dependent process9known as mitotic slippage13, 30. Inhibiting the APC/C has been therefore proposed as a therapeutic option to prevent mitotic slippage, a possible mechanism of resistance to mitotic therapies in cancer cells 5, 8, 11, 12. Cdc20-knockout cells display a permanent mitotic arrest until death 9, providing a clean genetic model to analyze molecular pathways that determine cell fate in mitosis.Cells are sensitive to multiple insults during mitosis and the cellular alterationsresulting from aberrant mitotic progression are collectively known as mitotic catastrophe 14Despite the broad use of this concept, the molecular mechanisms that determine cell death in response to these alterations are not well understood. Among cell death pathways, multiple evidences have established the involvement of intrinsic apoptosis in response to mitotic aberrations11, 13, whereas the extrinsic apoptotic pathway is thought to be inhibited at this stage of the cell cycle32. Our results confirm previous results suggesting the relevance of the Bcl2 family in response to mitotic defects11, 13, 15, 16, 33. It has also been recently described that Cdc20 can suppress apoptosis targeting the pro-apoptotic factor Bim34, suggesting that mitotically arrested cells in which Cdc20 is inhibited as a consequence of SAC activity are sensitive to this form of death. However, mitotic arrested cells also die in the absence of caspase activity or in Bax/Bak double knockout cells in the presence of necrotic figures (Fig. 1 and Supplementary Fig. 1).

The two major cell death pathways in the cell, apoptosis and necrosis, proceed via a loss in mitochondrial membrane potential, reduced ATP levels and generation of ROS22. It has been assumed that mitochondria are particularly active during the energy expensive process driving spindle formation and chromosome segregation36. In fact, recent data showed that Cdk1 activity is necessary to phosphorylate and activate several components of the mitochondrial complex I thus enhancing mitochondrial respiration during the G2/M transition24. Inhibition of Cdk1 results in decreased mitochondrial activity 24, impaired respiratory capacity (Fig. 4b,c), and reduced ATP levels (Fig. 4f).

Thus, Cdk1 activity provides cells with the bioenergy required for a normal mitosis by enhancing mitochondrial respiration. However, upon mitotic arrest, the mitochondrial mass declines after about 6 h, presumably as a result of deficient renovation of organelles. This process occurs in the

presence of mitophagy (Fig. 3), a critical autophagic process responsible for the clearance of damaged mitochondria in cells37, 38 .Although it was originally argued that autophagy was shut down during the later phases of the cell cycle19, 39, 40, it has been more recently shown that autophagy can persist during mitosis 36. Thus, the reduced biogenesis resulting from impaired transcription and reduced translation in mitotic cells likely perpetuates mitochondrial dysfunction (Fig. 3) and reduced ATP levels (Fig. 4) during mitotic arrest, a situation not easily compensated by glycolysis as this pathway is much less efficient in generating ATP. The rise in the AMP/ATP ratio during mitotic arrest likely contributes to the activation of AMPK, a major homeostatic regulator of cellular ATP levels41 . Whereas the activation of AMPK has been shown to be predominantly cytoplasmic25, mitotic cells may become more sensitive to AMPK due to the absence of the nuclear envelope. Once activated, AMPK stimulates catabolic pathways that generate ATP, and inhibits ATP-consuming processes such as biosynthesis, cell growth and proliferation41. AMPK activation can acutely increase glucose uptake and glycolysis, although in the long-term it promotes the more energy-efficient oxidative metabolism by upregulating mitochondrial biogenesis and expression of oxidative enzymes. However, the later process is thought to be transcription-dependent 42 and therefore inefficient in mitotic 16 arrested cells. Among other activities, AMPK forms stable complexes with Ulk1 and Ulk2 and directly phosphorylates Ulk1, triggering autophagy 43, 44. Thus, in the presence of mitochondrial dysfunction, AMPK likely determines a glycolytic switch, and can further promote autophagy during prolonged mitotic arrest (Fig. 4). It has been recently published that AMPK is active during mitosis and it is required for the completion of mitosis by phosphorylating components of the APC/C (APC1 and CDC27) and PP1 regulatory subunits45. In these studies, it was not obvious why a kinase activated by energy stress should be required for passage through mitosis42. However, it is important to note that nocodazole-arrested cells were used in these studies as a paradigm of mitotic cells45, raising the possibility that some of these conclusions may not apply to a normal, short (<1h) mitosis. Yet, AMPK deficiency in flies results in altered chromosome compositions, a phenotype likely linked to myosin regulatory light chain (MRLC) function46 and the links between AMPK and mitosis may be more complex than initially thought. AMPK activity is also pro-apoptotic, and necessary and sufficient for the activation of pro-apoptotic proteins such as Bim or Bmf and cell death during bioenergetics stress 47-49. Thus, we hypothesize that AMPK may have a dual role during mitotic arrest. On one hand, it senses loss of ATP and enhances glycolysis protecting from death. On the other hand, it may enhance autophagy and apoptosis through the modulation of Ulk1 and Bim/Bmf activities43, 44, 48, 49, thus explaining why both the inhibition (using siRNAs or small-molecule inhibitors) and the activation of AMPK (with metformin) results in reduced survival during mitosis (Fig. 5). The glycolytic activity of AMPK is thought to be determined by the phosphorylation and activation of PFKFB326, 50. PFKFB3 is a critical activator of 6-phosphofructo-1-kinase (PFK1), the rate-limiting enzyme in the conversion of glucose to pyruvate, the precursor of anaerobic ATP production. PFKFB3 is commonly overexpressed in human cancer26 contributing to the Warburg effect, a switch away from oxidative metabolism and towards rapid glucose uptake, glycolysis and lactate output that is characteristic of many tumor cells51

Since APC/C-Cdh1 is activated downstream of APC/C-Cdc20 after mitotic exit, the levels of PFKFB3 are high during mitosis (data not shown). In addition, whereas this protein is mostly nuclear during interphase, the combination of nuclear and cytoplasmic compartments during mitosis likely facilitates its AMPK-driven activation as well as its promoting function on the glycolytic machinery. As a summary, whereas recent data suggest that Cdk1-dependent activation of mitochondrial respiration is required for the G2/M transition, our observations suggest a switch to glycolysis during prolonged mitotic arrest. This switch is modulated by AMPK and requires key glycolytic enzymes such as PFKFB3. These observations may have important implications in cancer therapy. Mitotic slippage may be considered as a major mechanism of resistance in mitotic-targeted therapies8, 10. Whereas the combination between microtubule poisons and apoptotic inducers has been extensively studied13, 15, 16, 53, our data suggest that promoting autophagy or inhibiting glycolysis may therefore promote mitotic cell death before cells exit from mitosis. In fact,treatment with several small-molecule compounds directed against these pathways results in enhanced mitotic cell death in mitosis and cooperates with taxol in preventing cell proliferation of breast cancer cells both in vitro (Fig. 6) and in vivo (Fig. 7). Collectively, these data provide the cellular basis for new combinatory therapies targeting cell cycle and metabolic pathways in cancer

METHODS

Cell culture and synchronization. The Cdc20 conditional allele and its deletion by 4-OHT-inducible forms of Cre (RERT) were reported previously9. Atg5 and Bax/Bak mutant MEFs were described previously54-56. MEFs and human cell

lines were grown in Dulbecco's modified Eagle's medium (DMEM) or RPMI (Sigma) complemented with fetal bovine serum (FBS) and gentamycin at 37ºC and 5% CO2. For synchronization in G2, Cdc20(lox/lox); RERT MEFs and MDA-MB-231 cells were treated with RO-3306 (Calbiochem; 5 μM) for 18 hours and released in DMEM with or without 4-OHT (Sigma; 1 μM), or DMEM with or without Taxol (Sigma; 700 nM) and proTAME (Boston Biochem., Inc.; 10 μM). For mitotic synchronization of Cdc20-proficient mouse or human cultures, cells were treated for 12 hours with 200 nM nocodazole(Sigma) and released in fresh media containing 10μM MG132. Cells were treated withsmall molecule inhibitors as indicated in Supplementary Table 1. One μM TO-PRO®-3 Iodide (642⁄661; Invitrogen T3605) was added to cultures to monitor cell death.MEFs and human cells lines were transfected with Lipofectamine 2000 (Invitrogen) or Amaxa reagents (Dharmacon smart pool) in accordance with the manufacturer´s recommendations.

For quantitative RT-PCR studies, total RNA was isolated by using the Qiagen RNeasy kit, according to the manufacturer's instructions. cDNA was synthesized with a Superscript III reverse transcriptase (Invitrogen) and PCR amplification was performed using SYBR Green PCR Master mix (Applied Biosystems) with specific primers (Supplementary Table 2).

Cytometry. Cell cycle profiles were monitored by adding 0.2 μg/ml DAPI (Sigma) to the samples prior to their analysis on the LSR Fortessa (BD, San Jose). All data were analyzed using FlowJo v9.6.4 (Treestar, Oregon). For quantifying mitochondrial mass, adherent cells were trypsinized for 5 min at 37 ºC and resuspended in complete medium with 10 nM Mitotracker Deep Red (MTDR, M22426, Invitrogen) and 1 m/mL propidium iodide (P4864, Sigma) and then incubated for 15 min at 37 ºC. Using an FC500 flow cytometer (Beckman Coulter), 10,000 cells were acquired in the FL3 and FL4 channels. Mean fluorescence in the FL4 channel in the viable cell (PI-negative) population was plotted and normalized against that of untreated cells.

Biochemical analysis and immunofluorescence. For Western blotting, cells were lysed in RIPA or a buffer containing 50 mM Tris HCl, pH 7.5, 1 mM phenylmethylsulfonyl fluoride, 50 mM NaF, 5 mM sodium pyrophosphate, 1 mM sodium orthovanadate, 0.1% Triton X-100, 1 μg/ml leupeptin, 1mM EDTA, 1 mMEGTA and 10 mM sodium-glicerophosphate54. 30 μg of total protein was separated by SDS-PAGE and probed with antibodies as indicated in Supplementary Table 3. For immunofluorescence (IF) cells were fixed in 4% buffered paraformaldehyde for 10 min at RT, permeabilized in 0.15% Triton-X 100 for 5-10 min at RT and stained with 4,6 diaminophenylindole (DAPI; Prolong Gold antifade, Invitrogen) to visualize nuclei. Images were captured using a laser scanning confocal microscope TCS-SP5 (AOBS) Leica or a Leica DMI 6000B microscope and quantified with ImageJ. The tandem fluorescent-tagged LC3 reporter20 and the AMPK biosensor25 were described previously

Microscopy. For videomicroscopy human cell lines at 60-70% confluency were infected with lentiviruses containing H2B-GFP. lens, maintained at 37 °C in a humidified CO2 chamber. 1 μM TO-PRO®-3 Iodide 642⁄661; Invitrogen T3605) or 10 nM Mitotracker (Life Technologies) were added prior to recording. Images were acquired every 15 min, and processed and analyzed using ImageJ software.For high-throughput microscopy (HTM) cells were grown on μCLEAR bottom 96-well plates (Greiner Bio-One). After specific treatments, 1 μM TO-PRO®-3 Iodide (642⁄661; Invitrogen T3605) and 5 μg/ml Hoechst 33342 (Invitrogen H3570) were added. After 30 min at 37 ºC, images were automatically acquired from each well by an Opera High-Content Screening System (Perkin Elmer). A 20x magnification lens was used and pictures were taken at non-saturating conditions. Images were segmented using the Hoechst 33342 staining to generate masks matching cell nuclei from which the mean TO-PRO®-3 signal were calculated. To monitor ROS, cells were with specific drugs and incubated for 30 min at 37ºC as indicated in OxiSelect TM Intracellular ROS assay kit, Cell Biolabs and 5 μg/ml Hoechst 33342 (Invitrogen H3570). Images were automatically acquired from each well by an Opera High-Content Screening System (Perkin Elmer) as indicated above.For FRET analysis 25, cells were plated on eight-well flow chambers (Ibidi) and imaged with a Leica AF6000W equipped with a fast external filter wheels, Hamamatsu CCD Camera, HCX PL APO 40X/ oil 1.25 NA objective lens and AFC hardware autofocus system, maintained at 37 °C in a humidified CO2 chamber. Images were acquired every 1 or 10 min. Images were processed and analyzed using ImageJ software.

AMP/ATP levels, metabolic flux and NMR. Respirometry (OCR) and the extracellular acidification rate (ECAR) of cells were measured with an XF96 Extracellular Flux Analyzer (Seahorse Bioscience). In brief, cells were plated at 1.5-2×104 cells/well in buffered DMEM containing 25 mM glucose and 2 mM glutamine. Cells were incubated in a CO2-free incubator at 37°C for 1 h to allow for temperature and pH equilibration prior to loading into the XF96 apparatus. Assays consisted of sequential mix (2 min), pause (2 min), mix (0.33 min) and measurement (4 min) cycles, allowing for

determination of OCR/ECAR every 8.33 min. Mitotic cells were obtained after shake off and plated in BD Cell-TaK coated plates. Concentration of ATP was determined spectrophotometrically as described previously 57.For NMR analysis of cell media metabolites58, 0.5 x106 MEFs were plated in DMEM containing 13C-labeled–glucose and synchronized as described above. 500 μLof supernatant were recovered for every time point, centrifuged at 10000g for 10 min and filtered in 10Kd Spin Columns (BioVision). Before measurements by NMR,samples were dissolved 1:3 in buffer (0.3 mM TMSP, PBS 3X, 70% deuterated water and 0.09% azide). High-resolution NMR spectra were registered on a Bruker Avance spectrometer operating at 16.4T and integration regions were then manually defined using the AMIX3.8 software.

Transmission electron microscopy. Cells were fixed for 4 hours at 4°C in 4% paraformaldehyde (w/v) and 2.5% glutaraldehyde (v/v) in 0.4 M HEPES buffer pH 7.4, washed and fixed again in aqueous 1% (w/v) osmium tetroxide, and embedded in Epon.
Electron microscopy was performed with a JEOL 1230 transmission electron microscope, at 80 kV, on ultra-thin sections of 60 nm.

In vivo studies. Mice were injected subcutaneously in the right and the left flank with 3 x106 MDA-MB-231 cells in 0.1 ml of PBS + 0.5% BSA. 20 days after cell injection, 22 tumors had grown to an average volume of 150-200 mm3. Mice were then divided into different experimental groups of 5 animals each, which received the following treatments as intraperitoneal injections: saline (control); 5 mg/kg Taxol; 5 mg/kg 3PO;25 mg/kg 3PO; 50 mg/kg 3PO; 5 mg/kg Taxol + 5 mg/kg 3PO; 5 mg/kg Taxol + 25 mg/kg 3PO; 5 mg/kg Taxol + 50 mg/kg 3PO. The injection was repeated every two days and treatment was continued for 12 days. Tumor volumes were monitored using calliper measurements and were calculated by the formula: (4p/3) * (w/2)2 * (l/2).

Statistics. Statistical analysis was carried out using Prism 5 (GraphPad). All statistical tests were performed using two-sided, unpaired Student's t tests, or the Fisher's exact Test. Data with $p<0.05$ were considered statistically significant (*, $p<0.05$; **, $p<0.01$; ***, $p<0.001$).

Acknowledgements

We thank Marisol Soengas (CNIO, Madrid), Juan Pedro Bolaños (Salamanca), and Noboru Mizushima (Tokyo Medical and Dental University, Tokyo) for reagents. We also thank Susana Velasco (CNIO) for help with the Seahorse apparatus, and Fernando Escobar (CIB) for help with electron microscopy. E.D. and M.S-R. were supported by the Spanish Fondo de Investigaciones Sanitarias (Madrid) and Asociación Española contra el Cáncer (AECC), respectively. A.K.S. was supported by USPHS grants RO1DK19514, RO1DK67509. G.V. was supported by grants from the Spanish Ministry of Economy and Competitiveness (MINECO) and Fondo Europeo de Desarrollo Regional (FEDER) (PI12/02248), Fundació La Marató de TV3 (m12 20134031), and
Fundación Mutua Madrileña (AP101042012). M.L. was supported by the European Community's Seventh Framework Programme under grant agreement nº 281854 - the 23ObERStress (European Research Council project). E.R. was funded by a MINECO grant (SAF 2010-20256). Work in the M.M. laboratory was supported by grants from the MINECO (SAF2012-38215), the OncoCycle Programme (S2010/BMD-2470) from the Comunidad de Madrid, and the European Union Seventh Framework Programme(MitoSys project; HEALTH-F5-2010-241548).

Author Contribution

E.D. and M.S-R. performed most of the cellular and biochemical assays with the help of D.P., and L.E.-M. and P.B. collaborated in the analysis of mitophagy. R.C.-O. generated the NMR data. M.P. and D.M. helped with microscopy analysis. A.K.S. performed the AMP/ATP measurements and M.L. contributed to the analysis of AMPK. E.R. helped with metabolic measurements. E.D, M.S.-R., G.V., E.R., L.E.-M., P.B. and M.M. analyzed the data. M.M. designed the project and wrote the manuscript.

REFERENCES

1. Alvarez-Fernandez, M. & Malumbres, M. Preparing a cell for nuclear envelope breakdown: Spatio-temporal control of phosphorylation during mitotic entry. Bioessays (2014).
2. Musacchio, A. & Salmon, E.D. The spindle-assembly checkpoint in space and time. Nat Rev Mol Cell Biol 8, 379-393 (2007).
3. Peters, J.M. The anaphase promoting complex/cyclosome: a machine designed to destroy. Nat Rev Mol Cell Biol 7, 644-656 (2006).
4. Wurzenberger, C. & Gerlich, D.W. Phosphatases: providing safe passage through mitotic exit. Nat Rev Mol Cell Biol 12, 469-482 (2011).
5. Manchado, E., Guillamot, M. & Malumbres, M. Killing cells by targeting mitosis. Cell Death Differ 19, 369-377 (2012).

6. Komlodi-Pasztor, E., Sackett, D.L. & Fojo, A.T. Inhibitors targeting mitosis: tales of how great drugs against a promising target were brought down by a flawed rationale. Clin Cancer Res 18, 51-63 (2012).
7. Mitchison, T.J. The proliferation rate paradox in antimitotic chemotherapy. Mol Biol Cell 23, 1-6 (2012).
8. Domenech, E. & Malumbres, M. Mitosis-targeting therapies: a troubleshooting guide. Curr Opin Pharmacol (2013).
9. Manchado, E. et al. Targeting mitotic exit leads to tumor regression in vivo: Modulation by Cdk1, Mastl, and the PP2A/B55alpha,delta phosphatase. Cancer Cell 18, 641-654 (2010).
10. Gascoigne, K.E. & Taylor, S.S. Cancer cells display profound intra- and interline variation following prolonged exposure to antimitotic drugs. Cancer Cell 14, 111-122 (2008).
11. Huang, H.C., Shi, J., Orth, J.D. & Mitchison, T.J. Evidence that mitotic exit is a
better cancer therapeutic target than spindle assembly. Cancer Cell 16, 347-358 (2009).
12. Rieder, C.L. & Medema, R.H. No way out for tumor cells. Cancer Cell 16, 274-275 (2009).
13. Topham, C.H. & Taylor, S.S. Mitosis and apoptosis: how is the balance set? Curr Opin Cell Biol 25, 780-785 (2013).
14. Vitale, I., Galluzzi, L., Castedo, M. & Kroemer, G. Mitotic catastrophe: a mechanism for avoiding genomic instability. Nat Rev Mol Cell Biol 12, 385-392 (2011).
15. Wertz, I.E. et al. Sensitivity to antitubulin chemotherapeutics is regulated by MCL1 and FBW7. Nature 471, 110-114 (2011).
16. Inuzuka, H. et al. SCF(FBW7) regulates cellular apoptosis by targeting MCL1 for ubiquitylation and destruction. Nature 471, 104-109 (2011).
17. Tse, C. et al. ABT-263: a potent and orally bioavailable Bcl-2 family inhibitor. Cancer Res 68, 3421-3428 (2008).
18. Wei, M.C. et al. Proapoptotic BAX and BAK: a requisite gateway to mitochondrial dysfunction and death. Science 292, 727-730 (2001).
19. Eskelinen, E.L. et al. Inhibition of autophagy in mitotic animal cells. Traffic 3, 878-893 (2002).
20. Kimura, S., Noda, T. & Yoshimori, T. Dissection of the autophagosome maturation process by a novel reporter protein, tandem fluorescent-tagged LC3. Autophagy 3, 452-460 (2007).
21. Ashrafi, G. & Schwarz, T.L. The pathways of mitophagy for quality control and clearance of mitochondria. Cell Death Differ 20, 31-42 (2013).
22. Galluzzi, L., Bravo-San Pedro, J.M. & Kroemer, G. Organelle-specific initiation of cell death. Nat Cell Biol 16, 728-736 (2014).
23. Rambold, A.S., Kostelecky, B., Elia, N. & Lippincott-Schwartz, J. Tubular
network formation protects mitochondria from autophagosomal degradation during nutrient starvation. Proc Natl Acad Sci U S A 108, 10190-10195 (2011).
25. Tsou, P., Zheng, B., Hsu, C.H., Sasaki, A.T. & Cantley, L.C. A fluorescent reporter of AMPK activity and cellular energy stress. Cell Metab 13, 476-486 (2011).
26. Bando, H. et al. Phosphorylation of the 6-phosphofructo-2-kinase/fructose 2,6-bisphosphatase/PFKFB3 family of glycolytic regulators in human cancer. Clin Cancer Res 11, 5784-5792 (2005).
27. Lieber, J. et al. The BH3 mimetic ABT-737 increases treatment efficiency of paclitaxel against hepatoblastoma. BMC cancer 11, 362 (2011).
28. Campone, M. et al. Safety and pharmacokinetics of paclitaxel and the oral mTOR inhibitor everolimus in advanced solid tumours. British journal of cancer100, 315-321 (2009).
29. Meier, F. et al. Significant response after treatment with the mTOR inhibitor sirolimus in combination with carboplatin and paclitaxel in metastatic melanoma patients. Journal of the American Academy of Dermatology 60, 863-868 (2009).
30. Brito, D.A. & Rieder, C.L. Mitotic checkpoint slippage in humans occurs via cyclin B destruction in the presence of an active checkpoint. Curr Biol 16, 1194-1200 (2006).
31. Orth, J.D., Loewer, A., Lahav, G. & Mitchison, T.J. Prolonged mitotic arrest triggers partial activation of apoptosis, resulting in DNA damage and p53 induction. Mol Biol Cell 23, 567-576 (2012).
32. Matthess, Y., Raab, M., Sanhaji, M., Lavrik, I.N. & Strebhardt, K. Cdk1/cyclin B1 controls Fas-mediated apoptosis by regulating caspase-8 activity. Mol Cell Biol 30, 5726-5740 (2010).
33. Wang, P. et al. Phosphorylation of the proapoptotic BH3-only protein bid primes mitochondria for apoptosis during mitotic arrest. Cell reports 7, 661-671 (2014).
34. Wan, L. et al. APC(Cdc20) Suppresses Apoptosis through Targeting Bim for Ubiquitination and Destruction. Dev Cell 29, 377-391 (2014).
36. Liu, L., Xie, R., Nguyen, S., Ye, M. & McKeehan, W.L. Robust autophagy/mitophagy persists during mitosis. Cell Cycle 8, 1616-1620 (2009).
37. Youle, R.J. & Narendra, D.P. Mechanisms of mitophagy. Nat Rev Mol Cell Biol12, 9-14 (2011).
38. Okamoto, K. Organellophagy: Eliminating cellular building blocks via selective autophagy. J Cell Biol 205, 435-445 (2014).
39. Tasdemir, E. et al. Cell cycle-dependent induction of autophagy, mitophagy and reticulophagy. Cell Cycle 6, 2263-2267 (2007).
40. Tasdemir, E. et al. p53 represses autophagy in a cell cycle-dependent fashion. Cell Cycle 7, 3006-3011 (2008).
41. Hardie, D.G., Ross, F.A. & Hawley, S.A. AMP-activated protein kinase: a target for drugs both

ancient and modern. Chem Biol 19, 1222-1236 (2012).
42. Hardie, D.G., Ross, F.A. & Hawley, S.A. AMPK: a nutrient and energy sensor that maintains energy homeostasis. Nat Rev Mol Cell Biol 13, 251-262 (2012).
43. Egan, D.F. et al. Phosphorylation of ULK1 (hATG1) by AMP-activated protein kinase connects energy sensing to mitophagy. Science 331, 456-461 (2011).
44. Kim, J., Kundu, M., Viollet, B. & Guan, K.L. AMPK and mTOR regulate autophagy.
45. Banko, M.R. et al. Chemical genetic screen for AMPKalpha2 substrates uncovers a network of proteins involved in mitosis. Mol Cell 44, 878-892 (2011).
46. Lee, J.H. et al. Energy-dependent regulation of cell structure by AMP-activated protein kinase. Nature 447, 1017-1020 (2007).
47. Davila, D. et al. Two-step activation of FOXO3 by AMPK generates a coherent feed-forward loop determining excitotoxic cell fate. Cell Death Differ 19, 1677-1688 (2012).
48. Concannon, C.G. et al. AMP kinase-mediated activation of the BH3-only protein Bim couples energy depletion to stress-induced apoptosis. J Cell Biol189, 83-94 (2010).
49. Kilbride, S.M. et al. AMP-activated protein kinase mediates apoptosis in response to bioenergetic stress through activation of the pro-apoptotic Bcl-2 homology domain-3-only protein BMF. J Biol Chem 285, 36199-36206 (2010).
50. Marsin, A.S. et al. Phosphorylation and activation of heart PFK-2 by AMPK has

a role in the stimulation of glycolysis during ischaemia. Curr Biol 10, 1247-1255 (2000).
51. Vander Heiden, M.G., Cantley, L.C. & Thompson, C.B. Understanding the
Warburg effect: the metabolic requirements of cell proliferation. Science 324, 1029-1033 (2009).
53. Oltersdorf, T. et al. An inhibitor of Bcl-2 family proteins induces regression of solid tumours. Nature 435, 677-681 (2005).
54. Salazar, M. et al. Cannabinoid action induces autophagy-mediated cell death through stimulation of ER stress in human glioma cells. The Journal of clinical investigation 119, 1359-1372 (2009).55. Tsukamoto, S. et al. Autophagy is essential for preimplantation development of mouse embryos. Science 321, 117-120 (2008).
56. Buytaert, E., Callewaert, G., Vandenheede, J.R. & Agostinis, P. Deficiency in apoptotic effectors Bax and Bak reveals an autophagic cell death pathway initiated by photodamage to the endoplasmic reticulum. Autophagy 2, 238-240 (2006).
57. Saha, A.K. et al. Pioglitazone treatment activates AMP-activated protein kinase in rat liver and adipose tissue in vivo. Biochem Biophys Res Commun 314, 580-585 (2004).
58. Bradley, S.A. et al. Fermentanomics: monitoring mammalian cell cultures withNMR spectroscopy. Journal of the American Chemical Society 132, 9531-9533
(2010).

Available online at www.sciencedirect.com

SciVerse ScienceDirect

Current Opinion in Pharmacology

Mitosis-targeting therapies: a troubleshooting guide

Elena Domènech and Marcos Malumbres

Several mitotic kinases and kinesins are currently considered as cancer targets based on their critical role during the cell division cycle and their significant level of expression in human tumors. Yet, their use is limited by the lack of selectivity against tumor cells, the low percentage of mitotic cells in many human tumors, and dose-limiting side-effects. As a consequence, initial clinical trials have shown limited responses. Despite these drawbacks, inhibiting mitosis is a promising strategy that deserves further development. Future advances will benefit from more specific inhibitors with better pharmacodynamic properties, a clear physiological characterization and cell-type-specific requirements of old and new mitotic targets, and rational strategies based on synthetic lethal interactions to improve selectivity against tumor cells.

Addresses
Cell Division and Cancer Group, Spanish National Cancer Research Centre (CNIO), Madrid, Spain

Corresponding author: Malumbres, Marcos (malumbres@cnio.es, mmm@cnio.es)

Current Opinion in Pharmacology 2013, **13**:519–528

This review comes from a themed issue on **Cancer**

Edited by **Massimo Santoro** and **Francesca Carlomagno**

For a complete overview see the Issue and the Editorial

Available online 12th April 2013

1471-4892/$ – see front matter,

http://dx.doi.org/10.1016/j.coph.2013.03.011

Introduction

Cell cycle deregulation is a common feature of human cancers and multiple therapeutic strategies are aimed to inhibit the cell division cycle in tumor cells. Current efforts can be broadly divided into three different groups: first, preventing the commitment to cell cycle entry imposed by oncogenic signals [1]; second, abrogation of the DNA damage checkpoint to increase lethality in highly proliferating cells [2,3]; and third, taking advantage of the special sensitivity of cells to abnormal chromosome segregation during mitosis [4]. The two first approaches are clearly based on the specific signals originated from the oncogenic stress in tumor cells. This has been far more difficult to achieve in targeted therapies directed against mitosis given the conservation in the essential mechanism that regulates chromosome segregation in normal or tumor cells.

Classical antimitotic therapies have made use of spindle poisons that bind tubulin subunits and either stabilize, for example, taxanes (paclitaxel, Nab-paclitaxel and docetaxel), or de-stabilize, for example, vinka-alkaloids (vinorelbine, vinblastine, vincristine) and microtubules. In all these cases, these compounds prevent microtubule dynamics, a process required for the generation of a bipolar spindle and chromosome segregation during mitosis. Microtubules are also necessary for multiple cellular functions during interphase and the use of these spindle poisons is associated to side-effects such as neurotoxicity that can lead to irreversible neuropathologies. It is expected that dividing cells are more vulnerable to these microtubule-disturbing agents due to the increased rate or microtubule turnover during mitosis. In fact, microtubule poisons can be considered as one of the major additions to the clinic in the last decades. However, whether mitotic inhibition explains the clinical success of these drugs is now under debate [5,6•].

The success of spindle poisons and the susceptibility of cells to mitotic arrest have led in the last years to a search for improved therapeutic strategies based on specific mitotic targets (Figure 1). Several mitotic kinases have been evaluated including members of the Polo-like kinase (Plk) and Aurora families. Mitotic targets also include kinesins, a class of motor proteins with ATPase activity that move along microtubule filaments and are required for proper microtubule function. Abrogation of the mitotic checkpoint has been also considered to specifically generate lethal aberrations in chromosomally unstable tumor cells. Preventing mitotic exit has been recently proposed as a complementary alternative since cells cannot survive for long time in mitosis and they eventually die if components of the mitotic exit pathway, such as the E3 ubiquitin ligase APC/C (Anaphase Promoting Complex/Cyclosome) are inhibited. In this review we will discuss the recent data generated from these studies as well as proposals that need to be evaluated in the near future.

Mitotic kinases and kinesins

Multiple enzymatic activities are required for mitosis. These include centrosomal and mitotic kinases required for the maintenance of the mitotic state, generation of the mitotic spindle, and proper attachment of chromosomes to microtubules for segregation [7]. The cyclin-dependent kinase Cdk1 is a major driver of mitotic entry and progression. Its activity is essential for mitotic entry and lack of Cdk1 activity prevents cell proliferation in every cell type tested [8]. Inhibition of this kinase is thought to result in high levels of toxicity in normal cells and it is not frequently considered as an interesting target for cancer therapy [9]. However, some recent